



**Drug delivery to the nose:  
formulation, deposition and permeation  
of poorly soluble drugs**

**Michele Pozzoli**

A thesis submitted in fulfilment of the requirements  
for the degree of Doctor of Philosophy

Graduate Research School of Health  
Pharmacy

University of Technology Sydney

January 2017

# CERTIFICATE OF ORIGINAL AUTHORSHIP

I certify that the work in this thesis has not previously been submitted for a degree nor has it been submitted as part of requirements for a degree except as part of the collaborative doctoral degree and/or fully acknowledged within the text.

I also certify that the thesis has been written by me. Any help that I have received in my research work and the preparation of the thesis itself has been acknowledged. In addition, I certify that all information sources and literature used are indicated in the thesis.

Signature of Student:

Production Note:  
Signature removed prior to publication.

Date: January 2017

# ACKNOWLEDGMENTS

*"I was just guessing at numbers and figures*

*"Pulling your puzzles apart*

*Questions of science; science and progress*

*Do not speak as loud as my heart"*

*-The Scientist by Coldplay-*

To an amazing supervisory team – Associate Professor Fabio Sonvico, whose mentorship over the past few years has helped me to grow as a scientist and as an individual, words cannot explain my infinite gratitude; Professor Daniela Traini, who spurred me from the first day to put into words my work in the laboratory – if my English writing skills have improved even at the slightest, it is all your merit; Professor Paul Young, thank you for your brilliant ideas; lastly Dr. Maria Sukkar, thank you for accepting me at half way of my candidature.

A special thanks to Dr. Lyn Myor for helping me with my English, my writing and for instilling some "cell biology" into my brain; to Dr. Erick Bing Zhu for teaching me how to use all the equipment; to Dr. Hui Xin Ong (YY) for guiding me at the beginning of my PhD... Thank your Boss. Muito Obrigada Gabriela!

To all my Respitech buddies – Thank you Giulia, Emelie, Khanh, Stewie, Mic, Mariam, Alaa, Jesse "The Teddy Bear"; the post-docs: Yang, Wing & Judy, Mehra, Maliheh and Maree. Special thanks to Larissa and Roberto for being such amazing friends... thank you for all the coffee and beers we shared together. Thank you Lala for being the best messy desk mate I could ever ask for.

Thank you to the visiting student from Italy, thank you for making me feel like I was back home in my country: Mariateresa, Gialunca, Matteo, Angelo and the last crazy couple, the blonde and the brunette Carola & Cristina. Special thanks to my favourite

Sicilian girl Valentina. Thank you to all the others students especially Summit and Jasper.

In the Graduate School of Health, I would like to thank Sharon for being my friend... even before having the same supervisor.

A special thanks to all the students that I have met during my period abroad in Parma. Special thanks to Adryana, Kenji and Irene for getting me through it!

The lifelong friendship of who has always been there for me, Tommaso, from kindergarten, he has become a source of amazing and crazy experiences. Even though we are 14,000 kilometres apart, there is not day without talking to each other. Thank you Marty.

Thank you Chiara, Grace and Marta for the long-distance friendship... Thank you for your nice words during the dark period.

Thanks to all my Italian friends for their support and the joyful moments every time I return... Pado and Caste... and of course to all Basketball mates... Mitch, Bimbo, Mirco, Burghi and Simone to help me with 3D drawings.

Lastly, to my family, who have given me so much and to whom I am indebted to always – My Brother, Dad, Rosy and Sister in law (MaryCandy), thank you all for the continuous support and unconditional love. Thank you to my Aunty and Uncles for always believing in my abilities.

*I dedicate this thesis to the past and to the future*

*To my Grandma Carla as gratitude for raising me and allowing me to become the man which I am today and to my forthcoming nephew/ niece... you are just less than a centimetre now but I can't wait to hold you in my arms in a few months' time*

# TABLE OF CONTENTS

Certificate of original authorship .....	I
Table of Contents .....	IV
List of Figures and Tables.....	X
Glossary and Abbreviations .....	XV
Thesis Abstract .....	XVII
<b>Chapter 1 .....</b>	<b>1</b>
<b>1.1 General Introduction .....</b>	<b>2</b>
<b>1.2 Anatomy and Histology of the Nose.....</b>	<b>3</b>
<b>1.3 Commercial Nasal Products .....</b>	<b>7</b>
1.3.1 Liquid Dosage Forms and Metered Dose Spray Pumps .....	7
1.3.2 Nasal pressurized metered-dose inhalers (pMDIs).....	10
1.3.3 Dry Powder Dosage Forms and Devices .....	11
<b>1.4 Characterization of nasal delivery products .....</b>	<b>13</b>
<b>1.5 <i>In vitro</i> models for assessing nasal drug deposition .....</b>	<b>15</b>
<b>1.6 <i>In vitro</i> models for assessing nasal drug absorption .....</b>	<b>20</b>
1.6.1 <i>Ex vivo</i> models for studying drug permeation .....	20
1.6.2 Cell Cultures- Primary cells and cell lines.....	21
<b>1.7 Aim of the Study.....</b>	<b>25</b>
<b>1.8 Structure of the Thesis.....</b>	<b>26</b>
<b>1.9 References.....</b>	<b>29</b>

<b>Chapter 2</b> .....	<b>39</b>
<b>2.0 Preface</b> .....	<b>40</b>
<b>2.1 Abstract</b> .....	<b>41</b>
<b>2.2 Introduction</b> .....	<b>43</b>
<b>2.3 Materials and Methods</b> .....	<b>50</b>
2.3.1 The Puvlizer <sup>®</sup> device .....	50
2.3.2 Physico-chemical characterization .....	52
2.3.2.1 Powder bulk and tapped density .....	52
2.3.2.2 Dynamic Vapor Sorption .....	52
2.3.2.3 Specific Surface Area.....	53
2.3.2.4 Particle Size Distribution by Laser Diffraction .....	53
2.3.2.5 Scanning electron microscopy .....	53
2.3.2.6 Scanning Raman Spectroscopy .....	54
2.3.3 Analytical Characterization .....	55
2.3.3.1 BDP quantification using HPLC.....	55
2.3.3.2 Dose Content Uniformity .....	55
2.3.3.3 Shoot Weight and BDP Content.....	55
2.3.4 Aerosol performance of Teijin Rhinocort <sup>®</sup> .....	56
2.3.4.1 Cascade impaction .....	56
2.3.4.2 In-line In Vitro Aerosol Laser Diffraction Analysis.....	58
<b>2.4 Results and Discussion</b> .....	<b>59</b>
2.4.1 Physicochemical characterization of the formulation .....	59
2.4.2 Aerosol performance of Teijin Rhinocort .....	66
<b>2.5 Conclusion</b> .....	<b>70</b>
<b>2.6 Acknowledgements</b> .....	<b>71</b>

<b>2.7</b>	<b>Author Disclosure Statements</b> .....	<b>71</b>
<b>2.8</b>	<b>References</b> .....	<b>72</b>
<b>Chapter 3</b>	.....	<b>76</b>
<b>3.0</b>	<b>Preface</b> .....	<b>77</b>
<b>3.1`</b>	<b>Abstract</b> .....	<b>78</b>
<b>3.2</b>	<b>Introduction</b> .....	<b>79</b>
<b>3.3</b>	<b>Materials and Methods</b> .....	<b>83</b>
3.3.1	Materials.....	83
3.3.2	Cell Culture Nasal Cell Line.....	84
3.3.3	Transepithelial electrical resistance Measurements.....	84
3.3.4	Sodium Fluorescein Permeation Experiments.....	85
3.3.5	Evaluation of Mucus Production.....	86
3.3.6	Immunocytochemistry Experiment.....	86
3.3.7	Expression of Xenobiotic Transporters.....	87
3.3.7.1	RPMI 2650 Cell Culture and Sample Collection of Primary Nasal Cell.....	87
3.3.7.2	RNA Isolation, Target Synthesis, Microarray Data Analysis.....	88
3.3.8	Development and Validation of Aerosol Nasal Deposition Apparatus.....	89
3.3.8.1	Development of the Modified Expansion Chamber.....	89
3.3.8.2	Validation of the Impactor Deposition Performances: Standard vs. Modified Expansion Chamber	91
3.3.8.3	Validation of the Cell Layer Integrity in the Modified Chamber.....	92
3.3.9	Deposition and Transport of a Commercial Budesonide Nasal Spray on Optimized RPMI 2650 cell Model using the Modified Expansion Chamber.....	92
3.3.10	Analytical Quantification of Budesonide.....	93

3.3.11	Statistics .....	93
<b>3.4</b>	<b>Result and Discussion.....</b>	<b>94</b>
3.4.1	Transepithelial Electrical Resistance (TEER) Measurements .....	94
3.4.2	Sodium Fluorescein Permeation Experiments.....	96
3.4.3	Evaluation of Mucus Production .....	98
3.4.4	Immunocytochemical investigation.....	103
3.4.5	Expression of Xenobiotic Transporters.....	104
3.4.6	Development and Validation of the Modified Expansion Chamber .....	109
<b>3.5</b>	<b>Conclusion .....</b>	<b>113</b>
<b>3.6</b>	<b>Acknowledgements.....</b>	<b>114</b>
<b>3.7</b>	<b>Author Disclosure Statements.....</b>	<b>114</b>
<b>3.8</b>	<b>References .....</b>	<b>115</b>
<b>Chapter 4</b>	<b>.....</b>	<b>120</b>
<b>4.0</b>	<b>Preface .....</b>	<b>121</b>
<b>4.1</b>	<b>Introduction .....</b>	<b>122</b>
<b>4.2</b>	<b>Material and Methods .....</b>	<b>124</b>
4.2.1	Materials.....	124
4.2.2	Aerosol Performances and Modified Expansion Chamber Validation .....	124
4.2.3	In-line <i>In Vitro</i> Aerosol Laser Diffraction Analysis.....	127
4.2.4	Cultivation of RPMI 2650 cell line in Air Liquid Interface .....	127
4.2.5	Transport Studies on Nasal Cell Model (Conventional and after Deposition) .....	128
4.2.6	Chemical Quantification of Beclomethasone Dipropionate and its Metabolites .....	129
4.2.7	Statistics.....	130
<b>4.3</b>	<b>Results and Discussion .....</b>	<b>130</b>



4.3.1	Aerosol Performances Expansion Chamber Validation .....	130
4.3.2	Transport Studies on Nasal Cell Model.....	133
<b>4.4</b>	<b>Conclusion .....</b>	<b>136</b>
<b>4.5</b>	<b>References .....</b>	<b>137</b>
<b>Chapter 5</b>	<b>.....</b>	<b>139</b>
<b>5.0</b>	<b>Preface .....</b>	<b>140</b>
<b>5.1</b>	<b>Abstract .....</b>	<b>141</b>
<b>5.2</b>	<b>Introduction.....</b>	<b>142</b>
<b>5.3</b>	<b>Material and Methods .....</b>	<b>143</b>
5.3.1	Materials.....	143
5.3.2	Chemical Quantification of Budesonide by High Performance Liquid Chromatography 144	
5.3.3	Preparation of Freeze-dried formulation (LYO).....	145
5.3.4	Preparation of the Physical Mixture with Diluent .....	146
5.3.5	Physico-Chemical Characterization .....	146
5.3.5.1	Scanning electron microscopy .....	146
5.3.5.2	Specific Surface Area.....	147
5.3.5.3	Particle Size Distribution by Laser Diffraction .....	147
5.3.5.4	X-Ray Powder Diffractometry (XRPD) .....	147
5.3.5.5	Differential scanning calorimetry (DSC).....	148
5.3.6	<i>In Vitro</i> Drug Release Studies .....	148
5.3.7	Spray Performances and Interaction with Nasal Cell Model .....	149
5.3.7.1	Aerosol Performances by Cascade Impaction.....	149
5.3.7.2	In-line In Vitro Aerosol Laser Diffraction Analysis.....	150
5.3.7.3	Cultivation of RPMI 2650 cell line in Air Liquid Interface.....	150

5.3.7.4	Deposition and Transport Studies on Nasal Cell Model.....	151
5.3.8	Statistical Analysis .....	152
<b>5.4</b>	<b>Result and Discussion.....</b>	<b>153</b>
5.4.1	Physical Chemical Characterization .....	153
5.4.2	<i>In Vitro</i> Drug Release Studies .....	158
5.4.3	Aerosolization Performance and Interactions with Nasal Cell Model .....	162
<b>5.5</b>	<b>Conclusion .....</b>	<b>166</b>
<b>5.6</b>	<b>Acknowledgements.....</b>	<b>166</b>
<b>5.7</b>	<b>Author Disclosure Statements.....</b>	<b>166</b>
<b>5.8</b>	<b>References .....</b>	<b>167</b>
<b>Chapter 6</b>	<b>.....</b>	<b>172</b>
<b>6.1</b>	<b>General Conclusion.....</b>	<b>173</b>
<b>6.2</b>	<b>Future Directions.....</b>	<b>178</b>
<b>Appendices</b>	<b>.....</b>	<b>179</b>
<b>A.1</b>	<b>Publication List.....</b>	<b>180</b>
Journal articles included as thesis chapter .....		180
Conference Proceeding .....		181
<b>A.2</b>	<b>Other Publications During Candidacy Unrelated to Thesis .....</b>	<b>216</b>
<b>A.3</b>	<b>Copyrights Permissions .....</b>	<b>254</b>

# LIST OF FIGURES AND TABLES

Figure 1.1 Advantages and limitations of nasal drug delivery. Adapted from [4]. ....	3
Figure 1.2. Anatomy of the human nasal cavity schematic of a sagittal plane cut (A) and sample coronal plane midway through the nasal cavity (B). Reproduced from reference [5] with authorisation.....	4
Table 1.1 Summary of featuring of the nasal cavity and the different epithelium of the nasal mucosa .....	5
Figure 1.3. Metered dose spray pump. Reproduced from reference [33] with permission.....	10
Figure 1.4. Examples of nasal powder devices: A. Teijin Rhinocort (Teijin Pharma); B. Rhinocort Turbuhaler (Astrazeneca), from [33]; C. Optinose (Optinose), Reproduced from reference [21] with permission. ....	13
Figure 1.5. The two halves of the silicon nasal cast produced by Koken.....	16
Figure 1.6. Scheme representing the subdivision of the Bepak cast. Reproduced from reference [61] with permission. ....	17
Figure 1.7. Part composing Boehringer-Ingelheim nasal Cast. Reproduced from reference [65] with permission .....	18
Figure 2.1. Disassembled Teijin Puvlizer device with accessories .....	44
Table 2.1. Summary of nasal dry powder products and water-based alternatives marketed in U.K. ....	46
Table 2.2. Summarized Steps for the device preparation and administration of Teijin Rhinocort® .....	51

Figure 2.2. Apparatus E system used for the aerosol performance of the Teijin nasal powder device equipped with the nasal expansion chamber.....	57
Figure 2.3. SEM micrographs of the Teijin Rhinocort powder blend. ....	60
Table 2.3. Amount of Powder (mg) and BDP ( $\mu\text{g}$ ) emitted after each actuation ( $n=3 \pm \text{StDev}$ ) .....	62
Figure 2.4. Dynamic vapor sorption isotherm (two cycles) of Rhinocort Teijin Powder. ....	63
Figure 2.5. Particle size analysis by laser diffraction of Rhinocort Teijin powder blend measured with Malvern Mastersizer MS3000 ( $n=3 \pm \text{StDev}$ ).....	65
Figure 2.6. Overlay of Raman images on white light montage (BDP=green; HPC = blue and magnesium stearate = red). ....	66
Table 2.4. Percentage of Active ingredient in each stage of the Apparatus E Impactor equipped with the 2L expansion glass chamber for nasal delivery ( $n=3, \pm \text{StDev}$ ). ....	67
Figure 2.7. Particle size distribution of the powder emitted from Teijin Rhinocort using the Spraytech laser diffraction apparatus ( $n=3, \pm \text{StDev}$ ). ....	68
Figure 2.8. Equivalent volume diameter values ( $D_v 90, 50$ and $10$ ) measured by laser diffraction for Teijin Rhinocort, 8 insufflations for one dose ( $n=3, \pm \text{StDev}$ ). ...	69
Figure 3.1. 3D drawing of the modified expansion chamber. ....	90
Figure 3.2. British Pharmacopoeia apparatus E equipped with FDA glass expansion chamber (A) and modified expansion chamber (B).....	91
Figure 3.3. TEER of three different seeding densities of RPMI2650 cells cultured in the ALI conditions over time ( $n=3; \pm \text{StDev}$ ).....	95

Table 3.2. $P_{app}$ values ( $\times 10^{-6}$ cm/s) of Flu-Na across RPMI 2650 cultured in ALI conditions for three different seeding densities ( $n=3$ ; $\pm$ StDev) compared to values obtained for excised human nasal mucosa .....	97
Figure 3.4. Optical microscope images of Alcian blue mucus staining on RPMI 2650 grown on Snapwell <sup>®</sup> inserts at $2.50 \times 10^6$ cell/mL seeding density. ....	99
Figure 3.5. RGBb ratio values obtained after mucus staining as function of time in culture for the three different cell seeding densities ( $n=3$ ; $\pm$ StDev).....	102
Figure 3.6. Confocal Microscope Images of RPMI 2650 cells tight junction proteins-stained in green: E-cadherin (A) and ZO-1 (B-C). The blue and red colours in A and B respectively represent the DAPI staining of nuclei. C, the cross section of cell layers during confocal imaging: green ZO-1 and red cell nucleus.....	104
Table 3.1. List of drug transporters evaluated and their gene expression ( $\Delta Ct$ ) in RPMI2650 cultivated on Snapwells at $2.50 \times 10^6$ cell/mL, PNC: human primary nasal cells from brushing (average between male and female). Scale from not expressed (red) to highly expressed (dark green) .....	106
Table 3.3. Amount of Budesonide (% of the nominal dose) recovered from each Stage of the NGI using the Glass and Modified chamber ( $n=3 \pm$ StDev). ....	109
Figure 3.7. Amount of budesonide transported through RPMI 2650 nasal cell model after NGI aerosols deposition using the 3D modified chamber ( $n=5 \pm$ StDev). ....	111
Figure 3.8. Distribution of the budesonide recovered at the end of the experiment (4 hours) after the aerosol deposition using the 3D the modified expansion chamber ( $n=5 \pm$ StDev). ....	113

Figure 4.1. NGI configuration with Glass Expansion Chamber (A) and Modified Chamber printed in ABS (B).....	125
Figure 4.2. CAD 3D drawing of the Modified Expansion Chamber. Modified from Chapter 3. ....	126
Figure 4.3. Exemplification of conventional transport (A), Deposition of Nasal Products on cells (B).....	128
Table 4.1. Comparison of BDP mass deposition in the standard glass and the modified chamber using the NGI (n=3 ± StDev) .....	131
Table 4.2. Summary of the particle size of Teijin Rhinocort and Beconase (n=3, ± StDev) .....	133
Figure 4.4: Total amount (%) of BDP and BMP transported across the RPMI 2650 nasal cell model over 4 hours (n= 3, ± StDev). ....	134
Table 4.3. Percentage of BDP and BMP found ‘on’ the surface and inside ‘in’ RPMI2650 cells after 4 hours from the deposition/transport studies (n=3, ± StDev) .....	135
Table 5.1. Freeze-drying process for the Soluplus-budesonide formulation. ....	146
Figure 5.1. SEM micrographs of (A) micronized budesonide, (B) Soluplus and (C) LYO formulation .....	154
Figure 5.2. Particle size distribution of the lyophilized formulation, micronized budesonide and Soluplus. (n=3, ± StDev).....	155
Figure 5.3. X-rays diffraction patterns of micronized budesonide and LYO formulation. ....	157
Figure 5.4. Thermographs of budesonide, Soluplus, a physical mixture of Soluplus (80 %m/m) and budesonide (20%m/m) and lyophilized formulation (LYO). .	158

Figure 5.5. In vitro drug release of budesonide from: (A) LYO vs. water suspension.  
 (B) LYO vs. budesonide powders. (C) LYO, LYO-Ca, vs. budesonide and Ca-  
 BUD. (D) LYO vs. LYO after 3 months of storage. (n=3, ± StDev) ..... 159

Table 5.2. Percentage of Active ingredient in each stage of the apparatus E equipped  
 with the 2L expansion glass chamber for nasal delivery (n=3, ± StDev). No  
 Budesonide deposition could be detected for Stages 4-7..... 163

Table 5.3. Values of volumetric diameter ( $D_v$ ), span and percentage of particle  
 smaller than 10  $\mu\text{m}$  obtained for LYO-Ca (n=3, ± St.dev)..... 164

Figure 5.6. Amount (%) of budesonide transported across RPMI 2650 nasal cell  
 model after aerosol deposition using an apparatus E equipped with a modified  
 expansion chamber. (n=6, ± StDev)..... 165

# GLOSSARY AND ABBREVIATIONS

ABS	Acrylonitrile butadiene styrene
API	Active Pharmaceutical Ingredient
ALI	Air Liquid Interface
ATCC	American Type Culture Collection
Papp	Apparent permeability
BMP	Beclomethasone Monopropionate
BDP	Beclomethasone Dipropionate
BSA	Bovine Serum Albumin
BET	Brunauer–Emmett–Teller
Bud	Budesonide
CaCO <sub>3</sub>	Calcium Carbonate
CI	Cascade Impactor
R <sup>2</sup>	Coefficient of determination
f <sub>1</sub>	Difference factor
DSC	Differential Scanning Calorimetry
DMSO	dimethyl sulfoxide
DVS	Dynamic Vapor Sorption
EC	Expansion Chamber - Glass Chamber
FBS	Foetal Bovine Serum
T <sub>g</sub>	Glass Transition Temperature
HBSS	Hank's Buffer Salt Solution



HPLC	High Performances Liquid Chromatography
HPC	Hydroxypropyl cellulose
HPMC	Hydroxypropylmethyl cellulose
LCC	Liquid Cover Culture
Lyo	Lyophilized/ Freeze-dried
MEM	Minimum Essential Media
MC	Modified Chamber - Developed Apparatus
NGI	Next Generation Impactor/ Apparatus E
P-gap	P-Glycoprotein
PSD	Particle Size Distribution
PBS	Phosphate Buffer Saline
RGB	Red Green Blue
RH	Relative Humidity
SEM	Scanning Electron Microscopy
f2	Similarity factor
Flu-Na	Sodium Fluorescein
StDev	Standard Deviation
TGA	Thermogravimetric Analysis
TEER	Trans Epithelial Electric Resistance
FDA	United States of America Food and Drug Administration
Dv(X)	Volumetric diameter (percentage of population related to)
XRPD	X-Ray Powder Diffractometry
ZO-1	Zonula occludens-1

# THESIS ABSTRACT

The nose, is a promising site to deliver drugs with low oral bioavailability and for treatment of conditions that require a rapid onset of action. It is the first option to treat localized diseases such as rhinitis but also it can be used as site to deliver drug systemically. In the future, the number of product administered through the nose it is expected to increase, as more drugs will require an effective route for drug absorption. Hence, while the current characterization of nasal product focus mainly on the physicochemical properties of spray formulations, the biopharmaceutical evaluation of new nasal drug delivery products and formulations will require robust and reliable pre-clinical *in vitro* models.

The first aim of this study was to develop an apparatus able to perform deposition and permeation of nasal formulation at the same time, mimicking so the *in vivo* process of drug administration.

The second aim was the application of this model to the characterization of commercial products and the development of novel formulations.

In particular, to provide a physiologically relevant surface and barrier for the deposition and permeation studies, the cell line RPMI 2650 was chosen in order to establish a model of the nasal mucosa. The model was obtained using the air-liquid interface culturing method, in which the upper surface of the cell is exposed to air after the seeding on cell culture insert. The model developed showed production of

mucus, expression of xenobiotic transporters similar to primary nasal cells and barrier properties matching those reported in literature for excised human nasal mucosa.

The deposition apparatus was produced via 3D printing starting from an expansion chamber proposed by FDA for the determination the aerodynamic particle size of nasal sprays with cascade impactors. The apparatus developed consists of a plastic chamber able to accommodate cell culture inserts on its internal surface. This allows the deposition of aerosolised particles directly onto the surface of the RPMI 2650 cells previously cultured on inserts. The apparatus was validated against FDA glass expansion chamber using three different commercial products: two suspensions and one powder. The powder has shown faster permeation rate across RPMI 2650 cells nasal mucosa model.

In conclusion, this work has developed, validated and tested an *in vitro* method to assess particles deposition and drug permeation in conditions similar to those occurring *in vivo* and which will be useful for the characterization and development of future nasal products.

# CHAPTER 1

*Introduction to the Nose and Nasal Drug Delivery*

## 1.1 GENERAL INTRODUCTION

Nasal sprays are the first-line therapies for the treatment of localized diseases such as rhinitis, hay-fever, polyps or nasal hypersensitivity and they are used to offer relief for typical local symptoms such as congested nose related to the common cold and flu.

On the other hand, over the past decades, the interest in the use of the nose to deliver drugs for systemic treatments has dramatically increased. Nowadays it is possible to use the nasal route to treat migraine, to manage pain, for hormone replacement therapy, smoking cessation and flu vaccination [1-3]. Furthermore, nasal delivery has the potential to provide access to the central nervous system (Nose-to-Brain) avoiding the blood brain barrier. This delivery occurring through different pathways, including the olfactory epithelium, may open new opportunities for the treatment and symptoms management of neurodegenerative diseases such as Alzheimer's and Parkinson's. The possibility, to have different targets (local, systemic and brain), it is related to various aspect: physicochemical properties of the drug, presence in the formulation of additives such as permeation enhancer or nano-systems and lastly the site of deposition.

Such various and different therapeutic indications are possible as a consequence of the number of advantages of the nasal route (Figure 1.1). This delivery route is painless and non-invasive, increasing patient compliance and offers a rapid onset of drug action, due to the high vascularization and high permeability of the nasal mucosa, at the same time avoiding first pass metabolism.

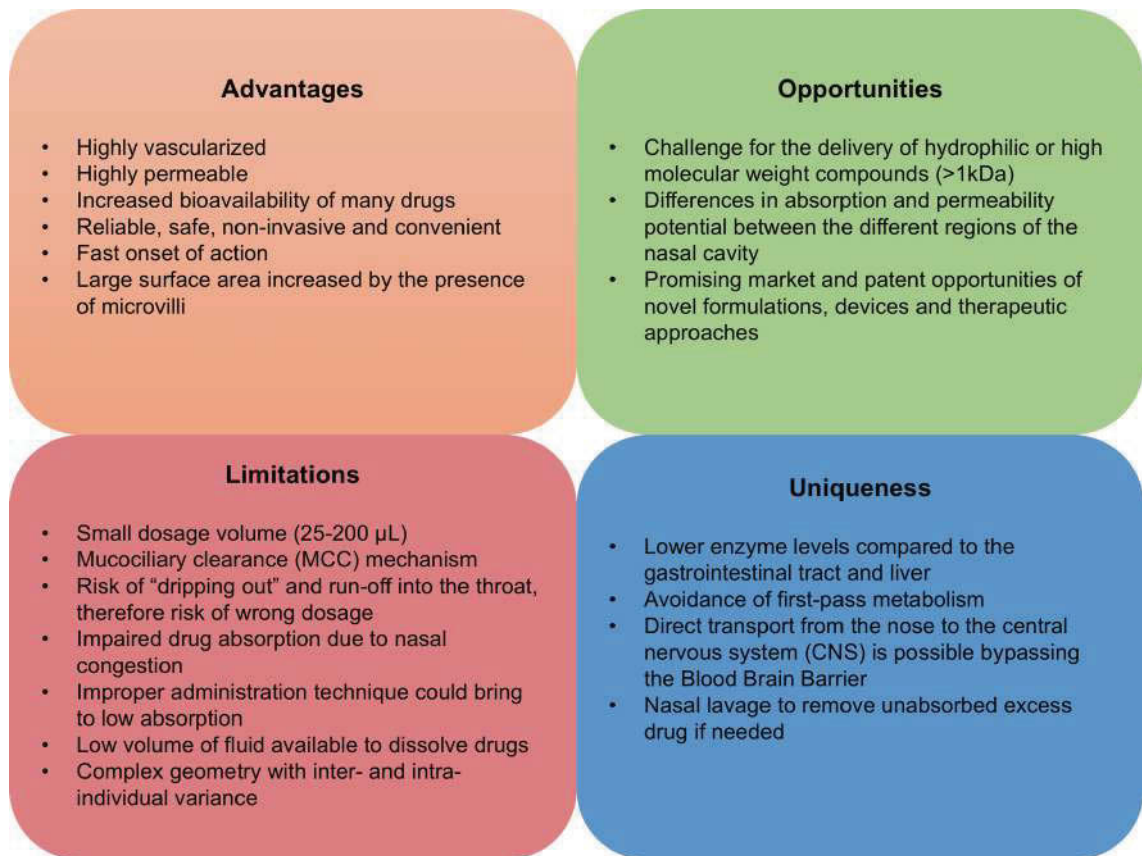


Figure 1.1 Advantages and limitations of nasal drug delivery. Adapted from [4].

## 1.2 ANATOMY AND HISTOLOGY OF THE NOSE

The nose is the first tract of the respiratory system. As its component it helps conditioning the air we normally breath; it helps to filtrate particulates present in the air; and, it is the main organ for olfaction and the first-line immunology defence.

The human nasal cavity is divided into two halves by the septum, each with a volume of about 7.5 mL. Both symmetrical halves consist of three main regions distinguished according to their anatomic and histological characteristics: the nasal vestibule, the respiratory region and the olfactory region.

The vestibular region is the anterior part of the nose and it is the narrowest part of the nasal cavity (the internal nostril; nasal valve), which is located about 1.5 cm from the external naris. The vibrissae, stiff hairs within the nostrils, cover most of this area allowing the efficient filtration of inhaled particles with an aerodynamic particle size larger than 10  $\mu\text{m}$ . In the vestibular region, the surface lining changes from skin, that covers the anterior part of the passage, to a stratified squamous epithelium.

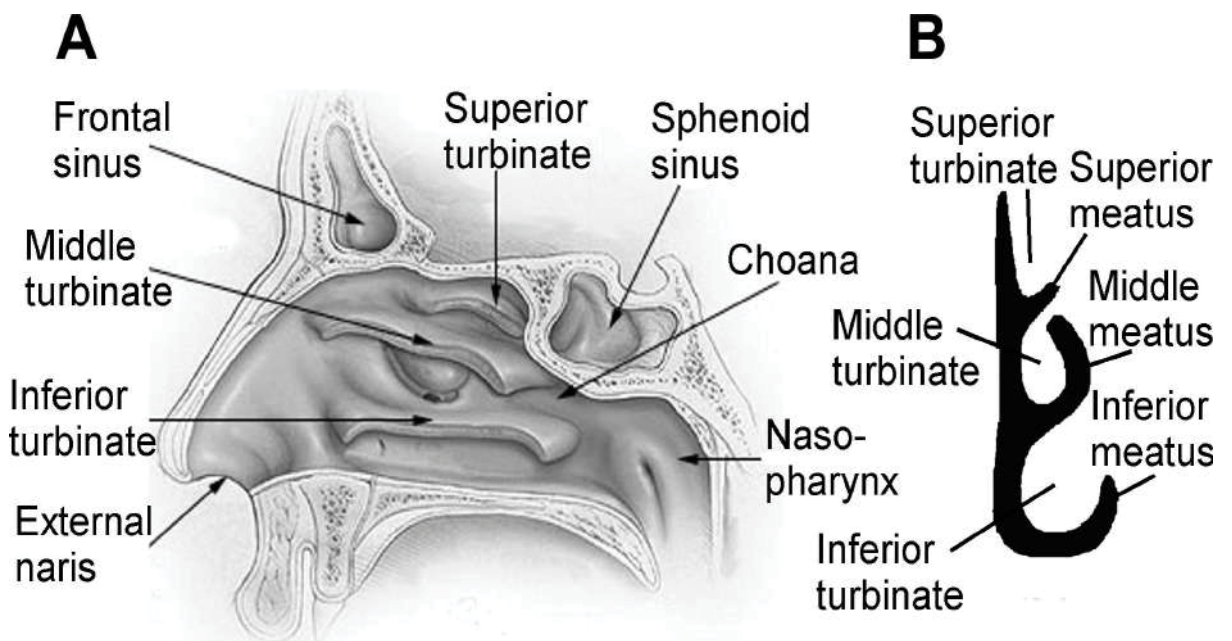


*Figure 1.2. Anatomy of the human nasal cavity schematic of a sagittal plane cut (A) and sample coronal plane midway through the nasal cavity (B). Reproduced from reference [5] with authorisation.*

The respiratory region is divided into three turbinate (conchae): superior, middle, and inferior. The turbinates are covered with a pseudostratified columnar epithelium. This epithelium is composed of four type of cells: mucus secreting, ciliated, non-ciliated and basal cells. The ciliated and non-ciliated cells are

covered with non-motile microvilli (300 microvilli per cell), which are responsible for increasing the surface area [6]. These structures because of this multi-folded structure, increase the total surface area of the nose to approximately 150 cm<sup>2</sup>.

*Table 1.1 Summary of featurig of the nasal cavity and the different epithelium of the nasal mucosa*

<b>Features of Nasal Cavity</b>	
Depth [7]	120 - 140 mm
Surface Area [8]	150 - 160 cm <sup>2</sup>
Total Volume [9]	16 -19 cm <sup>3</sup>
Olfactory Region Area [10,11]	8 cm <sup>2</sup> (2-10 cm <sup>2</sup> )
Mucosal pH [7]	5.5 - 6.5
Temperature [12]	32.5 - 35.0 °C
Humidity (RH) [12]	35%
Mucuciliary Clearance [13]	15 - 30 min
Cilia Length [9]	4-5 µm
Cilia Beat Frequency [14-16]	13 Hz (8.8-14 Hz)
Mucus Velocity (Respiratory region) [7]	6 mm/min
Mucus Velocity (Vestibular region) [7]	1–2 mm/h
Mucus Layer Thickness [17]	5 µm
Mucus Produced [18]	20 – 40 mL/day
Mucus Composition [9]	water (95%), mucus glycoproteins (2%), other proteins including albumin, immunoglobulins, lysozyme and lactoferin (1%),



	inorganic salts (1%) and lipids (<1%)
Regions [19,20]	<i>Vestibular/ Atrium:</i> Nasal hairs, epithelial cells are stratified, squamous and keratinized, low absorption. Barrier against toxic environmental substances
	<i>Turbinates/ Respiratory:</i> pseudo-stratified epithelia, mucus secreting, presence of microvilli. large vascularity and surface area, major site of absorption.
	<i>Olfactory:</i> Specialized ciliated olfactory nerve cells for smell perception, 3-5 % total nasal area, direct access to the brain.

Approximately 15-20% of the cells in the turbinate are ciliated cells, with about 100 cilia on the apical surface of a cell [20]. Ciliated cells are covered with motile cilia which are responsible for mucus transport and mucociliary clearance. Cilia are hair-like projections (2-4  $\mu\text{m}$ ) on the apical surface of the columnar cells. All cilia beat in a coordinated fashion, transporting the mucus towards the nasopharynx.

The human olfactory region is situated in the superior conchae and covers only about 3-5% (about 8  $\text{cm}^2$ ) of the nasal cavity [10]. The olfactory epithelium is a pseudo-stratified columnar structure. It consists of olfactory sensory neurons (OSN), supporting cells, serous and mucosal glands. The OSNs are bipolar neuronal cells, dendritic portions of these neurons extend above the epithelial

surface and terminate into a bulbous olfactory knob from which protrude on average 10–15 immotile cilia, providing an extensive surface area for reception of odorants. The olfactory neuro-epithelium is replaced approximately every 40 days [18].

## **1.3 COMMERCIAL NASAL PRODUCTS**

Drugs can be administered to the nasal cavity using different formulation strategies: liquid, solid or semisolid products.

Liquid formulations delivered by metered spray pumps, in form of solutions or suspensions, currently dominate the nasal drug market, but nasal powder formulations and devices do exist, and more are in development [21-25]. Additionally, the number of pressurized metered dose inhalers (pMDIs) dramatically decreased since the ban of chlorofluorocarbons (CFCs) in 1987.

Ointments, gels, creams and balms, liquid formulation delivered as drops and are just a small niche in the nasal market and will not be discussed in details [21,26,27].

### **1.3.1 Liquid Dosage Forms and Metered Dose Spray Pumps**

Liquid nasal formulations are generally aqueous solutions, but suspensions (e.g. corticosteroid for rhinitis treatment) and emulsions can also be delivered. Liquid formulation usually contains an agent to increase viscosity, typically a cellulose derivative, in order to prolong the residence of the formulation in the nose, to diminish the dripping out effect and to help to stabilize the formulation, especially in the case of suspensions and emulsions [28,29]. Surfactants are often added

to decrease the particle size of the spray droplets, to improve drug solubility and as stabilizers or emulsions stabilizers [29,30]. The main drawbacks in the use of surfactants are related to mucosal irritation and damage [31]. In aqueous formulations, the presence of preservatives is required in order to avoid microorganism growth and drug oxidation. However this is one major issues of nasal water-based dosage forms because preservatives can alter the mucociliary function especially in long-term treatments and they can be a major cause of irritation [21,27,32,33]. An additional disadvantage, of metered nasal pumps, might be related to the limited chemical stability of the drug when in solution or suspension. Lastly, the delivery of liquid formulation in the nasal cavity, especially in large volume, can lead to a “drip-out” effect, i.e. part of the formulation is lost after the administration because of the dripping of the liquid out of the nose leading to an incorrect dosing of the drug [1,34-36].

Since their introduction some four decades ago, metered spray pumps have come to a dominant position in the nasal drug delivery market [21].

Nasal spray systems consist of a container, the pump with the valve and the actuator. The pumps typically deliver around 100  $\mu\text{L}$ , even if delivered volumes can range between 25 and 250  $\mu\text{L}$  per spray actuation, and they offer high reproducibility of the dose delivered (Figure 1.3) [21,33]. In addition, the spray humidifying effect is considered convenient, as it appears useful towards symptoms often present in many allergic and chronic diseases (rhinitis) such as drying of mucous membranes.

The particle size and plume geometry of the spray can vary within certain limits and depend on the properties of the specific pump used and formulation. Formulation properties such as viscosity and rheological behaviour (in general thixotropic behaviour is expected for non-Newtonian fluid, as in pharmaceutical liquid formulations), surface tension and particle size of suspended particles can potentially influence droplet size and dose accuracy. Nozzle orifice, force and velocity applied to actuate the device are others factors affecting the spray performances pump related [21,30,33,37,38].

After the actuation, traditional spray pumps replace the emitted liquid volume introducing air in the bottle containing the formulation. During this process, microbes can enter the device and start to proliferate in the liquid, preservatives are therefore required to avoid contamination in multi-dose containers.

To avoid the issues related to the presence of preservative, disposable single-dose containers and airless/preservative-free multi-dose sprays have been developed and are now available on the market. These innovative devices however have a higher cost compared to traditional metered pumps.

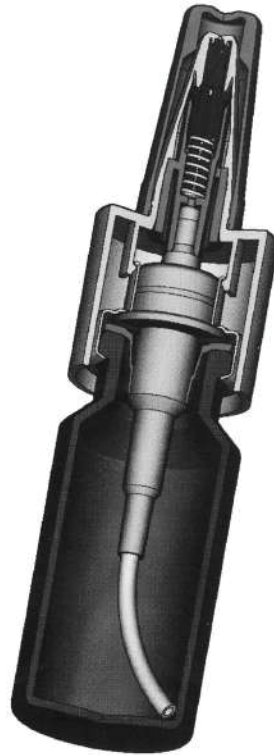


*Figure 1.3. Metered dose spray pump. Reproduced from reference [33] with permission.*

### **1.3.2 Nasal pressurized metered-dose inhalers (pMDIs)**

As mentioned above, only few nasal products exist that contain hydrofluoroalkane (HFA) propellants. Two of them were recently approved and marketed in 2014 in US as locally acting corticosteroids: Zetonna (Ciclesonide, Sunovion Pharmaceuticals) and QNASL (Beclomethasone Dipropionate, BDP, Teva Respiratory LLC). Major advantages of this new kind of nasal formulation are related to the quick evaporation of the propellant that help in limiting the drip effect and the high velocity of the spray produced that favour deposition by impaction [21,25].

### 1.3.3 Dry Powder Dosage Forms and Devices

Major advantages of using dry powder formulations over liquid formulations for nasal delivery are: lack of preservatives, improved chemical stability, high dose delivered, enhanced residency time on the nasal mucosa, decreased clearance rate and improved absorption rate [21,33,39-41]. Hence, administration of nasal powders may increase drug bioavailability and patient compliance [22,34,40].

Despite these advantages, dry powders are still less frequently used in nasal drug delivery compared to liquid formulations. Currently, only 4 products are available on the market: Teijin Rhinocort (Beclomethasone Dipropionate) and Erizas (Dexamethasone cipeccilate) are sold only in Japan for the treatment of rhinitis by Teijin Pharma and Nippon Shinyaku respectively; Rhinocort Turbuhaler (Budesonide) is commercialized by AstraZeneca in Canada and Europe; and more recently, ONZETRA™ Xsail™ (Sumatriptan) a new treatment for acute migraine, is marketed by Avanir Pharmaceuticals in United States of America.

Major drawbacks of powder formulation are related to the drug dissolution and solubility due to the low fluid volume in the nasal cavity. Additionally, powder properties such as particle size and shape, density and flow characteristics have an influence on the distribution, deposition, dissolution and absorption in the nose [33,36,42,43]. A thorough characterization of the formulation and of its behaviour in combination with a suitable device is required to develop powder-based nasal products.

Nasal devices to deliver dry powder formulations can broadly be divided into 3 categories:

1. Powder sprayers: these devices are usually composed by a compressible compartment which provides an air flow that creates a plume of powder. The Teijin (Figure 1.4A) and Erizas devices are based on this principle [21,39,44]. These two systems are capsule-based, therefore is possible to use the device with different formulations. However, the necessity to carry around the device and the capsules in a blister and to execute a sequence of manoeuvres for powder administration (capsule loading, piercing, actuation, unload of the empty capsule shell, eventual cleaning procedures) could somewhat decrease patient compliance.

2. Breath actuated-inhalers, where the subject uses his own inspiratory energy to inhale the powder throughout the nostril from the device. Astra Zeneca's Rhinocort Turbuhaler is based on this principle (Figure 1.4B) [1,21,23,34,45]. Among all the dry powder devices available on the market, Rhinocort Turbuhaler is the only multi-dose product. It is based Turbuhaler<sup>®</sup> technology, a reservoir system widely used in pulmonary drug delivery [46].

3. Breath powered bi-directional delivery nasal insufflator: this unique device consists of a mouthpiece connected to a nosepiece. The delivery of the powder is based on the blowing force of the patient. During the exhalation, the soft palate close, minimizing the risk for the formulation to reach the lungs, and optimizing the deposition in the respiratory region of the nose [21,47,48]. ONZETRA<sup>™</sup> Xsail<sup>™</sup> is based on this principle (Figure 1.4C).

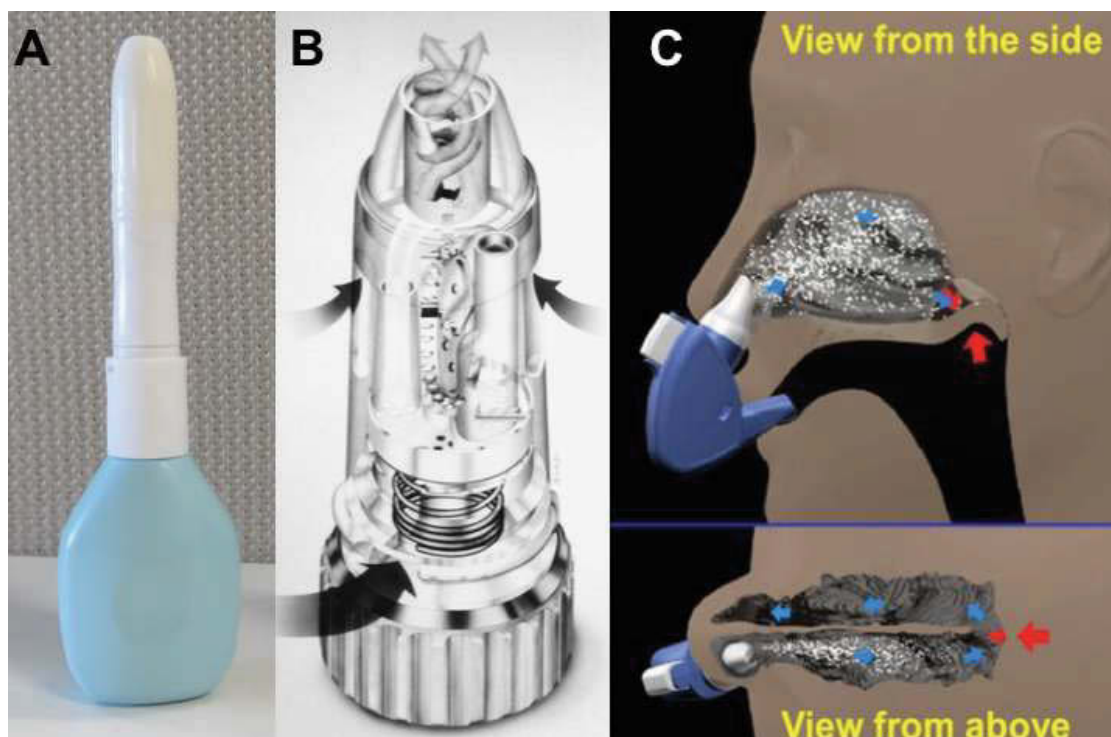


Figure 1.4. Examples of nasal powder devices: A. Teijin Rhinocort (Teijin Pharma); B. Rhinocort Turbuhaler (Astrazeneca), from [33]; C. Optinose (Optinose), Reproduced from reference [21] with permission.

## 1.4 CHARACTERIZATION OF NASAL DELIVERY PRODUCTS

For the *in vitro* characterization of nasal devices and formulations various regulatory agencies, like the Food and Drug Administration (FDA) and the European Medicines Agency (EMA), have published guidelines describing various testing methods [49,50].

According to the 2003 FDA Draft Guidance on “Bioavailability and Bioequivalence Studies for Nasal Aerosols and Nasal Sprays for Local Action”, the bioequivalence of a nasal spray solution product can be established by a number of *in vitro* tests to demonstrate equivalent product performance, in conjunction to



formulation sameness and device comparability between the test and reference products [29]. Specifically, six *in vitro* tests are indicated as critical to assess the performance of a nasal spray product and are required to demonstrate bioequivalence of the drug product. These tests are: single actuation content through container life, droplet size distribution by laser diffraction, particle/droplet size distribution by cascade impactor, spray pattern, plume geometry, and priming/re-priming [39,49,51].

All these tests are only based on analytical measures of physico-chemical properties of the nasal medicinal product and of the spray produced with it. Such an approach is valid especially in a quality control prospective. However, the suggested tests when applied to the development of an innovative product and to other type of formulations, such as dry powders, are inadequate for the thorough characterization of the product. In fact, these tests do not take in consideration the complexity of the geometry of the nasal cavity in term of deposition and the effect on drug absorption of the formulation properties. Several studies showed that these *in vitro* tests in some cases were capable of discriminating between nasal spray products, but these differences were not then translated to relevant differences *in vivo* [7,52,53].

The assessment of nasal products would benefit from the use of more clinically meaningful *in vitro* methods [54] and as a matter of fact, in the literature several deposition and absorption models have been suggested by different research groups.

## 1.5 *IN VITRO* MODELS FOR ASSESSING NASAL DRUG DEPOSITION

Due to nasal anatomy and physiology, the site of drug deposition is very important when trying to maximise drug absorption. Considering this, the respiratory region of the nasal cavity, which comprises the turbinates and the nasal septum, is the most promising area for drug absorption [55,56].

In order to determine how a nasal formulation is going to be deposited in such peculiar environment, nasal casts appear an interesting option.

Nasal cast are physically realistic nasal airway geometry models, which have been developed to study and assess the regional drug deposition of nasal formulation *in vitro*. Several type of nasal cast models have been proposed.

Nasal airway geometric models can be obtained post-mortem from human cadavers. The problem related with this kind of models is that, usually the techniques applied to obtain them can lead to loss of anatomical accuracy and they can pose biosafety issues during the handling of the cadaver specimens [57].

Furthermore, all these models are obtained from a specific individual and therefore they are neither idealized nor representative of the general population.

The Koken cast (Koken LM-005, Japan) is a transparent silicon replica of the nasal airways, divided in two sections, i.e. left and right cavity by a Plexiglas sheet, consequently a not anatomically correct representation of the septum (Figure 1.5).

The cast originated from a Japanese male cadaver. Despite the drawbacks of this model, it is one of the most used cast used in literature for nasal products *in vitro* deposition. In particular, being transparent allows the imaging of the product deposition in the nasal cavity [58-60].



*Figure 1.5. The two halves of the silicon nasal cast produced by Koken.*

Durand and co-workers have proposed plastination as technique to obtain anatomically correct nasal casts from cadavers [57]. However, this technique has not been utilised as yet to study nasal formulations deposition. The process consists in replacing water and lipids in biological tissue by curable polymers. Then, polymers are hardened resulting in dry, odourless and durable anatomic specimen.

Advanced imaging techniques, including magnetic resonance imaging (MRI) and computed tomography (CT), enable the measurement of nasal airway dimensions of human subjects with high accuracy and allow the creation of more accurate models compared to casts obtained post-mortem from human cadavers. A series of nasal casts have been developed with this approach by both academic groups and industries.

Models derived from single-person CT scans have been developed by Bepak and Boehringer-Ingelheim. The scans were obtained from an healthy female and male, respectively. Bepak cast is fabricated in nylon and it divided in 5 regions: Nasal vestibule, front and rear turbinates, olfactory region and nasal pharynx (Figure 1.6) [61-63].

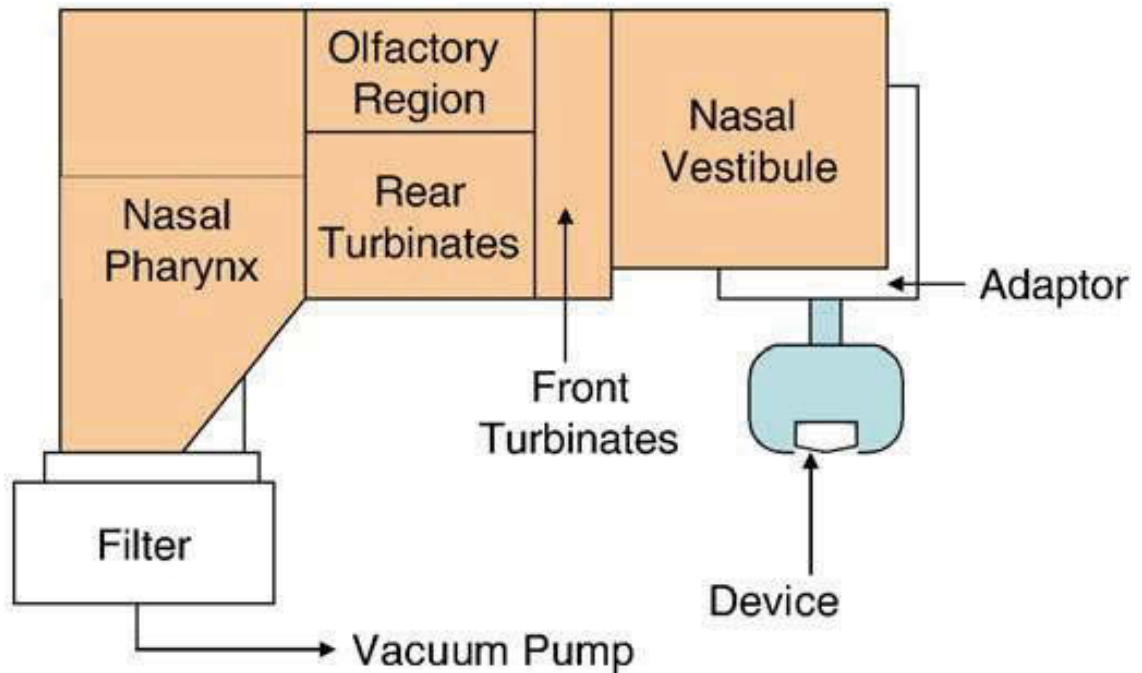


Figure 1.6. Scheme representing the subdivision of the Bepak cast. Reproduced from reference [61] with permission.

Boehringer-Ingelheim cast is also made of five sections representing the nostrils, nasal vestibule, lower, middle and upper turbinates and nasopharynx (Figure 1.7) [64,65]. Despite the accuracy and the sectioning of the model that helps the recovery of the material in the different sections of the nasal cavity, major drawbacks of this models are the rigidity of the material used for the cast and the fact that the model is representative of only one nasal cavity and not all the population.



*Figure 1.7. Part composing Boehringer-Ingelheim nasal Cast. Reproduced from reference [65] with permission*

Casts from MRI scan of single individuals have been developed by Cheng YS co-authors and Virginia Commonwealth University (VCU) [66]; both models are originated from data acquired from the same 53 years old healthy Caucasian male. VCU model is divided in 3 sections: anterior nose, middle passage and nasopharynx [54,67]. The model developed by Cheng, is made from acrylic plastic and it is segmented in 77 sagittal sections, feature that make the handling of the cast challenging [66].

Liu and collaborators have developed a model obtained constructing an average from 30 healthy volunteer CT scans. The major problem related to this model is linked to the segmentation of the cast that is divided in only 3 parts: anterior nose,

middle passages and nasopharynx, which does not discriminate different specific areas such as for example the olfactory region. Moreover, during the “averaging” process the nasal cavity was simplified, hence, losing in surface and geometry complexity [5].

Although nasal cast are powerful tools to study and even quantify regional deposition of nasal formulations *in vitro*, they have a series of drawback that are summarised here below:

- Nasal casts can be from single or multiple CT scans. Models from single CT scans are not representative of the general population, while models obtained from multiple CT scans of several generally lack of anatomic detail.
- Nasal casts made in either soft or hard plastic are not really representative of the nasal cavity surface. Furthermore, for the more rigid models, the nostrils geometry may restrict the positioning of the nasal device.
- The lack of mucus on the surface of deposition is a major problem. Casts have been coated on their inner surface with different type of viscous solutions like PEG 400 and glycerol, but these are poor representation of the *in vivo* mucosal surface [63,65].
- Finally, the use of different casts and analytical techniques make the set of measures obtainable very specific for the peculiar tool used.

## **1.6 IN VITRO MODELS FOR ASSESSING NASAL DRUG ABSORPTION**

To investigate the amount of active ingredient absorbed after nasal administration, two are the main approaches that have been widely used: *ex vivo* model from animal mucosa or cell culture based system.

### **1.6.1 *Ex vivo* models for studying drug permeation**

A number of studies have been published describing permeation experiments using excised nasal tissue of animal origin. Porcine [28,68-70], rabbit [71-74], bovine [75-78] and sheep nasal mucosae [79-81] have all been investigated and used in vertical Franz's diffusion cell or Ussing chambers [69,82].

The choice of a particular model or animal species is usually based on the availability of the tissue rather than because of morphological, functional, or biochemical similarities of the model to the human nasal mucosa [82]

Agu and collaborators have extensively reviewed the use of nasal excised mucosa as *ex vivo* model for assessing nasal drug permeation and metabolism [82]. They concluded that a correlation between nasal drug absorption in human and animal *ex vivo* tissues is difficult due to different factors:

- Lack of mucociliary clearance, which *in vivo* limit the time of exposure of the drug to the mucosa [82].
- Lack of reproducibility of the deposition and formulation related aspects occurring *in vivo*. *In vivo* the formulation in form of fine droplets or powder

particles get in contact with the mucosa and only then the absorption take place, the local viscosity and concentration of active ingredient in contact to the mucosa are difficult to reproduce [82].

Although animal nasal mucosal tissues are useful *ex vivo* tools to study nasal formulations, there are some limitations to their use, related to the variability in the mucosal tissues such as their thickness, viability, integrity observed with specimens of different individuals or as a consequence of the excision procedures and differences related to the species of origin of the mucosae [69,82].

### **1.6.2 Cell Cultures- Primary cells and cell lines**

Another approach to study drug permeation is the use of cultures of primary human nasal epithelial cells.

Both Min-ki Lee and Jin-Wook Yoo have characterized nasal mucosal models for drug transport studies, culturing primary nasal cells obtained harvesting nasal human cells from the inferior turbinate during surgeries [83-85]. These models were obtained growing primary cells as Liquid Cover Culture (LCC) where, once the cell are seeded, on a cell insert, the cell layer is covered with liquid media.

Results of permeation studies of anti-allergic drugs suggest that human nasal epithelial culture models may be a useful *in vitro* tool for studying the passive transport processes for nasal drug delivery [86].

Ong and co-authors have characterized primary nasal epithelia cell cultures obtained from nasal brushing of the inferior turbinate, a minimally invasive technique that can be easily reproduced. They validated a nasal epithelium model



using Air Liquid Interface (ALI) cultures, where the apical surface of the cells is exposed to air after seeding them on a porous membrane cell insert. The main focus of this research was the characterization of the model in terms of barrier formation, using trans-epithelial electrical resistance (TEER), permeability to marker compounds, mucus production, morphology, cilia formation, and motility. In addition, this cell model was able to produce inflammatory mediator (interleukins) in response to different stimuli [15].

Despite the advantages of using cell models which produce viable cilia, mucus, tight junction and inflammatory mediators to investigate nasal drug absorption, these models have inherent problems.

Firstly, the sampling procedure can be in some cases quite invasive and purification of the specimen obtained can be complex [87,88]. Secondly, the expensive culture conditions, limited lifespan of the primary cells (up to passage four), the high risk of culture contamination due to cell origin and the prolonged period of culturing need for the model to be ready to perform permeation studies (up to 5 weeks after seeding on cell inserts) [15,89,90]. Reproducibility of the model due to inter- and intra-variability of the cell samples could also be an issue [87,88].

Another approach is the use of immortalized cell lines of animal or human origin. These cells can be purchased and the culturing costs are lower compared to primary cells [89]. Cells lines usually grow faster than primary cells, therefore studies can be completed sooner. In addition, these cell lines can be used for

multiple passages without losing their features, limiting inter-laboratory variability related to cultures differences, unlike for primary cells.

*In vitro* cell lines have their own drawbacks. For instance, the loss of some features of the original tissue cells, e.g. expression of certain proteins, reduction of interleukins and other cell signalling molecules production, absence of cilia, can occur as a consequence of the cell transformation leading to immortalization or after a high number of passages [89,90]. Furthermore, differences in culture conditions (e.g. different media supplement, presence or not of culturing antibiotics) can also have an impact on cell characteristics.

Calu-3 cell line, derived from human lung adenocarcinoma, has been extensively used over the past years as a well-established and functional *in-vitro* model of airways epithelium for the investigation of novel nasal formulation [85,89,91-96]. Despite being a suitable and well established model of the airways epithelium, the use of Calu-3 cells have raised questions if they represent a suitable model of the nasal mucosa. The TEER and paracellular marker permeability values have been shown to be different from human excised mucosa, with TEER values 2 – 3 times higher compared to those reported for human mucosa ( $90 -180 \Omega \cdot \text{cm}^2$ ). Similarly, values of apparent permeability coefficient ( $P_{app}$ ) for a paracellular marker such as sodium fluorescein (Flu-Na) were found to be at least 10 times higher than values reported in literature for excised human nasal mucosa [97,98].

The cell line RPMI 2650, originated from an anaplastic squamous cell carcinoma of the nasal septum [99], is a commercially available human nasal cell line which is widely used as *in vitro* model for nasal drug transport studies.

Evidence for the suitability of this cell line as *in vitro* nasal cell model for drug transport studies have been presented by Bai, Wengst and Reichel [97,100]. Their results showed that the conversion of RPMI 2650 cells from the classical liquid cover culture to the air liquid interface (ALI) conditions, more representative of the nasal physiology where the upper surface of the cells is exposed to air, was able to induce cell differentiation leading to the formation of a cell continuous monolayer suitable for permeation experiments [97,100]. Indeed, under these culture conditions cell production of tight junction proteins was observed. Moreover, TEER values as well as values of permeability to the paracellular marker Flu-Na attained values similar to those of excised human nasal mucosa [97,100].

On the other hand, culturing conditions have been shown to affect the cell culture posing an eventual problem for the use of this model. Indeed, Reichl has shown how differences in term of cell inserts (membrane polymer and porosity) and media supplements (such as foetal bovine serum; FBS) affect the development and tightness of the model [88]. These imply further validation of the RPMI 2650 nasal cell are needed to optimize culture condition.

Nevertheless, RPMI 2650 is undoubted one the most promising model for the nasal drug permeation studies. Additionally, being this model relatively recent, there are opportunities to further investigate this cell line as a relevant model of the nasal mucosa.

## 1.7 AIM OF THE STUDY

Developing a new product for nasal route requires, before any *in vivo* test, the selection of a promising drug for nasal administration, the development of a suitable formulation and the selection of a device for the delivery of the formulation to the nasal cavity. In fact, the nasal bioavailability will depend on the permeation of the drug through the nasal mucosa as well as from the deposition pattern of the formulation in the nasal cavity.

As previously stated, different model for deposition and permeation have been developed. However, it is missing a tool able to assess both of them simultaneously.

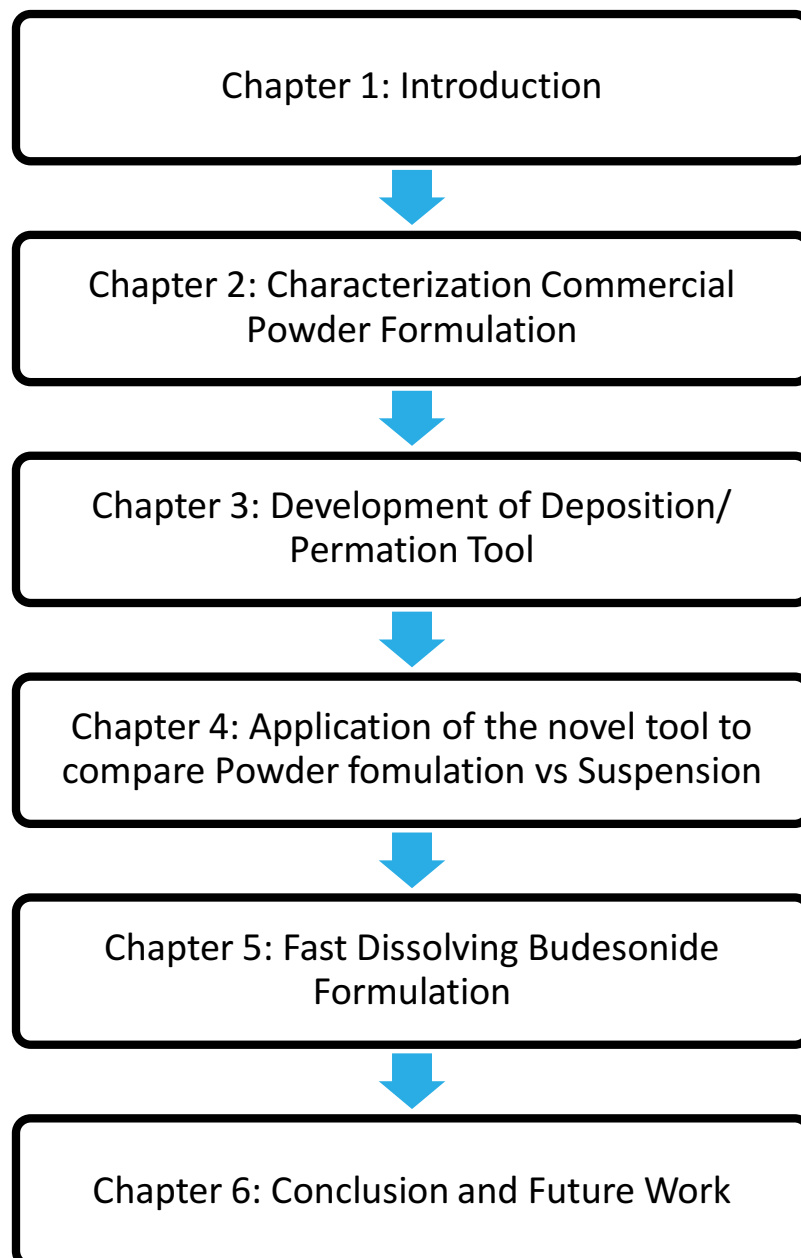
Hence, the primary aim of this study was to develop an apparatus able to perform deposition and permeation of nasal formulation at the same time, mimicking so the physiology of the process of drug administration occurring *in vivo*.

Secondly, demonstrate the usefulness of the novel apparatus by testing with it the performance of two different formulations (suspension and dry powder) of the same model drug.

Finally, after a full characterization of a commercial dry powder nasal product, the model of the nasal mucosa will be used to characterize a new formulation trying to overcome one of the major drawback of powder formulations of poorly soluble drugs, i.e. delayed dissolution.

## 1.8 STRUCTURE OF THE THESIS

Completion of the above research objectives was accomplished by carrying out a set of experiments presented in Chapter 2, 3, 4 and 5 as described below. Chapter one is a general introduction on nasal drug delivery, while Chapter 6 proposes a final conclusion and suggests future directions in this research field. The following diagram outlines the content of the chapter presented in this thesis aligning them to the research program.



Details of each chapter of the research program are also listed as follow:

*Chapter 1:*

- Overview of nasal anatomy
- General classification of commercial nasal products, special focus on liquid and powder dosage forms
- Outline analytical requirement to test nasal products
- Overview of nasal cast as deposition models
- Summary of absorption models for nasal drug delivery

*Chapter 2:*

- Overview of commercially available powder products and general knowledge on nasal powder formulation
- Full analytical characterization of a dry powder spray (Rhinocort, Teijin Pharma, Japan)

*Chapter 3:*

- RPMI 2650 cell culture on special cell inserts (Snapwell®)
- Optimization of the time of culture in terms of mucus production and barrier to permeation of substances
- Development of a 3D printed prototype (modified expansion chamber; MC) for the simultaneous nasal product deposition on cell and characterization of particle size
- Validation of the prototype with a commercial budesonide suspension

*Chapter 4:*

- Validation of the modified expansion chamber with a powder and a suspension product
- Evaluation of the deposition/ transport of the same active ingredient (beclomethasone dipropionate) from two different formulations (powder and suspension)
- Comparison between the innovative deposition/ transport method with traditional transport studies

*Chapter 5:*

- Application of solid amorphous dispersion to a poorly soluble drug (Budesonide) to overcome solubility issues in nasal drug delivery
- Characterization of dissolution properties and aerodynamic performances of the novel formulation
- Evaluation of deposition/ permeation profile across RPMI 2650 cell model
- Comparison of the novel formulation with a commercial suspension

*Chapter 6:*

- General conclusion and future works

## 1.9 REFERENCES

1. Birkhoff M, Leitz M, Marx D. Advantages of Intranasal Vaccination and Considerations on Device Selection. *Indian J. Pharm. Sci. India: Medknow Publications*; 2009;71:729–31.
2. Degenhard M, Gerallt W, Birkhoff M. Intranasal Drug Administration — An Attractive Delivery Route for Some Drugs, Drug Discovery and Development - From Molecules to Medicine. *InTech*; 2015. DOI: 10.5772/59468. Available from: <http://www.intechopen.com/books/drug-discovery-and-development-from-molecules-to-medicine/intranasal-drug-administration-an-attractive-delivery-route-for-some-drugs>
3. Bhise SB, Adhikrao Vyankatrao Yadav, Amelia Makrand Avachat, Malayandi R. Bioavailability of intranasal drug delivery system. *Asian j. pharm. (Online)*. 2008;2 (4):01–15.
4. Comfort C, Garrastazu G, Pozzoli M. Opportunities and Challenges for the Nasal Administration of Nanoemulsions. *Curr. Top. Med. Chem.* 2015;15:356–68.
5. Liu Y, Johnson MR, Matida EA, Kherani S, Marsan J. Creation of a standardized geometry of the human nasal cavity. *J. Appl. Physiol.* 2009;106:784–95.
6. Illum L. Nasal clearance in health and disease. *Journal of Aerosol Medicine.* 2006;19:92–9.
7. Suman JD. Current understanding of nasal morphology and physiology as a drug delivery target. *Drug Deliv. and Transl. Res. [Internet]*. 2013;3:4–15. Available from: <http://eutils.ncbi.nlm.nih.gov/entrez/eutils/elink.fcgi?dbfrom=pubmed&id=25787863&retmode=ref&cmd=prlinks>
8. Rygg A, Longest PW. Absorption and Clearance of Pharmaceutical Aerosols in the Human Nose: Development of a CFD Model. *Journal of Aerosol Medicine and Pulmonary Drug Delivery.* 2016;29:416–31.
9. Dahl R, Mygind N. Anatomy, physiology and function of the nasal cavities in health and disease. *Adv Drug Deliv Rev.* 2000 ed. 1998;29:3–12.



10. Harkema JR, Carey SA, Wagner JG. The nose revisited: a brief review of the comparative structure, function, and toxicologic pathology of the nasal epithelium. *Toxicol Pathol.* 2006;34:252–69.
11. Jones N, Rog D. Olfaction: a review. *The Journal of Laryngology & Otology.* Cambridge University Press; 1998;112:11–24.
12. Keck T, Leiacker R, Riechelmann H, Rettinger G. Temperature profile in the nasal cavity. *The Laryngoscope.* John Wiley & Sons, Inc; 2000;110:651–4.
13. Merkus F, Verhoef J, Schipper N, Marttin E. Nasal mucociliary clearance as a factor in nasal drug delivery. *Adv Drug Deliv Rev.* 1998;29:13–38.
14. Quraishi MS, Jones NS, Mason JD. The nasal delivery of drugs. *Clin Otolaryngol Allied Sci.* 1997 ed. 1997;22:289–301.
15. Ong HX, Jackson CL, Cole JL, Lackie PM, Traini D, Young PM, et al. Primary Air-Liquid Interface Culture of Nasal Epithelium for Nasal Drug Delivery. *Mol. Pharmaceutics.* 2016;13:2242–52.
16. Hirst RA, Jackson CL, Coles JL, Williams G, Rutman A, Goggin PM, et al. Culture of primary ciliary dyskinesia epithelial cells at air-liquid interface can alter ciliary phenotype but remains a robust and informative diagnostic aid. *PLoS ONE.* 2014;9:e89675.
17. Sahin-Yilmaz A, Naclerio RM. Anatomy and Physiology of the Upper Airway. *Proceedings of the American Thoracic Society.* 2011;8:31–9.
18. Jones N. The nose and paranasal sinuses physiology and anatomy. *Adv. Drug Deliv. Rev.* 2001;51:5–19.
19. Arora P, Sharma S, Garg S. Permeability issues in nasal drug delivery. *Drug Discov. Today.* 2002. 2002;7(18):967-75.
20. Ugwoke MI, Agu RU, Verbeke N, Kinget R. Nasal mucoadhesive drug delivery: background, applications, trends and future perspectives. *Adv. Drug Deliv. Rev.* 2005;57:1640–65.
21. Djupesland PG. Nasal drug delivery devices: characteristics and performance in a clinical perspective—a review. *Drug Deliv. and Transl. Res.* 2013;3:42–62.
22. Andersson M, Lindqvist N, Svensson C, Ek L, Pipkorn U. Dry powder inhalation of budesonide in allergic rhinitis. *Clin Otolaryngol Allied Sci.* 1993;18:30–3.

23. Agertoft L, Wolthers OD, Fuglsang G, Pedersen S. Nasal powder administration of budesonide for seasonal rhinitis in children and adolescents. *Pediatr Allergy Immunol.* 1993;4:152–6.
24. Benninger MS, Hadley JA, Osguthorpe JD, Marple BF, Leopold DA, Derebery MJ, et al. Techniques of intranasal steroid use. *Otolaryngol Head Neck Surg.* 2004 ed. 2004;130:5–24.
25. Li BV, Jin F, Lee SL, Bai T, Chowdhury B, Caramenico HT, et al. Bioequivalence for Locally Acting Nasal Spray and Nasal Aerosol Products: Standard Development and Generic Approval. *AAPS J.* 2013;15:875–83.
26. Laube BL. Devices for Aerosol Delivery to Treat Sinusitis. *Journal of Aerosol Medicine.* 2007;20:S5–S18.
27. Ghori MU, Mahdi MH, Smith AM. Nasal Drug Delivery Systems: An Overview. *Am J Pharmacol. Sci.* 2015;3 (5): 110-119
28. Hansen K, Kim G, Desai K-GH, Patel H, Olsen KF, Curtis-Fisk J, et al. Feasibility Investigation of Cellulose Polymers for Mucoadhesive Nasal Drug Delivery Applications. *Mol. Pharmaceutics.* 2015;12:2732–41.
29. Chudiwal SS, Dehghan MHG. Quality by design approach for development of suspension nasal spray products: a case study on budesonide nasal suspension. *Drug Dev. Ind. Pharm.* 2016;42:1643–52.
30. Trows S, Wuchner K, Spycher R, Steckel H. Analytical challenges and regulatory requirements for nasal drug products in europe and the u.s. *Pharmaceutics.* 2014;6:195–219.
31. Rosen PL, Palmer JN, O'Malley BW, Cohen NA. Surfactants in the management of rhinopathologies. *Am J Rhinol Allergy.* 2013;27:177–80.
32. Djupesland PG, Docekal P, Czech Migraine Investigators Group. Intranasal sumatriptan powder delivered by a novel breath-actuated bi-directional device for the acute treatment of migraine: A randomised, placebo-controlled study. *Cephalalgia.* 2010;30:933–42.
33. Kublik H, Vidgren MT. Nasal delivery systems and their effect on deposition and absorption. *Adv. Drug Deliv. Rev.* 1998;29:157–77.
34. Yang WH, Dolovich J, Drouin MA, Keith P, Haddon J, Jennings B. Comparison of budesonide Turbuhaler with budesonide aqua in the treatment of seasonal allergic rhinitis. Rhinocort Study Group. *Can. Respir. J.* 1998;5:455–60.

35. Alagusundaram M, Chengaiah B. Nasal drug delivery system-an overview. *Int. J. Res. Pharm. Sci.* 2010;1(4):454–65.
36. Djupesland PG, Skretting A. Nasal deposition and clearance in man: comparison of a bidirectional powder device and a traditional liquid spray pump. *Journal of Aerosol Medicine and Pulmonary Drug Delivery.* 2012;25:280–9.
37. Dayal P, Pillay V, Babu RJ, Singh M. Box-Behnken experimental design in the development of a nasal drug delivery system of model drug hydroxyurea: characterization of viscosity, in vitro drug release, droplet size, and dynamic surface tension. *AAPS PharmSciTech.* Springer-Verlag; 2005;6:E573–85.
38. Pennington J, Pandey P, Tat H, Willson J, Donovan B. Spray pattern and droplet size analyses for high-shear viscosity determination of aqueous suspension corticosteroid nasal sprays. *Drug Dev. Ind. Pharm.* 2008;34:923–9.
39. Pozzoli M, Rogueda P, Zhu B, Smith T, Young PM, Traini D, et al. Dry powder nasal drug delivery: challenges, opportunities and a study of the commercial Teijin Puvlizer Rhinocort device and formulation. *Drug Dev. Ind. Pharm.* 2016;42:1660–8.
40. Okuda M, Okamoto M, Nomura Y, Saito Y. Clinical study on beclomethasone dipropionate powder preparation (TL-102) in perennial nasal allergy. *Rhinology.* 1986.
41. Costantino HR, Illum L, Brandt G, Johnson PH, Quay SC. Intranasal delivery: Physicochemical and therapeutic aspects. *International Journal of Pharmaceutics.* 2007;337:1–24.
42. Kim J-E, Cho H-J, Kim D-D. Budesonide/cyclodextrin complex-loaded lyophilized microparticles for intranasal application. *Drug Dev. Ind. Pharm.* 2014;40:743–8.
43. Djupesland PG, Messina JC, Mahmoud RA. Breath powered nasal delivery: a new route to rapid headache relief. *Headache.* 2013;53 Suppl 2:72–84.
44. Russo P, Buttini F, Sonvico F, Bettini R. Chimeral agglomerates of microparticles for the administration of caffeine nasal powders. *J Drug Del Sci. Tech.* 2004.
45. Devalia JL, Prime D, Richards DH. Effect of Variable Inspiratory Flow Rate on the Performance of the Budesonide Rhinocort Turbuhaler™. *Clin Drug Investig.* Springer International Publishing; 2001;21:195–201.

46. Wetterlin K. Turbuhaler: a new powder inhaler for administration of drugs to the airways. *Pharm Res.* 1988;5:506–8.
47. Djupesland PG, Messina JC, Mahmoud RA. The nasal approach to delivering treatment for brain diseases: an anatomic, physiologic, and delivery technology overview. *Ther Deliv.* 2014;5:709–33.
48. Djupesland PG, Skretting A, Winderen M, Holand T. Bi-directional nasal delivery of aerosols can prevent lung deposition. *J Aerosol Med.* 2004;17:249–59.
49. U.S. Department of Health and Human Services, Food and Drug Administration, Center for Drug Evaluation and Research. Bioavailability and Bioequivalence Studies for Nasal Aerosols and Nasal Sprays for Local Action. 2003;1–37.
50. European Medicines Agency. Guideline on the Pharmaceutical Quality of Inhalation and Nasal Products; European Medicines Agency: London, UK, 2006; pp. 1–27.
51. Doub WH, Adams WP, Wokovich AM, Black JC, Shen M, Buhse LF. Measurement of drug in small particles from aqueous nasal sprays by Andersen Cascade Impactor. *Pharm Res.* 2012;29:3122–30.
52. Suman JD, Laube BL, Lin T-C, Brouet G, Dalby R. Validity of in vitro tests on aqueous spray pumps as surrogates for nasal deposition. *Pharm Res.* 2002;19:1–6.
53. Suman JD, Laube BL, Dalby R. Comparison of nasal deposition and clearance of aerosol generated by nebulizer and an aqueous spray pump. *Pharm Res.* 1999 ed. 1999;16:1648–52.
54. Azimi M, Longest PW, Hindle M. Towards Clinically Relevant In Vitro Testing of Locally Acting Nasal Spray Suspension Products. Dalby RN, Byron PR, Suman JD, Young PM, editors. *RDD Europe 2015.* 2015;1:121–9.
55. Illum L. Nasal drug delivery - recent developments and future prospects. *J Control Release.* 2012;161:254–63.
56. Newman SP, Pitcairn GR, Dalby RN. Drug delivery to the nasal cavity: in vitro and in vivo assessment. *Crit Rev Ther Drug Carrier Syst.* 2004;21:21–66.

57. Durand M, Pourchez J, Louis B, Pouget JF, Isabey D, Coste A, et al. Plastinated nasal model: a new concept of anatomically realistic cast. *Rhinology*. 2011;49:30–6.
58. Kundoor V, Dalby RN. Assessment of nasal spray deposition pattern in a silicone human nose model using a color-based method. *Pharm Res*. Springer US; 2010;27:30–6.
59. Kundoor V, Dalby RN. Effect of Formulation- and Administration-Related Variables on Deposition Pattern of Nasal Spray Pumps Evaluated Using a Nasal Cast. *Pharm Res*. 2011;28:1895–904.
60. Castile J, Cheng Y-H, Simmons B, Perelman M, Smith A, Watts P. Development of in vitro models to demonstrate the ability of PecSys®, an in situ nasal gelling technology, to reduce nasal run-off and drip. *Drug Dev. Ind. Pharm.* 2013;39:816–24.
61. Kaye RS, Purewal TS, Alpar OH. Development and testing of particulate formulations for the nasal delivery of antibodies. *J Control Release*. 2009;135:127–35.
62. Hughes R, Watterson J, Dickens C, Ward D, Banaszek A. Development of a nasal cast model to test medicinal nasal devices. *Proceedings of the Institution of Mechanical Engineers, Part H: Journal of Engineering in Medicine*. 2008;222:1013–22.
63. Shah SA, Dickens CJ, Ward DJ, Banaszek AA, George C, Horodnik W. Design of experiments to optimize an in vitro cast to predict human nasal drug deposition. *Journal of Aerosol Medicine and Pulmonary Drug Delivery*. 2014;27:21–9.
64. Coowanitwong I, de S, Somaraju S, Wu H, Mclaughlin K, Schoenbrodt T, et al. Regional Deposition of Beclomethasone Dipropionate Powder Exiting Puvlizer® in a Nasal Cast Connected to a Next Generation Impactor. Dalby RN, Byron PR, peart J, Suman JD, Young PM, editors. *RDD Europe 2011*. 2011;2:373–8.
65. Scherließ R, Trows S. Novel Formulation Concept for Particulate Uptake of Vaccines via the Nasal Associated Lymphoid Tissue. *Procedia in Vaccinology*. 2011;4:113–9.

66. Cheng YS, Holmes TD, Gao J, Guilmette RA, Li S, Surakitbanharn Y, et al. Characterization of nasal spray pumps and deposition pattern in a replica of the human nasal airway. *J Aerosol Med.* 2001st ed. 2001;14:267–80.
67. Xi J, Longest PW. Numerical predictions of submicrometer aerosol deposition in the nasal cavity using a novel drift flux approach. *International Journal of Heat and Mass Transfer.* 2008;51:5562–77.
68. Wadell C, Björk E, Camber O. Nasal drug delivery--evaluation of an in vitro model using porcine nasal mucosa. *Eur. J. Pharm. Sci.* 1999;7:197–206.
69. Wadell C, Björk E, Camber O. Permeability of porcine nasal mucosa correlated with human nasal absorption. *Eur. J. Pharm. Sci.* 2003;18:47–53.
70. Millotti G, Vetter A, Leithner K, Sarti F, Shahnaz Bano G, Augustijns P, et al. Development of thiolated poly(acrylic acid) microparticles for the nasal administration of exenatide. *Drug Dev. Ind. Pharm.* 2014;40:1677–82.
71. Fabrizio B, Giulia BA, Fabio S, Paola R, Gaia C. In vitro permeation of desmopressin across rabbit nasal mucosa from liquid nasal sprays: The enhancing effect of potassium sorbate. *Eur. J. Pharm. Sci.* 2009;37:36–42.
72. Russo P, Sacchetti C, Pasquali I, Bettini R, Massimo G, Colombo P, et al. Primary microparticles and agglomerates of morphine for nasal insufflation. *J. Pharm. Sci.* 2006;95:2553–61.
73. Balducci AG, Ferraro L, Bortolotti F, Nastruzzi C, Colombo P, Sonvico F, et al. Antidiuretic effect of desmopressin chimera agglomerates by nasal administration in rats. *Int J Pharm.* 2013;440:154–60.
74. Colombo G, Lorenzini L, Zironi E, Galligioni V, Sonvico F, Balducci AG, et al. Brain distribution of ribavirin after intranasal administration. *Antiviral Research.* 2011;92:408–14.
75. Zhang H, Prisinzano TE, Donovan MD. Permeation and metabolism of cocaine in the nasal mucosa. *Eur J Drug Metab Pharmacokinet.* 2012;37:255–62.
76. Richter T, Keipert S. In vitro permeation studies comparing bovine nasal mucosa, porcine cornea and artificial membrane: androstenedione in microemulsions and their components. *Eur J Pharm Biopharm.* 2004;58:137–43.
77. Tas C, Ozkan CK, Savaser A, Ozkan Y, Tasdemir U, Altunay H. Nasal absorption of metoclopramide from different Carbopol 981 based formulations: In

vitro, ex vivo and in vivo evaluation. *European Journal of Pharmaceutics and Biopharmaceutics* [Internet]. 2006;64:246–54. Available from: <http://eutils.ncbi.nlm.nih.gov/entrez/eutils/elink.fcgi?dbfrom=pubmed&id=16870409&retmode=ref&cmd=prlinks>

78. Bari NK, Fazil M, Hassan MQ, Haider MR, Gaba B, Narang JK, et al. Brain delivery of buspirone hydrochloride chitosan nanoparticles for the treatment of general anxiety disorder. *Int. J. Biol. Macromol.* [Internet]. 2015;81:49–59. Available from: <http://eutils.ncbi.nlm.nih.gov/entrez/eutils/elink.fcgi?dbfrom=pubmed&id=26210037&retmode=ref&cmd=prlinks>

79. Lindhardt K, Bagger M, Andreasen KH, Bechgaard E. Intranasal bioavailability of buprenorphine in rabbit correlated to sheep and man. *International Journal of Pharmaceutics.* 2001;217:121–6.

80. Shinde RL, Bharkad GP, Devarajan PV. Intranasal microemulsion for targeted nose to brain delivery in neurocysticercosis: Role of docosahexaenoic acid. *Eur J Pharm Biopharm.* 2015;96:363–79.

81. Alex AT, Joseph A, Shavi G, Rao JV, Udupa N. Development and evaluation of carboplatin-loaded PCL nanoparticles for intranasal delivery. *Drug Delivery.* 2015;:1–10.

82. Agu RU, Ugwoke MI. *In Situ and Ex Vivo Nasal Models for Preclinical Drug Development Studies. Drug Absorption Studies.* Boston, MA: Springer US; 2008. pp. 112–34.

83. Yoo J-W, Kim Y-S, Lee S-H, Lee M-K, Roh H-J, Jhun B-H, et al. Serially Passaged Human Nasal Epithelial Cell Monolayer for in Vitro Drug Transport Studies. *Pharmaceutical Research;* 2003;20:1690–6.

84. Lee M-K, Yoo J-W, Lin H, Kim Y-S, Kim D-D, Choi Y-M, et al. Air-liquid interface culture of serially passaged human nasal epithelial cell monolayer for in vitro drug transport studies. *Drug Delivery.* 2005;12:305–11.

85. Cho HJ, Termsarasab U, Kim JS. In vitro Nasal Cell Culture Systems for Drug Transport Studies. *Journal of Pharmaceutical Investigation.* 2010;40:321–32.

86. Lin H, Yoo J-W, Roh H-J, Lee M-K, Chung S-J, Shim C-K, et al. Transport of anti-allergic drugs across the passage cultured human nasal epithelial cell monolayer. *Eur J Pharm Sci.* 2005;26:203–10.

87. Dimova S, Brewster ME, Noppe M, Jorissen M, Augustijns P. The use of human nasal in vitro cell systems during drug discovery and development. *Toxicology in Vitro*. 2005;19:107–22.
88. Reichl S, Becker K. Cultivation of RPMI 2650 cells as an in-vitro model for human transmucosal nasal drug absorption studies: optimization of selected culture conditions. *J. Pharm. Pharmacol.* 2012 ed. 2012;64:1621–30.
89. Kim D-D. In Vitro Cellular Models for Nasal Drug Absorption Studies. *Biotechnology: Pharmaceutical Aspects*. 2008;Chapter 9 of a book:216–34.
90. Merkle HP, Ditzinger G, Lang SR, Peter H, Schmidt MC. In vitro cell models to study nasal mucosal permeability and metabolism. *Adv Drug Deliv Rev.* 2000 ed. 1998;29:51–79.
91. Wen Z, Yan Z, He R, Pang Z, Guo L, Qian Y, et al. Brain targeting and toxicity study of odorranalectin-conjugated nanoparticles following intranasal administration. *Drug Delivery*. 2011;18:555–61.
92. Zheng X, Shao X, Zhang C, Tan Y, Liu Q, Wan X, et al. Intranasal H102 Peptide-Loaded Liposomes for Brain Delivery to Treat Alzheimer's Disease. *Pharm Res* [Internet]. 2015;32:3837–49. Available from: <http://link.springer.com/10.1007/s11095-015-1744-9>
93. Ye Y, Xu Y, Liang W, Leung GPH, Cheung K-H, Zheng C, et al. DNA-loaded chitosan oligosaccharide nanoparticles with enhanced permeability across Calu-3 cells. *Journal of Drug Targeting*. 2013;21:474–86.
94. Cevher E, Salomon SK, Makrakis A, Li XW, Brocchini S, Alpar HO. Development of chitosan-pullulan composite nanoparticles for nasal delivery of vaccines: optimisation and cellular studies. *J Microencapsul.* 2015;32:755–68.
95. Wang S, Chow MSS, Zuo Z. An approach for rapid development of nasal delivery of analgesics--identification of relevant features, in vitro screening and in vivo verification. *Int J Pharm.* 2011;420:43–50.
96. Dalby R, Jin F. In Vitro Beclomethasone Dipropionate Dissolution and Uptake Rates from Nasal Suspensions Comprised of Differing Primary Drug Particle Sizes. *Respiratory Drug Delivery 2010*. 2010;:839–42.
97. Wengst A, Reichl S. RPMI 2650 epithelial model and three-dimensional reconstructed human nasal mucosa as in vitro models for nasal permeation studies. *Eur J Pharm Biopharm.* 2010;74:290–7.



98. Haghi M, Young PM, Traini D, Jaiswal R, Gong J, Bebawy M. Time- and passage-dependent characteristics of a Calu-3 respiratory epithelial cell model. *Drug Dev. Ind. Pharm.* 2010 ed. 2010;36:1207–14.
99. De Fraissinette A, Brun R, Felix H, Vonderscher J, Rummelt A. Evaluation of the human cell line RPMI 2650 as an in vitro nasal model. *Rhinology.* 1995 ed. 1995;33:194–8.
100. Bai S, Yang T, Abbruscato TJ, Ahsan F. Evaluation of human nasal RPMI 2650 cells grown at an air-liquid interface as a model for nasal drug transport studies. *J. Pharm. Sci.* 2007 ed. 2008;97:1165–78.

## CHAPTER 2

### *Characterization of a Commercial Powder Product*

This Chapter was published in *Drug Development and Industrial Pharmacy*, 42:1660–8 (2016) under the title “Dry powder nasal drug delivery: challenges, opportunities and a study of the commercial Teijin Puvlizer Rhinocort device and formulation”. Authours: Pozzoli M, Rogueda P, Zhu B, Smith T, Young PM, Traini D and Sonvico F. DOI: 10.3109/03639045.2016.1160110

## **2.0 PREFACE**

In Chapter 2 the advantages of nasal powder formulations and some of the test required to characterize nasal products are introduced. In this chapter, it was our interest to fully characterize Rhinocort<sup>®</sup> Teijin, one of the few marketed dry powder nasal products. The characterization was based on the analytical approach proposed by the US and European regulatory agencies in relevant guidelines (see Chapter 1). Furthermore, an overview of nasal products market was performed in order to contextualize this formulation under a clinical and commercial point of view.

## 2.1 ABSTRACT

**Purpose:** To discuss the challenges and opportunities for dry powder nasal medications and to put this in to perspective by evaluating and characterizing the performance of the Teijin- beclomethasone dipropionate dry powder nasal inhaler; providing a baseline for future nasal products development.

**Methods:** The aerosol properties of the formulation and product performance of Teijin powder intranasal spray were assessed, with a particular focus on particle size distribution (laser diffraction), powder formulation composition (confocal Raman microscope) and aerosol performance data (British Pharmacopoeia Apparatus E cascade impactor, aerosol laser diffraction).

**Results:** Teijin Rhinocort<sup>®</sup> (beclomethasone dipropionate, BDP) dry powder spray formulation is a simple blend of one active ingredient, BDP with hydroxypropylcellulose (HPC) carrier particles and a smaller quantity of lubricants (stearic acid and magnesium stearate). The properties of the blend are mainly those of the carrier ( $Dv_{50} = 98 \pm 1.3 \mu\text{m}$ ). Almost the totality of the capsule fill weight (96.5 %) was emitted with 8 actuations of the device. Using the pharmacopeia suggested nasal chamber deposition apparatus attached to an Apparatus E impactor. The BDP main site of deposition was found to be in the nasal expansion chamber ( $90.2 \pm 4.78 \%$ ), while  $4.64 \pm 1.38 \%$  of the BDP emitted dose was deposited on Stage 1 of the Apparatus E.

**Conclusions:** The Teijin powder nasal device is a simple and robust device to deliver pharmaceutical powder to the nasal cavity, thus highlighting the robustness of intranasal powder delivery systems. The large number of actuations needed to deliver the total dose (eight) should be taken in consideration when compared to aqueous sprays (usually 2 actuations), since

this will impact on patient compliance and consequently therapeutic efficacy of the formulation.

## 2.2 INTRODUCTION

The diminishing success rate in bringing new chemical entities to market has led pharmaceutical companies to focus their efforts on identifying new uses for existing drugs, including the development of alternative routes of administration. As a result, nasal drug delivery has emerged as an increasingly viable delivery technology. A number of publications on the development of nasal dry powder formulations for immunization, delivery of peptides and proteins as well as small molecules can be found in the literature [1-3]. This indicates a renewed interest from industry and academia in this area of research. Although nasal delivery is a well-established drug delivery route, surprisingly there are no dry powder nasal delivery systems marketed neither in Europe (EU) nor the United States (US). Globally, only three nasal dry powder inhalers are available on the market for local treatment: Rhinocort Turbuhaler<sup>®</sup> (Budesonide) marketed by AstraZeneca in Canada, Rhinocort Puvlizer<sup>®</sup> (beclomethasone dipropionate, BDP) by Teijin Japan (Figure 2.1), and Erizas<sup>®</sup> (dexamethasone cipeclate), recently launched by Nippon Shinyaku in Japan (Table 2.1). All these products are indicated for the treatment of rhinitis. Both the Japanese products are capsule-based, although using two different devices; while the AstraZeneca product uses a multi-dose breath-actuated prefilled device that is already in use for pulmonary administration of orally inhaled products. The Teijin BDP medicinal product can be used with either dry powder Rhinocort<sup>®</sup> capsules for nasal delivery or with Salcoat<sup>®</sup> capsules to be administered in the oral cavity, both containing BDP [4]. The nasal powder product (Rhinocort<sup>®</sup>) was launched in December 1986 in Japan, but is not currently available in the EU or in US. It is approved for both allergic and vasomotor rhinitis. The recommended dose is one capsule of 50 µg

in the nasal cavity twice daily, after waking up and just before bedtime, eight actuations are required to empty one capsule. Teijin Nasal Spray package comprises the device and a selection of 100, 500 or 700 unit capsules (hard gelatin capsules No. 2 color-coded white and blue). Ten capsules are contained in a blister and 10 blisters are wrapped together in a sealed aluminium pack. The Puvlizer<sup>®</sup> device can also be purchased on its own (Figure 2.1).

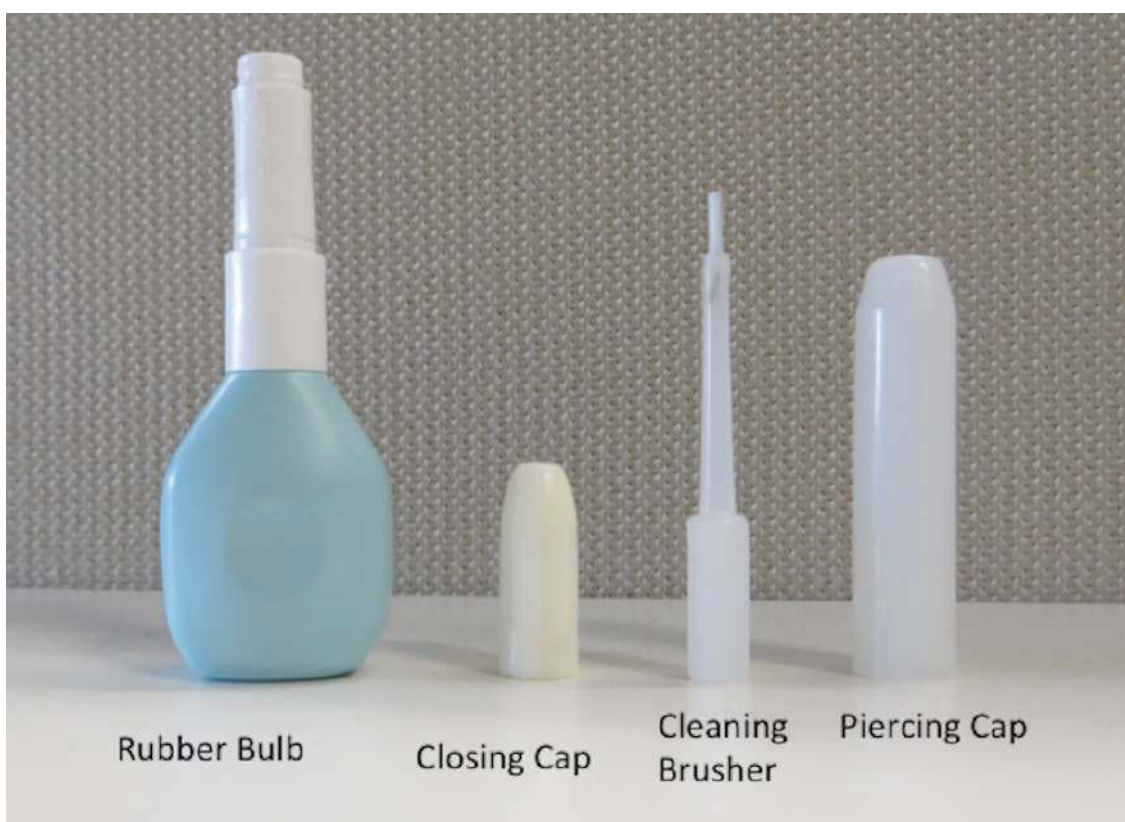


*Figure 2.1. Disassembled Teijin Puvlizer device with accessories*

In Europe, the current UK market for the treatment of rhinitis accommodates 3 generic versions of BDP in the form of nasal sprays: Nasobec (Teva, UK), Boots Blocked Nose Relief (The Boots Company Plc, UK) and Beconase (Omega Pharma Ltd, UK); all three are suspensions delivering 50 µg of drug for twice a day administration; usually morning and evening.

Nasal drug delivery is usually achieved with liquid aerosol sprays delivering solutions or suspensions. A quick review of the marketed nasal delivery products in the UK shows that out of the 53 over-the-counter and prescription products listed on the Electronic Medicines Compendium ([www.Medicines.org.uk](http://www.Medicines.org.uk), accessed January 2015), 3 are semisolids (Naseptin<sup>®</sup>, Alliance Pharmaceutical, chlorhexidine neomycin cream; Bactroban<sup>®</sup>, GSK, mupirocin ointment and Happinose Nasal Decongestant Balm<sup>®</sup>, Diomed Developments Limited, levomenthol ointment), 4 are nasal drop products (Ephedrine Nasal Drops, Thorton & Ross Ltd and Otrivine<sup>®</sup> xylometazoline HCl Nasal Drops, Novartis Consumer Health both in two dosages: adult and child), while the remaining 46 are liquid nasal sprays (15 suspensions vs. 31 solutions).



Table 2.1. Summary of nasal dry powder products and water-based alternatives marketed in U.K.

<b>Nasal Dry Powder</b>				
Product	Drug	Dosage	Features	Company/Country
Erizas Capsule	Dexamethasone cipeclate	400µg capsule	-First once daily dry powder type steroid nasal spray in Japan -Double nostril device -NO preservative, Less local irritation and NO dripping off from nasal cavities -Lactose hydrate is used as an additive	Nippon Shinyaku / Japan
Erizas Nasal Powder	Dexamethasone cipeclate	200µg 28 metered spray	-Once daily treatment, one spray per nostril -NO preservative, less local irritation and NO dripping off from nasal cavities -Lactose hydrate is used as an additive -NO Capsule	Nippon Shinyaku / Japan
Rhinocort Turbohaler®	Budesonide	100 µg 200 doses	-Treatment of rhinitis in both Child and Adults (400µg daily dosage), once daily application (2 per each nostril in the morning) -Treatment or Prevention of Nasal Polyps: One application (100 µg) into each nostril, morning and evening (total daily dose 400 µg) -NO additives or carrier substances are included	AstraZeneca / Canada
Puvlizer Rhinocort®	Beclometasone dipropionate	50µg Capsule	-Initially Marketed in December 1986 -Allergic rhinitis and vasomotor rhinitis -Additives: Hydroxypropylcellulose, Magnesium stearate, Stearic acid -One capsule each is sprayed into the nasal cavity, twice daily	Teijin Pharma Limited / Japan
<b>Water Based Spray Alternatives (UK Market)</b>				
Product	Drug	Dosage	Features	Company
Beconase Aqueous Nasal Spray	Beclometasone dipropionate monohydrate	50µg spray	-Suggested posology: 2 Sprays in each nostril, twice a day (morning and evening) -Contain Benzalkonium Chloride and Phenethyl alcohol	GlaxoSmithKline UK
Nasobec	Beclometasone dipropionate	50µg spray	-Suggested posology: 2 Sprays in each nostril, twice a day (morning and evening) -Contain Benzalkonium Chloride and Phenethyl alcohol	Teva UK
Boots Hayfever Relief	Beclometasone dipropionate	50µg spray	-Suggested posology: 200 to 400 µg/day -Contain Benzalkonium Chloride and Phenethyl alcohol	THE BOOTS COMPANY
Budesonide Aqueous Nasal Spray	Budesonide	64 µg 50µl spray	-Suggested initial posology: 256 µg per day, once or twice a day -Contain Ascorbic acid E300 and Disodium Edetate	Sandoz Limited
Rhinocort Aqua® 64 micrograms	Budesonide	64 µg 50µl spray	-Treatment of rhinitis 256 µg per day, once or twice a day -Treatment Nasal Polyps 256 µg per day twice a day -Contain Disodium Edetate -Shelf life: Use within 2 months of starting treatment	AstraZeneca UK Limited

The total volume of the nasal cavity ranges from 13 mL to 20 mL [5], allowing for a maximum delivery of 20 mg of powder [6-9]. Nasal deposition tends to be limited to the outer vestibule of the nasal cavity, following three mechanisms: impaction (primary factor), sedimentation and diffusion (related to olfaction). Deposition and subsequent absorption through the nasal mucosal surface are in competition with a series of mechanisms contributing to drug elimination from the nasal cavity such as physical clearance, mucociliary clearance and enzymatic metabolic activity. As a consequence, exposure and retention of the molecules to the nasal cavity is limited. The act of sniffing is said to enhance the diffusional deposition, particularly relevant for submicron particles deposition, by increasing the airflow rate and changing it from continuous to pulsatile [5]. Kaye *et al.* studied the powder deposition patterns in the nasal cavity with the Aptar Unit Dose Powder (UDP) device and found that 60 to 70% of the delivered dose was deposited no further than the nasal vestibule. The remaining 30–40% was deposited into deeper compartments of the nasal cavity [3].

The particle size required for efficient nasal delivery is above 10  $\mu\text{m}$ , i.e. cascade impactor induction port cut off point. A recent work by Schroeter and Kimbell indicated that particles above 20  $\mu\text{m}$  deposit fully in the nasal passageways, with lower sizes starting to deposit further down in the respiratory tract and only 15% of 1  $\mu\text{m}$  particles deposited in the nasal cavity [10].

The advantages of intranasal powder formulations include increased chemical stability (solid state stability), no requirement for small particles size (anything above 20  $\mu\text{m}$  can be delivered), no requirement for preservatives, no need for cold chain storage, possibility to formulate water insoluble compounds and increased bioavailability compared to liquid formulations [1-3,11]. This has been

demonstrated in a study by Ishikawa *et al.* whereby powder formulations were found to improve nasal bioavailability of elcatonine polypeptide when blended with a carrier such as CaCO<sub>3</sub>, talc, barium sulfate or ethyl cellulose [2,12]. This opened up the use of nasal formulation for systemic delivery of peptides and proteins. The increased bioavailability obtained by using an insoluble powder carrier, such as CaCO<sub>3</sub>, was due to the increase in residence time available for absorption in the nasal cavity, slowing drug elimination from the absorption site, facilitating permeation of the drug across the nasal epithelium [4,12]. However, further studies on transmucosal permeation are still needed to elucidate how insoluble powders contribute to nasal absorption enhancement. Colombo *et al.*, have proved that ribavirin has higher absorption, through rabbit nasal mucosa, when it was delivered as powder form instead of solution. This highlights possible future uses of powder in the nasal drug delivery and the brain targeting through this route [13].

Another important aspect to investigate in order to obtain an efficient deposition of the formulation in the nasal cavity is the choice of the delivery device. As already mentioned above, there are several devices available, however these technologies are at different stages of development, with some already used in clinical trials (Trivair, OptiNose Bidirectional device) while others at the development stage or only existing as blueprints [5,14]. Some of these devices rely on the inspiration effort of the patient in order to aerosolize the powder; while others, like the Puvlizer, requires a mechanically generated airflow, supplied by a squeeze bottle or a pump activated by the user. The Trivair [3,6-8] and the Optinose device [1,5,15] are unique technologies since they rely on the patient's own insufflation to propel the powder up the nasal cavities. In a way, these

devices can be described as breath actuated devices, and provide the additional advantage of minimizing lower airways deposition as a consequence of soft palate elevation isolating the nasal cavity [3,5,16].

According to the Food and Drug Administration (FDA) Guidance, the characterization of nasal droplet size distribution can be evaluated by either laser diffraction or cascade impaction (CI), with an additional 2 L expansion chamber [3,17]. However, neither methods are representative for investigating real time drug deposition in the nasal cavity.

As for the flow rate to be used during testing, 0 and 15 L/min are often quoted, [3,18] although nasal inspiratory flows can be much higher than this. More realistic peak nasal inspiratory flow should be 126-143 L/min for male adults and 104-122 L/min for female adults [19]. These values are lower for children [10,20] and should take into account ethnic differences [4,11].

As part of an ongoing study, the aim of this investigation was to investigate the physico-chemical properties and formulation attributes of a commercial dry powder intranasal product, Teijin Rhinocort<sup>®</sup> with a view to understanding how we may improve formulation of nasal dry powders and provide a baseline for future nasal products.

## 2.3 MATERIALS AND METHODS

Beclomethasone dipropionate (BDP) dry powder nasal device (Rhinocort<sup>®</sup>, batch # 9091) was obtained from Teijin Pharma Ltd. (Tokyo, Japan). Water used in the analyses was purified by reverse osmosis (MilliQ, Millipore, France). All solvents were obtained from Chem-Supply (South Australia, Australia) and were of HPLC grade.

### 2.3.1 The Puvlizer<sup>®</sup> device

The Puvlizer<sup>®</sup> is a single dose, capsule-based, patient operated device (Figure 2.1). The overall length of the device is 10.5 cm, similar to other classic nasal spray devices for liquid formulations. The device is made of two parts, a stem in which the Rhinocort<sup>®</sup> capsule is placed and pierced with the needle set in the cap, and the lower part of the device, which is a soft plastic bulb that can be squeezed to provide an air flow able to propel the powder from the capsule through the stem into the nasal cavity. Holes are punctured at both ends of the capsule and the forced airflow pass through the holes of the capsule, aerosolizing the medication. The rubber bulb dimensions are 3.7 cm height by 2 cm width. The length of the nasal applicator on top of the rubber ball is 6.8 cm. The activation of the device is performed in 9 steps. Five steps for the device setting, and four steps for the delivery to the nasal cavity, as shown in Table 2.2. To empty the content of the capsule fully, it is recommended to squeeze the rubber ball and inhale 4 times in each nostril, for a total of 8 inhalation acts.

*Table 2.2. Summarized Steps for the device preparation and administration of Teijin Rhinocort®*

Device Preparation	Delivery Steps
<ul style="list-style-type: none"> <li>• Pull off the large cap and twist off the small cap.</li> <li>• Place the capsule in the small cap.</li> <li>• Reaffix the small cap onto the rubber bulb.</li> <li>• Place large cap in its original position to pierce other end of capsules.</li> <li>• Remove the large cap to complete the preparation for spraying.</li> </ul>	<ul style="list-style-type: none"> <li>• Squeeze rubber bulb to spray medication into nasal cavity while inhaling through the nose.</li> <li>• Spray alternatively in each cavity.</li> <li>• Remove capsule from device.</li> <li>• Clean the device with the brusher</li> </ul>

The device can be dismantled in 3 parts (Figure 2.1): rubber bulb (pale blue color), small cap (cream color), large cap (white color, with piercing needle inside). Additionally a cleaning brush is provided, as well as a disposal bag. No special indications are given for the storage of the device, nor timing for its replacement. The device is packaged in a cardboard box, with the capsules and an extra plastic bag to carry the device with no extra moisture protection.

## 2.3.2 Physico-chemical characterization

### 2.3.2.1 Powder bulk and tapped density

For the bulk density, the content of 21 Rhinocort<sup>®</sup> capsules was accurately weighed (29.6mg each capsule) and emptied into a 5 mL graduated cylinder with an internal diameter of 5mm. The volume occupied by the powder was recorded to calculate the bulk density. The container was tapped for 30 min and the new volume reading was used to calculate the tapped density value of the powder. The tapping has been carried out manually with an amplitude and frequency of 2-5 mm and 1 tap/sec respectively. The bulk volume was measured at the beginning of the experiment and tapped volume values recorded every 10 minutes. No significant variation was observed between 20 and 30 minutes. The Carr index (CI) was calculated according the following formula, where  $V_b$  was the bulk volume and  $V_f$  was the volume after tapping. Values below 15 are considered with good flow characteristic, while over 25 powders are considered with poor flowability [21-23].

$$CI = \frac{(V_b - V_f)}{V_b} \cdot 100$$

### 2.3.2.2 Dynamic Vapor Sorption

In order to investigate the behavior of the formulation in response to different degrees of humidity, a dynamic vapor sorption (DVS) study was performed. In brief, ca. 20 mg of powder from one Teijin Rhinocort capsule was weighed into a stainless sample pan and placed in the sample chamber of the DVS analyzer (DVS Intrinsic, Particulate Systems, London, UK). The powder was exposed to two 0-90% relative humidity (RH) cycles at 25 °C with 10% RH increment steps

triggered when the sample reached the equilibrium. The equilibrium moisture content at each target RH level was determined when a weigh change rate lower than 0.002%/min was recorded.

#### 2.3.2.3 *Specific Surface Area*

The Brunauer–Emmett–Teller (BET) method was used to determine the specific surface area of the samples, using a Gemini VII apparatus (Micromeritics, Norcross, USA). Measurements were carried out on 300 mg of the powder from ten capsules, after a 24-hour degassing step at 30°C under vacuum (VacPrep 061, Micromeritics, Norcross, USA). Measurements were performed in triplicate.

#### 2.3.2.4 *Particle Size Distribution by Laser Diffraction*

The Mastersizer 3000 equipped with dry dispersion feeder unit Aero S (Malvern Instrument, UK) was used to measure the particle size of the powder by laser diffraction. The content of a single capsule was emptied into the hopper of the feeder and dispersed with a pressure of 4 bar, the total time of analysis was set at 10 seconds. In order to use the Mie theory to convert light scattering data to particle size values, experimental parameters such as refraction index and density of particles were set at 1.5 and 1, respectively, as suggested for standard opaque particles by the manufacturer [24]. Measurements were carried out in triplicate.

#### 2.3.2.5 *Scanning electron microscopy*

Scanning electron micrographs (SEM) of the Teijin powder samples were conducted using a Zeiss Ultra plus field emission scanning electron microscope



(FESEM, Zeiss GmbH, Germany) operated at 4 kV. Prior to imaging, samples were mounted on carbon sticky tabs and platinum-coated to ~10 nm thickness using a sputter coater (Edwards E306A Sputter coater, UK)

#### 2.3.2.6 *Scanning Raman Spectroscopy*

An inVia Raman microscope (Renishaw, UK), equipped with a 532 nm diode laser, was used to collect individual Raman reference spectra from the single components and Raman images data from the powder mixture.

The capsule powder was flattened onto a glass microscope slide to provide a nominal flat and levelled powder surface. Raman images were generated from 200,000 spectra collected using a step size of 3  $\mu\text{m}$ . The Raman images were used to show the relative location of each core species within the formulation, using previously collected reference spectra from pure materials.

Direct Classical Least Squares Method (DCLS) was used to produce the Raman images from over 70,000 spectra collected in roughly 1 hour. The images were then combined to enable comparison between the relative locations of the BDP and other components of the nasal powder.

The streamline image data were processed to remove cosmic ray features using a nearest neighbor approach with the WiRE 3.3 software (Renishaw, UK). The combined image shows green features as BDP, red magnesium stearate and blue HPC carrier particles.

### 2.3.3 Analytical Characterization

#### 2.3.3.1 *BDP quantification using HPLC*

The amount of active ingredient in each sample was determined using a high performance liquid chromatography (HPLC) system equipped with a SPD-20A UV-VIS detector (Shimadzu, Tokyo, Japan). A Novapack C18 column (150 X 3.9 mm, 4  $\mu\text{m}$ , Waters, Australia) was used with a mobile phase methanol/water 80:20 v/v. The flow rate was set at 1 mL/min and BDP was detected at  $\lambda = 243\text{nm}$ . The retention time of BDP was found to be between 7.5 and 8 minutes. Standards were prepared in the mobile phase, and 100  $\mu\text{L}$  injected in order to obtain a calibration curve which linearity was measured between 0.1  $\mu\text{g}\cdot\text{mL}^{-1}$  and 50  $\mu\text{g}\cdot\text{mL}^{-1}$ .

#### 2.3.3.2 *Dose Content Uniformity*

The dose content uniformity of the Rhinocort<sup>®</sup> formulation was determined as an average of three measurements. For each measurement, the powder contained in one capsule was dissolved in 10 mL of methanol. The solution was filtered using nylon filters (0.45  $\mu\text{m}$ , Sartorius, Australia) and samples collected for quantification by HPLC. The compatibility between the filter and the drug was assessed. No statistical difference in the BDP amount was found whether the solutions were filtered or not.

#### 2.3.3.3 *Shoot Weight and BDP Content*

The device was weighed after the capsule was placed inside and after each actuation. The device was positioned at 30° and the emitted powder was collected in a 15 mL centrifuge tube. In order to determine the amount of BDP

emitted after each actuation, 5 mL of a mixture of methanol water (80:20) were added to the container; subsequently the tubes were shaken, vortexed and sonicated for about 30 min. The analyses were conducted in triplicate and the amount of BDP was determined through the HPLC method previously described. The emitted BDP (%) was calculated from the ratio between the emitted mass of BDP for a certain actuation and the mass of powder emitted for the same actuation. The emitted dose fraction (%) was calculated from the ratio of mass of BDP emitted and the dose of drug contained in one capsule.

### **2.3.4 Aerosol performance of Teijin Rhinocort<sup>®</sup>**

#### *2.3.4.1 Cascade impaction*

The aerodynamic performance of the Rhinocort<sup>®</sup> formulation delivered via the Puvlizer device was assessed using a cascade impactor, British Pharmacopoeia apparatus E (Westech W7; Westech Ltd., UK) equipped with a 2 L glass expansion chamber according to the Food and Drug Administration (FDA) guidance [2,12,17,25-27]. The expansion chamber is a 2 L single-neck round-bottomed flask with 1 cm inlet hole at 30° angle from the neck axis (Figure 2.2).

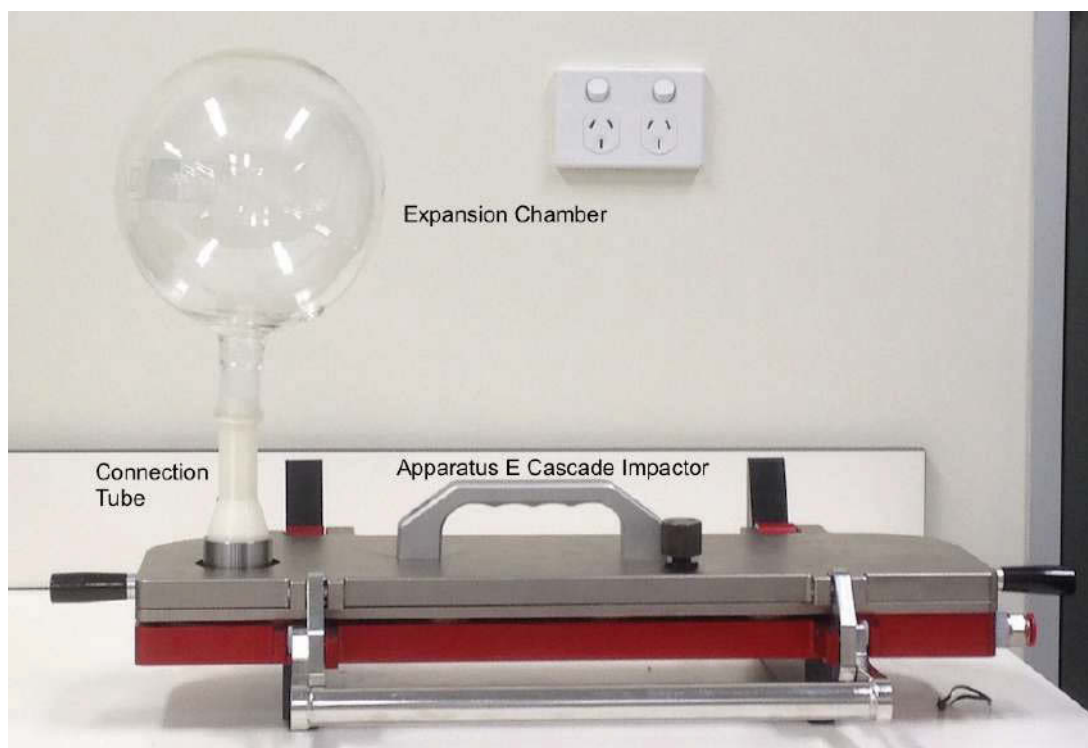


*Figure 2.2. Apparatus E system used for the aerosol performance of the Teijin nasal powder device equipped with the nasal expansion chamber.*

The Teijin device was connected to the inlet of the expansion chamber and the test was performed actuating the device 8 times for each capsule with airflow of 15 L/min calibrated using a flow meter (Model 3063; TSI Inc., MN, USA). For each test, 3 capsules were used to ensure an API concentration above detection limit of the HPLC method in the Apparatus E stages. Each Apparatus E stage was washed with the following volumes of a washing solution 80:20 methanol/water: expansion chamber 25 mL; capsules, connection tube, first and final stage 10 mL each; device and all other stages 5 mL. BDP amount in each sample was assayed using the HPLC method described above. Experiments were carried out in triplicate.

The emitted fraction (EF) was calculated as the total amount of drug emitted from the device (i.e. the sum of drug deposits on the chamber, connection tube and impactor stages) divided by the nominal dose (50µg/capsule).

#### 2.3.4.2 *In-line In Vitro Aerosol Laser Diffraction Analysis*

In order to measure the particle size distribution of the emitted powder from the Teijin device, laser diffraction was used (Spraytec, Malvern Instrument, UK). The device was placed at 2.5 cm from the measurement cell, at a fixed angle of 30° using an extraction flow rate of 15 L/min in order to mimic the *in vivo* drug administration. The analysis was performed for 10 seconds with an acquisition rate of 2.5 kHz. A total of three capsules were analyzed. For each, minimum of 6 puffs were measured in order to completely empty the device. In order to measure the particle size, using the Mie theory, values of refraction index 1.5 and 1 as density value for particles were used, respectively [24].

## **2.4 RESULTS AND DISCUSSION**

The regulatory requirements to characterize nasal products are well documented [6,17]. These include: i) Single actuation through container life, ii) Droplet size distribution by laser diffraction, iii) Drug in small particle/droplets, or particle/droplet size distribution by cascade impactor, iv) Drug particle size distribution by microscopy, v) Spray pattern vi) Plume geometry, and vii) Priming and re-priming. The particle size range to be studied is above 10  $\mu\text{m}$ , for which current impactors are not suited.

### **2.4.1 Physicochemical characterization of the formulation**

The formulation is composed of 50  $\mu\text{g}$  of BDP in a  $28.8 \pm 0.4$  mg powder blend containing hydroxypropylcellulose (HPC), magnesium stearate and stearic acid (0.5-1 % of the formulation). The original formulation is protected by a Japanese, US and EU patent [14,28-31]. Furthermore the formulation is a powder blend of large excipient particles with BDP, as shown by the SEM on Figure 2.3. The main dimension of the particles is typically 100  $\mu\text{m}$ , corresponding to HPC particles, and irregular in shape.

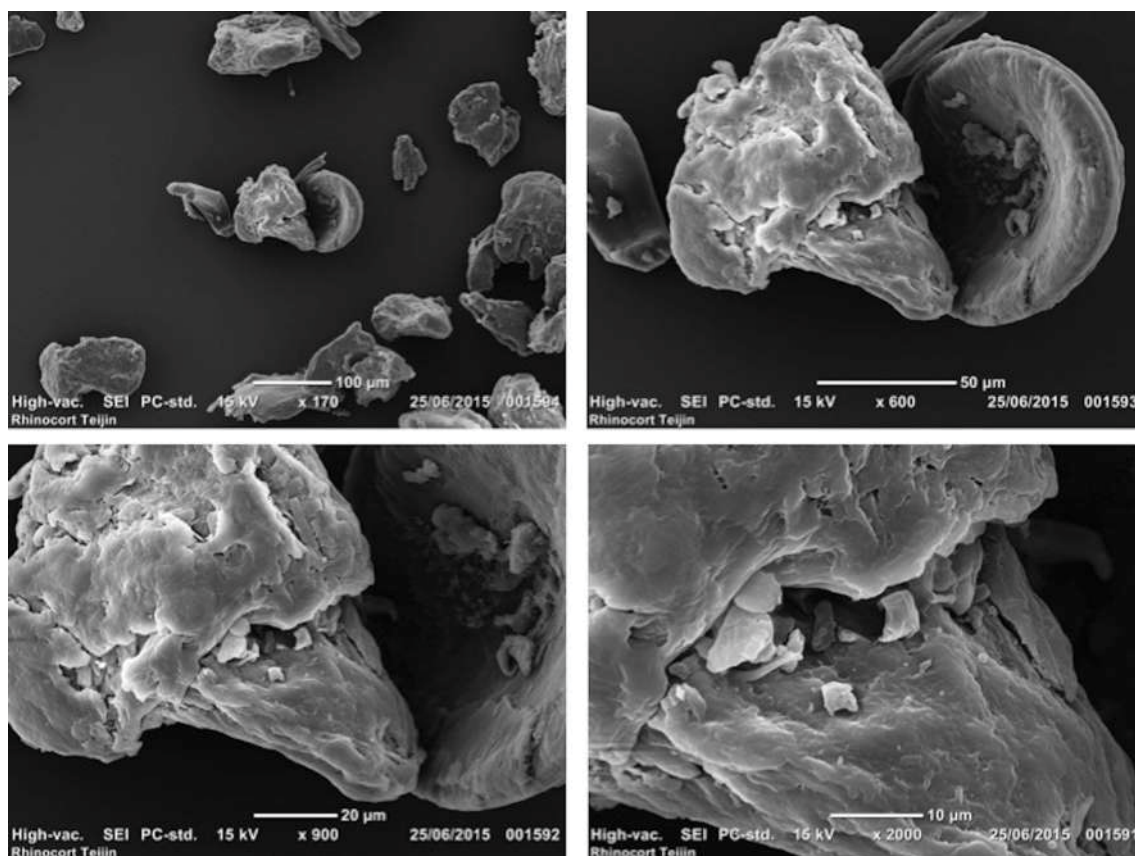


*Figure 2.3. SEM micrographs of the Teijin Rhinocort powder blend.*

The capsule content uniformity, as measured by HPLC, showed an average of  $48.11 \pm 2.75 \mu\text{g}/\text{capsule}$  of BDP. The bulk density of the powder was found to be  $0.564 \pm 0.004 \text{ g}/\text{cm}^3$ , and the tapped density was  $0.621 \pm 0.003 \text{ g}/\text{cm}^3$ , these values provide a Carr's index of 9 implying that the powder has good flowability properties. [22,23] As shown in Table 2.3, the amount of BDP emitted after each one of the eight actuations is never constant nor a decreasing trend can be described. Usually the first actuations release the highest amount of drug (and % of dose), and already seven of the eight actuations required are sufficient to deliver almost the totality of the dose. The same fluctuating trend is observed for the amount of powder emitted, this highlights how improvements on this type nasal powder device are needed, when compared to the liquid pumps that deliver

always the same amount of drug solution/suspension after each spray. The same trend was observed for the other two parameters.



Table 2.3. Amount of Powder (mg) and BDP ( $\mu\text{g}$ ) emitted after each actuation ( $n=3 \pm \text{StDev}$ )

	Actuation 1	Actuation 2	Actuation 3	Actuation 4	Actuation 5	Actuation 6	Actuation 7	Actuation 8
Emitted Powder (mg)	8.27 $\pm$ 0.83	4.23 $\pm$ 2.51	3.73 $\pm$ 1.17	3.77 $\pm$ 1.39	6.17 $\pm$ 4.02	2.03 $\pm$ 0.67	1.20 $\pm$ 0.35	0.07 $\pm$ 0.11
Emitted BDP ( $\mu\text{g}$ )	9.82 $\pm$ 1.89	7.76 $\pm$ 3.62	6.16 $\pm$ 1.49	6.74 $\pm$ 1.28	8.52 $\pm$ 4.09	3.90 $\pm$ 0.98	2.97 $\pm$ 1.36	0.83 $\pm$ 1.45
Emitted BDP (%)	0.12	0.18	0.17	0.18	0.14	0.19	0.25	1.25
Emitted Dose								
Fraction (%)	20.7	16.3	13.0	14.2	17.9	8.2	6.3	1.7

The interaction between the formulation and ambient environment (i.e. moisture) during use and storage is an important aspect to evaluate long-term stability and spray performances due to the possibility of powder cohesion and increased retention of powder in the device with consequent reduced emitted dose. [32]

Dynamic Vapor Sorption was used in order to gain a better understanding of the behavior of the powder at different relative humidity (RH) values. Figure 2.4 shows the moisture sorption isotherm (two cycles, sorption and desorption) for Rhinocort<sup>®</sup> formulation. The powder adsorbed roughly 20% w/w of moisture from 0 to 90% RH. The vapor sorption profile is comparable to reported values in literature for HPC over the same humidity range, which is the main component of the formulation and is similar to an isotherm type III, characteristic of not porous, or possibly macro-porous materials with low energy of adsorption [33-36].

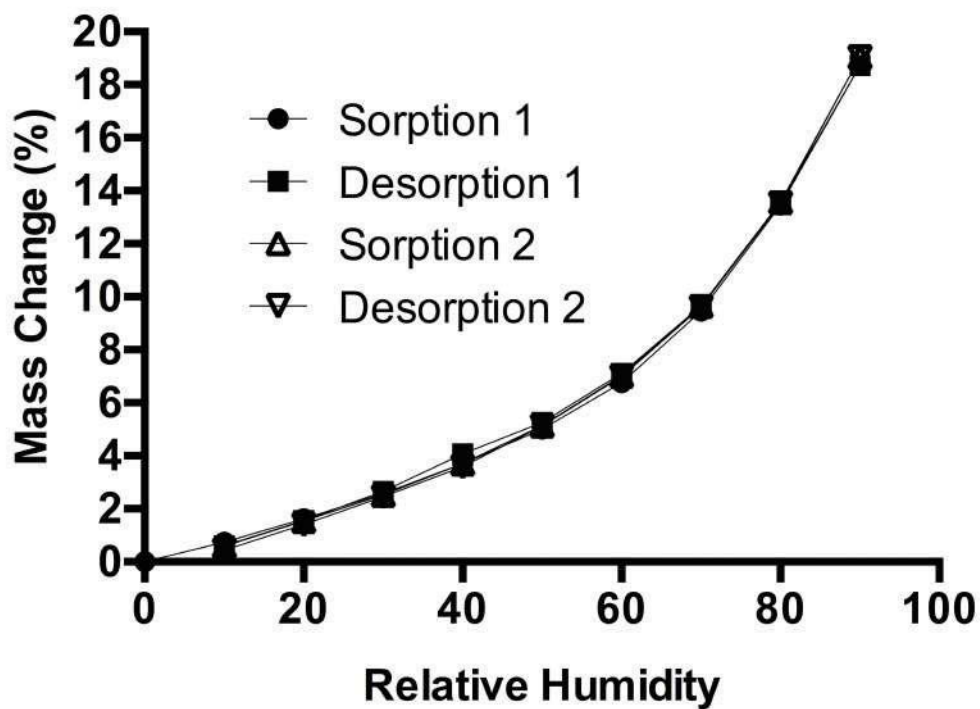


Figure 2.4. Dynamic vapor sorption isotherm (two cycles) of Rhinocort Teijin Powder.

There were no significant differences between two subsequent adsorption cycles, both cycles being completely reversible, suggesting moderate hygroscopicity. [37] The large amount of water that the powder can adsorb and the process of gelification observed during the hydration of the powder suggest the suitability of the formulation for nasal delivery allowing a longer residence time of the powder in the nasal cavity when hydrated [33,38,39].

The specific surface area is a derived property of powders that can be used to determine the type and properties of a material and it is not linked to particle size, in fact powders with similar particle size can have different area, suggesting different particle porosity. A large surface area can ensure a better dissolution or hydration allowing the powder to hydrate and possibly dissolve the associated drug faster [40].

The BET method was used to evaluate the surface area of the Teijin formulation and results showed a value of  $0.426 \pm 0.025 \text{ m}^2 \text{ g}^{-1}$ , comparable to low-substituted HPC available on the market, suggesting the main component of the formulation is determining this property of the powder [41].

In order to gain information regarding the powder particle size distribution, the capsule content was analyzed with Mastersizer 3000 equipped with Aero S system for dry dispersion. Figure 2.5 shows that the powder had a broad range of particle size (from 1 to 240  $\mu\text{m}$ ) divided into two distinct populations: 6.6 % of the volume was in the small size population (peak at 9.9  $\mu\text{m}$ ), while the rest (93%) presented a peak at 98  $\mu\text{m}$ . The volume diameters characterizing the powder obtained from three capsules were:  $Dv_{10} 51.7 \pm 0.7 \mu\text{m}$ ,  $Dv_{50} 98 \pm 1.3 \mu\text{m}$  and  $Dv_{90} 162.3 \pm 4.0 \mu\text{m}$ , respectively.

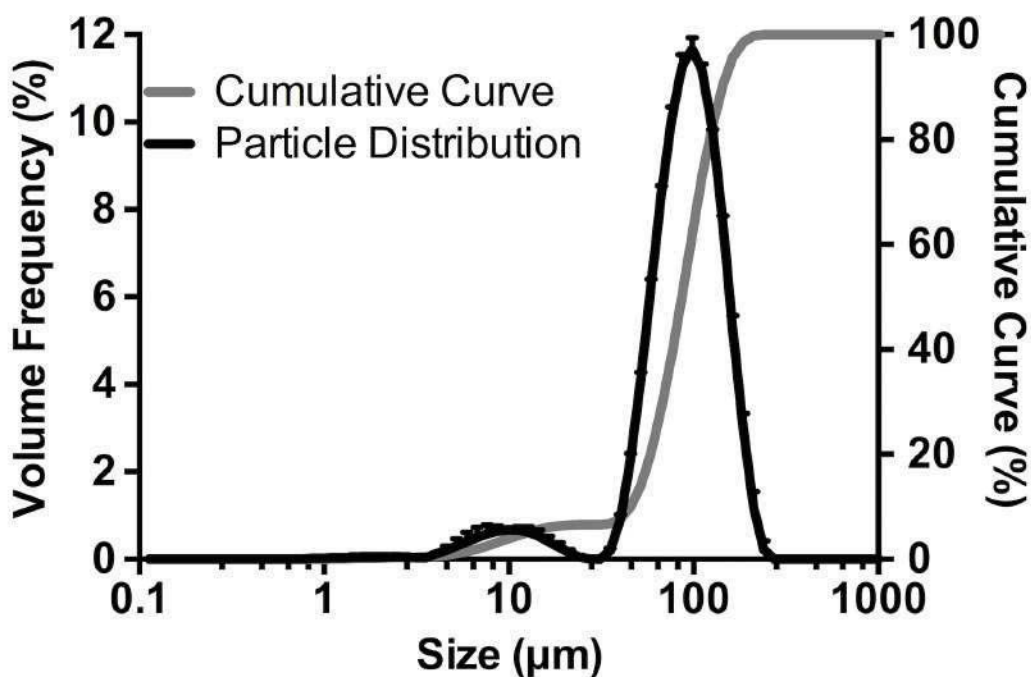
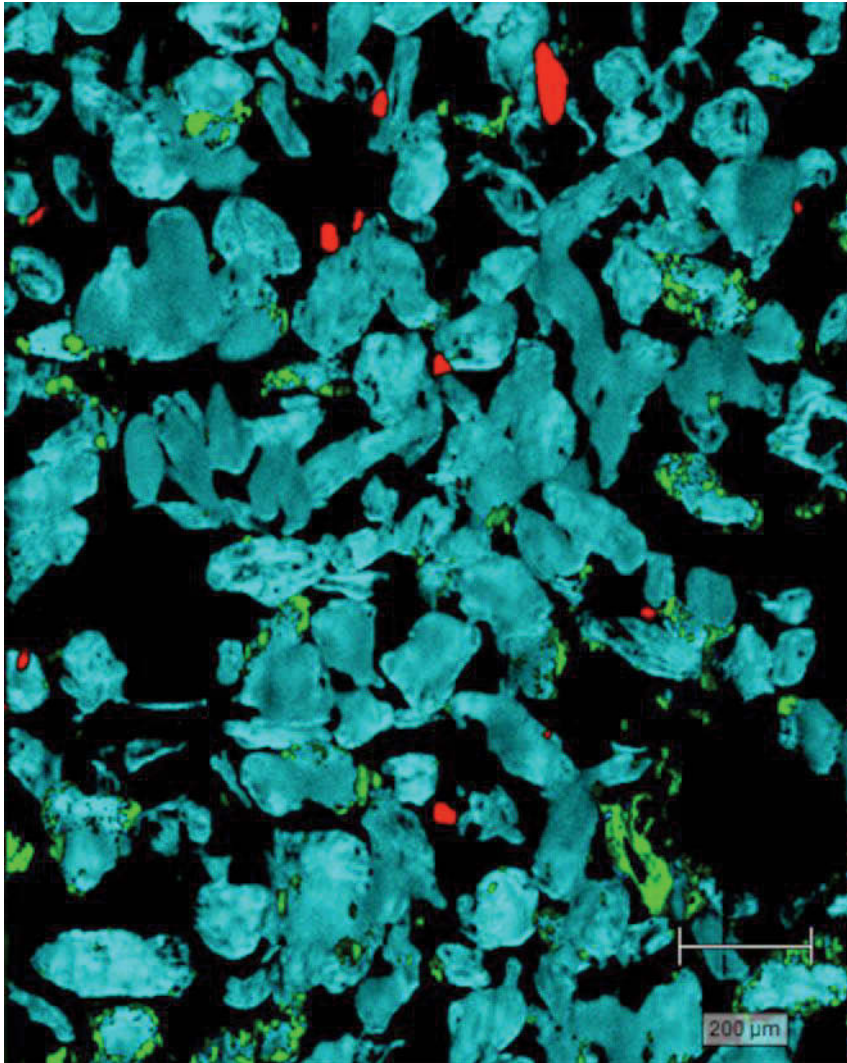


Figure 2.5. Particle size analysis by laser diffraction of Rhinocort Teijin powder blend measured with Malvern Mastersizer MS3000 ( $n=3 \pm \text{StDev}$ )

Figure 2.6 shows the scanning Raman map of the Teijin formulation powder, providing information about the localization of each component in the formulation blend. The larger and more abundant particles were hydroxyl propyl cellulose, supporting the DVS, BET and laser diffraction results. Sporadic particles of magnesium stearate were also observed. The BDP micronized particles were typically found on the surface of the large excipient particles but did not appear to be uniformly distributed, suggesting that probably the powder was not an ordered blend of the different components, see Figure 2.6.



*Figure 2.6. Overlay of Raman images on white light montage (BDP=green; HPC = blue and magnesium stearate = red).*

#### **2.4.2 Aerosol performance of Teijin Rhinocort**

The aerosol performance of the formulation was measured using Apparatus E equipped with a glass expansion chamber and by laser diffraction. According to the FDA draft guidance for industry, impactor and laser diffraction experiments should be performed to ascertain the absence of finer particles (aerodynamic diameter  $<10\ \mu\text{m}$ ) likely to penetrate the conductive airways and reach the lungs [17].

As shown in Table 2.4 almost the total amount of the BDP was found in the expansion chamber and roughly 95% of the API was deposited in stages with a cut-off diameter larger than 10  $\mu\text{m}$ . Around 3% remained in the capsule and the device, indicating that the dose was not completely emitted. In only one experiment some BDP was detected (0.24% of the total) on stage 4; no drug was found in any lower cut-off stages.

*Table 2.4. Percentage of Active ingredient in each stage of the Apparatus E Impactor equipped with the 2L expansion glass chamber for nasal delivery (n=3,  $\pm$  StDev).*

<b>Part or Stage</b>	<b>Cut off Diameter (<math>\mu\text{m}</math>)</b>	<b>% BDP (<math>\pm</math>StDev)</b>
Expansion Chamber	-	90.2 $\pm$ 4.78
Connection Tube	-	0.57 $\pm$ 0.12
Stage 1	> 14.1	4.64 $\pm$ 1.39
Stage 2	14.1 - 8.61	0.61 $\pm$ 0.25
Stage 3	8.61- 5.39	0.36 $\pm$ 0.17
Stage 4	5.39 - 3.3	0.08 $\pm$ 0.14
Stage 5	3.3 - 2.08	NA
Stage 6	2.08 - 1.36	NA
Stage 7	1.36 - 0.98	NA
Final Stage	< 0.98	NA
Capsules (3)	-	2.01 $\pm$ 0.46
Device	-	0.74 $\pm$ 0.11

In order to determine if any formulation excipient (i.e. HPC) could reach the lower airways, additional studies using Spraytech laser diffraction particle sizing were performed. The frequency and cumulative undersize particle size distribution profiles for the aerosolized powder are shown in Figure 2.7. It can be noticed that there are two populations, the first with a peak around 16  $\mu\text{m}$ , and the other one at 108  $\mu\text{m}$ . More than the 99% of the powder has a volume size larger than 10  $\mu\text{m}$  and the  $D_{v50}$  was  $93.7 \pm 2.9 \mu\text{m}$ . The  $D_{v50}$  value of the emitted dose is slightly smaller and significantly different from the one obtained for the capsule content, suggesting that a phenomenon of de-agglomeration is occurring during the *in vivo* simulated administration process using the Spraytech.

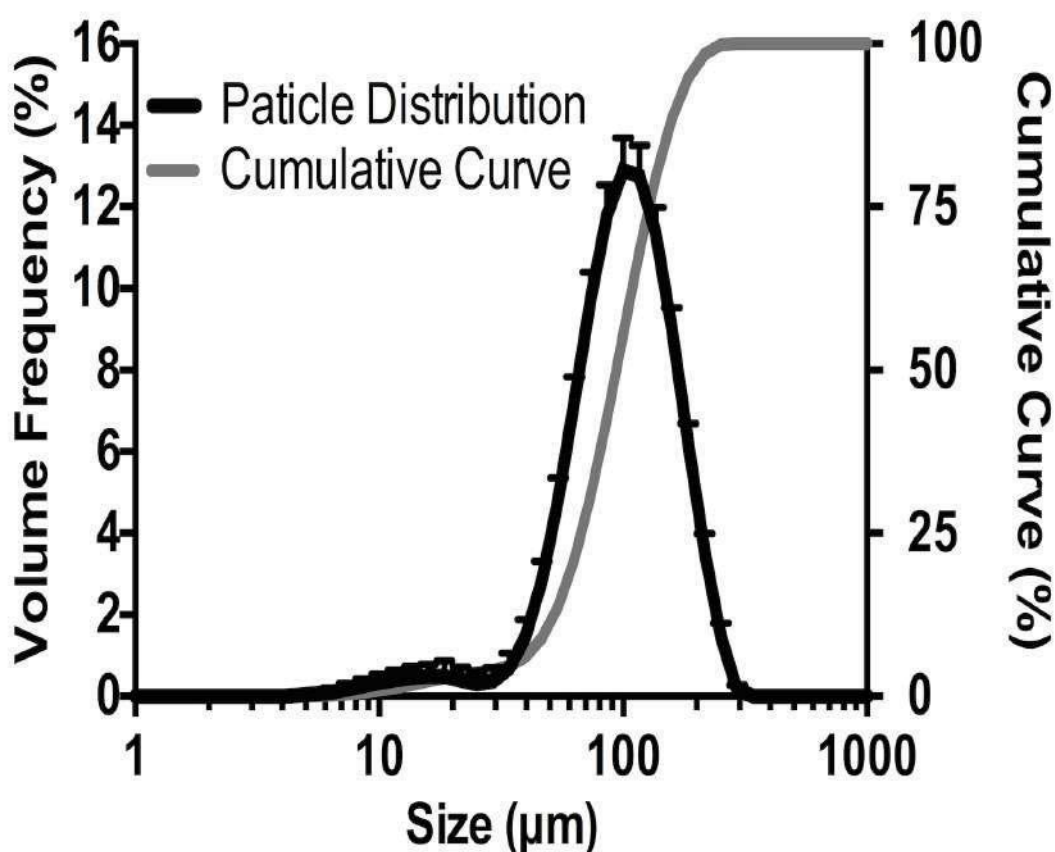


Figure 2.7. Particle size distribution of the powder emitted from Teijin Rhinocort using the Spraytech laser diffraction apparatus ( $n=3$ ,  $\pm$  StDev).

The  $D_{v10}$ ,  $D_{v50}$  and  $D_{v90}$  for each actuation necessary to empty one capsule were determined with the Spraytech. Figure 2.8 shows  $D_{v10}$ ,  $D_{v50}$  and  $D_{v90}$  for each actuation obtained averaging 3 capsules. No statistical difference was observed. However, it was not possible to obtain data for the last two actuations of the 8 required for drug administration, since six actuations were enough to empty the capsule to the point where any further emitted powder was not enough to trigger the analysis, in disagreement to what is suggested on the patient information leaflet, where 4 actuations for each nostril are indicated to complete the process.

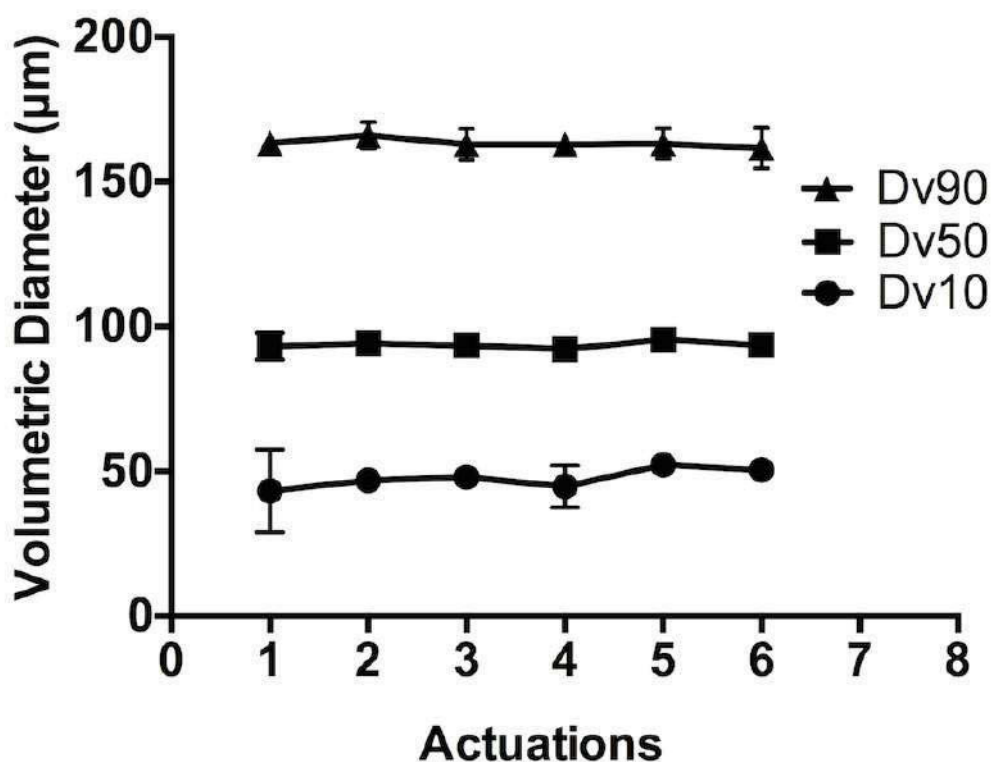


Figure 2.8. Equivalent volume diameter values ( $D_v$  90, 50 and 10) measured by laser diffraction for Teijin Rhinocort, 8 insufflations for one dose ( $n=3$ ,  $\pm$  StDev).



Clinical studies on the efficacy of Teijin formulation, on nasal allergies, were performed in Japan on over 220 people. Results from 1986 shows that the dry powder formulation was able to decrease the daily dosage by one quarter when compared to a pressurized nasal formulation (from 400µg to 100µg daily), with the same overall therapeutic improvement and less incidence of side effects. [42] The better efficacy of the powder formulation was explained as a result of the presence of HPC and its ability to prolong the residence of BDP in the nasal cavity. Furthermore, the fewer side effects were related to the lower daily frequency of administration needed and the reduced irritation due to the presence of the main excipient, HPC, compared to equivalent Freon based pMDI nasal formulations. [42] Similar results have been found in literature also for Rhinocort Turbuhaler<sup>®</sup> (Budesonide, AstraZenca), where patients were found to prefer the use of a dry powder device (formulation) compared to a water nasal spray. Specifically, the patients found the DPI product to have a less unpleasant taste and to cause less nasal irritation, compared to the reference liquid product [43].

In another study, the Optinose<sup>®</sup> device has been used for the systemic delivery of sumatriptan powder through the nose, reporting fast absorption ( $t_{max}$ = 20 minutes) of the drug and no bitter aftertaste [9]. Furthermore, in another study, it was shown that when compared to water spray, the Optinose powder formulation had less clearance in the first two minutes after the administration due to lack of anterior drip-out and less sniffing that prevented further dripping [15].

## **2.5 CONCLUSION**

Teijin Puvlizer Rhinocort<sup>®</sup> is one of the few nasal powder inhalers on the market worldwide and the oldest. The device comprises of a squeeze bulb-based

insufflator able to administer the powder loaded in a capsule via repeated actuations. Despite the simple device, the particle size distribution was highly reproducible, suggesting a consistent deposition of the drug in the nasal cavity, complying with the FDA guidance requirements for nasal formulations. Practically, the fact that six consecutive and repeated steps are required to administer the required dose can be considered as a limiting step for patient compliance, in comparison with multi-dose pre-metered water nasal products now on the market.

## **2.6 ACKNOWLEDGEMENTS**

A/Professor Traini is the recipient of an Australian Research Council Future Fellowship (project number FT12010063). A/Professor Young is the recipient of an Australian Research Council Future Fellowship (project number FT110100996).

## **2.7 AUTHOR DISCLOSURE STATEMENTS**

No conflicts of interest exist.

## 2.8 REFERENCES

1. Tafaghodi M, Rastegar S. Preparation and in vivo study of dry powder microspheres for nasal immunization. *J. Drug Target.* 2010;18:235–42.
2. Ishikawa F, Katsura M, Tamai I, Tsuji A. Improved nasal bioavailability of elcatonin by insoluble powder formulation. *Int. J Pharm.* 2001;224:105–14.
3. Kaye RS, Purewal TS, Alpar OH. Development and testing of particulate formulations for the nasal delivery of antibodies. *J. Control. Release.* 2009;135:127–35.
4. Kamide N, Ogino M, Yamashina N, Fukuda M. Sniff nasal inspiratory pressure in healthy Japanese subjects: mean values and lower limits of normal. *Respiration.* 2008;77:58–62.
5. Mistry A, Stolnik S, Illum L. Nanoparticles for direct nose-to-brain delivery of drugs. *Int J Pharm.* 2009;379:146–57.
6. Djupesland PG, Skretting A. Nasal deposition and clearance in man: comparison of a bidirectional powder device and a traditional liquid spray pump. *J. Aerosol Med. and Pulm. Drug Del.* 2012;25:280–9.
7. Djupesland PG, Skretting A, Winderen M, Holand T. Breath Actuated Device Improves Delivery to Target Sites Beyond the Nasal Valve. *The Laryngoscope.* 2006;116:466–72.
8. Birkhoff M, Leitz M, Marx D. Advantages of Intranasal Vaccination and Considerations on Device Selection. *Indian J. Pharm. Sci. India: Medknow Publications;* 2009;71:729–31.
9. Luthringer R, Djupesland PG, Sheldrake CD, Flint A, Boeijinga P, Danjou P, et al. Rapid absorption of sumatriptan powder and effects on glyceryl trinitrate model of headache following intranasal delivery using a novel bi-directional device. *J. Pharm. Pharmacol.* 2009;61:1219–28.
10. Schroeter JD, Garcia GJM, Kimbell JS. A computational fluid dynamics approach to assess interhuman variability in hydrogen sulfide nasal dosimetry. *Inhal. Toxicol.* 2010;22:277–86.
11. Balducci AG, Ferraro L, Bortolotti F, Nastruzzi C, Colombo P, Sonvico F, et al. Antidiuretic effect of desmopressin chimera agglomerates by nasal administration in rats. *AAPS PharmSciTech* [Internet]. 2014;440:956–62. Available from:

<http://eutils.ncbi.nlm.nih.gov/entrez/eutils/elink.fcgi?dbfrom=pubmed&id=23046665&retmode=ref&cmd=prlinks>

12. Ishikawa F, Murano M, Hiraishi M, Yamaguchi T, Tamai I, Tsuji A. Insoluble powder formulation as an effective nasal drug delivery system. *Pharm Res.* 2002;19:1097–104.
13. Colombo G, Lorenzini L, Zironi E, Galligioni V, Sonvico F, Balducci AG, et al. Brain distribution of ribavirin after intranasal administration. *Antiviral Res.* 2011;92:408–14.
14. Tepper SJ, Cady RK, Silberstein S, Messina J, Mahmoud RA, Djupesland PG, et al. AVP-825 breath-powered intranasal delivery system containing 22 mg sumatriptan powder vs 100 mg oral sumatriptan in the acute treatment of migraines (The COMPASS study): a comparative randomized clinical trial across multiple attacks. *Headache.* 2015;55:621–35.
15. Djupesland PG, Docekal P, Czech Migraine Investigators Group. Intranasal sumatriptan powder delivered by a novel breath-actuated bi-directional device for the acute treatment of migraine: A randomised, placebo-controlled study. *Cephalalgia.* 2010;30:933–42.
16. Djupesland PG. Nasal drug delivery devices: characteristics and performance in a clinical perspective—a review. *Drug Deliv. and Transl. Res.* 2013;3:42–62.
17. U.S. Department of Health and Human Services, Food and Drug Administration, Center for Drug Evaluation and Research. Bioavailability and Bioequivalence Studies for Nasal Aerosols and Nasal Sprays for Local Action. 2003;1–37.
18. Coowanitwong I, de S, Somaraju S, Wu H, Mclaughlin K, Schoenbrodt T, et al. Regional Deposition of Beclomethasone Dipropionate Powder Exiting Puvlizer® in a Nasal Cast Connected to a Next Generation Impactor. *RDD Europe 2011.* 2011;2:373–8.
19. Ottaviano G, Scadding GK, Coles S, Lund VJ. Peak nasal inspiratory flow; normal range in adult population. *Rhinology.* 2006;44:32–5.
20. Papachristou A, Bourli E, Aivazi D, Futzila E, Papastavrou T, Konstandinidis T, et al. Normal peak nasal inspiratory flow rate values in Greek children and adolescents. *Hippokratia.* 2008;12:94–7.

21. Jallo LJ, Ghoroi C, Gurumurthy L, Patel U, Davé RN. Improvement of flow and bulk density of pharmaceutical powders using surface modification. *Int. J Pharm.* 2012; 423:213–25.
22. Carr RL. Evaluating flow properties of solids. *Chemical Engineering.* 1965.
23. Schüssele A, Bauer-Brandl A. Note on the measurement of flowability according to the European Pharmacopoeia. *Int. J Pharm.* 2003; 257(1-2):301-4
24. Dayal P, Shaik MS, Singh M. Evaluation of different parameters that affect droplet-size distribution from nasal sprays using the Malvern Spraytec™. *J. Pharm. Sci.* 2004;93:1725–42.
25. U.S. Department of Health and Human Services, Food and Drug Administration, Centre for Drug Evaluation and Research. Bioavailability and Bioequivalence Studies for Nasal Aerosols and Nasal Sprays for Local Action. 2003;1–37.
26. Doub WH, Adams WP, Wokovich AM, Black JC, Shen M, Buhse LF. Measurement of drug in small particles from aqueous nasal sprays by Andersen Cascade Impactor. *Pharm. Res.* 2012;29:3122–30.
27. Great Britain SO. British Pharmacopoeia. London: Stationery Office; Appendix XII C. Consistency of Formulated Preparations.
28. Suzuki Y, Sekine K, Nagai T, Nambu N, Nishimoto Y. Powdery pharmaceutical composition for nasal administration. Google Patents; 1986.
29. Dohi M, Nishibe Y, Makino Y, Fujii T. Powdery composition for nasal administration. Google Patents; 2010.
30. Kobayashi H, Makino Y, Suzuki Y. Pharmaceutical preparation for intra-airway administration. Google Patents; 2001.
31. Makino Y, Kobayashi H, Suzuki Y. Pharmaceutical preparation for intra-airway administration. Google Patents; 1996.
32. Young PM, Price R, Tobyn MJ, Buttrum M, Dey F. Effect of humidity on aerosolization of micronized drugs. *Drug Dev. Ind. Pharm.* 2003;29:959–66.
33. Baumgartner S, Kristl J, Peppas NA. Network structure of cellulose ethers used in pharmaceutical applications during swelling and at equilibrium. *Pharm Res.* 2002;19:1084–90.
34. Yakimets I, Paes SS, Wellner N, Smith AC, Wilson RH, Mitchell JR. Effect of water content on the structural reorganization and elastic properties of biopolymer films: a comparative study. *Biomacromolecules.* 2007;8:1710–22.

35. Condon JB. Surface Area and Porosity Determinations By Physisorption: Measurements and Theory. Elsevier Science 2006:1–297.
36. Storey RA, Ymén I. Solid State Characterization of Pharmaceuticals 3rd Edition. John Wiley & Sons; 2011. pp. 1–42.
37. Callahan JC, Cleary GW, Elefant M, Kaplan G, Kensler T, Nash RA. Equilibrium Moisture Content of Pharmaceutical Excipients. *Drug Dev. Ind. Pharm.* 1982;8:355–69.
38. Dohi M, Nishibe Y, Makino Y, Fujii T. Powdery composition for nasal administration. Google Patents; 2005.
39. Hansen K, Kim G, Desai K-GH, Patel H, Olsen KF, Curtis-Fisk J, et al. Feasibility Investigation of Cellulose Polymers for Mucoadhesive Nasal Drug Delivery Applications. *Mol. Pharmaceutics.* 2015;12:2732–41.
40. Khadka P, Ro J, Kim H, Kim I, Kim JT. Pharmaceutical particle technologies: an approach to improve drug solubility, dissolution and bioavailability. *Asian J Pharm Sci.* 2014;9:304–16.
41. Rowe RC, Sheskey PJ, Cook WG, Fenton ME, Association AP. Handbook of Pharmaceutical Excipients. Pharmaceutical Press; 2012.
42. Okuda M, Okamoto M, Nomura Y, Saito Y. Clinical study on beclomethasone dipropionate powder preparation (TL-102) in perennial nasal allergy. *Rhinology.* 1986;24:113-123.
43. Yang WH, Dolovich J, Drouin MA, Keith P, Haddon J, Jennings B. Comparison of budesonide Turbuhaler with budesonide aqua in the treatment of seasonal allergic rhinitis. Rhinocort Study Group. *Can. Respir. J.* 1998;5:455–60.

## CHAPTER 3

### *Development of an in vitro tool to test nasal products*

This chapter was published in European Journal of Pharmaceutics and Biopharmaceutics, 107:223–33 (2016) under the title “Application of RPMI 2650 nasal cell model to a 3D printed apparatus for the testing of drug deposition and permeation of nasal products”. Authors: Pozzoli M, Ong HX, Morgan L, Sukkar M, Traini D, Young PM and Sonvico F. DOI: 10.1016/j.ejpb.2016.07.010

### **3.0 PREFACE**

Chapter 2 has shown the use of analytical methods to characterize a nasal formulation and the robustness of dry powder formulation. In detail, the application of the FDA expansion chamber in order to characterize aerodynamic particle size of a nasal product. However, that traditional approach for the characterization of nasal product heightened the need for a novel tool able to integrate analytical tools with a biological model. In this chapter an *in vitro* tool was developed to allow the deposition of nasal product over a nasal mucosa model. A conventional nasal liquid formulation was used in this chapter to validate the novel apparatus in order to demonstrate the applicability of this to be applied to the majority products.



### 3.1` ABSTRACT

The aim of this study was to incorporate an optimized RPMI2650 nasal cell model into a 3D printed model of the nose to test deposition and permeation of drugs intended for use in the nose. The nasal cell model was optimized for barrier properties in terms of permeation marker and mucus production. RT-PCR was used to determine the xenobiotic transporter gene expression of RPMI 2650 cells in comparison with primary nasal cells. After 14 days in culture, the cells were shown to produce mucus, and to express TEER (define) values and sodium fluorescein permeability consistent with values reported for excised human nasal mucosa. In addition, good correlation was found between RPMI 2650 and primary nasal cells transporters expression values.

The purpose built 3D printed model of the nose takes the form of an expansion chamber with inserts for cells and an orifice for insertion of a spray drug delivery device. This model was validated against the FDA glass chamber with cascade impactors that is currently approved for studies of nasal products. No differences were found between the two apparatus.

The apparatus including the nasal cell model was used to test a commercial nasal product containing budesonide (Rhinocort, AstraZeneca, Australia). Drug deposition and transport studies on RPMI 2650 were successfully performed.

The new 3D printed apparatus that incorporate cells can be used as valid *in vitro* model to test nasal products in conditions that mimic the delivery from nasal devices in real life conditions.

## 3.2 INTRODUCTION

Over recent decades, interest in the nose as an alternative site for drug administration has increased steadily [1]. The nose is attractive for drug delivery because the highly vascularised mucosa with low enzymatic activity potentiates peptide permeation and rapid, high concentration drug absorption that avoids first pass metabolism. [2-6]. However, there are a number of limitations and challenges associated with nasal drug delivery. Normal mucociliary clearance would clear the nasal cavity of liquid formulations within 45 minute. The nasal cavity, even in health, is a small volume and geometrically complex space, rendered smaller by mucosal inflammation. Finally, the small volume of the cavity and the relatively low volume of fluid available for drug dissolution limits the doses that can be administered [7-10].

Together, these highlight the specificity of this administration route and the need for further research into the development of new nasal formulations that are able to overcome the challenges related to efficient administration. In particular, there is an increasing need for reliable preclinical tools to screen new products and formulations intended for nasal delivery that can predict deposition and permeation through the mucosa and transport across the epithelium.

Different *in vitro* models have been proposed to investigate the deposition of nasal products. One approach is the use of transparent silicone anatomical casts such as one originated from a Japanese male cadaver Koken (Koken LM-005,

Bunkyo-ku Tokyo, Japan). However, this as well as other casts, appears to have some limitations related to the fact that the Food and Drug Administration (FDA) do not regulate the deposition experiments, each cast is not representative of the anatomical variability of different nasal cavities and its polymeric surface is far from representative of the mucosal surface present in the nose.

Another approach is to use Pharmacopoeia impactors, which have been used to predict aerodynamic particle size distributions and thus deposition profiles of aerosolized particles/droplets in the lower respiratory tract [11]. Specifically, for nasal drug delivery, the FDA guidance for industry on “Bioavailability and Bioequivalence Studies for Nasal Aerosols and Nasal Sprays for Local Action” suggests to determine particles/droplets size distribution using a cascade Impactor (CI) [12]. In particular, the guideline suggests the use of an induction port, i.e. a glass expansion chamber (EC), to be connected to a cascade impactor in order to maximise drug deposition below the top stages of the CI [11-13]. This allows a better discrimination of particles with aerodynamic diameters smaller than 10  $\mu\text{m}$  that could be inhaled and therefore not suitable for the nasal deposition.

While impactors and casts are important tools to determine deposition on the different areas of the respiratory tract, they don't offer any information related to either drug dissolution or permeation through the mucosa in the nasal cavity. Recently, various approaches that integrate lower airway epithelia cell cultures into compendia-based impactors have been proposed and used to study the deposition and permeation of particles emitted by dry powder inhalers and

pressurized metered dose inhalers [14-16]. To our knowledge, nothing similar has been proposed for nasal products as yet.

Among the *in vitro* cell lines available commercially, RPMI 2650 is the only immortalized human nasal cell line. It has been studied as a drug permeation tool by different researchers [2,17-22]. Initially, it was reported that this cell line was unsuitable for permeation studies because it was not able to form a confluent layer in conventional culture conditions [17]. However, Bai and collaborators and, two years later, Wengst and Reichel, started to further investigate culture condition for this cell line and to characterize some of the culture features using transepithelial electrical resistance measurements (TEER), permeation of paracellular markers and tight junctions' protein expression. The key findings of these studies were that the change from the conventional Liquid Cover Culture (LCC) to an Air Liquid Interface cultures (ALI), where the upper surface of the cells was exposed to air, was able to induce cell differentiation leading to the formation of cells layers suitable for permeation experiments [18,19]. A few years later, Reichel and colleagues tried to optimize culturing conditions using different cell growth media and different types of cell-culture insert membrane; the main studies were based on TEER observation and paracellular marker permeation. A pronounced dependence of TEER on medium and membrane material were observed; with the best culture condition being achieved when using polyethylene terephthalate (PET) 3  $\mu\text{m}$  porosity Transwell™ inserts, using Minimum Essential Medium (MEM) supplemented with 10% of foetal bovine serum with cells cultivated using the ALI condition [21].

Based on these previous findings, the aim of the present study is to incorporate RPMI 2650 nasal cell epithelia, grown under ALI conditions into a modified expansion chamber connected to a cascade impactor. This approach, will allow the study of real nasal aerosols products, their deposition and permeation after nasal device actuation. In order to develop this new impactor/deposition apparatus, larger Snapwell™ cell culture inserts detachable from its plastic frame that can be accommodated in to the 3D apparatus without altering the aerosol performances of the impactor have been selected [14]. Firstly, the optimization of the RPMI 2650 cell line culture conditions on Snapwell inserts as nasal drug permeation model, specifically focusing on parameters that characterize the barrier properties of the model, i.e. TEER measurement, para-cellular marker permeation, tight junction localization and mucus production, were investigated. To further validate the model, a thorough analysis of the xenobiotic transporter expression in comparison with that of freshly brushed human nasal cells was carried out.

Then, RPMI 2650 grown in ALI conditions on Snapwell inserts were accommodated into a custom-built 3D printed modified expansion chamber in order to study nasal product deposition and permeation after device actuation. This new apparatus was validated against the original glass expansion chamber, recommended in the FDA guidelines, in terms of drug deposition on the CI stages and was tested in terms of drug deposition and permeation through the RPMI 2650 nasal cell model, using a commercially available budesonide nasal spray.

There is a clear need for a reliable preclinical model to test new products and formulations intended for nasal delivery that can predict drug deposition, permeation and transport across the epithelium.

### **3.3 MATERIALS AND METHODS**

#### **3.3.1 Materials**

Minimum essential medium added with phenol red (MEM), non-essential amino acids solution ( $\times 100$ ), fetal bovine serum (FBS), L-glutamine (200 mM), Hank's balanced salt solution (HBSS), TrypLE Express, bovine serum albumin (BSA) and phosphate buffered saline (PBS) were purchased from Gibco, Invitrogen (Sydney, NSW, Australia). Snapwell™ cell culture inserts (1.13 cm<sup>2</sup> polyester, 0.4  $\mu$ m pore size) and black 96-well black plates were supplied by Corning Costar (Lowell, MA, USA). All other culture plastics were from Sarstedt (Adelaide, SA, Australia). Trypan blue solution (0.4%, w/v), paraformaldehyde and dimethyl sulfoxide (DMSO) were obtained from Sigma-Aldrich (Sydney, NSW, Australia). Fluorescein-sodium (Flu-Na) was purchased from May & Baker Ltd. (Dagenham, England). Alcian blue 1% (pH 2.5) in 3% acetic acid was purchased from Fronine laboratory (Sydney, NSW, Australia). NucleoSpin® RNA extraction kit was kindly provided by Scientifix (Cheltenham, VIC, Australia), a custom TaqMan® Array-96 well plate and all buffers were purchased by Applied Biosystem (ThermoFisher Scientific, Scoresby, VIC, Australia). Rhinocort nasal spray (AstraZeneca, North Ryde, NSW, Australia) was purchased at a local pharmacy. All chemicals and reagents were of the highest analytical grade.

### **3.3.2 Cell Culture Nasal Cell Line**

The cell line RPMI 2650 (CCL-30) was purchased from the American Type Cell Culture Collection (ATCC, Manassas, VA, USA). Cells between passage 16-30 were grown in 75 cm<sup>2</sup> flasks in complete Minimum Essential Medium (MEM) containing 10% (v/v) foetal bovine serum, 1% (v/v) non-essential amino acid solution and 2mM L-glutamine and maintained in a humidified atmosphere of 95% air 5% CO<sub>2</sub> at 37°C. Cells were propagated and sub-cultured according to ATCC protocol. The cell culture inserts were coated with 250uL of 1µg/mL collagen solution in PBS (rat collagen type 1 in PBS, BD Biosciences, Australia) and left overnight to increase the adherence of cells to the membrane [18]. In order to establish the ALI model, 200 uL of cell suspension were seeded on to the collagen coated Snapwell inserts at three different seeding concentrations: 1.25, 2.5, 5.0 x10<sup>6</sup> cells/mL (equivalent to 221, 442, 885 x10<sup>5</sup> cells/cm<sup>2</sup>). The media on the apical compartment was removed after 24 hours post-seeding. Media in the basolateral chamber was replaced 3 times per week. Cell layers were allowed to grow and differentiate under ALI conditions up to 21 days.

### **3.3.3 Transepithelial electrical resistance Measurements**

Transepithelial electrical resistance was recorded with EVOM2<sup>®</sup> epithelial voltohmmeter (World Precision Instruments, Sarasota, FL, USA) every 2-3 days from day one. Briefly, pre-warmed media was added to the apical chamber and allowed to equilibrate for at least 30 minutes in a cell culture incubator (humidified air with 5% CO<sub>2</sub> at 37°C). Blank filter values were subtracted and TEER values were calculated normalizing the resistance values with the Snapwell inserts area (1.13 cm<sup>2</sup>).

### 3.3.4 Sodium Fluorescein Permeation Experiments

Sodium Fluorescein, a paracellular marker (Flu-Na, MW 367 Da), was used to evaluate barrier formation and tight junction functionality in the ALI culture. Three time-points were chosen to conduct the experiments (1, 2, 3 weeks) and at each time point, three Snapwell inserts were washed twice with warm HBSS before each experiment. 250  $\mu$ L of 2.5 mg/mL Flu-Na solution were added to the apical chamber (donor) and 1.5 mL of pre-warmed HBSS into the basolateral chamber (acceptor). At pre-determined time points, 200  $\mu$ L of solution are sampled from the acceptor chamber every 30 minutes over 4 hours and equal volume of fresh HBSS was added for replacement.

Samples were collected into a black 96-well plates and fluorescence of Flu-Na was measured with a SpectraMax M2 plate reader (Molecular Devices, Sunnyvale, CA, USA), using excitation and emission wavelengths of 485 nm and 535 nm, respectively. The calibration coefficient of determination was 0.999, with standards prepared between 1.25 and 0.0125  $\mu$ g/mL.

Samples were analysed and the permeation coefficient ( $P_{app}$ ) was calculated according Eq. (1.1):

$$P_{app} = \frac{dQ}{dt \cdot C_0 \cdot A}$$

Where  $dQ/dt$  is the flux ( $\mu$ g/s) of the Flu-Na across the barrier,  $C_0$  is the initial donor concentration ( $\mu$ g/mL) and  $A$  is the surface area ( $\text{cm}^2$ ).



### **3.3.5 Evaluation of Mucus Production**

To assess the ability of the cell line RPMI 2650 to produce mucus when cultured at the ALI configuration, Alcian Blue was used according to a previously established method [23]. Mucus production of the ALI model was assessed at different time points (1, 7, 14, 21 days) for three seeding densities (1.25, 2.5, 5.0 x10<sup>6</sup> cells/mL), respectively. On the day of the experiment, cell layers were washed twice with 300  $\mu$ L of pre-warmed PBS and fixed using 4% (w/v) paraformaldehyde for 20 minutes. After the fixing agent was washed with PBS, the surface of the cells was stained with Alcian Blue. Excess staining was washed with PBS and inserts allowed to air-dried for approximately three hours. The membrane was cut from the insert and mounted on to the glass slide with Entellan™ mounting medium (ProSciTech, Thuringowa, QLD, Australia) and sealed. Subsequently, images were taken using an Olympus BX60 (Olympus, Hamburg, Germany) microscope equipped with an Olympus DP71 camera. Three images were taken per well, with all conditions performed in triplicate. Images were analysed using Image J software (NIH, Bethesda, MD, USA) and values of RGB (Red Green Blue) were measured for each image [24]. The ratio of blue (RGBb ratio) was calculated by dividing the mean RGBb by the sum of the RGB values for each image (RGBr + RGBg + RGBb) [23].

### **3.3.6 Immunocytochemistry Experiment**

In order to visualise the tight junction proteins on RPMI 2650 cells: ZO-1 (zone occluding 1) and E-cadherin immunocytochemistry was performed. RPMI 2650 cells grown on Snapwell inserts for 14 days under ALI condition were used for immunocytochemistry. The cells were washed 3 times for 30 min with PBS to

decrease the amount of mucus on the cell layers and improve visualisation. Then, the cells were fixed with 4% paraformaldehyde solution for 10 min. Afterwards, the cells were incubated for 10 min in PBS containing 50 mM NH<sub>4</sub>Cl, followed by 8 min with 0.1% (w/v) Triton X-100 in PBS for permeabilization of the cell membrane.

Cells were then incubated for 60 min with primary antibodies, i.e. 200 µL of E-cadherin (H-108) rabbit polyclonal IgG (1:100, Santa Cruz Biotechnology, Dallas, TX, USA) and ZO-1 (D7D12) rabbit monoclonal IgG (1:1000, Cell Signaling Technology, Danvers, MA, USA). Afterwards, cell monolayers were rinsed three times with PBS containing BSA 2%, before 30 minutes incubation with 200 µL of a 1:500 dilution in PBS containing 2% BSA of a goat anti-Rabbit IgG secondary antibody labelled with Alexa Fluor<sup>®</sup> 488 (LifeTechnologies, Waltham, MA, USA). 4',6-diamidino-2-phenylindole (DAPI, 1 µg/mL in PBS) was used to counterstain cell nuclei. After 30 min of incubation, the specimens were again rinsed three times with PBS containing 2% BSA and embedded in Entellan<sup>™</sup> new mounting medium (Merk-Millipore, Darmstadt, Germany). Images were obtained using a confocal laser-scanning microscope (Nikon A1, Nikon Instruments Inc., Melville, NY, USA), using a laser at 488 nm and 60x objective.

### **3.3.7 Expression of Xenobiotic Transporters**

#### *3.3.7.1 RPMI 2650 Cell Culture and Sample Collection of Primary Nasal Cell*

RPMI 2650 cells were cultured for 14 days on Snapwell porous membranes under ALI conditions at a density of  $2.5 \times 10^6$  cells/mL. To obtain primary nasal cells,

bilateral nasal mucosal brushing was performed using a disposable cytology brush (Model BC-202D-2010, Olympus Australia Pty. Ltd., Notting Hill, VIC, Australia) on human subjects to collect nasal epithelium as described previously [25-28]. Samples were pooled together from eight healthy volunteers between ages 20 and 40, with two groups of four people per gender. Samples were washed and centrifuged twice with PBS solution and left in -80°C freezer overnight prior to RNA extraction.

#### 3.3.7.2 *RNA Isolation, Target Synthesis, Microarray Data Analysis*

In order to analyse the protein transporter expression in the cells samples, RNA was isolated and purified using the NucleoSpin<sup>®</sup> RNA kit (Machery-Nagel, Düren, Germany). The RNA samples were treated with RNase-free DNase sets and dissolved in RNase-free water. Concentration and purity was determined by spectrophotometry (NanoDrop 2000, ThermoFischer Scientific, Scoresby, VIC, Australia). TaqMan<sup>®</sup> Array Plates (LifeTechnologies, Sydney, NSW, Australia) was used to perform rt-PCR assays. The array, *ad hoc* designed, enabled the assessment of 46 human drug transporter genes, including 13 ATP-binding cassette transporters, 23 solute carrier transporters, and 10 solute carrier organic anion transporters (see Table 3.1 for a list of all genes and proteins). Reverse transcription was carried out using a standardized internal protocol. Briefly, to 5 uL of RNA were added a mixture of general primer and deoxynucleotide (dNTP, 1:1) and 5 uL of PCR grade water; the mixture was heat at 65°C for 5 min and quickly cooled in ice. Subsequently, 4 uL of first strand buffer, 2 uL of 0.1 M solution of DTT (Dithiothreitol) and 1 uL of ribonuclease inhibitor were added; the solution was incubated at 37°C for 2 minutes and 1 uL of M-MLV (Moloney Murine

Leukemia Virus) reverse transcriptase was added. The mixture was incubated firstly at 25°C for 10 minutes and then at 37°C for 50 minutes; in order to stop the reaction the temperature was raised to 70°C for 15 min. The cDNA for all the samples was uniformly diluted to 20 ng/uL and mixed with TaqMan® mastermix. Thermal-cycling conditions were set to manufacturer specifications, with 20 uL of mixture (sample and mastermix 1:1) were added to each well. The plates were analysed using the StepOnePlus™ Real-Time PCR System (Applied biosystem, ThermoFisher Scientific, Scoresby, VIC, Australia) for a total of 40 cycles. Data analysis was performed using the  $\Delta Cq$  method, where the  $\Delta Cq$  value is normalized to the 18S ribosomal RNA (18S rRNA) used as a reference gene. Ribosomal RNA, the central component of the ribosome is an abundant and one of the most conserved genes in all cells. Recently, 18S rRNA has been indicated as the most suitable reference gene for RT-qPCR normalization of data from primary human bronchial epithelial cells [29].

### **3.3.8 Development and Validation of Aerosol Nasal Deposition**

#### **Apparatus**

##### *3.3.8.1 Development of the Modified Expansion Chamber*

Rapid prototyping with 3D printing technique was used to manufacture the custom-made modified expansion chamber (MC) (Figure 3.1). The MC was designed to accommodate up to 3 Snapwell cell culture inserts, using CAD software (Catia 3D, 3DS, Boston, MA, USA). The modified expansion chamber was designed based on the 2 L glass expansion chamber (EC) as suggested in the FDA guidance for nasal products [12]. The MC comprises of two interlocking

hemispheres: the lower part presents the connection to the cascade impactors (through a connection adaptor), and an inlet hole for nasal devices at 30° from the axis. The upper half is designed to allow the incorporation of three Snapwell cell culture inserts, located opposite to the inlet hole (Figure 3.1).

Acrylonitrile butadiene styrene (ABS) was used as printing material using a commercial 3D printer (Dimension Elite, StrataSys, Eden Prairie, MN, USA), at layer thickness of 178 µm. Due to the intrinsic porosity of the printed material, the internal and external surfaces were chemically treated with small quantities of acetone to seal internal surfaces; absence of leakage was successfully tested with different mixtures of water and methanol.

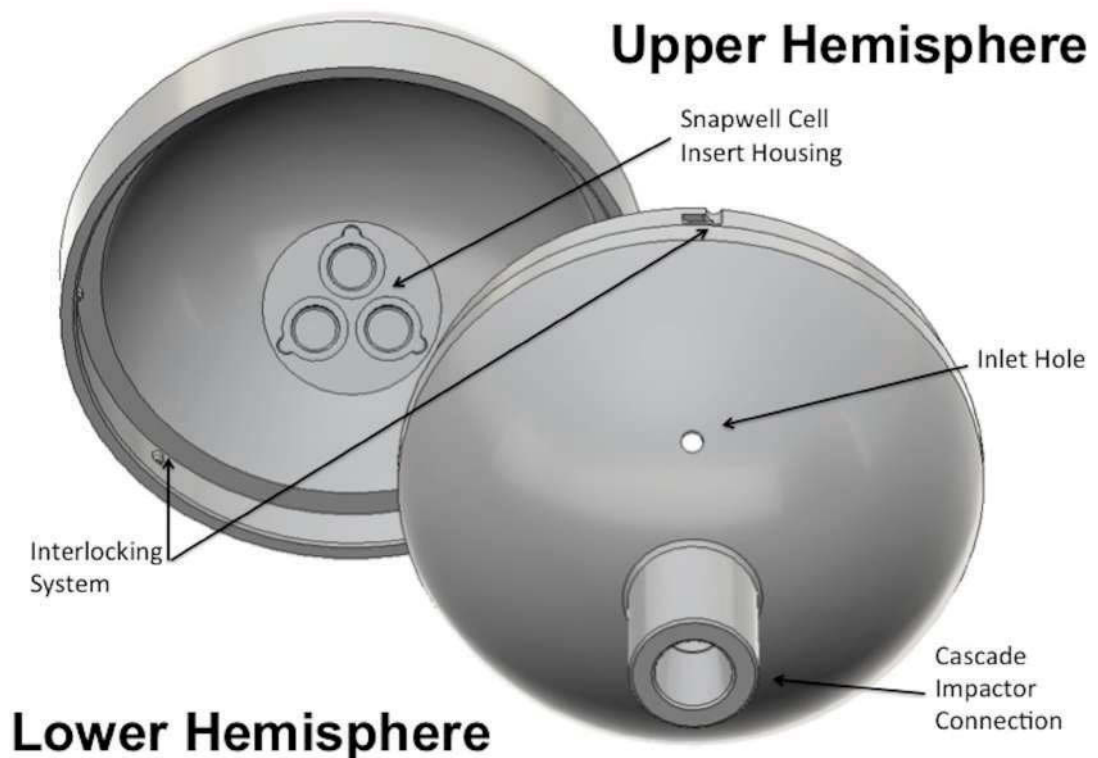


Figure 3.1. 3D drawing of the modified expansion chamber.

### 3.3.8.2 Validation of the Impactor Deposition Performances: Standard vs. Modified Expansion Chamber

Rhinocort, a commercial available nasal spray for the treatment of rhinitis (AstraZeneca, North Ryde, NSW, Australia), containing a suspension of Budesonide (32 µg/spray) as active ingredient, was used to validate the modified chamber. Aerodynamic particle size distributions were evaluated using a British Pharmacopoeia Apparatus E – Next Generation Impactor (Westech W7; Westech Scientific Instruments, Upper Stondon, UK) (Figure 3.2). Analyses were performed in triplicate with either the glass expansion chamber or the modified chamber fitted with Snapwell inserts. The device was primed to waste and for each analysis, three actuations were fired. Briefly, the impactor was connected to a rotary pump (Westech Scientific Instruments, Upper Stondon, UK) at a flow-rate of 15 L/min using a calibrated flow meter (Model 4040, TSI Precision Measurement Instruments, Aachen, Germany). Each impactor stage was washed with a solution 80:20 (% v/v) methanol/water and samples analysed by high performance liquid chromatography (HPLC) using a validated method [30].

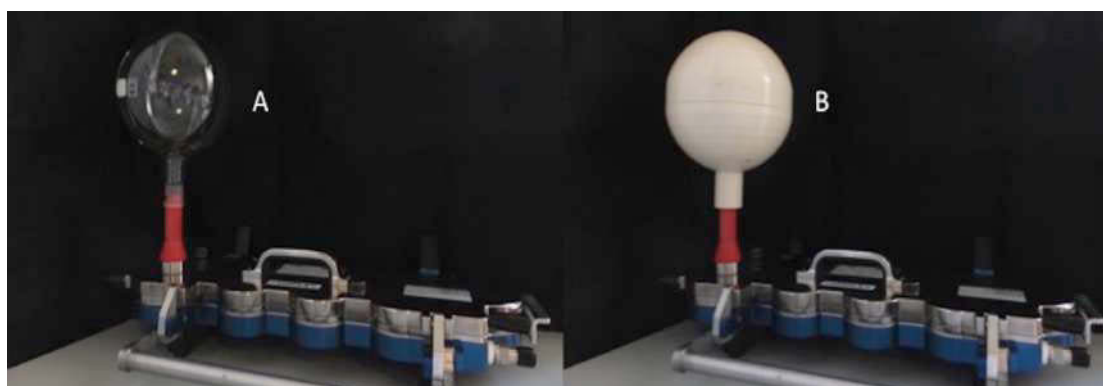


Figure 3.2. British Pharmacopoeia apparatus E equipped with FDA glass expansion chamber (A) and modified expansion chamber (B).

### 3.3.8.3 *Validation of the Cell Layer Integrity in the Modified Chamber*

RPMI 2650 were cultivated on Snapwells at the optimized seeding condition. At day 14, three cell inserts were washed with pre-warmed HBSS, and placed into the modified expansion chamber. An HBSS solution into a VP3 Aptar nasal pump (Aptar, Le Vaudreuil, France) was used as blank to simulate the deposition process into the modified chamber. After 6 actuations of the buffer blank solution, with the same deposition method previously described, the inserts were transferred into a cell culture plate. Flu-Na permeation studies were performed as mentioned above in order to confirm that the integrity of the cell layers after aerosol deposition. The  $P_{app}$  was compared with untreated control cells.

### **3.3.9 Deposition and Transport of a Commercial Budesonide Nasal Spray on Optimized RPMI 2650 cell Model using the Modified Expansion Chamber**

RPMI 2650 cells were used after 14 days from seeding on Snapwells ( $2.5 \times 10^6$  cells/mL). Three cell inserts were washed with pre-warmed HBSS buffer and fitted into the upper hemisphere of the modified expansion chamber. The aerosol deposition of budesonide on the cell surface from the Rhinocort device (AstraZeneca, North Ryde, NSW, Australia) was obtained according method described above, with a total dose of 96  $\mu\text{g}$  of budesonide (3 sprays) was delivered into the chamber. The cell inserts were then removed from the modified chamber and transferred to a 6-well plate containing 1.5 mL of fresh pre-warmed HBSS. Samples of 200  $\mu\text{L}$  were collected from the basal chamber every hour and replaced with the same volume of fresh buffer. After four hours, the apical surface

of the epithelia was washed twice in order to collect any remaining drug. Subsequently, cells were scraped from the insert membrane and lysed with CellLytic™ buffer (Invitrogen, Sydney, NSW, Australia) in order to quantify the amount of budesonide inside the cells by HPLC. TEER measurements were performed prior and after the deposition in order to confirm that the integrity of the cell layer was maintained.

### **3.3.10 Analytical Quantification of Budesonide**

The amount of budesonide in each sample was determined according to a validated method in literature; using an HPLC system equipped with a SPD-20A UV-Vis detector (Shimadzu, Tokyo, Japan) [30]. A Luna C18 column (150 X 4.6 mm, 3  $\mu$ m, Phenomenex, Lane Cove, NSW, Australia) was used with a mobile phase methanol/water 80:20 % v/v. The flow rate was set at 1 mL/min and Budesonide was detected at  $\lambda$ =240 nm. The retention time of budesonide was ~ 5 minutes. Standards were prepared in the mobile phase, and 100  $\mu$ l injections were used. Linearity was confirmed between 0.1  $\mu$ g/mL and 50  $\mu$ g/mL [30].

### **3.3.11 Statistics**

Unless differently stated, data represent the mean  $\pm$  standard deviation of at least three independent experiments. t-Test was used to compare data, with differences considered significant for  $p < 0.05$ .



## **3.4 RESULT AND DISCUSSION**

### **3.4.1 Transepithelial Electrical Resistance (TEER)**

#### **Measurements**

Transepithelial electrical resistance can be used as an indicator of the development and integrity of the epithelial barrier. Various studies have tried to optimize and standardize the culture conditions of RPMI 2650 [21]. However, the effects of seeding density on RPMI 2650 cultured in the ALI conditions on this Snapwell insert with a larger surface area has not been previously evaluated. The Snapwell inserts offers a more flexible membrane compared to the more common 0.33 cm<sup>2</sup> Transwell inserts due to their larger surface area and different support structure.

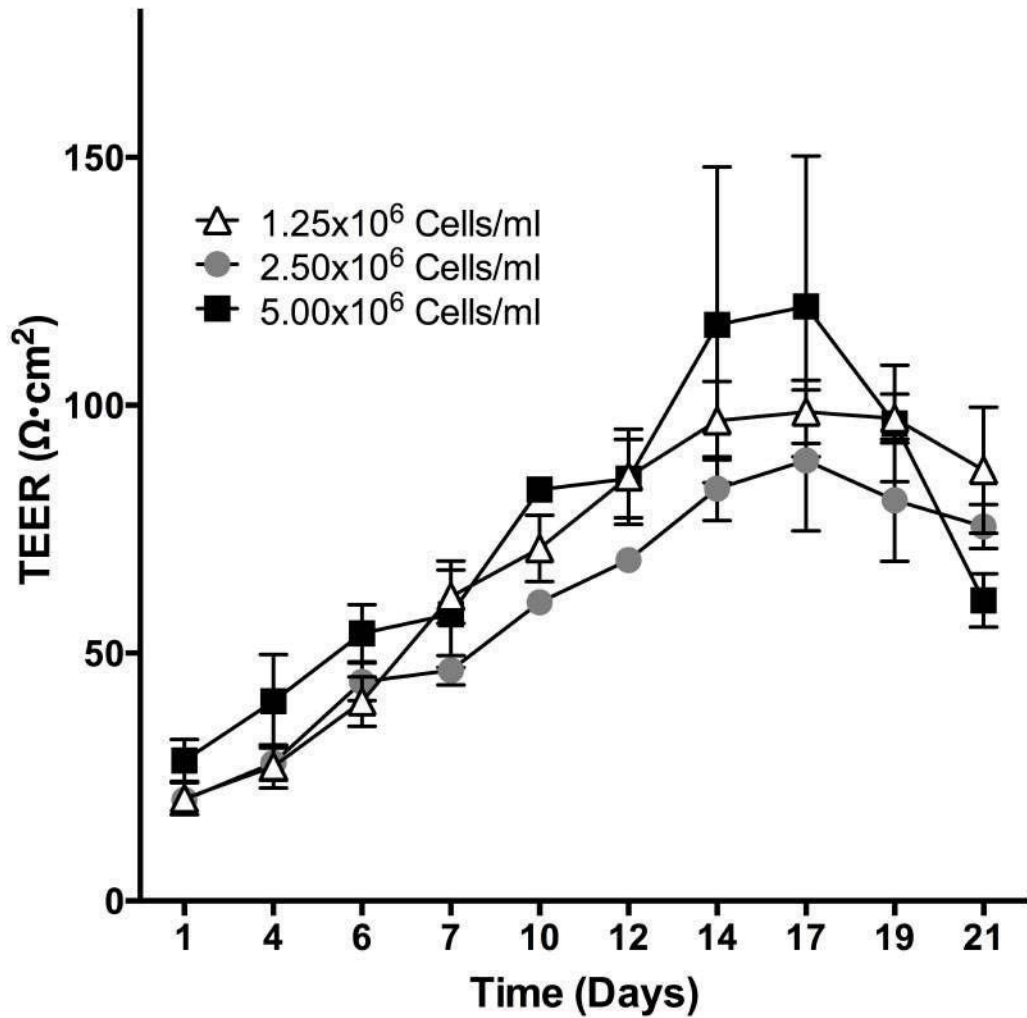


Figure 3.3. TEER of three different seeding densities of RPMI2650 cells cultured in the ALI conditions over time ( $n=3$ ;  $\pm$  StDev).

The progressive formation of the tight junction barrier by cultured RPMI 2650 cells seeded onto Snapwell inserts with respect to time is shown in Figure 3.3. The TEER for the three different seeding densities steadily increases with time until day 14, starting from values around  $20 \Omega \cdot \text{cm}^2$  and reaching a plateau between  $115 \Omega \cdot \text{cm}^2$  ( $5 \times 10^6$  cells/mL seeding) and  $150$  ( $1.25 \times 10^6$  cell/mL seeding) up to day 17 when the TEER starts to decrease. Data indicate that at least 14 days are required for the cell to reach a tight confluent layer with the highest TEER barrier

when cultured in the ALI conditions. After 17 days, a decrease of the TEER values is observed, suggesting that the cells either start to die or lose their tight junction integrity a few days after full maturation. This trend is similar to previously published data [21]. Regarding the three different seeding levels, no statistical differences were found at days 14 and 17, reaching values around 90-150  $\Omega\cdot\text{cm}^2$ . Therefore, values above 90  $\Omega\cdot\text{cm}^2$  were considered sufficient to perform experiments.

We report a clear correlation with the range of TEER values reported for human nasal mucosa. our results are very similar to those reported previously [18,21,31]. In particular, TEER values from excised human mucosa obtained from turbinectomy surgeries and used within an hour from the extraction, showed TEER values around 90-180  $\Omega\cdot\text{cm}^2$ . Therefore, this data support the use of ALI cultured RPMI 2650 as a representative model of the nasal mucosa.

### **3.4.2 Sodium Fluorescein Permeation Experiments**

The relatively high variability in TEER values reported in literature for RPMI 2650 cells suggests that this measurement is affected by many factors related to the technique (inter/intra laboratory), therefore other parameters have to be considered when trying to establish a model for drug deposition and transport. Thus, permeation studies of Flu-Na were performed in order to confirm and support the TEER measurements. Sodium fluorescein, due to its hydrophilic characteristic, is used as a paracellular permeation marker. The transport of Flu-Na across RPMI 2650 cell layer was evaluated over a period of 4 hours (Table 3.2). In order to confirm that, the Snapwell insert membrane were not the rate-

limiting step of the permeation process, permeability of Flu-Na through the Snapwells membrane alone was also tested and showed a significantly higher value ( $1.38 \times 10^{-5}$  cm/s).

*Table 3.2.  $P_{app}$  values ( $\times 10^{-6}$  cm/s) of Flu-Na across RPMI 2650 cultured in ALI conditions for three different seeding densities ( $n=3$ ;  $\pm$  StDev) compared to values obtained for excised human nasal mucosa*

Flu-Na $P_{app}$ values ( $\times 10^{-6}$ cm/s)					
Seeding Density	1.25 ( $\times 10^6$ cells/mL)	2.50 ( $\times 10^6$ cells/mL)	5.00 ( $\times 10^6$ cells/mL)	Human Mucosa	Nasal Mucosa
Freshly excised	-	-	-	3.12 $\pm$ 1.99 [18]	
Week 1	5.32 $\pm$ 0.37	5.21 $\pm$ 0.27	5.47 $\pm$ 0.49		
Week 2	3.67 $\pm$ 0.21	2.68 $\pm$ 0.60	2.95 $\pm$ 0.17		
Week 3	3.47 $\pm$ 0.20	3.55 $\pm$ 0.30	2.69 $\pm$ 0.18		

As shown in Table 3.2, no statistical difference was observed between the  $P_{app}$  values of the three different seeding densities after a week of culture, suggesting that seven days in ALI conditions are not sufficient to have a tight confluent cell layer. After 14 day of culture, the  $P_{app}$  values significantly decreased, when compared to the values of week 1, supporting the findings of the TEER experiments. It was also found that the intermediate seeding density reaches the lowest value of  $2.68 \pm 0.60 \times 10^{-6}$  cm/s after two weeks in culture. On the other hand, the lowest seeding density ( $1.25 \times 10^6$  cells/mL) shows higher permeability compared to the others two, suggesting that the amount of cell may not sufficient

to guarantee enough barrier properties. No significant differences between the Papp values for the two higher seeding densities were observed. After three weeks in culture, no significant difference in the Flu-Na permeability was found for any of the seeding densities, suggesting two weeks in culture is enough to reach a mature model with confluent cells for RPMI 2650.

Different research groups have tried to characterize the paracellular permeability of RPMI 2650 grown in ALI conditions: Bai et al obtained values of  $5.07 \times 10^{-6}$  using mannitol as marker [19]; Wengst and Reichel, using Flu-Na, on cells grown on Transwell<sup>®</sup> polycarbonate membrane, presented values of  $6.09 \times 10^{-6}$  cm/s [18]; and Reichel obtained lower values of  $1.91 \times 10^{-6}$  cm/s using Thincert<sup>®</sup> inserts with polyethylene terephthalate membranes, confirming that the supporting material may affect the adhesion and the layer/barrier formation of RPMI 2650 cell line [18,21]. More recently, Kreft reported  $P_{app}$  values of  $6.08 \times 10^{-7}$  cm/s using dextran conjugated to fluorescein isothiocyanate (MW 10,000), an extremely low value that is related to the higher molecular weight of the molecule used for the investigation [20].

### **3.4.3 Evaluation of Mucus Production**

Mucus plays an important role in protecting the nasal epithelium. Furthermore, this mucus is the first barrier that any drug administered into the nose has to overcome in order to be absorbed; it has a key role also in the dissolution process of drug that will allow subsequent permeation [32]. Thus, an appropriate model of the nasal epithelium requires mucus of specific depth, biochemistry and

rheology. Therefore, the production of mucus in the RPMI 2650 cellular model grown in ALI condition was investigated.

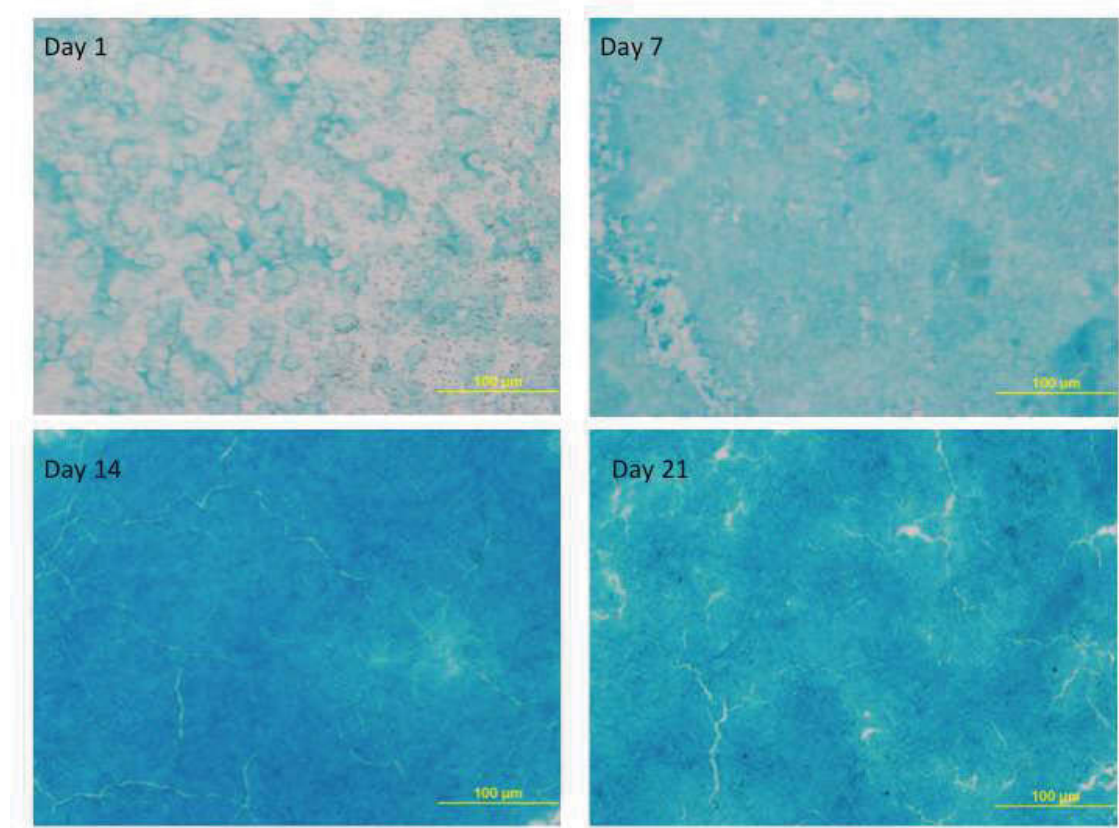


*Figure 3.4. Optical microscope images of Alcian blue mucus staining on RPMI 2650 grown on Snapwell® inserts at  $2.50 \times 10^6$  cell/mL seeding density.*

Alcian Blue allows mucus detection by reaction with acidic polysaccharides (mucopolysaccharides) and sialic acid containing glycoproteins, producing a blue color. Figure 3.4 shows an example of the staining of the mucus layer of RPMI2650 seeded at  $2.50 \times 10^6$  cell/mL over a 3 weeks period.

Observing the images in Figure 3.4 it can be seen that, after one day of culture, just few light blue spots appear, most probably due to the staining of the extracellular matrix. After one week of culture the cell layer is almost completely

covered by a thin but discontinuous light blue layer, but the increased blue intensity implies that a small amount of mucus has been produced. At 14 days, the higher intensity of the colour and its uniformity suggest that the production of mucus has increased and that a mucus blanket uniformly covers the cell layer. At day 21, the mucus still covers all the area but not uniformly, dark blue areas are alternate to light ones; this could be related to the concurrent decrease in TEER between day 14-21 suggesting cell integrity and/or death occurs.

The relative quantification of the mucus production was measured by the RGBb ratio. Figure 3.5 shows the mucus production in terms of RGBb ratio over three weeks. No differences in mucus production can be observed between the different seeding densities at day 1 and day 7. However, at week 2, the intermediate ( $2.50 \times 10^6$  cell/mL) seeding shows a statistically significant increase in mucus production that was statistically higher than the other two densities. This RGBb value subsequently plateaus from day 14 to day 21. While the lowest and highest seeding densities ( $1.25$  and  $5.0 \times 10^6$  cell/mL) showed no statistically differences at both day 14 and 21. These two seeding conditions showed a steady increase in the RGBb ratio value indicating a build-up in the mucus production during all the culturing time. Finally, at day 21, all three seeding density managed to attain similar amount of mucus produced with no significant differences observed between them.

These results suggest that the intermediate seeding density ( $2.50 \times 10^6$  cell/mL) is the optimum condition that allows the cells to form confluent layer with a uniform mucus blanket in 2 weeks in the Snapwell insert. This is probably due to

the optimisation of the growth conditions that allow for the cells to proliferate, sufficient nutrients and space to interact and form tight junctions and produce mucus.

The plateau observed for the intermediate seeding density, can also be a result of the limitations of measurement technique leading to a saturation of the blue RGBb ratio [23]. In addition, being an *in vitro* model, one of the limitations is the static nature of this system where the mucus cannot be cleared leading to build up in the wells with the increasing cell numbers.

Based on the above results for mucus production, TEER measurements and Flu-Na permeability, the optimal seeding density was found to be  $2.50 \times 10^6$  cell/mL for RPMI 2650 cells grown on Snapwell inserts.



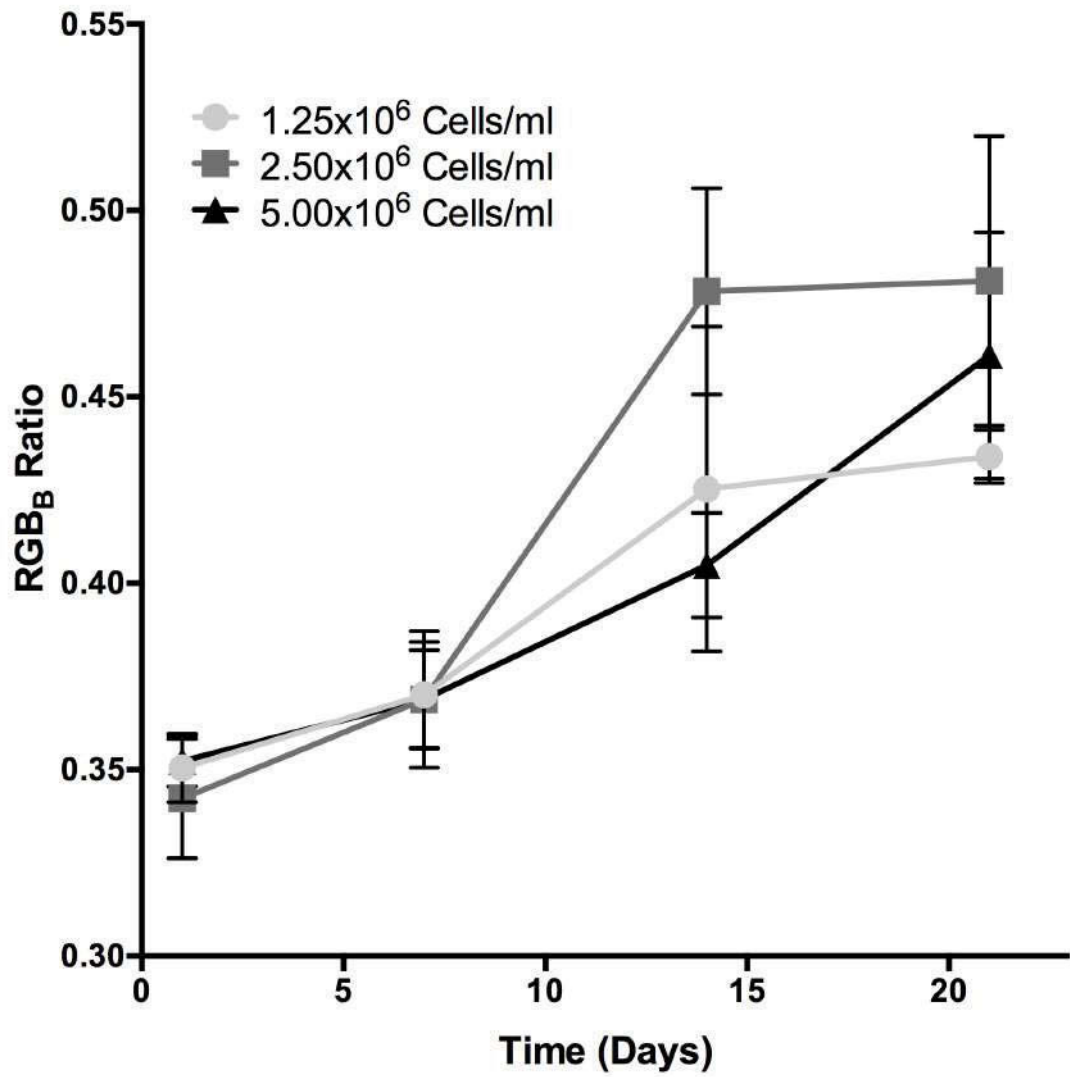
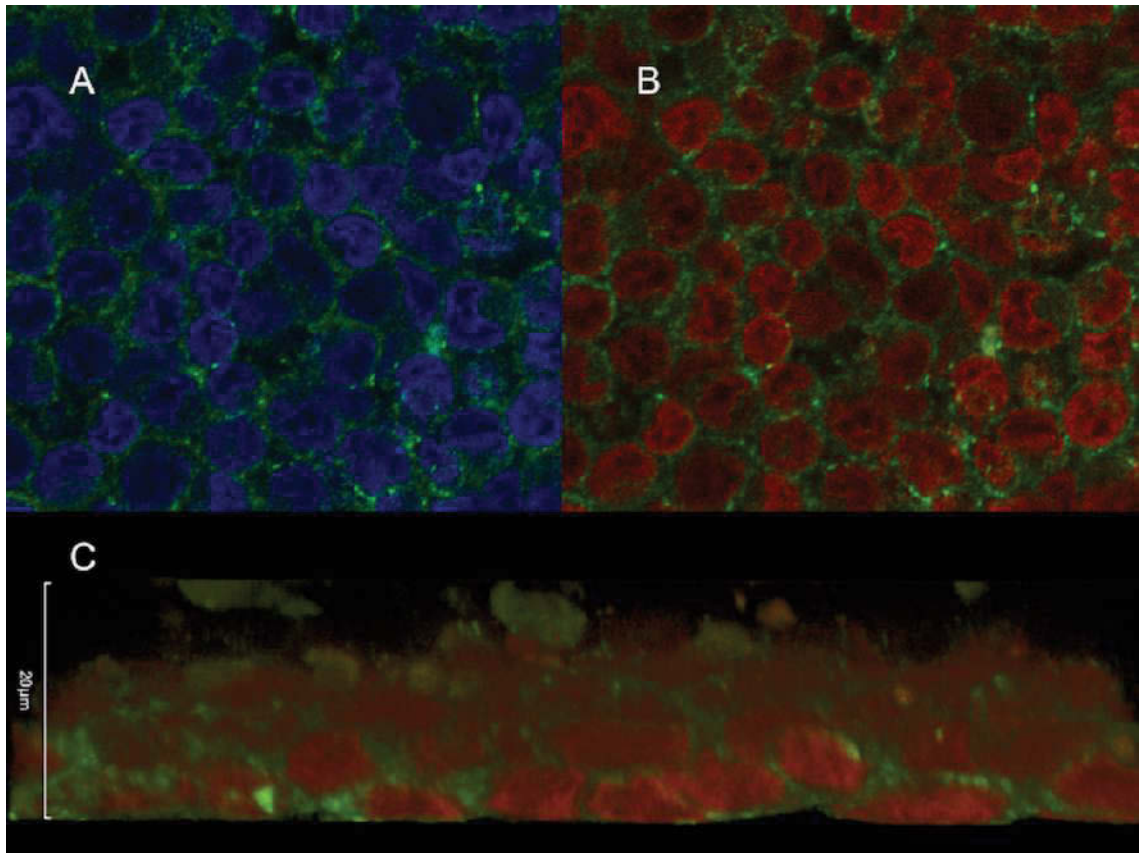


Figure 3.5. RGB<sub>B</sub> ratio values obtained after mucus staining as function of time in culture for the three different cell seeding densities ( $n=3$ ;  $\pm$  StDev).

### 3.4.4 Immunocytochemical investigation

Tight junctions play an important role in the control of the paracellular permeation across the epithelia [33]. In order to confirm that the RPMI 2650 cells on Snapwell inserts were also able to produce tight junctions, the expression and localization of two proteins essential for the formation and maintenance of tight junction were investigated; specifically, E-cadherin and *zonula occludens* protein 1 (ZO-1) (Figure 3.6). Figure 3.6A shows the localization of E-cadherin (green) around the nucleus stained with DAPI (blue) and Figures 2.6B and C show in green the expression of ZO-1 and in red DAPI.

As expected, the proteins are found at the edge of the cells where they are involved in the formation of tight junction in the RPMI 2650 cells. Furthermore, the RPMI 2650 cells was found to form multilayers as seen with the overlapping nuclei in Figure 3.6C. This is different from what Bai et al as observed, where cells were forming a monolayer. However it is in good agreement with Kreft et al that noticed a multi-layering growth of RPMI 2650 when cultured in ALI conditions [19,20].



*Figure 3.6. Confocal Microscope Images of RPMI 2650 cells tight junction proteins- stained in green: E-cadherin (A) and ZO-1 (B-C). The blue and red colours in A and B respectively represent the DAPI staining of nuclei. C, the cross section of cell layers during confocal imaging: green ZO-1 and red cell nucleus.*

### **3.4.5 Expression of Xenobiotic Transporters**

When paracellular transport across epithelia is not involved, membrane carrier proteins can have a key role in the absorption, distribution and elimination processes of both endogenous compounds and xenobiotics [34,35]. In order to cross the epithelia a molecule needs to pass through two barriers; specifically, it needs to be taken up from apical membrane and effluxed from the basal membrane. These processes are often carrier mediated [36].

In order to evaluate if RPMI 2650 could be a representative model of the nasal mucosa, further investigation on the transporters expression in the cell line model was performed and was compared with freshly brushed human nasal cells.

Specifically, 47 xenobiotic transporters were investigated. The genes investigated were those expressing ATP Binding Cassette (ABC), Solute Carrier (SLC) and Solute Carrier Organic anion (SLCO) proteins. Table 3.1 graphically summarizes which of these 47 xenobiotic transporters were present in the RPMI 2650 cells and compared with gene present on PNC: human primary nasal cells from brushing (average between male and female).

Table 3.1. List of drug transporters evaluated and their gene expression ( $\Delta C_t$ ) in RPMI2650 cultivated on Snapwells at  $2.50 \times 10^6$  cell/mL, PNC: human primary nasal cells from brushing (average between male and female). Scale from not expressed (red) to highly expressed (dark green)

Protein Name	Protein Description	Gene code	RPMI 2650	PNC	$\Delta C_t$	Classification
p-gp	P-glycoprotein	ABCB1			30	No Expression
BSEP	Bile Salt Export Pump	ABCB11			15 to 30	Poorly Expressed
MDR3	Multidrug resistance protein 3	ABCB4			5 to 15	Expressed
MRP1	Multidrug resistance-associated protein 1	ABCC1			<5	Highly Expressed
MRP7	Multidrug resistance-associated protein 7	ABCC10				
MRP8	Multidrug resistance-associated protein 8	ABCC11				
MRP9	Multidrug resistance-associated protein 9	ABCC12				
MRP2	Multidrug resistance-associated protein 2	ABCC2				
MRP3	Multidrug resistance-associated protein 3	ABCC3				
MRP4	Multidrug resistance-associated protein 4	ABCC4				
MRP5	Multidrug resistance-associated protein	ABCC5				
MRP6	Multidrug resistance-associated protein 6	ABCC6				
BCRP	breast cancer resistance protein	ABCG2				
NTCP	Sodium-taurocholate cotransporting polypeptide	SLC10A1				
PEPT1	Peptide transporter 1	SLC15A1				
PEPT2	Peptide transporter 2	SLC15A2				
MCT1	Monocarboxylate transporter 1	SLC16A1				
MCT2	Monocarboxylate transporter 2	SLC16A7				
NaPi1	Renal type I sodium/phosphate transporter	SLC17A1				
(OCT1)	Organic cation transporter 1	SLC22A1				
URAT1	Organic anion/urate transporter 1	SLC22A12				
(OCT2)	Organic cation transporter 2	SLC22A2				
(OCT3)	Organic cation transporter 3	SLC22A3				
OCTN1	Organic cation transporter, novel 1	SLC22A4				
OCTN2	Organic cation transporter, novel 2	SLC22A5				
OAT1	Organic anion transporter 1	SLC22A6				
OAT2	Organic anion transporter 2	SLC22A7				
OAT3	Organic anion transporter 3	SLC22A8				
CNT1	Anti-Concentrative Nucleoside Transporter 1	SLC28A1				
CNT2	Anti-Concentrative Nucleoside Transporter 2	SLC28A2				
CNT3	Anti-Concentrative Nucleoside Transporter 3	SLC28A3				
ENT1	Equilibrative nucleoside transporter 1	SLC29A1				
ENT2	Equilibrative nucleoside transporter 2	SLC29A2				
ENT3	Equilibrative nucleoside transporter 3	SLC29A3				
ENT4	Equilibrative nucleoside transporter 4	SLC29A4				
OST $\alpha$	Organic Solute Transporter, Alpha	SLC51A				
ATB(0+)	Sodium- and chloride-dependent neutral and basic amino acid transporter B(0+)	SLC6A14				
OATP-A	Organic anion transporter polypeptide A	SLCO1A2				
OATP-C	Organic anion transporter polypeptide C	SLCO1B1				
OATP-8	Organic anion transporter polypeptide 8	SLCO1B3				
OATP-F	Organic anion transporter polypeptide F	SLCO1C1				
PGT	Prostaglandin Transporter	SLCO2A1				
OATP-B	Organic anion transporter polypeptide B	SLCO2B1				
OATP-D	Organic anion transporter polypeptide D	SLCO3A1				
OATP-E	Organic anion transporter polypeptide E	SLCO4A1				
OATP-H	Organic anion transporter polypeptide H	SLCO4C1				
OATP-J	Organic anion transporter polypeptide J	SLCO5A1				

For the RPMI 2650 cells, the highly expressed genes ( $\Delta Ct < 5$ ) were found to be MRP1 and MRP9 proteins while the poorly expressed genes ( $\Delta Ct > 15$ ) were found to be for the following transporters: BSEP (Bile Salt Export Pump), MRP5 (Multidrug Resistance-associated Protein 5), MRP7, MRP8, OCT3 (Organic Cation Transporter 3), CNT3 (Anti-Concentrative Nucleoside Transporter 3), ENT1 (Equilibrative nucleoside transporter 1) and ENT3. Some genes, such as those expressing MRP6, PEPT1 (Peptide transporter 1), PEPT2, NaPi1 (Renal type I sodium/phosphate transporter), OCT1, OCT2, URAT1 (Organic anion/urate transporter 1), ATB(0+) (Sodium- and chloride-dependent neutral and basic amino acid transporter B(0+)), OATP-C (Organic anion transporter polypeptide C), OATP-8, OATP-F, OATP-B were not expressed at all. All the other genes were expressed at an intermediate level ( $5 < \Delta Ct < 15$ ).

In terms of the primary nasal cells obtained by nasal mucosa brushing, no differences were found between male and female volunteers. Highly expressed genes were those encoding for the following transporter proteins: MDR3, MRP1, MRP9, MRP2, MRP3, MRP4, NTCP (Sodium-taurocholate cotransporting polypeptide), MCT1 (Monocarboxylate transporter 1), OCTN2 (Organic cation transporter, novel 2), CNT3, ENT1, ENT2 and OATP-H. No genes were classified as poorly expressed and only 11 genes were not expressed at all (MRP6, OCT1/2, OCTN1, OAT1/2/3, CNT1/2, ATB (0+) and OATP-F). Corticosteroids, which are one of the main topical nasal active ingredients, are an example of a drug class that is associated with these cell transporters [37,38]. In particular, budesonide and beclomethasone dipropionate (BDP) have shown effect of the expression of BCRP, PGP, OCT1 and OCT2 in Calu-3 and breast cancer cell lines [39,40]. In

addition, budesonide has been identified as substrate of P-glycoprotein (ABCB1) during transport across Caco-2 cell line [41].

Nevertheless, to our knowledge there is a lack of information about their role in the nose [35]. Our data shows that BRCP and PGP are expressed in the nasal epithelium and in the RPMI 2650 model, suggesting that an avenue for future investigations in this direction.

Although the xenobiotic genes expression was found to be higher for primary cells than for RPMI 2650 in general, the same genes were expressed in both primary human mucosa nasal cells and RPMI 2650, highlighting the potential use of RPMI2650 grown on ALI as a suitable model for nasal mucosa. In addition, from the 47 genes that encode for transporter proteins, the 11 that were not expressed in primary cells were also absent in RPMI 2650, further supporting a good correlation between the RPMI 2650 cell model and human nasal mucosa. The following proteins: NaPi1, URAT1, PEPT1, PEPT2, OATP-C and OATP-8 were found to be expressed in brushed nasal cells, but not in RPMI 2650; this could be considered as a limitation to the RPMI 2650 model in terms of transport of peptides and organic anionic substances.

Kreft et al. had previously described the expression of some of xenobiotic transporter genes in RPMI 2650 grown in ALI conditions with two different culturing media and at two culturing time points: 1 and 3 weeks, without finding any relevant differences [20]. Our data correlate nicely with those published by Kreft, suggesting good reproducibility of RPMI2650 cell model.

### 3.4.6 Development and Validation of the Modified Expansion Chamber

The different materials used for the manufacturing of the FDA guideline expansion chamber (glass) and the 3D printed modified chamber (ABS) could raise the question whether or not the aerosol performances and particle deposition in the two chambers could be different. Therefore, in order to validate the 3D printed modified chamber, the aerosol performance of a commercially available nasal spray (Rhinocort Nasal Spray, AstraZeneca, Australia) was evaluated using a NGI cascade impactor using both expansion chambers. Table 3.3 shows the percentage of budesonide (calculate from the nominal dose emitted: 96 µg) recovered in each stage of NGI after 3 actuations of the Rhinocort device (average of 3 runs), using both devices.

*Table 3.3. Amount of Budesonide (% of the nominal dose) recovered from each Stage of the NGI using the Glass and Modified chamber (n=3 ± StDev).*

	<b>Chamber</b>	<b>Connection Tube</b>	<b>Stage 1</b>	<b>Stage 2*</b>
<b>Glass Chamber</b>	98.75±0.09	0.57±0.05	0.50±0.03	0.18±0.04
<b>Modified Chamber</b>	98.73±0.09	0.57±0.07	0.51±0.03	0.19±0.01

\* No Budesonide was found below Stage 2

The amount of drugs in the 3D printed modified chamber was calculated as sum of the mass recovered from both the upper and lower hemisphere and the three



Snapwells in the chamber. As expected, the majority of the drug was found in the chamber demonstrating that the device produced a coarse spray with an aerodynamic diameter that is higher than 10  $\mu\text{m}$ , with minimal respirable fraction. Overall, there were no statistical differences in aerosol performance for Rhinocort between the modified and the glass chamber for all NGI stages (no drug was recovered for stages lower than 2). With the deposition onto the Snapwell inserts,  $13.12 \pm 0.07 \mu\text{g}$  of budesonide were recovered from the three cell inserts after the extraction with 80:20 (v/v) methanol/ water, with approximately 4.4  $\mu\text{g}$  of budesonide on each well. This is equivalent to roughly 13.7% of the dose emitted with each spray of the Rhinocort suspension that reaches each Snapwell inserts.

Having validated the modified chamber in terms of aerosol performance, the RPMI 2650 cells grown on Snapwell inserts were introduced into the modified chamber in order to perform cells permeation experiments. The maintenance of barrier properties and the integrity of the cell layers are key factors for permeation studies. In order to confirm that the handling of the Snapwell inserts and the process of deposition into the modified chamber were not hampering the barrier properties of RPMI 2650 nasal cell model, a solution of HBSS was sprayed 6 times on the RPMI2650 nasal cells into the chamber. The cells were removed from the chamber and after 4 hours of Flu-Na permeation studies, the  $P_{\text{app}}$  was calculated. No statistical differences were found ( $p < 0.05$ ) between the  $P_{\text{app}}$  values of control and treated cells.

Finally, deposition and permeation experiments were performed using a budesonide commercial spray and with the 3D printed modified expansion

chamber connected to the cascade impactor, using the three Snapwells inserts with RPMI 2650 cells grown for 14 days. The formulation was deposited on the cells after device actuation and RPMI 2650 cells inserts were placed back in cell culture plates to perform the permeation study.

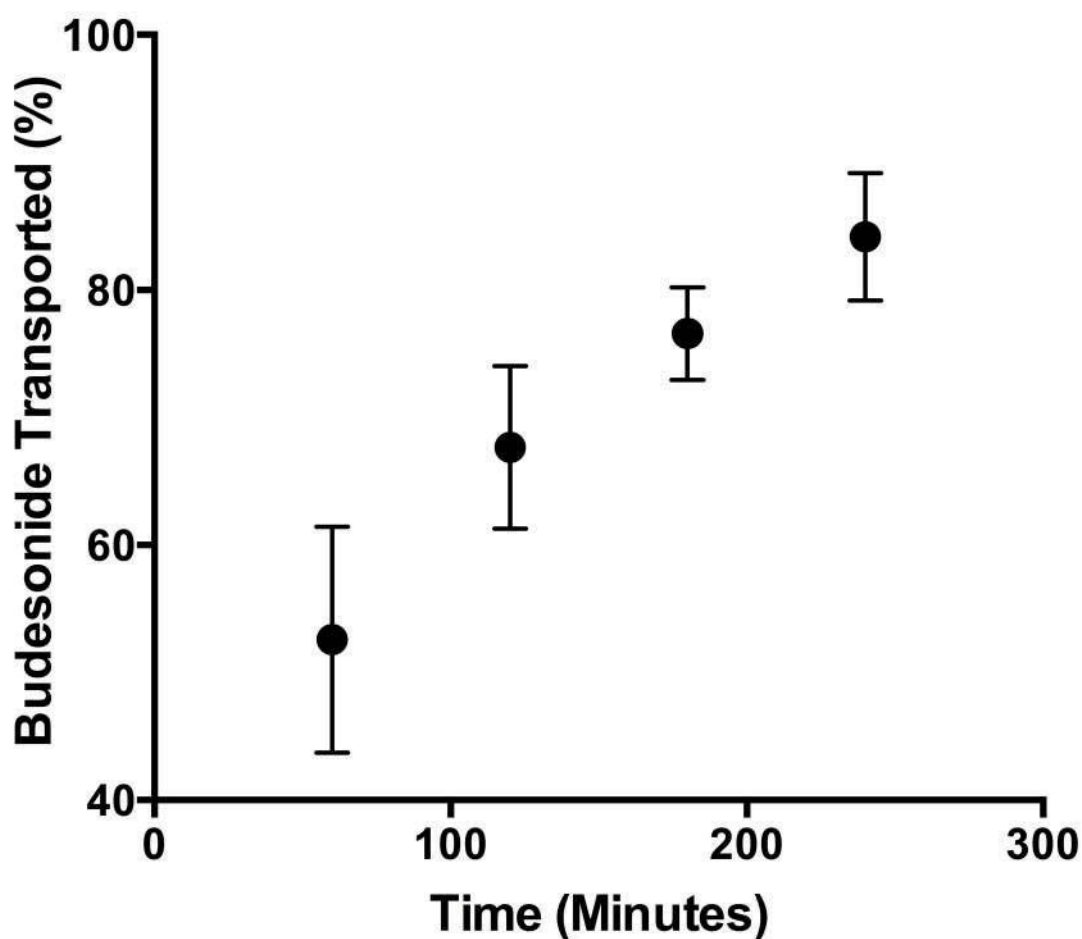


Figure 3.7. Amount of budesonide transported through RPMI 2650 nasal cell model after NGI aerosols deposition using the 3D modified chamber ( $n=5 \pm StDev$ ).

Figure 3.7 shows the percentage of budesonide transported across the nasal cell model after deposition in the 3D MC; the In the first hour, approximately  $47.3 \pm$

5.0 % of the drug was transported. This can be explained, as suggested by Baumann, due to the high quantity of available budesonide dissolved in the commercially available product to bind and diffuse readily through the epithelium [42,43]. At the end of the experiment (4 hours),  $83.1 \pm 6.3$  % of the total drug deposited reached the basal compartment. Between three to four hours, a decreased permeation rate was observed, probably due to the depletion of budesonide on the surface of the cells that consequently decreases the gradient between the two compartments (apical and basal). The total amount of budesonide found on each well was on average of  $0.79 \pm 0.25$   $\mu\text{g}$ . This was calculated from the sum of the budesonide on, in and transported across the cell layer; the total amount recovered from each ~~single~~ well was used as 100% reference values for the calculation in the cell deposition/ transport studies. This variability of the amount of budesonide deposited on each well could be related to both the plume geometry of Rhinocort nasal spray and the manual activation of the device, that don't allow a uniform deposition on each well. The integrity of the cell layer was maintained within the time scaled study with no statistical differences ( $p > 0.05$ ) was found between TEER values before ( $126 \pm 21 \Omega \cdot \text{cm}^2$ ) and after ( $127 \pm 14 \Omega \cdot \text{cm}^2$ ) the transport studies.

As shown in Figure 3.8, after 4 hours  $14.4 \pm 4.9$  % of the drug remains on the surface of the cell and  $2.5 \pm 1.6$  % of budesonide was found inside the cells, suggesting low binding and internalization within the cells of the RPMI 2650 nasal mucosa model. This is in good agreement with results found by Baumann where lower levels of budesonide drug bind to human nasal tissue when compared with other glucocorticoids [42].

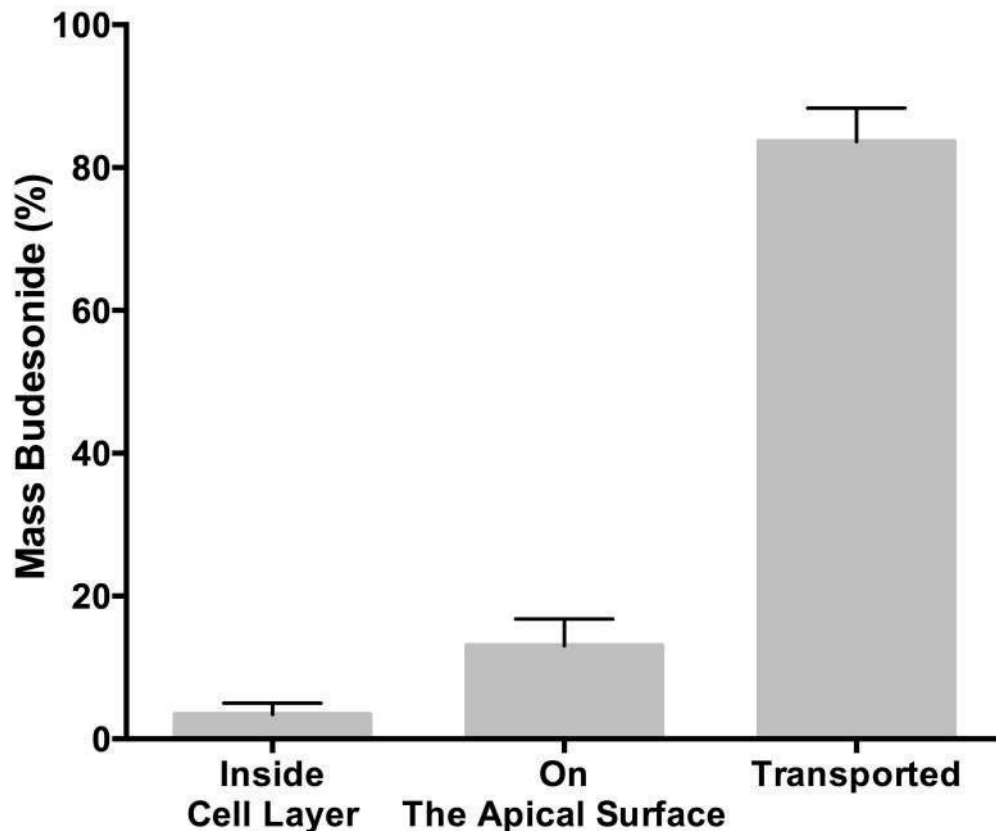


Figure 3.8. Distribution of the budesonide recovered at the end of the experiment (4 hours) after the aerosol deposition using the 3D the modified expansion chamber ( $n=5 \pm StDev$ ).

### 3.5 CONCLUSION

This research has shown that RPMI 2650 cells could be successfully grown on Snapwell inserts. The cells form a continuous layer offering a permeation barrier similar in terms of trans-epithelial electrical resistance and sodium fluorescein paracellular permeation to previously reported nasal epithelium models and more importantly to excised human nasal mucosa. It was also shown that RPMI 2650 cells produce mucus and its production is related to seeding density and time in culture. The optimal conditions for RPMI 2650 to achieve the highest epithelial

barrier and a complete coating with mucus layer are: Snapwell polycarbonate inserts at seeding density of  $2.50 \times 10^6$  cell/mL and cultured for 14 days in ALI culture. Regarding protein transporters expression, RPMI 2650 cells represent a good model of the nasal epithelium, correlating well with gene expression of freshly collected human nasal epithelial cells. A 3D printed modified expansion chamber, which allow deposition of nasal formulation directly on RPMI 2650 grown on Snapwell inserts has been successfully designed, validated and tested using a commercial nasal spray, showing that this model could be used concomitantly to study nasal formulations aerosol deposition and permeation through a nasal epithelium model of the aerosolized formulation.

### **3.6 ACKNOWLEDGEMENTS**

A/Professor Traini is the recipient of an Australian Research Council Future Fellowship (project number FT12010063). A/Professor Young is the recipient of an Australian Research Council Future Fellowship (project number FT110100996).

### **3.7 AUTHOR DISCLOSURE STATEMENTS**

No conflicts of interest exist.

### 3.8 REFERENCES

1. Illum L. Nasal drug delivery - recent developments and future prospects. *J. Control. Release.* 2012;161:254–63.
2. Merkle HP, Ditzinger G, Lang SR, Peter H, Schmidt MC. In vitro cell models to study nasal mucosal permeability and metabolism. *Adv. Drug. Deliv. Rev.* 2000 ed. 1998;29:51–79.
3. Saluja V, Amorij JP, van Roosmalen ML, Leenhouts K, Huckriede A, Hinrichs WLJ, et al. Intranasal delivery of influenza subunit vaccine formulated with GEM particles as an adjuvant. *AAPS J.* 2010;12:109–16.
4. Grassin-Delyle S, Buenestado A, Naline E, Faisy C, Blouquit-Laye S, Couderc L-J, et al. Intranasal drug delivery: an efficient and non-invasive route for systemic administration: focus on opioids. *Pharmacol. Ther.* [Internet]. 2012;134:366–79. <http://dx.doi.org/10.1016/j.pharmthera.2012.03.003>
5. Touitou E, Lisbeth I. Nasal drug delivery. *Drug Deliv. and Transl. Res.* 2013;3:1–3.
6. Wu H, Hu K, Jiang X. From nose to brain: understanding transport capacity and transport rate of drugs. *Expert Opin. Drug Deliv.* 2008;5:1159–68.
7. Quraishi MS, Jones NS, Mason JD. The nasal delivery of drugs. *Clin Otolaryngol Allied Sci.* 1997;22:289–301.
8. Djupesland PG. Nasal drug delivery devices: characteristics and performance in a clinical perspective—a review. *Drug Deliv. and Transl. Res.* 2013;3:42–62.
9. Comfort C, Garrastazu G, Pozzoli M. Opportunities and Challenges for the Nasal Administration of Nanoemulsions. *Curr. Top. Med. Chem.* 2015;15:356–68.
10. Merkus F, Verhoef J, Schipper N, Marttin E. Nasal mucociliary clearance as a factor in nasal drug delivery. *Adv Drug Deliv Rev.* 1998;29:13–38.
11. Great Britain SO. *British Pharmacopoeia.* London: Stationery Office;

## Appendix XII C. Consistency of Formulated Preparations.

12. U.S. Department of Health and Human Services, Food and Drug Administration, Center for Drug Evaluation and Research. Bioavailability and Bioequivalence Studies for Nasal Aerosols and Nasal Sprays for Local Action. 2003;1–37.

13. Doub WH, Adams WP, Wokovich AM, Black JC, Shen M, Buhse LF. Measurement of drug in small particles from aqueous nasal sprays by Andersen Cascade Impactor. *Pharm Res.* 2012;29:3122–30.

14. Haghi M, Traini D, Young P. In vitro cell integrated impactor deposition methodology for the study of aerodynamically relevant size fractions from commercial pressurised metered dose inhalers. *Pharm Res.* 2014;31:1779–87.

15. Grainger CI, Greenwell LL, Martin GP, Forbes B. The permeability of large molecular weight solutes following particle delivery to air-interfaced cells that model the respiratory mucosa. *Eur. J. Pharm. Biopharm.* 2009;71:318–24. <http://dx.doi.org/10.1016/j.ejpb.2008.09.006>

16. Bur M, Rothen-Rutishauser B, Huwer H, Lehr C-M. A novel cell compatible impingement system to study in vitro drug absorption from dry powder aerosol formulations. *Eur. J. Pharm. Biopharm.* 2009; 72:350–7. <http://dx.doi.org/10.1016/j.ejpb.2008.07.019>

17. De Fraissinette A, Brun R, Felix H, Vonderscher J, Rummelt A. Evaluation of the human cell line RPMI 2650 as an in vitro nasal model. *Rhinology.* 1995 ed. 1995;33:194–8.

18. Wengst A, Reichl S. RPMI 2650 epithelial model and three-dimensional reconstructed human nasal mucosa as in vitro models for nasal permeation studies. *Eur J Pharm Biopharm.* 2010;74:290–7.

19. Bai S, Yang T, Abbruscato TJ, Ahsan F. Evaluation of human nasal RPMI 2650 cells grown at an air-liquid interface as a model for nasal drug transport studies. *J. Pharm. Sci.* 2007 ed. 2008;97:1165–78.

20. Kreft ME, Jerman UD, Lasič E, Lanišnik Rižner T, Hevir-Kene N, Peternel L, et al. The characterization of the human nasal epithelial cell line RPMI 2650 under different culture conditions and their optimization for an appropriate in vitro nasal model. *Pharm Res.* 2015;32:665–79.
21. Reichl S, Becker K. Cultivation of RPMI 2650 cells as an in-vitro model for human transmucosal nasal drug absorption studies: optimization of selected culture conditions. *J. Pharm. Pharmacol.* 2012 ed. 2012;64:1621–30.
22. Kim D-D. In Vitro Cellular Models for Nasal Drug Absorption Studies. *Biotechnology: Pharmaceutical Aspects.* 2008;Chapter 9 of a book:216–34.
23. Haghi M, Young PM, Traini D, Jaiswal R, Gong J, Bebawy M. Time- and passage-dependent characteristics of a Calu-3 respiratory epithelial cell model. *Drug Dev. Ind. Pharm.* 2010 ed. 2010;36:1207–14.
24. Schneider CA, Rasband WS, Eliceiri KW. NIH Image to ImageJ: 25 years of image analysis. *Nat methods.* 2012.
25. Clarke LA, Sousa L, Barreto C, Amaral MD. Changes in transcriptome of native nasal epithelium expressing F508del-CFTR and intersecting data from comparable studies. *Respir. Res.* 2013;14:38.
26. Harris CM, Mendes F, Dragomir A, Doull IJM, Carvalho-Oliveira I, Bebok Z, et al. Assessment of CFTR localisation in native airway epithelial cells obtained by nasal brushing. *J. Cyst. Fibros.* 2004;3 Suppl 2:43–8.
27. Ong HX, Traini D, Ballerin G, Morgan L, Buddle L, Scalia S, et al. Combined inhaled salbutamol and mannitol therapy for mucus hyper-secretion in pulmonary diseases. *AAPS J* [Internet]. 2014;16:269–80. Available from: <http://eutils.ncbi.nlm.nih.gov/entrez/eutils/elink.fcgi?dbfrom=pubmed&id=24431080&retmode=ref&cmd=prlinks>
28. Beck S, Beck S, Penque D, Penque D, Garcia S, Garcia S, et al. Cystic fibrosis patients with the 3272-26A?G mutation have mild disease, leaky alternative mRNA splicing, and CFTR protein at the cell membrane. *Hum. Mutat.* 1999;14:133–44.



29. Kuchipudi SV, Tellabati M, Nelli RK, White GA, Perez BB, Sebastian S, et al. 18S rRNA is a reliable normalisation gene for real time PCR based on influenza virus infected cells. *Viol. J.* 2012;9:230.
30. Naikwade SR, Bajaj AN. Development of validated specific HPLC method for budesonide and characterization of its alkali degradation product. *Can J Anak Sci Spect* [Internet]. 2008;53:113–22. Available from: [https://www.researchgate.net/profile/Sonali\\_Bharate/publication/224910736\\_Development\\_of\\_validated\\_specific\\_HPLC\\_method\\_for\\_budesonide\\_and\\_characterization\\_of\\_its\\_alkali\\_degradation\\_product/links/09e41510127fcc9d56000000.pdf](https://www.researchgate.net/profile/Sonali_Bharate/publication/224910736_Development_of_validated_specific_HPLC_method_for_budesonide_and_characterization_of_its_alkali_degradation_product/links/09e41510127fcc9d56000000.pdf)
31. Cotton CU, Stutts MJ, Knowles MR, Gatzky JT, Boucher RC. Abnormal apical cell membrane in cystic fibrosis respiratory epithelium. An in vitro electrophysiologic analysis. *J. Clin. Invest.* 1987;79:80–5.
32. Suman JD. Current understanding of nasal morphology and physiology as a drug delivery target. *Drug Deliv. and Transl. Res.* 2013;3:4–15.
33. Subramanian VS, Marchant JS, Ye D, Ma TY, Said HM. Tight junction targeting and intracellular trafficking of occludin in polarized epithelial cells. *AJP: Cell Physiology.* 2007;293:C1717–26.
34. Salomon JJ, Muchitsch VE, Gausterer JC, Schwagerus E, Huwer H, Daum N, et al. The Cell Line NCI-H441 Is a Useful in Vitro Model for Transport Studies of Human Distal Lung Epithelial Barrier. *Mol. Pharmaceutics.* 2014.
35. Nickel S, Clerkin CG, Selo MA, Ehrhardt C. Transport mechanisms at the pulmonary mucosa: implications for drug delivery. *Expert Opin. Drug Deliv.* 2016;:1–24.
36. Bleasby K, Castle JC, Roberts CJ, Cheng C, Bailey WJ, Sina JF, et al. Expression profiles of 50 xenobiotic transporter genes in humans and pre-clinical species: a resource for investigations into drug disposition. *Xenobiotica.* 2006;36:963–88.
37. Trangsrud AJ, Whitaker AL, Small RE. Intranasal corticosteroids for allergic

rhinitis. *Pharmacotherapy*. 2002;22:1458–67.

38. Berger WE, Godfrey JW, Slater AL. Intranasal corticosteroids: the development of a drug delivery device for fluticasone furoate as a potential step toward improved compliance. *Expert Opin. Drug Deliv*. 2007;4:689–701.

39. Hamilton KO, Yazdanian MA, Audus KL. Modulation of P-glycoprotein activity in Calu-3 cells using steroids and beta-ligands. *International Journal of Pharmaceutics* [Internet]. 2001;228:171–9. Available from: <http://linkinghub.elsevier.com/retrieve/pii/S0378517301008365>

40. Cooray HC, Shahi S, Cahn AP, van Veen HW, Hladky SB, Barrand MA. Modulation of p-glycoprotein and breast cancer resistance protein by some prescribed corticosteroids. *Eur. J. Pharmacol*. 2006;531:25–33.

41. Dilger K, Schwab M, Fromm MF. Identification of budesonide and prednisone as substrates of the intestinal drug efflux pump P-glycoprotein. *Inflamm. Bowel Dis*. 2004;10:578–83.

42. Baumann D, Bachert C, Högger P. Development of a novel model for comparative evaluation of intranasal pharmacokinetics and effects of anti-allergic nasal sprays. *Eur J Pharm Biopharm*. 2012;80:156–63.

43. Baumann D, Bachert C, Högger P. Dissolution in nasal fluid, retention and anti-inflammatory activity of fluticasone furoate in human nasal tissue ex vivo. *Clin. Exp. Allergy*. 2009;39:1540–50.

## CHAPTER 4

### *Evaluation of Beclomethasone Dipropionate formulations: Suspension VS Powder*

This chapter is the combination of two peer-reviewed conference proceeding:

1. Validation of a Novel Apparatus for Deposition Studies of Nasal Products. In Respiratory Drug Delivery Europe (RDD 2015). 2015: 537-541. Authors: Pozzoli M, Cattaneo S, Zhu B, Traini D, Young PM and Sonvico F.
2. . Transport of Beclometasone Dipropionate Across RPMI 2650 Model of Nasal Epithelium: Evaluation of Two Different Approaches to Drug Delivery. In Respiratory Drug Delivery (RDD 2016). 2016: 607–610. Authors: Pozzoli M, Ong HX, Sonvico F., Young PM and Traini D.

## **4.0 PREFACE**

In Chapter 3, RPMI 2650 cell line was developed and characterized as nasal model for drug absorption using ALI culturing conditions. Subsequently, the cell model was integrated with a modified expansion chamber for cascade impactor studies and validated using a commercial nasal suspension.

In this chapter, the main focus was the validation of the apparatus with two different commercial products, containing the same active ingredient but delivered with different dosage forms (powder and suspension). Secondly, the evaluation of their absorption profiles after the drug is deposited on RPMI 2650 using the modified expansion chamber. Lastly, a comparison between the novel approach of deposition/ transport studies and a more conventional way.

## 4.1 INTRODUCTION

Allergic rhinitis is a hypersensitivity reaction to inhaled allergens. It produces inflammation of the nasal mucosa characterized by nasal congestion, sneezing, itching and rhinorrhoea [1]. Intranasal corticosteroids are highly effective in preventing and relieving early- and late-phase symptoms. Different types of formulations are available on the market for the treatment of rhinitis.

As discussed in Chapter 1, powder formulations present some potential advantages, such as the absence of harmful preservatives and higher chemical stability, compared to water spray pumps [2-4].

An important parameter for the development of a nasal product, both in form of powder or suspension, is the particle size distribution of the aerosolized particles [5-7]. Indeed, particle size affects the area of deposition inside the nasal cavity and thereafter the absorption profiles [4,8,9]. Specifically, droplets or particles are required to provide optimal nasal deposition and prevent inhalation into the lower airways, with an aerodynamic diameter requirement exciding  $9\ \mu\text{m}$  [10]. According to the 2003 Food and Drug Administration (FDA) draft guidance “Bioavailability and Bioequivalence Studies for Nasal Aerosols and Nasal Sprays for Local Action”, the evaluation of nasal droplet size distribution can be performed by either laser diffraction or cascade impaction (CI), employing in this latter case an additional 2 L expansion chamber as induction port [11]. However, neither methods are suitable for investigating real-time drug deposition on the nasal mucosa.

In Chapter 3 the development of a new apparatus to test the deposition/permeation of a nasal spray was described. The new apparatus was validated using a commercial budesonide nasal spray suspension. However,

different drugs and formulations are available on the nasal products market. Therefore, the need to validate and evaluate the performances of other different formulations arises. This is of special interest for the characterisation of powder formulations. Indeed, the interactions (e.g. electrostatic) between the different materials composing the chambers (glass and plastic) could have an effect on the aerosol performances of the formulation [12].

Beclomethasone dipropionate (BDP) is a commonly used glucocorticoid pro-drug which is hydrolysed to its active form, beclomethasone-17-monopropionate (BMP) [13]. In Australia, BDP is commercially available over the counter as an aqueous suspension, e.g. Beconase (Glaxosmithkline), delivered via a metered-dose nasal spray pump. In Japan, BDP is also available as a powder formulation commercialized as Rhinocort (Teijin Pharma, Tokyo, Japan) [14].

Furthermore, the conventional way to test *in vitro* permeation of drugs through cells monolayers is to add the drug solution or suspension at different concentrations to their apical side when growing on transwell inserts [15,16]. However, this method is not representative of the *in vivo* processes that occur following nasal steroid administration, where aerosolized drugs in either suspension or powder form are deposited on to the nasal mucosa by impaction. The first aim of this study was to validate the modified expansion chamber, presented in Chapter 3, using two different type of formulation of the corticosteroid pro-drug BDP: a water based suspension (Beconase) and a dry powder spray (Rhinocort).

The second aim this study was to compare the conventional *in vitro* BDP drug permeation of a suspension with a novel deposition method that allows the

delivery of drug aerosols generated from both liquid-based and powder-based nasal devices directly onto the surface of cultured nasal cells.

## **4.2 MATERIAL AND METHODS**

### **4.2.1 Materials**

Beclomethasone dipropionate and monopropionate (BDP and BMP) powder standards were kindly provided by Chiesi Farmaceutici (Chippenham, UK).

Water used in the analyses was purified by reverse osmosis (MilliQ, Millipore-Merck, Germany). Beconase (Glaxosmithkline, Abbotsford, VIC, Australia) BDP suspension nasal spray and Rhinocort (Teijin Pharma, Tokyo, Japan) dry powder spray were purchased and used as supplied.

Human nasal septum carcinoma derived cells (RPMI 2650) were purchased from the American Type Cell Culture Collection (ATCC, Rockville, USA). Minimum Essential Medium (MEM), Phosphate Buffer Saline (PBS) and Hank's Balanced Salt Solution (HBSS) were all purchased from Life Technologies (Sydney, Australia). CellLytic™ M reagent was purchased from Sigma-Aldrich (Sydney, Australia). All solvents were obtained from Chem-Supply (South Australia, Australia) and were of HPLC grade.

### **4.2.2 Aerosol Performances and Modified Expansion Chamber Validation**

A Next Generation Impactor (NGI, Westech Ltd., UK) equipped with a standard glass expansion chamber for nasal testing was used for determining the aerodynamic particle size distribution of nasal product (Figure 4.1A).

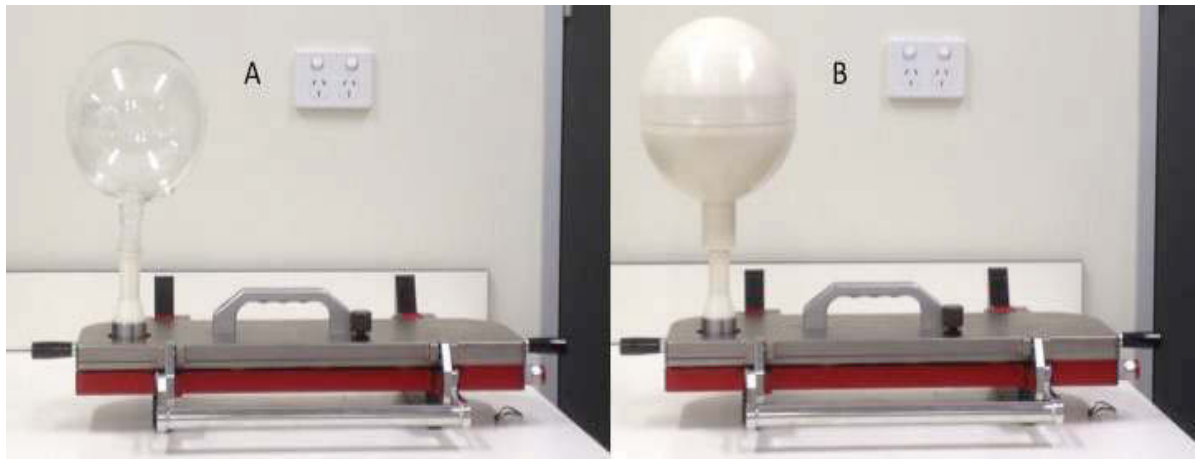


*Figure 4.1. NGI configuration with Glass Expansion Chamber (A) and Modified Chamber printed in ABS (B).*

A 2 L single-neck round bottomed glass flask with a 1 cm inlet hole at 30° from the neck axis was used as an expansion chamber (EC) for the aerosol deposition experiments (Fig 4.1A). The modified expansion chamber (MC, Fig 2A) was designed using Catia 3D design software (3DS, Boston, USA, see Figures 1B and 2) as previously described in Chapter 3. Briefly, computer designed drawings were printed in acrylonitrile butadiene styrene (ABS) using a 3D printer (Dimension Elite, USA).

The modified expansion chamber was composed of two spherical interlocking hollow hemispheres. The lower hemisphere contained the opening for the NGI connection and the inlet hole for the nasal device at 30° from the neck axis. The upper hemisphere was designed in order to accommodate three cell culture inserts (Snapwell™, Corning Costar, USA) located directly opposite to the inlet hole, Figure 4.2.



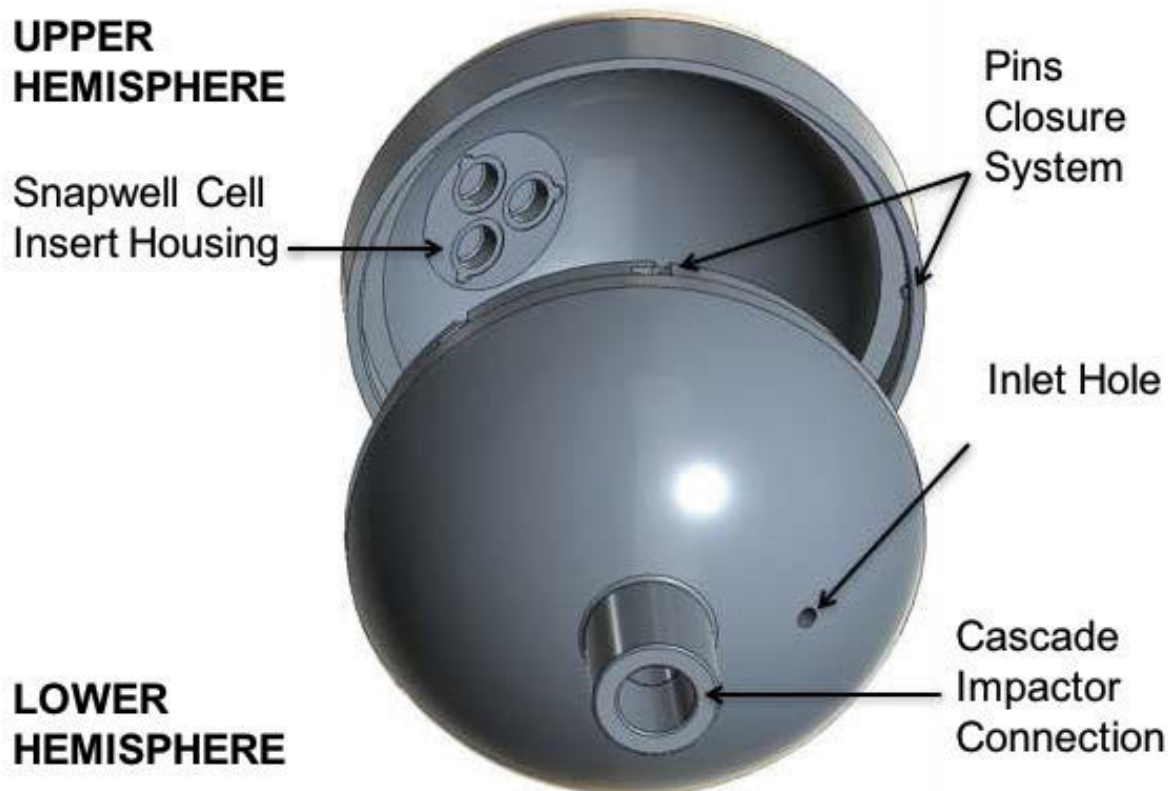


Figure 4.2. CAD 3D drawing of the Modified Expansion Chamber. Modified from Chapter 3.

The system design allowed easy access to the expansion chamber inner surface and handling of cell inserts.

Two different nasal products used for the treatment of rhinitis, both containing beclomethasone dipropionate (BDP) as active ingredient, were chosen to compare the two expansion chambers and validate the deposition in the modified expansion chamber.

Beconase<sup>®</sup> (GSK, Australia) was used as it is a nasal liquid product providing a nominal dose of 50 µg/spray with a 100 uL spray. It contains microcrystalline cellulose, sodium carboxymethylcellulose, dextrose, polysorbate 80, phenylethyl alcohol (2.5 uL/g) and benzalkonium chloride (0.2 mg/g). Teijin Rhinocort<sup>®</sup> (Teijin,

Japan) was used as the BDP nasal dry powder formulation. Teijin Rhinocort is a capsule-based device with each capsule containing a nominal dose of 50 µg of BDP, hydroxypropylcellulose (HPC) as carrier and magnesium stearate.

For each product (dry powder and liquid suspension) aerosol deposition experiments were performed, using both the glass EC and the 3D printed MC. The NGI was connected to a pump (Westech Scientific, UK) and flow rate set at 15 L.min<sup>-1</sup>, using a calibrated flow meter (Model 4040F; TSI Incorporated, MN, USA).

For each experiment, 3 capsules were used (8 actuations for each capsule) for the Teijin Rhinocort and 3 actuations and Beconase, respectively.

#### **4.2.3 In-line *In Vitro* Aerosol Laser Diffraction Analysis**

Particle sizing of the emitted dose was measured using laser diffraction (Spraytec™, Malvern Instrument, UK). Briefly, the devices were placed at 2.5 cm from the Inhaler Nebulizer Accessory (i.e. 5.5 cm from the laser beam), tilted at a fixed angle of 30° and actuated at a flow rate of 15 L.min<sup>-1</sup>, resembling the *in vivo* process of drug administration. Data were analysed considering the stable phase of the spray only.

#### **4.2.4 Cultivation of RPMI 2650 cell line in Air Liquid Interface**

A nasal epithelia cell line (RPMI 2650; ATCC, USA), was grown and passaged according to ATCC protocol, with complete Minimum Essential Medium containing 10% foetal bovine serum (Gibco, Life Technologies, Australia) 1X non-essential amino acid solution (Sigma Aldrich, Australia) and 2 mM L-glutamine, which was incubated at 37°C in a humidified atmosphere containing 5% CO<sub>2</sub>. To

establish an air-liquid interface (ALI) model, 200  $\mu\text{L}$  of nasal cells suspensions ( $2.5 \times 10^6$  cell/ mL) were seeded on Snapwell™ polyester membrane inserts (1.13  $\text{cm}^2$ , 0.4  $\mu\text{m}$  pore size, Corning Costar, USA). After 24 hours, the media from the apical compartment was removed. Transport studies were performed after 14 days of cell differentiation at the ALI configuration [17].

#### 4.2.5 Transport Studies on Nasal Cell Model (Conventional and after Deposition)

To investigate and compare the effects of BDP aerosol deposition, a 'conventional' transport study was performed by adding 250  $\mu\text{L}$  of 15  $\mu\text{g}/\text{mL}$  BDP HBSS (Hanks' Balanced Salt Solution, Life Technologies, Australia) suspension directly to the apical surface of RPMI 2650 nasal cells (control formulation) Figure 4.3A [16].

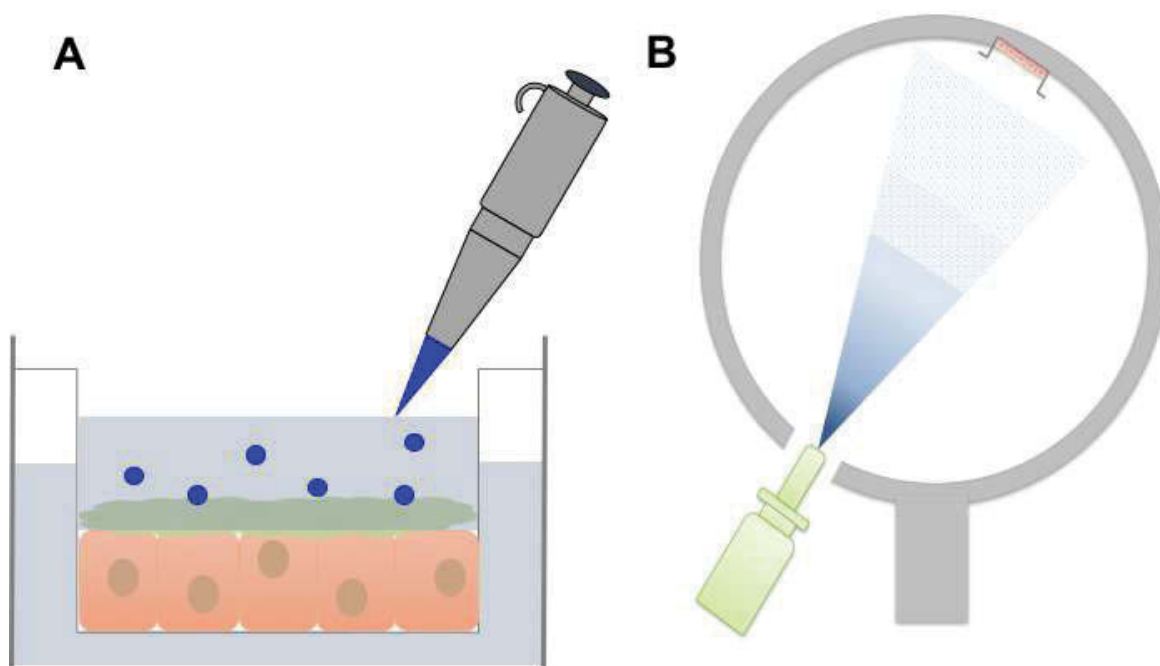


Figure 4.3. Exemplification of conventional transport (A), Deposition of Nasal Products on cells (B)

To study the transport of BDP after aerosol deposition, Apparatus E British Pharmacopoeia (Westech Scientific, Bedfordshire, UK) equipped with a previously described modified expansion chamber, that holds Transwell Cell inserts, was used to mimic the deposition of BDP from both the dry powder and suspension nasal formulations (Figure 4.3B) [18,19]. Briefly, cell inserts were removed from the cultured plates and washed with pre-warmed HBSS. Subsequently, the Snapwell inserts were transferred into the modified nasal deposition chamber. For each formulation (dry powder and liquid suspension) a total of 150 µg of BPD was delivered into the chamber where the wells were located. Apparatus E was connected to a pump (Westech Scientific, Bedfordshire, UK) and flow rate was set to 15 L.min<sup>-1</sup>, using a calibrated flow-meter (Model 4040F; TSI Incorporated, MN, USA). Cell inserts after deposition were repositioned on culture plates and transport studies were performed for a total of 4 hours. Samples (200 µL) were withdrawn every hour and media restored with fresh HBSS buffer to maintain the same buffer level. At the end of the experiment, the cell layer surface was washed to collect the drug on the surface of the cells before cell lysis to analyse the intracellular content of drugs.

#### **4.2.6 Chemical Quantification of Beclomethasone Dipropionate and its Metabolites**

BDP and BMP samples were quantified using reverse phase HPLC system equipped with UV-detector (Shimadzu Corporation, Japan) and Luna C18 column (3 µm, 4.6x150 mm, Phenomenex, NSW, Australia). Mobile phase was a mixture methanol: water (80:20 %v/v), flow rate 0.8 mL.min<sup>-1</sup>, with detector operating at

243 nm and retention time of ~ 6 and 9 minutes for BMP and BDP respectively. Standards were prepared in the mobile phase, and 100 uL injections were used. Linearity was confirmed between 0.1 µg/mL and 50 µg/mL.

#### **4.2.7 Statistics**

Unless stated otherwise, data represent the mean ± standard deviation of at least three independent experiments. A student t-Test was used to compare data, with differences considered statistically significant where  $p < 0.05$ .

### **4.3 RESULTS AND DISCUSSION**

#### **4.3.1 Aerosol Performances Expansion Chamber Validation**

The difference in aerosol deposition between the MC and reference EC for the two nasal products were evaluated using NGI and results are listed below in Table 4.1.

Table 4.1. Comparison of BDP mass deposition in the standard glass and the modified chamber using the NGI ( $n=3 \pm \text{StDev}$ )

	Mass BDP		Mass BDP		Mass BDP	
	Expansion Chamber ( $\mu\text{g}$ )		Throat (Connection) ( $\mu\text{g}$ )		Stage 1 ( $\mu\text{g}$ )	
	Standard	Modified	Standard	Modified	Standard	Modified
<b>Rhinocort</b>	130.2 $\pm$ 6.9	126.8 $\pm$ 6.9	0.83 $\pm$ 0.17	0.85 $\pm$ 0.13	6.7 $\pm$ 2.0	6.4 $\pm$ 0.3
<b>Beconase</b>	158.1 $\pm$ 2.5	155.1 $\pm$ 2.5	0.44 $\pm$ 0.15	0.34 $\pm$ 0.13	NA	NA

No BDP was deposited on stages below Stage 1 of the NGI, confirming that the aerodynamic diameter of the products is suitable for nasal purposes. For both Rhinocort and Beconase, no statistical difference ( $p \geq 0.05$ ) was found between the amount of BDP deposited in the glass and the modified chamber, suggesting that the modified expansion chamber could be used routinely for aerodynamic size fractioning and deposition studies. For the powder formulation tested, Rhinocort, BDP was found deposited also on the first stage of the NGI. On the contrary, no BDP reached stage 1 of the NGI when a suspension formulation, Beconase, was used. Regarding BDP deposited on the Snapwells using the modified chamber, for the liquid suspension formulation 40.0% of the BDP was recovered on the 3 Snapwell inserts, while only 3.4% was recovered on the Snapwell inserts when the dry powder formulation was used. This could be attributed to the different shape and velocity of the aerosol plume obtained from the two devices.

Cascade impaction does not provide information about the final particle size of the whole formulation, but only the fraction containing the active ingredients. In order to fully characterize the particle size distribution of the emitted droplets/particles from the two nasal devices, laser diffraction was used.

As shown in Table 4.2, the particle size distribution of the BDP powder is larger than the particle size of the droplets obtained with the spray device.

Table 4.2. Summary of the particle size of Teijin Rhinocort and Beconase ( $n=3$ ,  $\pm$  StDev)

	Rhinocort ( $\mu\text{m}$ )	Beconase ( $\mu\text{m}$ )
Dv10	47.7 $\pm$ 6.6	24.2 $\pm$ 3.7
Dv50	93.7 $\pm$ 2.9	58.5 $\pm$ 11.1
Dv90	163.3 $\pm$ 4.2	122.7 $\pm$ 24.7
%<10 $\mu\text{m}$	1.0 $\pm$ 0.7	1.1 $\pm$ 0.3

The absence of BDP on NGI Stage 1 for Beconase (despite a lower Dv50 and the higher percentage of deposition on the Snapwell) could be explained by the higher kinetic energy provided to the particles expelled from the liquid pump, resulting in the spray hitting the wall of the expansion chamber without complete aerosolization [10]. The lower energy provided by the dry powder formulation and device allows a complete development of the plume in the expansion chamber and the deposition of a small particle fraction in NGI Stage 1.

#### 4.3.2 Transport Studies on Nasal Cell Model

The sum of BDP and BMP (expressed as a percentage of total drug recovered) transported across the RPMI 2650 nasal cell model is shown in Figure 4.4. Overall, the 15  $\mu\text{g}/\text{mL}$  suspension delivered by direct addition on the surface of the cells, showed the highest drug permeation across the cell layer, with 35% of the drug transported after 4 hours. The Beconase aerosol suspension showed the highest drug permeation of 10.5% after one hour, while only 3.2% of drug was transported from the BDP dry powder formulation (Rhinocort). This may be



because dry powder aerosols require additional time for wetting and dissolution once in contact with the nasal mucus layer. No statistical difference ( $p < 0.05$ ) was found between the two commercial formulations after 4 hours, suggesting that dissolution was the rate-limiting step for the transport of BDP across cells. It is envisaged that, upon deposition, the particles in both formulations start to dissolve in the nasal mucus creating an *in situ* saturated BDP area leading to a higher concentration gradient driving the diffusion process [20].

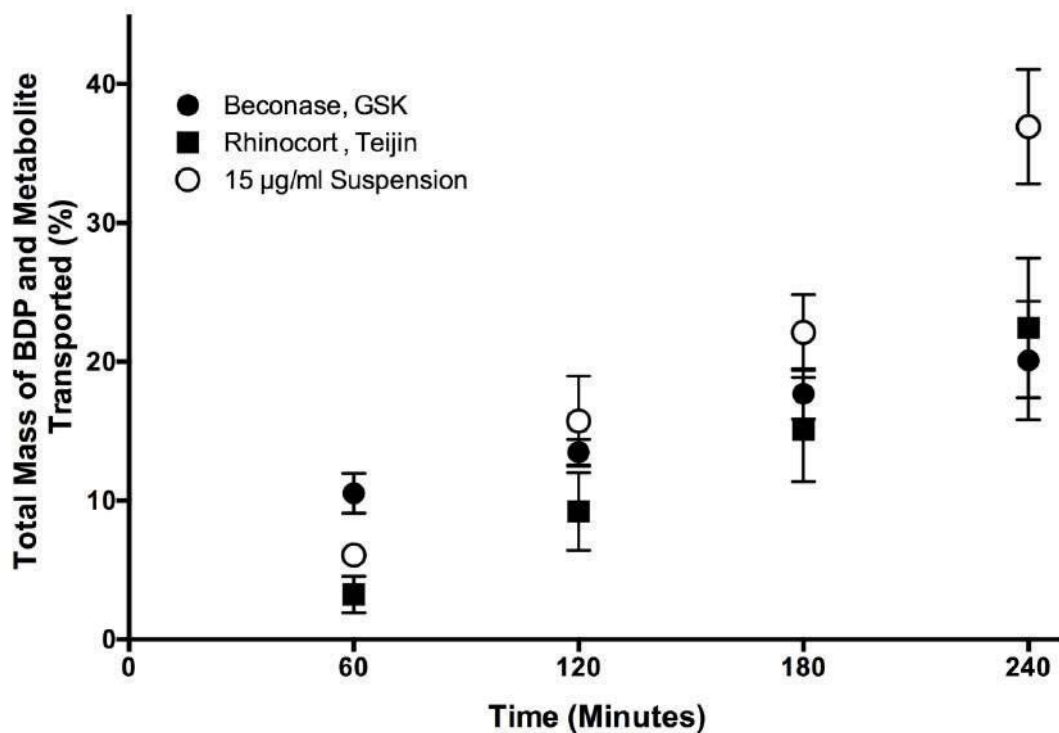


Figure 4.4: Total amount (%) of BDP and BMP transported across the RPMI 2650 nasal cell model over 4 hours ( $n = 3$ ,  $\pm$  StDev).

The amount (%) of BDP and BMP found on the surface and inside the nasal cells is shown in Table 4.3. It was found that around 25% of the BDP remained on the surface of the cell when BDP was delivered as a suspension, either by conventional transport method or as an aerosol using the nasal spray. Meanwhile,

for the dry powder formulation, only 9.4% was found to remain on the cells surface, confirming that the dry powder particles provide a higher permeation into the cell membrane after the deposition; this could be possibly due to a higher local gradient during the powder dissolution. As for the values of BMP, the dry powder formulation showed the highest percentage of BMP inside the cells, with 64% of total drug deposited, suggesting that once penetrated into the cells, the BDP is rapidly converted into the active compound, BMP. However, no statistical differences were found between the Beconase and the Rhinocort formulations. The 15 µg/mL suspension showed the lowest percentage of BMP inside the cell but the highest drug transport across the cell layers. This could be due to the liquid-liquid interface conditions of the transport study. This approach may dilute the mucus layer barrier present on cell surface and ultimately maximize the paracellular permeation rate of the drug. Therefore, the new approach/ model is believed to be more representative of the physiological conditions during nasal drug deposition.

*Table 4.3. Percentage of BDP and BMP found 'on' the surface and inside 'in' RPMI2650 cells after 4 hours from the deposition/transport studies (n=3, ± StDev)*

	BDP		BMP	
	ON	IN	ON	IN
15 µg/mL Suspension	25.4±0.7	1.4±0.2	0.7±0.1	34.7±2.1
Beconase, GSK	26.4±8.4	1.0±0.1	1.7±1.2	52.9±3.3
Rhinocort, Teijin	9.4±3.6	3.0±0.9	0.9±0.6	64.0±15.2

## 4.4 CONCLUSION

Overall, the 3D printed modified expansion chamber for assessing nasal formulation can be reliably used as an alternative to the standard glass chamber when using the Next Generation Impactor.

The model has been proved to be reliable for both powder and suspension formulations. Indeed, both Rhinocort (50 µg per capsule) and Beconase (100 uL/spray) have shown similarity in results.

Furthermore, it has been shown that there were no statistical differences between two commercially available nasal BDP formulations, for both the total drug permeated and the amount of active compound (BMP) recovered inside the cells after deposition studies. However, differences were found between classical aliquot addition based transport studies and the *in vitro* deposition method described herein, highlighting the importance of choosing a more physiological method to assess nasal formulations *in vitro*.

The good performances of the Teijin Rhinocort, raise the desire to further investigate deeply powder formulations and try to improve possible issues related to lack of solubility.

## 4.5 REFERENCES

1. Trangsrud AJ, Whitaker AL, Small RE. Intranasal corticosteroids for allergic rhinitis. *Pharmacotherapy*. 2002;22:1458–67.
2. Pozzoli M, Rogueda P, Zhu B, Smith T, Young PM, Traini D, et al. Dry powder nasal drug delivery: challenges, opportunities and a study of the commercial Teijin Puvlizer Rhinocort device and formulation. *Drug Dev. Ind. Pharm.* 2016;42:1660–8.
3. Djupesland PG. Nasal drug delivery devices: characteristics and performance in a clinical perspective—a review. *Drug Deliv. and Transl. Res.* 2013;3:42–62.
4. Kublik H, Vidgren MT. Nasal delivery systems and their effect on deposition and absorption. *Adv. Drug Deliv. Rev.* 1998;29:157–77.
5. Trows S, Wuchner K, Spycher R, Steckel H. Analytical challenges and regulatory requirements for nasal drug products in Europe and the U.S. *Pharmaceutics*. 2014;6:195–219.
6. Kippax P, Fracassi J. Particle size characterisation in nasal sprays and aerosols. *LabPlus Int (Feb/March)*. 2003.
7. Dayal P, Pillay V, Babu RJ, Singh M. Box-Behnken experimental design in the development of a nasal drug delivery system of model drug hydroxyurea: characterization of viscosity, in vitro drug release, droplet size, and dynamic surface tension. *AAPS PharmSciTech*. Springer-Verlag; 2005;6:E573–85.
8. Suman JD, Laube BL, Lin T-C, Brouet G, Dalby R. Validity of in vitro tests on aqueous spray pumps as surrogates for nasal deposition. *Pharm Res.* 2002;19:1–6.
9. Djupesland PG, Skretting A, Winderen M, Holand T. Breath Actuated Device Improves Delivery to Target Sites Beyond the Nasal Valve. 2006;116:466–72. Available from: <http://doi.wiley.com/10.1097/01.MLG.0000199741.08517.99>
10. Doub WH, Adams WP, Wokovich AM, Black JC, Shen M, Buhse LF. Measurement of drug in small particles from aqueous nasal sprays by Andersen Cascade Impactor. *Pharm Res.* 2012;29:3122–30.
11. U.S. Department of Health and Human Services, Food and Drug Administration, Center for Drug Evaluation and Research. Bioavailability and Bioequivalence Studies for Nasal Aerosols and Nasal Sprays for Local Action. 2003;1–37.

12. Kaialy W. A review of factors affecting electrostatic charging of pharmaceuticals and adhesive mixtures for inhalation. *Int J Pharm.* 2016;503:262–76.
13. Roberts JK, Moore CD, Ward RM, Yost GS, Reilly CA. Metabolism of beclomethasone dipropionate by cytochrome P450 3A enzymes. *Journal of Pharmacology and Experimental Therapeutics.* 2013;345:308–16.
14. Okuda M, Okamoto M, Nomura Y, Saito Y. Clinical study on beclomethasone dipropionate powder preparation (TL-102) in perennial nasal allergy. *Rhinology.* 1986; 24:113-123
15. Borchard G, Cassará ML, Roemelé PEH, Florea BI, Junginger HE. Transport and local metabolism of budesonide and fluticasone propionate in a human bronchial epithelial cell line (Calu-3). *J. Pharm. Sci.* 2002;91:1561–7.
16. Lin H, Yoo J-W, Roh H-J, Lee M-K, Chung S-J, Shim C-K, et al. Transport of anti-allergic drugs across the passage cultured human nasal epithelial cell monolayer. *Eur J Pharm Sci.* 2005;26:203–10.
17. Pozzoli M, Fabio S, Ong HX, Traini D, Young PM. Optimization of RPMI 2650 Cells as a Model for Nasal Mucosa. *RDD.* 2014. pp. 1–4.
18. Pozzoli M, Zhu B, Traini D, Young PM, Fabio S. Validation of a Novel Apparatus for Deposition Studies of Nasal Products. *RDD Europe 2015.* 2015;3:537–41.
19. Great Britain SO. *British Pharmacopoeia.* London: Stationery Office; Appendix XII C. Consistency of Formulated Preparations.
20. Ong HX, Traini D, Loo C-Y, Sarkissian L, Lauretani G, Scalia S, et al. Is the cellular uptake of respiratory aerosols delivered from different devices equivalent? *Eur J Pharm Biopharm.* 2015;93:320–7.

# CHAPTER 5

*Poorly Soluble Drugs:*

*Development of a Novel Nasal Formulation*

This chapter has been accepted for publication by the *Drug Development and Industrial Pharmacy* on the 13-April- 2017 with the title “Development of a Soluplus<sup>®</sup> Budesonide Freeze-Dried Powder for Nasal Drug Delivery”. Authors: Pozzoli M, Traini D, Young PM, Sukkar BM and Sonvico F. ID LDDI-2017-0063.R1

## 5.0 PREFACE

In the previous chapters were highlighted the advantages of powder formulations for nasal delivery such as increased chemical stability, longer permanence in the nasal cavity and as shown in Chapter 4 faster permeation across a cell monolayer absorption model such as RPMI 2650. In this chapter an innovative formulation approach is proposed to overcome one of the possible limitations of nasal powders, i.e. lack of solubility. In detail, the objective is to increase the dissolution properties of a poorly soluble active ingredient, through the use of amorphous solid dispersion. Budesonide was chosen as drug model instead the previously described BDP, as BDP has the inconvenient of being easily metabolized in BMP. MIAT nasal sprayer was used instead of Teijin Puvlizer in order to avoid the multiple actuations required to deliver the dose for the latter (see Chapter 2).

## 5.1 ABSTRACT

The small volume of fluid present in the nasal cavity limits the absorption of poorly soluble drug. Budesonide is a corticosteroid, practically insoluble, and normally administered as suspension-based nasal spray.

Amorphous solid dispersions/solutions (ASD) have been proposed to increase permeation and dissolution rate for different administration routes. The aim of this work was to develop an ASD of a poorly soluble drug, Budesonide (BUD) with a novel polymer Soluplus<sup>®</sup> (BASF, Germany) using a freeze-drying technique. The formulation was assessed for its physico-chemical and aerodynamic properties as well as transport *in vitro* using RPMI 2650 nasal cells, in order to elucidate the efficacy of the Soluplus-budesonide formulation.

The freeze-dried Soluplus-budesonide formulation (LYO) showed a porous structure with a specific surface area of  $1.4334 \pm 0.0178 \text{ m}^2/\text{g}$ . Calorimetric analysis confirmed an interaction between budesonide and Soluplus and X-ray powder diffraction the amorphous status of the drug. The freeze-dried formulation (LYO) showed faster release compared to both water-based suspension and dry powder commercial products. Furthermore, a LYO formulation, bulked with calcium carbonate (LYO-Ca), showed suitable aerodynamic characteristics for nasal drug delivery. The permeation across RPMI 2650 nasal cell model was higher compare to a commercial water-based BUD suspension.



[Production note:

This chapter is not included in this digital copy due to copyright restrictions.]

Pozzoli, M., Traini, D., Young, P. M., Sukkar, M. B. & Sonvico, F. 2017, 'Development of a Soluplus budesonide freeze-dried powder for nasal drug delivery', *Drug Development and Industrial Pharmacy*, in press.

DOI: 10.1080/03639045.2017.1321659

View/Download from: [Publisher's site](#)

# CHAPTER 6

## 6.1 GENERAL CONCLUSION

The main aim of this work was to develop and validate a new *in vitro* apparatus as a preclinical tool for the evaluation of nasal products. This apparatus comprised of the RPMI 2650 nasal cell line as a biological model of nasal mucosa, grown as ALI, included in a 3D printed modification of the FDA approved expansion chamber for testing aerosol performances by cascade impaction (analytical model).

In Chapter 1, a general introduction of the nose and the advantages and limitation of nasal drug delivery is proposed. A brief overview of the various nasal products, with a focus on liquid and powder dosage forms, leads to the description of the test required by authorities to develop a product. Subsequently, a summary of tools developed in the literature to study the formulation deposition in the nasal cavity and biological model to study drug absorption is proposed.

Chapter 2 offered a brief overview of powder formulations for nasal drug administration, highlighting features of marketed products and strategies to improve these formulations. The full analytical characterization of Teijin Rhinocort, one of the few marketed nasal powder products, showed the robustness of its intranasal powder delivery systems. In fact, Rhinocort was found to be quite consistent in its performance despite the high number of repeated actuations required to deliver one dose. On the other hand, it was highlighted the need for a new approach able to bring to an upper level the characterization and development of nasal products.

The use of RPMI 2650 cells as a model for drug transport studies is relatively novel. This thesis has demonstrated for the first time the ability of RPMI 2650 cells to produce mucus and express xenobiotic transporters under ALI conditions and thus highlighting the importance of creating a model with characteristics closer to the human nasal mucosa for drug absorption studies. Furthermore, the values obtained for the permeation of paracellular marker and TEER are comparable to the ones reported in literature for excised human nasal mucosa. Even the expression of a number of cell transporters was showed to be comparable to that of freshly brushed human nasal cells.

All this evidences strengthen even more RPMI 2650 as powerful *in vitro* tool to study drug permeation across the nasal mucosa.

A modified expansion chamber able to accommodate cell culture inserts has been proved to be a valid alternative to the FDA proposed glass expansion chamber for cascade impactor studies on nasal products (Chapter 3). This modified chamber was intentionally designed to be geometrically identical to the FDA one. ABS was chosen as plastic material because offered the same performances compared to glass. The holes to allocate the Snapwell were positioned directly opposite to the inlet in order to maximize the deposition of nasal products on cells. Furthermore, the ability to deposit drug aerosol on the blank cell inserts opens up opportunities to study drug dissolution more in detail. Even though the modified chamber could be used as a powerful tool to develop a new formulation, due to its simple design, it cannot be used the predict the site of deposition in the nasal cavity. Therefore, it will not be able to discriminate products for “special targeting” such as the nose to brain delivery.

From the results obtained during the comparison between the classical transport studies and the proposed model of deposition/transport through a cell monolayer it is clear that the innovative model undoubtedly offers some advantages such as the maintenance of the ALI cell model conditions. Indeed, this is clearly lacking during classical transport studies when the cells are covered with a large volume of fluid containing drug (Chapter 4). Furthermore, the proposed model offers a better representation of the *in vivo* process, where aerosolized particles interact with the mucosa and not a large volume of fluid.

In Chapter 4, the effect of formulation type on nasal drug absorption has been investigated. Whilst suspension formulations are more commonly available than powder products for nasal drug delivery, powder formulations have some known advantages. These include increased chemical stability and longer residence time in the nasal cavity. Results have showed that powder formulations have the ability to permeate faster across the RPMI 2650 nasal ALI model. This could be explained through the higher concentration gradient generated when a powder particle hit the nasal mucosa surface. This is beneficial as it will allow for better drug delivery and potentially increased bioavailability and reduced side effects.

A limitation of the delivery of powder to the nose is represented by the small volume of fluid present in the nasal cavity that may delay the dissolution of the powder formation. In Chapter 5, a new formulation based on amorphous solid dispersion was proposed (Chapter 5). This formulation was obtained through freeze-drying of budesonide (poorly soluble drug) with an amphiphilic polymer

(Soluplus<sup>®</sup>). This combination showed increased dissolution properties in a Franz's diffusion cell and permeation across the proposed RPMI 2650 cell model of nasal mucosa. This formulation platform opens up opportunities to formulate and increase dissolution profiles of other nasally administered poorly soluble drugs.

Corticosteroids, such as Budesonide and Beclomethasone dipropionate, were used throughout the thesis for various reasons. Firstly, corticosteroids are available as a commercial product in various formulation types such as water-based suspensions, dry powder inhaler, and pressurized metered dose inhaled. Therefore, they are the best option to validate the different in-vitro testing tools developed in this thesis. Secondly, considered the fact that they are supposed to have a local effect on the nasal mucosa and epithelial cell might be their major cellular target; drugs, in order to be effective, need to dissolve and penetrate through the mucus layer, then be absorbed by the epithelial cell layer and possibly permeate in the lower layer of the mucosa. Consequently, the use of corticosteroids to test RPMI 2650 nasal cell model is still meaningful due to the presence of mucus in the model and to the fact, the epithelial cells are not the only target of this drug class. Lastly, the delivery of corticosteroids and in general of poorly soluble drugs is challenging, therefore it opens up opportunities to develop new a type of formulation approaches and platforms that could be used for different type of drugs in the future.

The current market of nasal product and formulation is really simplistic.

The majority of the nasal products present on the market nowadays are for local use. The regulation of the manufacturing of these products is based on the FDA and EMEA guidelines which require a simple analytical test to guarantee the performances. Under this regulations, product cannot be really ranked.

Indeed, these products are mostly based on traditional water-based pumps; with the exception of a couple of products, to whom some particular technology has been applied to the formulation in order to gain some advantages such as prolonged residence in the nasal cavity.

Overall, the research work presented has addressed some of the limitations still existing for nasal product characterization. First of all, RPMI 2650 cells cultivated in Air-Liquid Interface condition have been optimized and validated as a model of the human nasal mucosa suitable for drug permeation studies. Furthermore, a 3D printed apparatus able to include cell culture inserts was developed to test at the same time formulation deposition and permeation and has been shown to be more representative of real nasal product administration compared to conventional methods. Finally, the advantages of powder formulation and strategies to overcome the downsides have unfold opportunities for future developments in this area.

## 6.2 FUTURE DIRECTIONS

Whilst the work presented in this thesis has expanded the current knowledge on nasal drug delivery through the development of a nasal cell culture model, a novel *in vitro* deposition model and the investigation of different formulations, further studies should be focused to investigate:

- Develop further the RPMI 2650 ALI model to mimic a diseased state such as rhinitis; to evaluate the production of inflammatory mediators and increased mucus production.
- Investigate a co-culture of RPMI2650 with neuronal cells in order to model specific regions of the nasal cavity such as the olfactory epithelium.
- Incorporate the RPMI 2650 ALI model into an anatomical nasal cast to improve the relevance of aerosol deposition experiments. This will help to better mimic the *in vivo* process of drug administration.
- Apply Soluplus® amorphous solid dispersion platform formulation to various type of drugs (soluble and not soluble) and compare them with conventional solution and suspensions formulations in order to gain better knowledge of mechanisms behind nasal drug absorption.



# APPENDICES

## A.1 PUBLICATION LIST

### Journal articles included as thesis chapter

- Pozzoli, M., Ong, H.X., Morgan, L., Sukkar, M., Traini, D., Young, P.M., Sonvico, F., 2016a. Application of RPMI 2650 nasal cell model to a 3D printed apparatus for the testing of drug deposition and permeation of nasal products. *Eur J Pharm Biopharm* 107, 223–233. doi:10.1016/j.ejpb.2016.07.010
- Pozzoli, M., Rogueda, P., Zhu, B., Smith, T., Young, P.M., Traini, D., Sonvico, F., 2016b. Dry powder nasal drug delivery: challenges, opportunities and a study of the commercial Teijin Puvlizer Rhinocort device and formulation. *Drug Dev. Ind. Pharm.* 42, 1660–1668. doi:10.3109/03639045.2016.1160110

## Conference Proceeding

Bolded titles are related to the thesis

- Pozzoli, M., Traini, D., Fabio, S., Young, P.M., Ong, H.X., 2016c. **Transport of Beclometasone Dipropionate Across RPMI 2650 Model of Nasal Epithelium: Evaluation of Two Different Approaches to Drug Delivery.** Presented at the Respiratory Drug Delivery 2016, pp. 607–610.
- Pozzoli, M., Zhu, B., Traini, D., Young, P.M., Fabio, S., 2015. **Validation of a Novel Apparatus for Deposition Studies of Nasal Products.** Presented at the Respiratory Drug Delivery Europe 2015, pp. 537–541.
- Pozzoli, M., Fabio, S., Ong, H.X., Traini, D., Young, P.M., 2014. Optimization of RPMI 2650 Cells as a Model for Nasal Mucosa. Presented at the Respiratory Drug Delivery 2014, pp. 738–742.



Contents lists available at ScienceDirect

European Journal of Pharmaceutics and Biopharmaceutics

journal homepage: [www.elsevier.com/locate/ejpb](http://www.elsevier.com/locate/ejpb)

Research paper

## Application of RPMI 2650 nasal cell model to a 3D printed apparatus for the testing of drug deposition and permeation of nasal products



Michele Pozzoli<sup>a</sup>, Hui Xin Ong<sup>b</sup>, Lucy Morgan<sup>c</sup>, Maria Sukkar<sup>a</sup>, Daniela Traini<sup>b</sup>, Paul M. Young<sup>b</sup>, Fabio Sonvico<sup>a,d,\*</sup>

<sup>a</sup> Graduate School of Health – Pharmacy, University of Technology Sydney, 15 Broadway, Ultimo, NSW 2007, Australia

<sup>b</sup> Respiratory Technology, The Woolcock Institute of Medical Research and Discipline of Pharmacology, Sydney Medical School, University of Sydney, 431 Glebe Point Road, Glebe, NSW 2037, Australia

<sup>c</sup> Concord Repatriation General Hospital, Sydney Medical School-Concord Clinical School, University of Sydney, Sydney, NSW, Australia

<sup>d</sup> Department of Pharmacy, University of Parma, 27A, Parco area delle Scienze, Parma 43124, Italy

### ARTICLE INFO

#### Article history:

Received 25 May 2016

Revised 8 July 2016

Accepted in revised form 8 July 2016

Available online 11 July 2016

#### Keywords:

RPMI 2650

Transporter expression

Nasal permeation

Mucus

Air Liquid Interface

Primary nasal cell

3D printing

Deposition

Dissolution

Permeation

### ABSTRACT

The aim of this study was to incorporate an optimized RPMI2650 nasal cell model into a 3D printed model of the nose to test deposition and permeation of drugs intended for use in the nose. The nasal cell model was optimized for barrier properties in terms of permeation marker and mucus production. RT-qPCR was used to determine the xenobiotic transporter gene expression of RPMI 2650 cells in comparison with primary nasal cells. After 14 days in culture, the cells were shown to produce mucus, and to express TEER (define) values and sodium fluorescein permeability consistent with values reported for excised human nasal mucosa. In addition, good correlation was found between RPMI 2650 and primary nasal cell transporter expression values.

The purpose-built 3D printed model of the nose takes the form of an expansion chamber with inserts for cells and an orifice for insertion of a spray drug delivery device. This model was validated against the FDA glass chamber with cascade impactors that is currently approved for studies of nasal products. No differences were found between the two apparatus.

The apparatus including the nasal cell model was used to test a commercial nasal product containing budesonide (Rhinocort, AstraZeneca, Australia). Drug deposition and transport studies on RPMI 2650 were successfully performed.

The new 3D printed apparatus that incorporates cells can be used as valid *in vitro* model to test nasal products in conditions that mimic the delivery from nasal devices in real life conditions.

© 2016 Elsevier B.V. All rights reserved.

### 1. Introduction

Over recent decades, interest in the nose as an alternative site for drug administration has increased steadily [1]. The nose is attractive for drug delivery because the highly vascularized mucosa with low enzymatic activity potentiates peptide permeation and rapid, high concentration drug absorption that avoids first pass metabolism [2–6]. However, there are a number of limitations and challenges associated with nasal drug delivery. Normal mucociliary clearance would clear the nasal cavity of liquid formulations within 45 min. The nasal cavity, even in health, is a small volume and geometrically complex space, rendered smaller by

mucosal inflammation. Finally, the small volume of the cavity and the relatively low volume of fluid available for drug dissolution limit the doses that can be administered [7–10].

Together, these aspects highlight the specificity of this administration route and the need for further research into the development of new nasal formulations that are able to overcome the challenges related to efficient administration. In particular, there is an increasing need for reliable preclinical tools to screen new products and formulations intended for nasal delivery that can predict deposition and permeation through the mucosa and transport across the epithelium.

Different *in vitro* models have been proposed to investigate the deposition of nasal products. One approach is the use of transparent silicone anatomical casts such as one originated from a Japanese male cadaver Koken (Koken LM-005, Bunkyo-ku Tokyo, Japan). However, this as well as other casts, appears to have some

\* Corresponding author at: Department of Pharmacy, University of Parma, 27A, Parco area delle Scienze, Parma 43124, Italy.

E-mail address: [fabio.sonvico@unipr.it](mailto:fabio.sonvico@unipr.it) (F. Sonvico).

<http://dx.doi.org/10.1016/j.ejpb.2016.07.010>

0939-6411/© 2016 Elsevier B.V. All rights reserved.

limitations related to the fact that the Food and Drug Administration (FDA) do not regulate the deposition experiments, each cast is not representative of the anatomical variability of different nasal cavities and its polymeric surface is far from representative of the mucosal surface present in the nose.

Another approach is to use Pharmacopoeia impactors, which have been used to predict aerodynamic particle size distributions and thus deposition profiles of aerosolized particles/droplets in the lower respiratory tract [11]. Specifically, for nasal drug delivery, the FDA guidance for industry on "Bioavailability and Bioequivalence Studies for Nasal Aerosols and Nasal Sprays for Local Action" suggests to determine particles/droplets size distribution using a cascade impactor (CI) [12]. In particular, the guideline suggests the use of an induction port, i.e. a glass expansion chamber (EC), to be connected to a cascade impactor in order to maximize drug deposition below the top stages of the CI [11–13]. This allows a better discrimination of particles with aerodynamic diameters smaller than 10  $\mu\text{m}$  that could be inhaled and therefore not suitable for the nasal deposition.

While impactors and casts are important tools to determine deposition on the different areas of the respiratory tract, they don't offer any information related to either drug dissolution or permeation through the mucosa in the nasal cavity. Recently, various approaches that integrate lower airway epithelia cell cultures into compendia-based impactors have been proposed and used to study the deposition and permeation of particles emitted by dry powder inhalers and pressurized metered dose inhalers [14–16]. To our knowledge, nothing similar has been proposed for nasal products as yet.

Among the *in vitro* cell lines available commercially, RPMI 2650 is the only immortalized human nasal cell line. It has been studied as a drug permeation tool by different researchers [2,17–22]. Initially, it was reported that this cell line was unsuitable for permeation studies because it was not able to form a confluent layer in conventional culture conditions [17]. However, Bai and collaborators and, two years later, Wengst and Reichl, started to further investigate culture condition for this cell line and to characterize some of the culture features using transepithelial electrical resistance measurements (TEER), permeation of paracellular markers and tight junctions' protein expression. The key findings of these studies were that the change from the conventional Liquid Cover Culture (LCC) to an Air Liquid Interface cultures (ALI), where the upper surface of the cells was exposed to air, was able to induce cell differentiation leading to the formation of cell layers suitable for permeation experiments [18,19]. A few years later, Reichl and colleagues tried to optimize culturing conditions using different cell growth media and different types of cell-culture insert membrane; the main studies were based on TEER observation and paracellular marker permeation. A pronounced dependence of TEER on medium and membrane material was observed; with the best culture condition being achieved when using polyethylene terephthalate (PET) 3  $\mu\text{m}$  porosity Transwell™ inserts, using Minimum Essential Medium (MEM) supplemented with 10% of fetal bovine serum with cells cultivated using the ALI condition [21].

Based on these previous findings, the aim of the present study was to incorporate RPMI 2650 nasal cell epithelia, grown under ALI conditions into a modified expansion chamber connected to a cascade impactor. This approach, will allow the study of real nasal aerosols products, their deposition and permeation after nasal device actuation. In order to develop this new impactor/deposition apparatus, larger Snapwell™ cell culture inserts detachable from its plastic frame that can be accommodated into the 3D apparatus without altering the aerosol performances of the impactor have been selected [14]. Firstly, the optimization of the RPMI 2650 cell line culture conditions on Snapwell inserts as nasal drug permeation model, specifically focusing on parameters that characterize

the barrier properties of the model, i.e. TEER measurement, paracellular marker permeation, tight junction localization and mucus production, was investigated. To further validate the model, a thorough analysis of the xenobiotic transporter expression in comparison with that of freshly brushed human nasal cells was carried out.

Then, RPMI 2650 grown in ALI conditions on Snapwell inserts was accommodated into a custom-built 3D printed modified expansion chamber in order to study nasal product deposition and permeation after device actuation. This new apparatus was validated against the original glass expansion chamber, recommended in the FDA guidelines, in terms of drug deposition on the CI stages and was tested in terms of drug deposition and permeation through the RPMI 2650 nasal cell model, using a commercially available budesonide nasal spray.

There is a clear need for a reliable preclinical model to test new products and formulations intended for nasal delivery that can predict drug deposition, permeation and transport across the epithelium.

## 2. Materials and methods

### 2.1. Materials

Minimum essential medium added with phenol red (MEM), non-essential amino acids solution (100 $\times$ ), fetal bovine serum (FBS), L-glutamine (200 mM), Hank's balanced salt solution (HBSS), TrypLE Express, bovine serum albumin (BSA) and phosphate buffered saline (PBS) was purchased from Gibco, Invitrogen (Sydney, NSW, Australia). Snapwell™ cell culture inserts (1.13  $\text{cm}^2$  polyester, 0.4  $\mu\text{m}$  pore size) and black 96-well black plates were supplied by Corning Costar (Lowell, MA, USA). All other culture plastics were from Sarstedt (Adelaide, SA, Australia). Trypan blue solution (0.4%, w/v), paraformaldehyde and dimethyl sulfoxide (DMSO) were obtained from Sigma-Aldrich (Sydney, NSW, Australia). Fluorescein-sodium (Flu-Na) was purchased from May & Baker Ltd. (Dagenham, England). Alcian blue 1% (pH 2.5) in 3% acetic acid was purchased from Fronine laboratory (Sydney, NSW, Australia). NucleoSpin® RNA extraction kit was kindly provided by Scientifix (Cheltenham, VIC, Australia), a custom TaqMan® Array-96 well plate and all buffers were purchased by Applied Biosystem (ThermoFisher Scientific, Scoresby, VIC, Australia). Rhinocort nasal spray (AstraZeneca, North Ryde, NSW, Australia) was purchased at a local pharmacy. All chemicals and reagents were of the highest analytical grade.

### 2.2. Cell culture nasal cell line

The cell line RPMI 2650 (CCL-30) was purchased from the American Type Cell Culture Collection (ATCC, Manassas, VA, USA). Cells between passage 16–30 were grown in 75  $\text{cm}^2$  flasks in complete Minimum Essential Medium (MEM) containing 10% (v/v) fetal bovine serum, 1% (v/v) non-essential amino acid solution and 2 mM L-glutamine and maintained in a humidified atmosphere of 95% air 5%  $\text{CO}_2$  at 37 °C. Cells were propagated and sub-cultured according to ATCC protocol. The cell culture inserts were coated with 250  $\mu\text{l}$  of 1  $\mu\text{g}/\text{ml}$  collagen solution in PBS (rat collagen type 1 in PBS, BD Biosciences, Australia) and left overnight to increase the adherence of cells to the membrane [18]. In order to establish the ALI model, 200  $\mu\text{l}$  of cell suspension was seeded onto the collagen coated Snapwell inserts at three different seeding concentrations: 1.25, 2.5, and 5.0  $\times 10^5$  cells/ml (equivalent to 221, 442, 885  $\times 10^5$  cells/ $\text{cm}^2$ ). The media on the apical compartment were removed after 24 h post-seeding. Media in the basolateral chamber

were replaced 3 times per week. Cell layers were allowed to grow and differentiate under ALI conditions up to 21 days.

### 2.3. Transepithelial electrical resistance measurements

Transepithelial electrical resistance was recorded with EVOM2<sup>®</sup> epithelial voltohmmeter (World Precision Instruments, Sarasota, FL, USA) every 2–3 days from day one. Briefly, pre-warmed media were added to the apical chamber and allowed to equilibrate for at least 30 min in a cell culture incubator (humidified air with 5% CO<sub>2</sub> at 37 °C). Blank filter values were subtracted and TEER values were calculated normalizing the resistance values with the Snapwell inserts area (1.13 cm<sup>2</sup>).

### 2.4. Sodium fluorescein permeation experiments

Sodium Fluorescein, a paracellular marker (Flu-Na, MW 367 Da), was used to evaluate barrier formation and tight junction functionality in the ALI culture. Three time points were chosen to conduct the experiments (1, 2, and 3 weeks) and at each time point, three Snapwell inserts were washed twice with warm HBSS before each experiment. 250 µl of 2.5 mg/ml Flu-Na solution was added to the apical chamber (donor) and 1.5 ml of pre-warmed HBSS into the basolateral chamber (acceptor). At pre-determined time points, 200 µl of solution is sampled from the acceptor chamber every 30 min over 4 h and equal volume of fresh HBSS was added for replacement.

Samples were collected into a black 96-well plates and fluorescence of Flu-Na was measured with a SpectraMax M2 plate reader (Molecular Devices, Sunnyvale, CA, USA), using excitation and emission wavelengths of 485 nm and 535 nm, respectively. The calibration coefficient of determination was 0.999, with standards prepared between 1.25 and 0.0125 µg/ml.

Samples were analyzed and the permeation coefficient ( $P_{app}$ ) was calculated according to Eq. (1):

$$P_{app} = \frac{dQ}{dt \cdot C_0 \cdot A} \quad (1)$$

where  $dQ/dt$  is the flux (µg/s) of the Flu-Na across the barrier,  $C_0$  is the initial donor concentration (µg/ml) and  $A$  is the surface area (cm<sup>2</sup>).

### 2.5. Evaluation of mucus production

To assess the ability of the cell line RPMI 2650 to produce mucus when cultured at the ALI configuration, Alcian Blue was used according to a previously established method [23]. Mucus production of the ALI model was assessed at different time points (1, 7, 14, 21 days) for three seeding densities (1.25, 2.5, and 5.0 × 10<sup>6</sup> cells/ml), respectively. On the day of the experiment, cell layers were washed twice with 300 µl of pre-warmed PBS and fixed using 4% (w/v) paraformaldehyde for 20 min. After the fixing agent was washed with PBS, the surface of the cells was stained with Alcian Blue. Excess staining was washed with PBS and inserts were allowed to air-dry for approximately three hours. The membrane was cut from the insert and mounted onto the glass slide with Entellan<sup>™</sup> mounting medium (ProSciTech, Thuringowa, QLD, Australia) and sealed. Subsequently, images were taken using an Olympus BX60 (Olympus, Hamburg, Germany) microscope equipped with an Olympus DP71 camera. Three images were taken per well, with all conditions performed in triplicate. Images were analyzed using ImageJ software (NIH, Bethesda, MD, USA) and values of RGB (Red Green Blue) were measured for each image [24]. The ratio of blue (RGBb ratio) was calculated by dividing the mean RGBb by the sum of the RGB values for each image (RGBr + RGBg + RGBb) [23].

### 2.6. Immunocytochemistry experiment

In order to visualize the tight junction proteins on RPMI 2650 cells, ZO-1 (zone occluding 1) and E-cadherin immunocytochemistry was performed. RPMI 2650 cells grown on Snapwell inserts for 14 days under ALI condition were used for immunocytochemistry. The cells were washed 3 times for 30 min with PBS to decrease the amount of mucus on the cell layers and improve visualization. Then, the cells were fixed with 4% paraformaldehyde solution for 10 min. Afterward, the cells were incubated for 10 min in PBS containing 50 mM NH<sub>4</sub>Cl, followed by 8 min with 0.1% (w/v) Triton X-100 in PBS for permeabilization of the cell membrane.

Cells were then incubated for 60 min with primary antibodies, i.e. 200 µl of E-cadherin (H-108) rabbit polyclonal IgG (1:100, Santa Cruz Biotechnology, Dallas, TX, USA) and ZO-1 (D7D12) rabbit monoclonal IgG (1:1000, Cell Signaling Technology, Danvers, MA, USA). Afterward, cell monolayers were rinsed three times with PBS containing BSA 2%, before 30 min incubation with 200 µl of a 1:500 dilution in PBS containing 2% BSA of a goat anti-Rabbit IgG secondary antibody labeled with Alexa Fluor<sup>™</sup> 488 (Life Technologies, Waltham, MA, USA). 4',6-diamidino-2-phenylindole (DAPI, 1 µg/ml in PBS) was used to counterstain cell nuclei. After 30 min of incubation, the specimens were again rinsed three times with PBS containing 2% BSA and embedded in Entellan<sup>™</sup> new mounting medium (Merk-Millipore, Darmstadt, Germany). Images were obtained using a confocal laser-scanning microscope (Nikon A1, Nikon Instruments Inc., Melville, NY, USA), using a laser at 488 nm and 60× objective.

### 2.7. Expression of xenobiotic transporters

#### 2.7.1. RPMI 2650 cell culture and sample collection of primary nasal cell

RPMI 2650 cells were cultured for 14 days on Snapwell porous membranes under ALI conditions at a density of 2.5 × 10<sup>6</sup> cells/ml. To obtain primary nasal cells, bilateral nasal mucosal brushing was performed using a disposable cytology brush (Model BC-202D-2010, Olympus Australia Pty. Ltd., Notting Hill, VIC, Australia) on human subjects to collect nasal epithelium as described previously [25–28]. Samples were pooled together from eight healthy volunteers between ages 20 and 40, with two groups of four people per gender. Samples were washed and centrifuged twice with PBS solution and left in –80 °C freezer overnight prior to RNA extraction.

#### 2.7.2. RNA isolation, target synthesis, microarray data analysis

In order to analyze the protein transporter expression in the cell samples, RNA was isolated and purified using the NucleoSpin<sup>®</sup> RNA kit (Macherey-Nagel, Düren, Germany). The RNA samples were treated with RNase-free DNase sets and dissolved in RNase-free water. Concentration and purity were determined by spectrophotometry (NanoDrop 2000, ThermoFischer Scientific, Scoresby, VIC, Australia). TaqMan<sup>®</sup> Array Plates (Life Technologies, Sydney, NSW, Australia) was used to perform RT-qPCR assays. The array, *ad hoc* designed, enabled the assessment of 46 human drug transporter genes, including 13 ATP-binding cassette transporters, 23 solute carrier transporters, and 10 solute carrier organic anion transporters (see Table 1 for a list of all genes and proteins). Reverse transcription was carried out using a standardized internal protocol. Briefly, to 5 µl of RNA was added a mixture of general primer and deoxynucleotide (dNTP, 1:1) and 5 µl of PCR grade water; the mixture was heat at 65 °C for 5 min and quickly cooled in ice. Subsequently, 4 µl of first strand buffer, 2 µl of 0.1 M solution of DTT (Dithiothreitol) and 1 µl of ribonuclease inhibitor were added; the solution was incubated at 37 °C for 2 min and 1 µl of M-MLV

**Table 1**

List of drug transporters evaluated and their gene expression ( $\Delta Cq$ ) in RPMI 2650 cultivated on Snapwells at  $2.50 \times 10^6$  cell/ml, PNC: human primary nasal cells from brushing (average between male and female). Scale from not expressed (red) to highly expressed (dark green).

Protein Name	Protein Description	Gene code	RPMI 2650	PNC	$\Delta Cq$	Classification
P-gp	P-glycoprotein	ABC B1			30	No Expression
BSEP	Bile Salt Export Pump	ABC B11			15	Poorly Expressed
MDR3	Multidrug resistance protein 3	ABC B4			5 to 15	Highly Expressed
MRP1	Multidrug resistance-associated protein 1	ABC C1			>9	Highly Expressed
MRP7	Multidrug resistance-associated protein 7	ABC C10				
MRP8	Multidrug resistance-associated protein 8	ABC C11				
MRP9	Multidrug resistance-associated protein 9	ABC C12				
MRP2	Multidrug resistance-associated protein 2	ABC C2				
MRP3	Multidrug resistance-associated protein 3	ABC C3				
MRP4	Multidrug resistance-associated protein 4	ABC C4				
MRP5	Multidrug resistance-associated protein 5	ABC C5				
MRP6	Multidrug resistance-associated protein 6	ABC C6				
BCRP	breast cancer resistance protein	ABC G2				
NCP	Sodium-taurocholate cotransporting polypeptide	SLC1 0A1				
PEPT1	Peptide transporter 1	SLC1 5A1				
PEPT2	Peptide transporter 2	SLC1 5A2				
MCT1	Monocarboxylate transporter 1	SLC1 6A1				
MCT2	Monocarboxylate transporter 2	SLC1 6A2				
NAP1	Renal type 1 sodium/phosphate transporter	SLC1 7A1				
OCT1	Organic cation transporter 1	SLC2 2A1				
URAT1	Organic anion/urate transporter 1	SLC2 2A12				
OCT2	Organic cation transporter 2	SLC2 2A2				
OCT3	Organic cation transporter 3	SLC2 2A3				
OCTN1	Organic cation transporter, novel 1	SLC2 2A4				
OCTN2	Organic cation transporter, novel 2	SLC2 2A5				
OAT1	Organic anion transporter 1	SLC2 2A6				
OAT2	Organic anion transporter 2	SLC2 2A7				
OAT3	Organic anion transporter 3	SLC2 2A8				
CNT1	Anti-Concentrative Transporter 1	Nucleoside SLC2 8A1				
CNT2	Anti-Concentrative Transporter 2	Nucleoside SLC2 8A2				
CNT3	Anti-Concentrative Transporter 3	Nucleoside SLC2 8A3				
ENT1	Equilibrative transporter 1	nucleoside SLC2 9A1				
ENT2	Equilibrative transporter 2	nucleoside SLC2 9A2				
ENT3	Equilibrative transporter 3	nucleoside SLC2 9A3				
ENT4	Equilibrative transporter 4	nucleoside SLC2 9A4				
OST $\alpha$	Organic Solute Transporter, Alpha	SLC5 1A				
ATB(0+)	Sodium- and chloride-dependent neutral and basic amino acid transporter B(0+)	SLC6 A14				
OATP-A	Organic anion transporter polypeptide A	SLC O1A2				
OATP-C	Organic anion transporter polypeptide C	SLC O1B1				
OATP-B	Organic anion transporter polypeptide B	SLC O1B3				
OATP-F	Organic anion transporter polypeptide F	SLC O1C1				
PGT	Prostaglandin Transporter	SLC O2A1				
OATP-B	Organic anion transporter polypeptide B	SLC O2B1				
OATP-D	Organic anion transporter polypeptide D	SLC O3A1				
OATP-E	Organic anion transporter polypeptide E	SLC O4A1				
OATP-H	Organic anion transporter polypeptide H	SLC O4C1				
OATP-J	Organic anion transporter polypeptide J	SLC O5A1				

(Moloney Murine Leukemia Virus) reverse transcriptase was added. The mixture was incubated firstly at 25 °C for 10 min and then at 37 °C for 50 min; in order to stop the reaction the temperature was raised to 70 °C for 15 min. The cDNA for all the samples was uniformly diluted to 20 ng/ $\mu$ l and mixed with TaqMan<sup>®</sup> mastermix. Thermal-cycling conditions were set to manufacturer specifications, with 20  $\mu$ l of mixture (sample and mastermix 1:1) was added to each well. The plates were analyzed using the StepOne-Plus<sup>™</sup> Real-Time PCR System (Applied biosystem, ThermoFisher Scientific, Scoresby, VIC, Australia) for a total of 40 cycles. Data analysis was performed using the  $\Delta Cq$  method, where the  $\Delta Cq$  value is normalized to the 18S ribosomal RNA (18S rRNA) used as a reference gene. Ribosomal RNA, the central component of the ribosome is an abundant and one of the most conserved genes in all cells. Recently, 18S rRNA has been indicated as the most suitable reference gene for RT-qPCR normalization of data from primary human bronchial epithelial cells [29].

## 2.8. Development and validation of aerosol nasal deposition apparatus

### 2.8.1. Development of the modified expansion chamber

Rapid prototyping with 3D printing technique was used to manufacture the custom-made modified expansion chamber (MC) (Fig. 1). The MC was designed to accommodate up to 3 Snapwell cell culture inserts, using CAD software (Catia 3D, 3DS, Boston, MA, USA). The modified expansion chamber was designed based on the 2 L glass expansion chamber (EC) as suggested in the FDA guidance for nasal products [12]. The MC comprises of two interlocking hemispheres: the lower part presents the connection to the cascade impactors (through a connection adaptor), and an inlet hole for nasal devices at 30° from the axis. The upper half is designed to allow the incorporation of three Snapwell cell culture inserts, located opposite to the inlet hole (Fig. 1).

Acrylonitrile butadiene styrene (ABS) was used as printing material using a commercial 3D printer (Dimension Elite, StrataSys, Eden Prairie, MN, USA), at layer thickness of 178  $\mu$ m. Due to the intrinsic porosity of the printed material, the internal and external surfaces were chemically treated with small quantities of acetone to seal internal surfaces; the absence of leakage was successfully tested with different mixtures of water and methanol.

### 2.8.2. Validation of the impactor deposition performances: Standard vs. modified expansion chamber

Rhinocort, a commercial available nasal spray for the treatment of rhinitis (AstraZeneca, North Ryde, NSW, Australia), containing a suspension of budesonide (32  $\mu$ g/spray) as active ingredient, was used to validate the modified chamber. Aerodynamic particle size

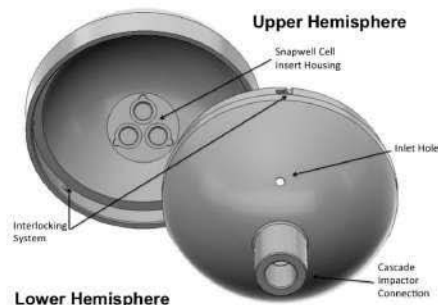


Fig. 1. 3D drawing of the modified expansion chamber.

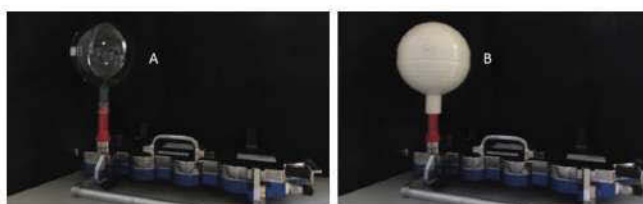


Fig. 2. British Pharmacopoeia Apparatus E equipped with FDA glass expansion chamber (A) and modified expansion chamber (B).

distributions were evaluated using a British Pharmacopoeia Apparatus E – Next Generation Impactor (Westech W7; Westech Scientific Instruments, Upper Stondon, UK) (Fig. 2). Analyses were performed in triplicate with either the glass expansion chamber or the modified chamber fitted with Snapwell inserts. The device was primed to waste and for each analysis, three actuations were fired. Briefly, the impactor was connected to a rotary pump (Westech Scientific Instruments, Upper Stondon, UK) at a flow rate of 15 L/min using a calibrated flow meter (Model 4040, TSI Precision Measurement Instruments, Aachen, Germany). Each impactor stage was washed with a solution 80:20 (% v/v) methanol/water and samples were analyzed by high performance liquid chromatography (HPLC) using a validated method [30].

#### 2.8.3. Validation of the cell layer integrity in the modified chamber

RPMI 2650 were cultivated on Snapwells at the optimized seeding condition. At day 14, three cell inserts were washed with pre-warmed HBSS, and placed into the modified expansion chamber. An HBSS solution into a VP3 Aptar nasal pump (Aptar, Le Vaudreuil, France) was used as blank to simulate the deposition process into the modified chamber. After 6 actuations of the buffer blank solution, with the same deposition method previously described, the inserts were transferred into a cell culture plate. Flu-Na permeation studies were performed as mentioned above in order to confirm the integrity of the cell layers after aerosol deposition. The  $P_{app}$  was compared with untreated control cells.

#### 2.9. Deposition and transport of a commercial budesonide nasal spray on optimized RPMI 2650 cell model using the modified expansion chamber

RPMI 2650 cells were used after 14 days from seeding on Snapwells ( $2.5 \times 10^6$  cells/ml). Three cell inserts were washed with pre-warmed HBSS buffer and fitted into the upper hemisphere of the modified expansion chamber. The aerosol deposition of budesonide on the cell surface from the Rhinocort device (AstraZeneca, North Ryde, NSW, Australia) was obtained according to the method described above, with a total dose of 96  $\mu\text{g}$  of budesonide (3 sprays) was delivered into the chamber. The cell inserts were then removed from the modified chamber and transferred to a 6-well plate containing 1.5 ml of fresh pre-warmed HBSS. Samples of 200  $\mu\text{l}$  were collected from the basal chamber every hour and replaced with the same volume of fresh buffer. After four hours, the apical surface of the epithelia was washed twice in order to collect any remaining drug. Subsequently, cells were scraped from the insert membrane and lysed with CellLytic<sup>TM</sup> buffer (Invitrogen, Sydney, NSW, Australia) in order to quantify the amount of budesonide inside the cells by HPLC. TEER measurements were performed prior and after the deposition in order to confirm that the integrity of the cell layer was maintained.

#### 2.10. Analytical quantification of budesonide

The amount of budesonide in each sample was determined using an HPLC system equipped with a SPD-20A UV-vis detector (Shimadzu, Tokyo, Japan) according to a validated method reported in the literature [30]. Briefly, a Luna C18 column ( $150 \times 4.6$  mm, 3  $\mu\text{m}$ , Phenomenex, Lane Cove, NSW, Australia) was used with a mobile phase methanol/water 80:20% v/v. The flow rate was set at 1 ml/min and budesonide was detected at  $\lambda = 240$  nm. The retention time of budesonide was around 5 min. Standards were prepared in the mobile phase, and 100  $\mu\text{l}$  injections were used. Linearity was confirmed between 0.1  $\mu\text{g/ml}$  and 50  $\mu\text{g/ml}$  [30].

#### 2.11. Statistics

Unless differently stated, data represent the mean  $\pm$  standard deviation of at least three independent experiments. *t*-Test was used to compare data, with differences considered significant for  $p < 0.05$ .

### 3. Result and discussion

#### 3.1. Transepithelial electrical resistance (TEER) measurements

Transepithelial electrical resistance can be used as an indicator of the development and integrity of the epithelial barrier. Various studies have tried to optimize and standardize the culture conditions of RPMI 2650 [21,22]. However, the effects of seeding density on RPMI 2650 cultured in the ALI conditions on this Snapwell insert with a larger surface area has not been previously evaluated. The Snapwell inserts offer a more flexible membrane compared to the more common 0.33  $\text{cm}^2$  Transwell inserts due to their larger surface area and different support structure.

The progressive formation of the tight junction barrier by cultured RPMI 2650 cells seeded onto Snapwell inserts with respect to time is shown in Fig. 3. The TEER for the three different seeding densities steadily increases with time until day 14, starting from values around 20  $\Omega \text{cm}^2$  and reaching a plateau between 115  $\Omega \text{cm}^2$  ( $5 \times 10^6$  cells/ml seeding) and 150 ( $1.25 \times 10^6$  cell/ml seeding) up to day 17 when the TEER starts to decrease. Data indicate that at least 14 days are required for the cell to reach a tight confluent layer with the highest TEER barrier when cultured in the ALI conditions. After 17 days, a decrease in the TEER values is observed, suggesting that the cells either start to die or lose their tight junction integrity a few days after full maturation. This trend is similar to previously published data [21]. Regarding the three different seeding levels, no statistical differences were found at days 14 and 17, reaching values around 90–150  $\Omega \text{cm}^2$ . Therefore, values above 90  $\Omega \text{cm}^2$  were considered sufficient to perform experiments.

We report a clear correlation with the range of TEER values reported for human nasal mucosa. Our results are very similar to



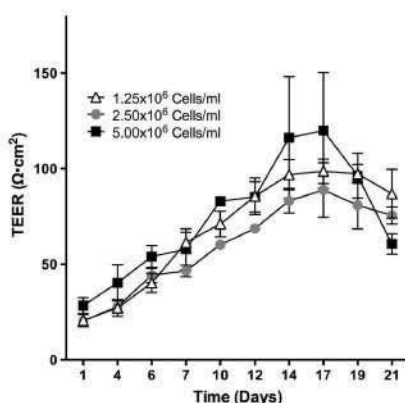


Fig. 3. TEER of three different seeding densities of RPMI 2650 cells cultured in the ALI conditions over time ( $n=3$ ;  $\pm$ StDev).

those reported previously [18,21,31]. In particular, TEER values from excised human mucosa obtained from turbinectomy surgeries and used within an hour from the extraction, showed TEER values around 90–180  $\Omega$   $\text{cm}^2$ . Therefore, these data support the use of ALI cultured RPMI 2650 as a representative model of the nasal mucosa.

### 3.2. Sodium fluorescein permeation experiments

The relatively high variability in TEER values reported in the literature for RPMI 2650 cells suggests that this measurement is affected by many factors related to the technique (inter/intra laboratory); therefore, other parameters have to be considered when trying to establish a model for drug deposition and transport. Thus, permeation studies of Flu-Na were performed in order to confirm and support the TEER measurements. Sodium fluorescein, due to its hydrophilic characteristic, is used as a paracellular permeation marker. The transport of Flu-Na across RPMI 2650 cell layer was evaluated over a period of 4 h (Table 2). In order to confirm that, the Snapwell insert membrane was not the rate-limiting step of the permeation process, and permeability of Flu-Na through the Snapwells membrane alone was also tested and showed a significantly higher value ( $1.38 \times 10^{-5}$  cm/s).

As shown in Table 2, no statistical difference was observed between the  $P_{app}$  values of the three different seeding densities after a week of culture, suggesting that seven days in ALI conditions are not sufficient to have a tight confluent cell layer. After 14 days of culture, the  $P_{app}$  values significantly decreased, when compared to the values of week 1, supporting the findings of the

Table 2  
 $P_{app}$  values ( $\times 10^{-6}$  cm/s) of Flu-Na across RPMI 2650 cultured in ALI conditions for three different seeding densities ( $n=3$ ;  $\pm$ StDev) compared to values obtained for excised human nasal mucosa.

	Flu-Na $P_{app}$ values ( $\times 10^{-6}$ cm/s)			Human nasal mucosa
	Seeding density 1.25 ( $\times 10^6$ cells/ml)	2.50 ( $\times 10^6$ cells/ml)	5.00 ( $\times 10^6$ cells/ml)	
Freshly excised	–	–	–	$3.12 \pm 1.99$ [18]
Week 1	$5.32 \pm 0.37$	$5.21 \pm 0.27$	$5.47 \pm 0.49$	
Week 2	$3.67 \pm 0.21$	$2.68 \pm 0.60$	$2.95 \pm 0.17$	
Week 3	$3.47 \pm 0.20$	$3.55 \pm 0.30$	$2.69 \pm 0.18$	

TEER experiments. It was also found that the intermediate seeding density reaches the lowest value of  $2.68 \pm 0.60 \times 10^{-6}$  cm/s after two weeks in culture. On the other hand, the lowest seeding density ( $1.25 \times 10^6$  cells/ml) shows higher permeability compared to the other two, suggesting that the amount of cell may not sufficient to guarantee enough barrier properties. No significant differences between the  $P_{app}$  values for the two higher seeding densities were observed. After three weeks in culture, no significant difference in the Flu-Na permeability was found for any of the seeding densities, suggesting two weeks in culture are enough to reach a mature model with confluent cells for RPMI 2650.

Different research groups have tried to characterize the paracellular permeability of RPMI 2650 grown in ALI conditions: Bai et al. obtained values of  $5.07 \times 10^{-6}$  using mannitol as marker [19]; Wengst and Reichl, using Flu-Na, on cells grown on Transwell<sup>®</sup> polycarbonate membrane, presented values of  $6.09 \times 10^{-6}$  cm/s [18]; and Reichl obtained lower values of  $1.91 \times 10^{-6}$  cm/s using Thincert<sup>®</sup> inserts with polyethylene terephthalate membranes, confirming that the supporting material may affect the adhesion and the layer/barrier formation of RPMI 2650 cell line [18,21]. More recently, Kreft reported  $P_{app}$  values of  $6.08 \times 10^{-7}$  cm/s using dextran conjugated to fluorescein isothiocyanate (MW 10,000), an extremely low value that is related to the higher molecular weight of the molecule used for the investigation [20].

### 3.3. Evaluation of mucus production

Mucus plays an important role in protecting the nasal epithelium. Furthermore, this mucus is the first barrier that any drug administered into the nose has to overcome in order to be absorbed; it has a key role also in the dissolution process of drug that will allow subsequent permeation [32]. Thus, an appropriate model of the nasal epithelium requires mucus of specific depth, biochemistry and rheology. Therefore, the production of mucus in the RPMI 2650 cellular model grown in ALI condition was investigated.

Alcian Blue allows mucus detection by reaction with acidic polysaccharides (mucopolysaccharides) and sialic acid containing glycoproteins, producing a blue color. Fig. 4 shows an example of the staining of the mucus layer of RPMI 2650 seeded at  $2.50 \times 10^6$  cell/ml over a 3 week period.

Observing the images in Fig. 4 it can be seen that, after one day of culture, just few light blue spots appear, most probably due to the staining of the extracellular matrix. After one week of culture the cell layer is almost completely covered by a thin but discontinuous light blue layer, but the increased blue intensity implies that a small amount of mucus has been produced. At 14 days, the higher intensity of the color and its uniformity suggest that the production of mucus has increased and that a mucus blanket uniformly covers the cell layer. At day 21, the mucus still covers all the areas but not uniformly, dark blue areas are alternate to light ones; this could be related to the concurrent decrease in TEER between day 14 and 21 suggesting cell integrity and/or death occurs.

The relative quantification of the mucus production was measured by the RGBb ratio. Fig. 5 shows the mucus production in terms of RGBb ratio over three weeks. No differences in mucus production can be observed between the different seeding densities at day 1 and day 7. However, at week 2, the intermediate ( $2.50 \times 10^6$  cell/ml) seeding shows a statistically significant increase in mucus production that was statistically higher than the other two densities. This RGBb value subsequently plateaus from day 14 to day 21, while the lowest and highest seeding densities ( $1.25$  and  $5.0 \times 10^6$  cell/ml) showed no statistically differences at both day 14 and 21. These two seeding conditions showed a steady increase in the RGBb ratio value indicating a build-up in the mucus production during all the culturing time.

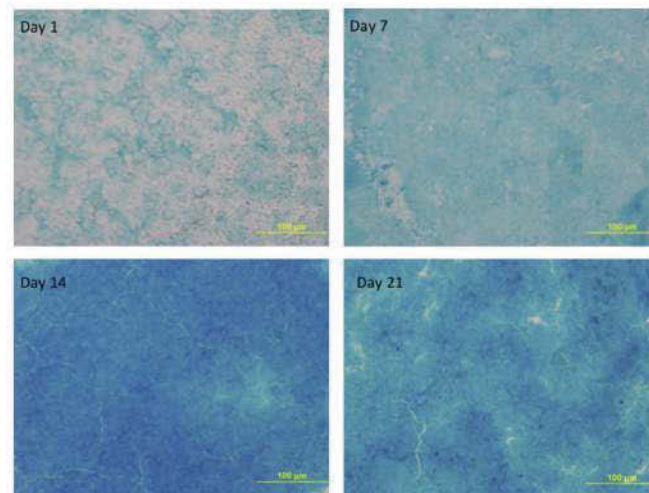


Fig. 4. Optical microscope images of Alcian blue mucus staining on RPMI 2650 grown on Snapwell® inserts at  $2.50 \times 10^6$  cell/ml seeding density. (For interpretation of the references to color in this figure legend, the reader is referred to the web version of this article.)

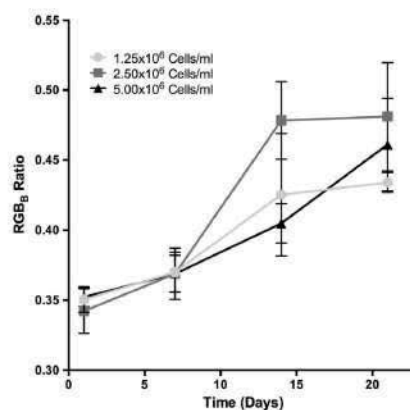


Fig. 5. RGBb ratio values obtained after mucus staining as function of time in culture for the three different cell seeding densities ( $n = 3$ ;  $\pm$ StDev).

Finally at day 21, all three seeding density managed to attain similar amount of mucus produced with no significant differences observed between them.

These results suggest that the intermediate seeding density ( $2.50 \times 10^6$  cell/ml) is the optimum condition that allows the cells to form confluent layer with a uniform mucus blanket in 2 weeks in the Snapwell insert. This is probably due to the optimization of the growth conditions that allow for the cells to proliferate, sufficient nutrients and space to interact and form tight junctions and produce mucus.

The plateau observed for the intermediate seeding density, can also be a result of the limitations of measurement technique leading to a saturation of the blue RGBb ratio [23]. In addition, being an

*in vitro* model, one of the limitations is the static nature of this system where the mucus cannot be cleared leading to build up in the wells with the increasing cell numbers.

Based on the above results for mucus production, TEER measurements and Flu-Na permeability, the optimal seeding density was found to be  $2.50 \times 10^6$  cell/ml for RPMI 2650 cells grown on Snapwell inserts.

### 3.4. Immunocytochemical investigation

Tight junctions play an important role in the control of the paracellular permeation across the epithelia [33]. In order to confirm that the RPMI 2650 cells on Snapwell inserts were also able to produce tight junctions, the expression and localization of two proteins essential for the formation and maintenance of tight junction were investigated: specifically, E-cadherin and zonula occludens protein 1 (ZO-1) (Fig. 6). Fig. 6A shows the localization of E-cadherin (green) around the nucleus stained with DAPI (blue) and Fig. 6B and C show in green the expression of ZO-1 and in red DAPI.

As expected, the proteins are found at the edge of the cells where they are involved in the formation of tight junction in the RPMI 2650 cells. Furthermore, the RPMI 2650 cells were found to form multilayers as seen with the overlapping nuclei in Fig. 6C. This is different from what Bai et al. as observed, where cells were forming a monolayer. However it is in good agreement with Kreft et al. that noticed a multi-layering growth of RPMI 2650 when cultured in ALI conditions [19,20].

### 3.5. Expression of xenobiotic transporters

When paracellular transport across epithelia is not involved, membrane carrier proteins can have a key role in the absorption, distribution and elimination processes of both endogenous compounds and xenobiotics [34,35]. In order to cross the epithelia a molecule needs to pass through two barriers; specifically, it needs

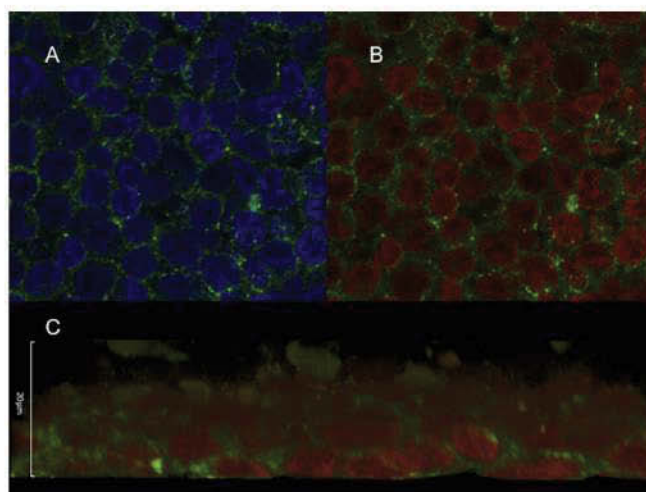


**Fig. 6.** Confocal microscope images of RPMI 2650 cells tight junction proteins-stained in green: E-cadherin (A) and ZO-1 (B and C). The blue and red colors in A and B respectively represent the DAPI staining of nuclei. C, the cross section of cell layers during confocal imaging: green ZO-1 and red cell nucleus. (For interpretation of the references to color in this figure legend, the reader is referred to the web version of this article.)

to be taken up from apical membrane and effluxed from the basal membrane. These processes are often carrier mediated [36].

In order to evaluate whether RPMI 2650 could be a representative model of the nasal mucosa, further investigation on the transporters expression in the cell line model was performed and was compared with freshly brushed human nasal cells.

Specifically, 47 xenobiotic transporters were investigated. The genes investigated were those expressing ATP Binding Cassette (ABC), Solute Carrier (SLC) and Solute Carrier Organic anion (SLCO) proteins. Table 1 graphically summarizes which of these 47 xenobiotic transporters were present in the RPMI 2650 cells and compared with gene present on PNC: human primary nasal cells from brushing (average between male and female).

For the RPMI 2650 cells, the highly expressed genes ( $\Delta Cq < 5$ ) were found to be MRP1 and MRP9 proteins while the poorly expressed genes ( $\Delta Cq > 15$ ) were found to be for the following transporters: BSEP (Bile Salt Export Pump), MRP5 (Multidrug Resistance-associated Protein 5), MRP7, MRP8, OCT3 (Organic Cation Transporter 3), CNT3 (Anti-Concentrative Nucleoside Transporter 3), ENT1 (Equilibrative nucleoside transporter 1) and ENT3. Some genes, such as those expressing MRP6, PEPT1 (Peptide transporter 1), PEPT2, NaPi1 (Renal type 1 sodium/phosphate transporter), OCT1, OCT2, URAT1 (Organic anion/urate transporter 1), ATB(0+) (Sodium- and chloride-dependent neutral and basic amino acid transporter B(0+)), OATP-C (Organic anion transporter polypeptide C), OATP-8, OATP-F, and OATP-B were not expressed at all. All the other genes were expressed at an intermediate level ( $5 < \Delta Cq < 15$ ).

In terms of the primary nasal cells obtained by nasal mucosa brushing, no differences were found between male and female volunteers. Highly expressed genes were those encoding for the following transporter proteins: MDR3, MRP1, MRP9, MRP2, MRP3, MRP4, Ntcp (Sodium-taurocholate cotransporting polypeptide), MCT1 (Monocarboxylate transporter 1), OCTN2 (Organic cation transporter, novel 2), CNT3, ENT1, ENT2 and OATP-H. No genes were classified as poorly expressed and only 11 genes were not

expressed at all (MRP6, OCT1/2, OCTN1, OAT1/2/3, CNT1/2, ATB (0+) and OATP-F). Gene expressions were calculated using 18S rRNA as reference gene. Using a single reference gene could represent a limitation of the study; however, 18S rRNA has been indicated as the most suitable reference gene in qPCR normalization of data in the case of other primary human airway epithelial tissues [29].

Corticosteroids, which are one of the main topical nasal active ingredients, are an example of a drug class that is associated with these cell transporters [37,38]. In particular, budesonide and beclomethasone dipropionate (BDP) have shown effect of the expression of BCRP, PGP, OCT1 and OCT2 in Calu-3 and breast cancer cell lines [39,40]. In addition, budesonide has been found to be a substrate of P-glycoprotein (ABCB1) in transport experiments across Caco-2 cell line [41].

Nevertheless, to our knowledge there is a lack of information about their role in the nose [35]. Our data show that BCRP and PGP are expressed in the nasal epithelium and in the RPMI 2650 model, suggesting that an avenue for future investigations in this direction.

Although the xenobiotic gene expression was found to be higher for primary cells than for RPMI 2650 in general, the same genes were expressed in both primary human mucosa nasal cells and RPMI 2650, highlighting the potential use of RPMI2650 grown on ALI as a suitable model for nasal mucosa. In addition, from the 47 genes that encode for transporter proteins, the 11 that were not expressed in primary cells were also absent in RPMI 2650, further supporting a good correlation between the RPMI 2650 cell model and human nasal mucosa. The following proteins: NaPi1, URAT1, PEPT1, PEPT2, OATP-C and OATP-8 were found to be expressed in brushed nasal cells, but not in RPMI 2650; this could be considered as a limitation to the RPMI 2650 model in terms of transport of peptides and organic anionic substances.

Kreft et al. had previously described the expression of some of xenobiotic transporter genes in RPMI 2650 grown in ALI conditions with two different culturing media and at two culturing time

points: 1 and 3 weeks, without finding any relevant differences [20]. Our data correlate nicely with those published by Kreft, suggesting good reproducibility of RPMI 2650 cell model.

### 3.6. Development and validation of the modified expansion chamber

The different materials used for the manufacturing of the FDA guideline expansion chamber (glass) and the 3D printed modified chamber (ABS) could raise the question whether or not the aerosol performances and particle deposition in the two chambers could be different. Therefore, in order to validate the 3D printed modified chamber, the aerosol performance of a commercially available nasal spray (Rhinocort Nasal Spray, AstraZeneca, Australia) was evaluated using a NGI cascade impactor using both expansion chambers. Table 3 shows the percentage of budesonide (calculated as percentage of the emitted nominal dose, 96 µg) recovered in each stage of NGI after 3 actuations of the Rhinocort device (average of 3 runs), using both devices.

The amount of drugs in the 3D printed modified chamber was calculated as sum of the mass recovered from both the upper and lower hemispheres and the three Snapwells in the chamber. As expected, the majority of the drug was found in the chamber demonstrating that the device produced a coarse spray with an aerodynamic diameter that is higher than 10 µm, with minimal respirable fraction. Overall, there were no statistical differences in aerosol performance for Rhinocort between the modified and the glass chamber for all NGI stages (no drug was recovered for stages lower than 2). With the deposition onto the Snapwell inserts, 13.12 ± 0.07 µg of budesonide was recovered from the three cell inserts after the extraction with 80:20 (v/v) methanol/water, with approximately 4.4 µg of budesonide on each well. This is equivalent to roughly 13.7% of the dose emitted with each spray of the Rhinocort suspension that reaches each Snapwell inserts.

Having validated the modified chamber in terms of aerosol performance, the RPMI 2650 cells grown on Snapwell inserts were introduced into the modified chamber in order to perform cell permeation experiments. The maintenance of barrier properties and the integrity of the cell layers are key factors for permeation studies. In order to confirm that the handling of the Snapwell inserts and the process of deposition into the modified chamber were not hampering the barrier properties of RPMI 2650 nasal cell model, a solution of HBSS was sprayed 6 times on the RPMI 2650 nasal cells into the chamber. The cells were removed from the chamber and after 4 h of Flu-Na permeation studies, the  $P_{app}$  was calculated. No statistical differences were found ( $p < 0.05$ ) between the  $P_{app}$  values of control and treated cells.

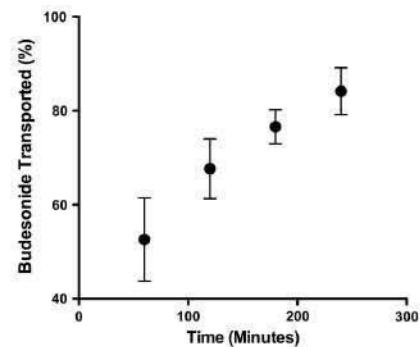
Finally, deposition and permeation experiments were performed using a budesonide commercial spray and with the 3D printed modified expansion chamber connected to the cascade impactor, using the three Snapwells inserts with RPMI 2650 cells grown for 14 days. The formulation was deposited on the cells after device actuation and RPMI 2650 cells inserts were placed back in cell culture plates to perform the permeation study.

Fig. 7 shows the percentage of budesonide transported across the nasal cell model after deposition in the 3D MC. In the first hour,

**Table 3**  
Amount of budesonide (% of nominal dose) recovered from each stage of the NGI using the glass and modified chamber (n = 3; ±StDev).

	Chamber	Connection tube	Stage 1	Stage 2 <sup>a</sup>
Glass chamber	98.75 ± 0.09	0.57 ± 0.05	0.50 ± 0.03	0.18 ± 0.04
Modified chamber	98.73 ± 0.09	0.57 ± 0.07	0.51 ± 0.03	0.19 ± 0.01

<sup>a</sup> No budesonide was found below stage 2.



**Fig. 7.** Amount of budesonide transported through RPMI 2650 nasal cell model after NGI aerosols deposition using the 3D modified chamber (n = 5; ±StDev).

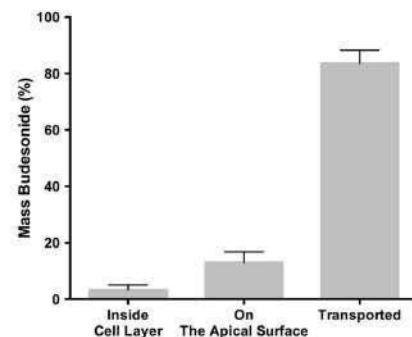


**Fig. 8.** Distribution of the budesonide recovered at the end of the experiment (4 h) after the aerosol deposition using the 3D the modified expansion chamber (n = 5; ±StDev).

approximately 47.3 ± 5.0% of the drug was transported. This can be explained, as suggested by Baumann, due to the high quantity of available budesonide dissolved in the commercially available product to bind and diffuse readily through the epithelium [42,43]. At the end of the experiment (4 h), 83.1 ± 6.3% of the total drug deposited reached the basal compartment. Between three to four hours, a decreased permeation rate was observed, probably due to the depletion of budesonide on the surface of the cells that consequently decreases the gradient between the two compartments (apical and basal). The total amount of budesonide found on each well was on average of 0.79 ± 0.25 µg. This was calculated from the sum of the budesonide on, in and transported across the cell layer; the total amount recovered from each well was used as 100% reference value for the calculation in the cell deposition/transport studies. This variability of the amount of budesonide deposited on each well could be related to both the plume geometry of Rhinocort nasal spray and the manual activation of the device, that don't allow a uniform deposition on each well. The integrity of the cell layer was maintained within the time scaled study with no statistical differences ( $p > 0.05$ ) was found between TEER values before ( $126 ± 21 \Omega \text{ cm}^2$ ) and after ( $127 ± 14 \Omega \text{ cm}^2$ ) the transport studies.

As shown in Fig. 8, after 4 h  $14.4 \pm 4.9\%$  of the drug remains on the surface of the cell and  $2.5 \pm 1.6\%$  of budesonide was found inside the cells, suggesting low binding and internalization within the cells of the RPMI 2650 nasal mucosa model. This is in good agreement with data published by Baumann showing that lower levels of budesonide bind to human nasal tissue when compared with other glucocorticoids [42].

#### 4. Conclusion

This research has shown that RPMI 2650 cells could be successfully grown on Snapwell inserts. The cells form a continuous layer offering a permeation barrier similar in terms of trans-epithelial electrical resistance and sodium fluorescein paracellular permeation to previously reported nasal epithelium models and more importantly to excised human nasal mucosa. It was also shown that RPMI 2650 cells produce mucus and its production is related to seeding density and time in culture. The optimal conditions for RPMI 2650 to achieve the highest epithelial barrier and a complete coating with mucus layer are as follows: Snapwell polycarbonate inserts at seeding density of  $2.50 \times 10^6$  cell/ml and cultured for 14 days in ALI culture. Regarding protein transporter expression, RPMI 2650 cells represent a good model of the nasal epithelium, correlating well with gene expression of freshly collected human nasal epithelial cells. A 3D printed modified expansion chamber, which allows deposition of nasal formulation directly on RPMI 2650 grown on Snapwell inserts has been successfully designed, validated and tested using a commercial nasal spray, showing that this model could be used concomitantly to study nasal formulation aerosol deposition and permeation through a nasal epithelium model of the aerosolized formulation.

#### Author disclosure statements

No conflict of interests exist.

#### Acknowledgments

A/Professor Traini is the recipient of an Australian Research Council Future Fellowship (project number FT12010063). A/Professor Young is the recipient of an Australian Research Council Future Fellowship (project number FT110100996).



#### References

- [1] L. Illum, Nasal drug delivery – recent developments and future prospects, *J. Controlled Release* 161 (2012) 254–263.
- [2] M. Pozzoli, P. Rogueda, B. Zhu, T. Smith, P.M. Young, D. Traini, F. Sonvico, Dry powder nasal drug delivery: challenges, opportunities and a study of the commercial Teijin Puvlizer Rhinocort® device and formulation, *Drug Dev. Ind. Pharm.* (2016), <http://dx.doi.org/10.3109/03639045.2016.1160110>.
- [3] V. Saluja, J.P. Amorij, M.L. van Rossmalen, K. Leenhouts, A. Huckriede, W.L.J. Hinrichs, H.W. Frijlink, Intranasal delivery of influenza subunit vaccine formulated with GEM particles as an adjuvant, *AAPS J.* 12 (2010) 109–116.
- [4] S. Grassin-Delye, A. Buenestado, E. Naline, C. Faisy, S. Blouquit-Laye, L.J. Couderc, M. Le Guen, M. Fischler, P. Devillier, Intranasal drug delivery: an efficient and non-invasive route for systemic administration: focus on opioids, *Pharmacol. Ther.* 134 (2012) 366–379.
- [5] E. Tountou, L. Illum, Nasal drug delivery, *Drug Deliv. Trans. Res.* 3 (2013) 1–3.
- [6] H. Wu, K. Hu, X. Jiang, From nose to brain: understanding transport capacity and transport rate of drugs, *Expert Opin. Drug Deliv.* 5 (2008) 1159–1168.
- [7] M.S. Quraishi, N.S. Jones, J.D. Mason, The nasal delivery of drugs, *Clin. Otolaryngol. Allied Sci.* 22 (1997) 289–301.
- [8] P.G. Duplessand, Nasal drug delivery devices: characteristics and performance in a clinical perspective—a review, *Drug Deliv. Trans. Res.* 3 (2013) 42–62.
- [9] C. Comfort, G. Garrastazu, M. Pozzoli, F. Sonvico, Opportunities and challenges for the nasal administration of nanoemulsions, *Curr. Topics Med. Chem.* 15 (2015) 356–368.
- [10] F. Merkus, J. Verhoef, N. Schipper, E. Marttin, Nasal mucociliary clearance as a factor in nasal drug delivery, *Adv. Drug Deliv. Rev.* 29 (1998) 13–38.
- [11] British Pharmacopoeia Commission, Appendix XII C. Consistency of formulated preparations, in: *British Pharmacopoeia 2016 – Volume V*, TSO, London, UK, 2016.
- [12] FDA Center for Drug Evaluation and Research, Draft Guidance for Industry, Bioavailability and Bioequivalence Studies for Nasal Aerosols and Nasal Sprays for Local Action, 2003.
- [13] W.H. Doub, W.P. Adams, A.M. Wokovich, J.C. Black, M. Shen, L.F. Buhse, Measurement of drug in small particles from aqueous nasal sprays by Andersen cascade impactor, *Pharm. Res.* 29 (2012) 3122–3130.
- [14] M. Hagi, D. Traini, P. Young, *In vitro* cell integrated impactor deposition methodology for the study of aerodynamically relevant size fractions from commercial pressurised metered dose inhalers, *Pharm. Res.* 31 (2014) 1779–1787.
- [15] C.I. Grainger, L.L. Greenwell, G.P. Martin, B. Forbes, The permeability of large molecular weight solutes following particle delivery to air-liquid interface cells that model the respiratory mucosa, *Eur. J. Pharm. Biopharm.* 71 (2009) 318–324.
- [16] M. Bur, B. Rothen-Rutishauser, H. Huwer, C.M. Lehr, A novel cell compatible impingement system to study *in vitro* drug absorption from dry powder aerosol formulations, *Eur. J. Pharm. Biopharm.* 72 (2009) 350–357.
- [17] A. De Fraissinette, R. Brun, H. Felix, J. Vonderscher, A. Rummelt, Evaluation of the human cell line RPMI 2650 as an *in vitro* nasal model, *Rhinology* 33 (1995) 194–198.
- [18] A. Wengst, S. Reichl, RPMI 2650 epithelial model and three-dimensional reconstructed human nasal mucosa as *in vitro* models for nasal permeation studies, *Eur. J. Pharm. Biopharm.* 74 (2010) 290–297.
- [19] S. Bai, T. Yang, T.J. Abruscato, F. Ahsan, Evaluation of human nasal RPMI 2650 cells grown at an air-liquid interface as a model for nasal drug transport studies, *J. Pharm. Sci.* 97 (2007) 1165–1178.
- [20] M.E. Kreft, U.D. Jerman, E. Laskó, T. Lanišnik Ržemer, N. Hovir-Kene, L. Petermel, K. Kristan, The characterization of the human nasal epithelial cell line RPMI 2650 under different culture conditions and their optimization for an appropriate *in vitro* nasal model, *Pharm. Res.* 32 (2015) 665–679.
- [21] S. Reichl, K. Becker, Cultivation of RPMI 2650 cells as an *in vitro* model for human transmucosal nasal drug absorption studies: optimization of selected culture conditions, *J. Pharm. Pharmacol.* 64 (2012) 1621–1630.
- [22] D.D. Kim, *In vitro* cellular models for nasal drug absorption studies, in: C. Ehrhardt, K.J. Kim (Eds.), *Drug Absorption Studies In Situ, In Vitro and In Silico Models*, Springer, New York, 2008, pp. 216–234.
- [23] M. Hagi, P.M. Young, D. Traini, R. Jaiswal, J. Gong, M. Bewawy, Time- and passage-dependent characteristics of a Calu-3 respiratory epithelial cell model, *Drug Dev. Ind. Pharm.* 36 (2010) 1207–1214.
- [24] C.A. Schneider, W.S. Rasband, K.W. Eliceiri, NIH Image to ImageJ: 25 years of image analysis, *Nat. Methods* 9 (2012) 671–675.
- [25] L.A. Clarke, L. Sousa, C. Barreto, M.D. Amaral, Changes in transcriptome of native nasal epithelium expressing F508del-CFTR and intersecting data from comparable studies, *Respir. Res.* 14 (2013) 38.
- [26] S. Beck, D. Penque, S. Garcia, A. Gomes, C. Farinha, L. Mata, S. Gulbenkian, K. Gil-Ferreira, A. Duarte, P. Pacheco, C. Barreto, B. Lopes, J. Cavaco, J. Lavinha, M. D. Amaral, Cystic fibrosis patients with the 3272–26A→G mutation have mild disease, leaky alternative mRNA splicing, and CFTR protein at the cell membrane, *Hum. Mutat.* 14 (1999) 133–144.
- [27] C.M. Harris, F. Mendes, A. Dragomir, I.J.M. Doull, I. Carvalho-Oliveira, Z. Bebok, J.P. Clancy, V. Eubanks, E.J. Sorscher, G.M. Roomans, M.D. Amaral, M.A. McPherson, D. Penque, R.L. Dormer, Assessment of CFTR localisation in native airway epithelial cells obtained by nasal brushing, *J. Cyst. Fibros.* 3 (2004) 43–48.
- [28] H.X. Ong, D. Traini, G. Ballerin, L. Morgan, L. Buddle, S. Scalia, P.M. Young, Combined inhaled salbutamol and mannitol therapy for mucus hypersecretion in pulmonary diseases, *AAPS J.* 16 (2014) 269–280.
- [29] S.V. Kuchipudi, M. Teflabati, R.K. Nelli, G.A. White, B.B. Perez, S. Sebastian, M.J. Slomka, S.M. Brookes, I.H. Brown, S.P. Dunham, K.C. Chang, 18S rRNA is a reliable normalisation gene for real time PCR based on influenza virus infected cells, *Virology* 49 (2012) 230.
- [30] S.R. Naikwade, A.N. Rajai, Development of validated specific HPLC method for budesonide and characterization of its alkali degradation product, *Can. J. Anal. Sci. Spectr.* 53 (2008) 113–122.
- [31] C.J. Cotton, M.J. Statts, M.R. Knowles, J.T. Gatzky, R.C. Baucher, Abnormal apical cell membrane in cystic fibrosis respiratory epithelium. An *in vitro* electrophysiologic analysis, *J. Clin. Invest.* 79 (1987) 80–85.
- [32] J.D. Suman, Current understanding of nasal morphology and physiology as a drug delivery target, *Drug Deliv. Trans. Res.* 3 (2013) 4–15.
- [33] V.S. Subramanian, J.S. Marchant, D. Ye, T.Y. Ma, H.M. Said, Tight junction targeting and intracellular trafficking of occludin in polarized epithelial cells, *AJP: Cell Physiol.* 293 (2007) C1717–C1726.
- [34] J.J. Salomon, V.E. Muchitsch, J.C. Gausterer, E. Schwagerus, H. Huwer, N. Daum, C.M. Lehr, C. Ehrhardt, The cell line NCI-H461 is a useful *in vitro* model for transport studies of human distal lung epithelial barrier, *Mol. Pharm.* 11 (2014) 995–1006.
- [35] S. Nickel, C.G. Clerkin, M.A. Selo, C. Ehrhardt, Transport mechanisms at the pulmonary mucosa: implications for drug delivery, *Expert Opin. Drug Deliv.* 13 (2016) 667–690.
- [36] R. Bleasby, J.C. Castle, C.J. Roberts, C. Cheng, W.J. Bailey, J.F. Sina, A.V. Kulkarni, M.J. Hafez, R. Evers, J.M. Johnson, R.G. Ulrich, J.C. Slater, Expression profiles of 50 xenobiotic transporter genes in humans and pre-clinical species: a resource for investigations into drug disposition, *Xenobiotica* 36 (2006) 963–988.

- [37] A.J. Traneusud, A.L. Whitaker, R.E. Small, Intranasal corticosteroids for allergic rhinitis, *Pharmacotherapy* 22 (2002) 1458–1467.
- [38] W.E. Berger, J.W. Godfrey, A.L. Slater, Intranasal corticosteroids: the development of a drug delivery device for fluticasone furoate as a potential step toward improved compliance, *Expert Opin. Drug Deliv.* 4 (2007) 689–701.
- [39] K.O. Hamilton, M.A. Yazdani, K.L. Audus, Modulation of P-glycoprotein activity in Calu-3 cells using steroids and beta-ligands, *Int. J. Pharm.* 228 (2001) 171–179.
- [40] H.E. Cooney, S. Shahi, A.P. Cahn, H.W. van Veen, S.B. Hladky, M.A. Baird, Modulation of p-glycoprotein and breast cancer resistance protein by some prescribed corticosteroids, *Eur. J. Pharmacol.* 531 (2006) 25–33.
- [41] K. Dilger, M. Schwab, M.F. Fromm, Identification of budesonide and prednisone as substrates of the intestinal drug efflux pump P-glycoprotein, *Inflamm. Bowel Dis.* 10 (2004) 578–583.
- [42] D. Baumann, C. Bachert, P. Högger, Development of a novel model for comparative evaluation of intranasal pharmacokinetics and effects of anti-allergic nasal sprays, *Eur. J. Pharm. Biopharm.* 80 (2012) 156–163.
- [43] D. Baumann, C. Bachert, P. Högger, Dissolution in nasal fluid, retention and anti-inflammatory activity of fluticasone furoate in human nasal tissue *ex vivo*, *Clin. Exp. Allergy* 39 (2009) 1540–1550.

RESEARCH ARTICLE

## Dry powder nasal drug delivery: challenges, opportunities and a study of the commercial Teijin Puvlizer Rhinocort device and formulation

Michele Pozzoli<sup>a</sup>, Philippe Rogueda<sup>b</sup>, Bing Zhu<sup>c</sup>, Timothy Smith<sup>d</sup>, Paul M. Young<sup>c</sup>, Daniela Traini<sup>c</sup>  and Fabio Sonvico<sup>a,e</sup> 

<sup>a</sup>Graduate School of Health – Pharmacy, University of Technology Sydney, Ultimo, NSW, Australia; <sup>b</sup>Aedestra Ltd., AEDESTRA Ltd Unit 2205, Hong Kong, Hong Kong; <sup>c</sup>Respiratory Technology, The Woolcock Institute of Medical Research and Discipline of Pharmacology, Sydney Medical School, University of Sydney, NSW, Australia; <sup>d</sup>Renishaw Ltd., Wotton-under-Edge, Old Town, Gloucestershire; UK; <sup>e</sup>Department of Pharmacy, University of Parma, Parma, Italy

### ABSTRACT

**Purpose:** To discuss the challenges and opportunities for dry powder nasal medications and to put this in perspective by evaluating and characterizing the performance of the Teijin beclomethasone dipropionate (BDP) dry powder nasal inhaler; providing a baseline for future nasal products development.

**Methods:** The aerosol properties of the formulation and product performance of Teijin powder intranasal spray were assessed, with a particular focus on particle size distribution (laser diffraction), powder formulation composition (confocal Raman microscope) and aerosol performance data (British Pharmacopoeia Apparatus E cascade impactor, aerosol laser diffraction).

**Results:** Teijin Rhinocort<sup>®</sup> (BDP) dry powder spray formulation is a simple blend of one active ingredient, BDP with hydroxypropylcellulose (HPC) carrier particles and a smaller quantity of lubricants (stearic acid and magnesium stearate). The properties of the blend are mainly those of the carrier ( $D_{0.50} = 98 \pm 1.3 \mu\text{m}$ ). Almost the totality of the capsule fill weight (96.5%) was emitted with eight actuations of the device. Using the pharmacopoeia suggested nasal chamber deposition apparatus attached to an Apparatus E impactor. The BDP main site of deposition was found to be in the nasal expansion chamber ( $90.2 \pm 4.78\%$ ), while  $4.64 \pm 1.38\%$  of the BDP emitted dose was deposited on Stage 1 of the Apparatus E.

**Conclusions:** The Teijin powder nasal device is a simple and robust device to deliver pharmaceutical powder to the nasal cavity, thus highlighting the robustness of intranasal powder delivery systems. The large number of actuations needed to deliver the total dose (eight) should be taken in consideration when compared to aqueous sprays (usually two actuations), since this will impact on patient compliance and consequently therapeutic efficacy of the formulation.

### ARTICLE HISTORY

Received 11 November 2015  
Revised 17 February 2016  
Accepted 19 February 2016  
Published online 22 March 2016

### KEYWORDS

BDP; dry powder nasal delivery; nasal drug delivery; particle size; Teijin Rhinocort

### Introduction



The diminishing success rate in bringing new chemical entities to market has led pharmaceutical companies to focus their efforts on identifying new uses for existing drugs, including the development of alternative routes of administration. As a result, nasal drug delivery has emerged as an increasingly viable delivery technology. A number of publications on the development of nasal dry powder formulations for immunization, delivery of peptides and proteins as well as small molecules can be found in the literature<sup>1-3</sup>. This indicates a renewed interest from industry and academia in this area of research. Although nasal delivery is a well-established drug delivery route, surprisingly there are no dry powder nasal delivery systems marketed neither in Europe (EU) nor in the United States (US). Globally, only three nasal dry powder inhalers are available on the market for local treatment: Rhinocort Turbohaler<sup>®</sup> (Budesonide) marketed by AstraZeneca (London, UK) in Canada, Rhinocort Puvlizer<sup>®</sup> (beclomethasone dipropionate [BDP]) by Teijin (Osaka, Japan) (Figure 1), and Erizas<sup>®</sup> (dexamethasone cipeccilate), recently launched by Nippon Shinyaku (Kyoto, Japan) in Japan. All these products are indicated for the treatment of rhinitis. Both the Japanese products are capsule-based, although using two different devices; while the AstraZeneca product uses a multi-dose breath-actuated prefilled device that is already in use for pulmonary

administration of orally inhaled products. The Teijin BDP medicinal product can be used with either dry powder Rhinocort<sup>®</sup> capsules for nasal delivery or with Salcoat<sup>®</sup> capsules to be administered in the oral cavity, both containing BDP<sup>4</sup>.

The nasal powder product (Rhinocort<sup>®</sup>) was launched in December 1986 in Japan, but is not currently available in the EU or in US. It is approved for both allergic and vasomotor rhinitis. The recommended dose is one capsule of 50  $\mu\text{g}$  in the nasal cavity twice daily, after waking up and just before bedtime, eight actuations are required to empty one capsule. Teijin Nasal Spray package comprises the device and a selection of 100, 500 or 700 units capsules (hard gelatin capsules No. 2 color-coded white and blue). Ten capsules are contained in a blister and 10 blisters are wrapped together in a sealed aluminum pack. The Puvlizer<sup>®</sup> device can also be purchased on its own (Figure 1).

In Europe, the current UK market for the treatment of rhinitis accommodates three generic versions of BDP in the form of nasal sprays: Nasobec (Teva, Petach Tikva, Israel), Boots Blocked Nose Relief (The Boots Company Plc, Nottingham, UK) and Beconase (Omega Pharma Ltd., London, UK); all three are suspensions delivering 50  $\mu\text{g}$  of drug for twice a day administration; usually morning and evening.

Nasal drug delivery is usually achieved with liquid aerosol sprays delivering solutions or suspensions. A quick review of the

**CONTACT** Professor Fabio Sonvico  [fabio.sonvico@unipr.it](mailto:fabio.sonvico@unipr.it)  Graduate School of Health Pharmacy, University of Technology Sydney, A5 Broadway, Ultimo, NSW 2007, Australia

© 2016 Informa UK Limited, trading as Taylor & Francis Group

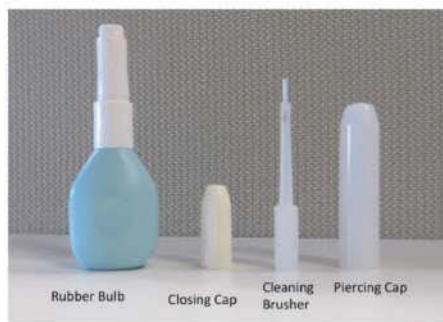


Figure 1. Disassembled Teijin Puvlizer device with accessories.

marketed nasal delivery products in the UK shows that out of the 53 over-the-counter and prescription products listed on the Electronic Medicines Compendium ([www.Medicines.org.uk](http://www.Medicines.org.uk), accessed January 2015), three are semisolids (Naseptin<sup>®</sup>, Alliance Pharmaceutical, Chippenham, UK, chlorhexidine neomycin cream; Bactroban<sup>®</sup>, GSK, Brentford, UK, mupirocin ointment and Happinose Nasal Decongestant Balm<sup>®</sup>, Diomed Developments Limited, Hitchin, UK, levomenthol ointment), four are nasal drop products (Ephedrine Nasal Drops, Thornton & Ross Ltd., Linthwaite, UK; and Otrivine<sup>®</sup> xylometazoline HCl Nasal Drops, Novartis Basel, Switzerland both in two dosages: adult and child), while the remaining 46 are liquid nasal sprays (15 suspensions versus 31 solutions). For a summary of marketed nasal dry powder products and water-based spray alternatives in UK market see Table 1.

The total volume of the nasal cavity ranges from 13 mL to 20 mL<sup>5</sup>, allowing for a maximum delivery of 20 mg of powder<sup>6-9</sup>. Nasal deposition tends to be limited to the outer vestibule of the nasal cavity, following three mechanisms: impaction (primary factor), sedimentation and diffusion (related to olfaction). Deposition and subsequent absorption through the nasal mucosal surface are in competition with a series of mechanisms contributing to drug elimination from the nasal cavity such as physical clearance, mucociliary clearance and enzymatic metabolic activity. As a consequence, exposure and retention of the molecules to the nasal cavity is limited. The act of sniffing is said to enhance the diffusional deposition, particularly relevant for submicron particles deposition, by increasing the airflow rate and changing it from continuous to pulsatile<sup>5</sup>. Kaye et al. studied the powder deposition patterns in the nasal cavity with the Aptar Unit Dose Powder (UDP, Aptar, Louveciennes, France) device and found that 60–70% of the delivered dose was deposited no further than the nasal vestibule. The remaining 30–40% was deposited into deeper compartments of the nasal cavity<sup>3</sup>.

The particle size required for efficient nasal delivery is above 10 µm, i.e. cascade impactor induction port cut off point. A recent work by Schroeter and Kimbell indicated that particles above 20 µm deposit fully in the nasal passageways, with lower sizes starting to deposit further down in the respiratory tract and only 15% of 1 µm particles deposited in the nasal cavity<sup>10</sup>.

The advantages of intranasal powder formulations include increased chemical stability (solid state stability), no requirement for small particles size (anything above 20 µm can be delivered), no requirement for preservatives, no need for cold chain storage, possibility to formulate water insoluble compounds and increased

bioavailability compared to liquid formulations<sup>1-3,11</sup>. This has been demonstrated in a study by Ishikawa et al. whereby powder formulations were found to improve nasal bioavailability of elcatonine polypeptide when blended with a carrier such as CaCO<sub>3</sub>, talc, barium sulfate or ethyl cellulose<sup>2,12</sup>. This opened up the use of nasal formulation for systemic delivery of peptides and proteins. The increased bioavailability obtained by using an insoluble powder carrier, such as CaCO<sub>3</sub>, was due to the increase in residence time available for absorption in the nasal cavity, slowing drug elimination from the absorption site, facilitating permeation of the drug across the nasal epithelium<sup>4,12</sup>. However, further studies on transmucosal permeation are still needed to elucidate how insoluble powders contribute to nasal absorption enhancement. Colombo et al., have proved that ribavirin has higher absorption, through rabbit nasal mucosa, when it was delivered as powder form instead of solution. This highlights possible future uses of powder in the nasal drug delivery and the brain targeting through this route<sup>13</sup>.

Another important aspect to investigate in order to obtain an efficient deposition of the formulation in the nasal cavity is the choice of the delivery device. As already mentioned above, there are several devices available, however these technologies are at different stages of development, with some already used in clinical trials (Trivair, Acerus Pharma, Mississauga, Canada; OptiNose Bidirectional device, Yardley, PA) while others at the development stage or only existing as blueprints<sup>5,14</sup>. Some of these devices rely on the inspiration effort of the patient in order to aerosolize the powder; while others, like the Puvlizer, requires a mechanically generated airflow, supplied by a squeeze bottle or a pump activated by the user. The Trivair<sup>3,6-8</sup> and the Optinose device<sup>1,5,15</sup> are unique technologies since they rely on the patient's own insufflation to propel the powder up the nasal cavities. In a way, these devices can be described as breath actuated devices, and provide the additional advantage of minimizing lower airways deposition as a consequence of soft palate elevation isolating the nasal cavity<sup>3,5,16</sup>.

According to the Food and Drug Administration (FDA) Guidance, the characterization of nasal droplet size distribution can be evaluated by either laser diffraction or cascade impaction (CI), with an additional 2 L expansion chamber<sup>3,17</sup>. However, neither methods are representative for investigating real time drug deposition in the nasal cavity.

As for the flow rate to be used during testing, 0 and 15 L/min are often quoted<sup>3,18</sup>, although nasal inspiratory flows can be much higher than this. More realistic peak nasal inspiratory flow should be 126–143 L/min for male adults and 104–122 L/min for female adults<sup>19</sup>. These values are lower for children<sup>10,20</sup> and ethnic differences should be taken into account<sup>4,11</sup>.

As part of an ongoing study, the aim of this investigation was to investigate the physico-chemical properties and formulation attributes of a commercial dry powder intranasal product, Teijin Rhinocort<sup>®</sup> with a view to understanding how we may improve formulation of nasal dry powders and provide a baseline for future nasal products.

## Materials and methods

BDP dry powder nasal device (Rhinocort<sup>®</sup>, batch # 9091) was obtained from Teijin Pharma Ltd. (Tokyo, Japan). Water used in the analyses was purified by reverse osmosis (MilliQ, Millipore, France). All solvents were obtained from Chem-Supply (South Australia, Australia) and were of high performance liquid chromatography (HPLC) grade.



**Table 1.** Summary of nasal dry powder products and water-based alternatives marketed in UK.

Nasal dry powder				
Product	Drug	Dosage	Features	Company/Country
Erizas capsule	Dexamethasone cipeclate	400 µg capsule	<ul style="list-style-type: none"> <li>• First once daily dry powder type steroid nasal spray in Japan</li> <li>• Double nostril device</li> <li>• NO preservative, less local irritation and NO dripping off from nasal cavities</li> </ul>	Nippon Shinyaku/Japan
Erizas nasal powder	Dexamethasone cipeclate	200 µg 28 metered spray	<ul style="list-style-type: none"> <li>• Lactose hydrate is used as an additive</li> <li>• Once daily treatment, one spray per nostril</li> <li>• NO preservative, less local irritation and NO dripping off from nasal cavities</li> <li>• Lactose hydrate is used as an additive</li> <li>• NO capsule</li> </ul>	Nippon Shinyaku/Japan
Rhinocort Turbohaler®	Budesonide	100 µg 200 doses	<ul style="list-style-type: none"> <li>• Treatment of rhinitis in both child and adults (400 µg daily dosage), once daily application (2 per each nostril in the morning)</li> <li>• Treatment or Prevention of Nasal Polyps: One application (100 µg) into each nostril, morning and evening (total daily dose 400 µg)</li> </ul>	AstraZeneca/Canada
Puvlizer Rhinocort®	Beclometasone dipropionate	50 µg Capsule	<ul style="list-style-type: none"> <li>• NO additives or carrier substances are included</li> <li>• Initially marketed in December 1986</li> <li>• Allergic rhinitis and vasomotor rhinitis</li> <li>• Additives: hydroxypropylcellulose, magnesium stearate, stearic acid</li> <li>• One capsule each is sprayed into the nasal cavity, twice daily</li> </ul>	Teijin Pharma Limited/Japan
<i>Water based spray alternatives (UK market)</i>				
Product	Drug	Dosage	Features	Company
Beconase aqueous nasal spray	Beclometasone dipropionate monohydrate	50 µg spray	<ul style="list-style-type: none"> <li>• Suggested posology: two sprays in each nostril, twice a day (morning and evening)</li> <li>• Contain benzalkonium chloride and phenethyl alcohol</li> </ul>	GlaxoSmithKline/UK
Nasobec	Beclometasone dipropionate	50 µg spray	<ul style="list-style-type: none"> <li>• Suggested posology: two sprays in each nostril, twice a day (morning and evening)</li> <li>• Contain benzalkonium chloride and phenethyl alcohol</li> </ul>	Teva/UK
Boots hayfever relief	Beclometasone dipropionate	50 µg spray	<ul style="list-style-type: none"> <li>• Suggested posology: 200–400 µg/day</li> <li>• Contain benzalkonium chloride and phenethyl alcohol</li> </ul>	The Boots Company/UK
Budesonide aqueous nasal spray	Budesonide	64 µg, 50 µl spray	<ul style="list-style-type: none"> <li>• Suggested initial posology: 256 µg per day, once or twice a day</li> </ul>	Sandoz Limited/UK
Rhinocort Aqua® 64 micrograms	Budesonide	64 µg, 50 µl spray	<ul style="list-style-type: none"> <li>• Contain ascorbic acid E300 and disodium edetate</li> <li>• Treatment of rhinitis 256 µg per day, once or twice a day</li> <li>• Treatment nasal polyps 256 µg per day twice a day</li> <li>• Contain disodium edetate</li> <li>• Shelf life: use within two months of starting treatment</li> </ul>	AstraZeneca UK Limited

**The Puvlizer device**

The Puvlizer® is a single dose, capsule-based, patient operated device (Figure 1). The overall length of the device is 10.5 cm, similar to other classic nasal spray devices for liquid formulations. The device is made of two parts, a stem in which the Rhinocort® capsule is placed and pierced with the needle set in the cap, and the lower part of the device, which is a soft plastic bulb that can be squeezed to provide an air flow sufficient to propel the powder from the capsule through the stem into the nasal cavity. Holes are punctured at both ends of the capsule and the forced airflow pass through the holes of the capsule, aerosolizing the medication.

The rubber bulb dimensions are 3.7 cm height by 2 cm width. The length of the nasal applicator on top of the rubber ball is 6.8 cm. The activation of the device is performed in nine steps. Five steps for the device setting, and four steps for the delivery to the nasal cavity, as shown in Table 2. To empty the content of the capsule fully, it is recommended to squeeze the rubber ball and inhale four times in each nostril, for a total of eight inhalation acts.

The device can be dismantled in three parts (Figure 1): rubber bulb (pale blue color), small cap (cream color), large cap (white

color, with piercing needle inside). Additionally a cleaning brush is provided, as well as a disposal bag. No special indications are given for the storage of the device, nor timing for its replacement. The device is packaged in a cardboard box, with the capsules and an extra plastic bag to carry the device with no extra moisture protection.

**Physico-chemical characterization****Powder bulk and tapped density**

For the bulk density, the content of 21 Rhinocort® capsules was accurately weighed (29.6 mg each capsule) and emptied into a 5 mL graduated cylinder with an internal diameter of 5 mm. The volume occupied by the powder was recorded to calculate the bulk density. The container was tapped for 30 min and the new volume reading was used to calculate the tapped density value of the powder. The tapping has been carried out manually with an amplitude and frequency of 2–5 mm and 1 tap/s, respectively. The bulk volume was measured at the beginning of the experiment and tapped volume values recorded every 10 min. No significant

**Table 2.** Summarized Steps for the device preparation and administration of Teijin Rhinocort®.

Device preparation	Delivery steps
<ul style="list-style-type: none"> <li>• Pull off the large cap and twist off the small cap</li> <li>• Place the capsule in the small cap</li> <li>• Reaffix the small cap onto the rubber bulb</li> <li>• Place large cap in its original position to pierce other end of capsules</li> <li>• Remove the large cap to complete the preparation for spraying</li> </ul>	<ul style="list-style-type: none"> <li>• Squeeze rubber bulb to spray medication into nasal cavity while inhaling through the nose</li> <li>• Spray alternatively in each cavity</li> <li>• Remove capsule from device</li> <li>• Clean the device with the brusher</li> </ul>

variation was observed between 20 and 30 min. The Carr index (CI) was calculated according to the following formula, where  $V_b$  was the bulk volume and  $V_f$  was the volume after tapping. Values below 15 are considered with good flow characteristic, while over 25 powders are considered with poor flowability<sup>21–23</sup>.

$$CI = \frac{(V_b - V_f)}{V_b} \cdot 100$$

**Dynamic vapor sorption.** In order to investigate the behavior of the formulation in response to different degrees of humidity, a dynamic vapor sorption (DVS) study was performed. In brief, ca. 20 mg of powder from one Teijin Rhinocort capsule was weighed into a stainless sample pan and placed in the sample chamber of the DVS analyzer (DVS Intrinsic, Particulate Systems, London, UK). The powder was exposed to two 0–90% relative humidity (RH) cycles at 25 °C with 10% RH increment steps triggered when the sample reached the equilibrium. The equilibrium moisture content at each target RH level was determined when a weigh change rate lower than 0.002%/min was recorded.

**Specific surface area.** The Brunauer–Emmett–Teller (BET) method was used to determine the specific surface area of the samples, using a Gemini VII apparatus (Micromeritics, Norcross, GA). Measurements were carried out on 300 mg of the powder from ten capsules, after a 24-h degassing step at 30 °C under vacuum (VacPrep 061, Micromeritics, Norcross, GA). Measurements were performed in triplicate.

**Particle size distribution by laser diffraction.** The Mastersizer 3000 equipped with dry dispersion feeder unit Aero 5 (Malvern Instrument, Malvern, UK) was used to measure the particle size of the powder by laser diffraction. The content of a single capsule was emptied into the hopper of the feeder and dispersed with a pressure of four bar, the total time of analysis was set at 10 s. In order to use the Mie theory to convert light scattering data to particle size values, experimental parameters such as refraction index and density of particles were set at 1.5 and 1, respectively, as suggested for standard opaque particles by the manufacturer<sup>24</sup>. Measurements were carried out in triplicate.

#### Scanning electron microscopy

Scanning electron micrographs (SEM) of the Teijin powder samples were conducted using a Zeiss Ultra plus field emission scanning electron microscope (FESEM, Zeiss GmbH, Germany) operated at 4 kV. Prior to imaging, samples were mounted on carbon sticky tabs and platinum-coated to ~10 nm thickness using a sputter coater (E306A Sputter coater, Edwards Vacuum, Crawley, UK).

**Scanning Raman spectroscopy.** An inVia Raman microscope (Renishaw, Wotton-under-Edge, UK), equipped with a 532 nm diode laser, was used to collect individual Raman reference spectra from the single components and Raman images data from the powder mixture.

The capsule powder was flattened onto a glass microscope slide to provide a nominal flat and leveled powder surface. Raman images were generated from 200 000 spectra collected using a step size of 3 μm. The Raman images were used to show the relative location of each core species within the formulation, using previously collected reference spectra from pure materials.

Direct Classical Least Squares Method (DCLS) was used to produce the Raman images from over 70,000 spectra collected in roughly 1 h. The images were then combined to enable comparison between the relative locations of the BDP and other components of the nasal powder.

The streamline image data were processed to remove cosmic ray features using a nearest neighbor approach with the WIRE 3.3 software (Renishaw, Wotton-under-Edge, UK). The combined image shows green features as BDP, red magnesium stearate and blue HPC carrier particles.

#### Analytical characterization

##### BDP quantification using HPLC

The amount of active ingredient in each sample was determined using a HPLC system equipped with a SPD-20A UV-VIS detector (Shimadzu, Tokyo, Japan). A Novapak C18 column (150 × 3.9 mm, 4 μm, Waters, Australia) was used with a mobile phase methanol/water 80:20 v/v. The flow rate was set at 1 mL/min and BDP was detected at  $\lambda = 243$  nm. The retention time of BDP was found to be between 7.5 and 8 min. Standards were prepared in the mobile phase, and 100 μl injected in order to obtain a calibration curve whose linearity was measured between 0.1 μg mL<sup>-1</sup> and 50 μg mL<sup>-1</sup>.

**Dose content uniformity.** The dose content uniformity of the Rhinocort® formulation was determined as an average of three measurements. For each measurement, the powder contained in one capsule was dissolved in 10 mL of methanol. The solution was filtered using nylon filters (0.45 μm, Sartorius, Goettingen, Germany) and samples collected for quantification by HPLC. The compatibility between the filter and the drug was assessed. No statistical difference in the BDP amount was found whether the solutions were filtered or not.

**Shoot weight and BDP content.** The device was weighed after the capsule was placed inside and after each actuation. The device was positioned at 30° and the emitted powder was collected in a 15 ml centrifuge tube. In order to determine the amount of BDP emitted after each actuation, 5 ml of a mixture of methanol water (80:20) were added to the container; subsequently the tube were shaken, vortexed and sonicated for about 30 min. The analyses were conducted in triplicate and the amount of BDP was determined through the HPLC method previously described. The emitted BDP (%) was calculated from the ratio between the emitted mass of BDP for a certain actuation and the mass of powder emitted for the same actuation. The emitted dose fraction (%) was calculated from the ratio of mass of BDP emitted and the dose of drug contained in one capsule.

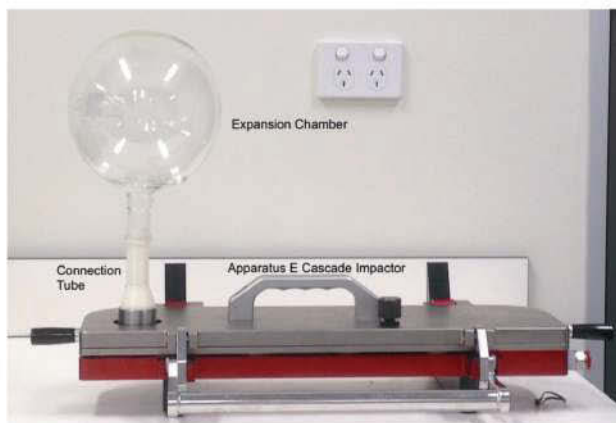


Figure 2. Apparatus E system used for the aerosol performance of the Teijin nasal powder device equipped with the nasal expansion chamber.

#### Aerosol performance of Teijin Rhinocort

##### Cascade impaction

The aerodynamic performance of the Rhinocort<sup>®</sup> formulation delivered via the Puvlizer device was assessed using a cascade impactor, British Pharmacopeia apparatus E (Westech W7; Westech Ltd., Henlow, UK) equipped with a 2 L glass expansion chamber according to the Food and Drug Administration (FDA) guidance<sup>2,12,25–27</sup>. The expansion chamber is a 2 L single-neck round-bottomed flask with 1 cm inlet hole at 30° angle from the neck axis (Figure 2).

The Teijin device was connected to the inlet of the expansion chamber and the test was performed actuating the device eight times for each capsule with airflow of 15 L/min calibrated using a flow meter (Model 3063; TSI Inc., Shoreview, MN). For each test, three capsules were used to ensure an API concentration above detection limit of the HPLC method in the Apparatus E stages. Each Apparatus E stage was washed with the following volumes of a washing solution 80:20 methanol/water: expansion chamber 25 mL; capsules, connection tube, first and final stage 10 mL each; device and all other stages 5 mL. BDP amount in each sample was assayed using the HPLC method described above. Experiments were carried out in triplicate.

The emitted fraction (EF) was calculated as the total amount of drug emitted from the device (i.e. the sum of drug deposits on the chamber, connection tube and impactor stages) divided by the nominal dose (50 µg/capsule).

**In-line in vitro aerosol laser diffraction analysis.** In order to measure the particle size distribution of the emitted powder from the Teijin device, laser diffraction was used (Spraytec, Malvern Instrument, Malvern, UK). The device was placed at 2.5 cm from the measurement cell, at a fixed angle of 30° using an extraction flow rate of 15 L/min in order to mimic the *in vivo* drug administration. The analysis was performed for 10 s with an acquisition rate of 2.5 kHz. A total of three capsules were analyzed. For each, minimum of six puffs were measured in order to completely empty the device. In order to measure the particle size, using the Mie theory, values of refraction index 1.5 and 1 as density value for particles were used, respectively<sup>24</sup>.

#### Results and discussion

The regulatory requirements to characterize nasal products are well documented<sup>6–25</sup>. These include: (i) Single actuation through container life, (ii) Droplet size distribution by laser diffraction, (iii) Drug in small particle/droplets, or particle/droplet size distribution by cascade impactor, (iv) Drug particle size distribution by microscopy, (v) Spray pattern, (vi) Plume geometry and (vii) Priming and re-priming. The particle size range to be studied is above 10 µm, for which current impactors are not suited.

##### Physicochemical characterization of the formulation

The formulation is composed of 50 µg of BDP in a 28.8 ± 0.4 mg powder blend containing hydroxypropylcellulose (HPC), magnesium stearate and stearic acid (0.5–1% of the formulation). The original formulation is protected by a Japanese, US and EU patent<sup>14,28–31</sup>. Furthermore, the formulation is a powder blend of large excipient particles with BDP, as shown by the SEM on Figure 3. The main dimension of the particles is typically 100 µm, corresponding to HPC particles, and irregular in shape.

The capsule content uniformity, as measured by HPLC, showed an average of 48.11 ± 2.75 µg/capsule of BDP. The bulk density of the powder was found to be 0.564 ± 0.004 g/cm<sup>3</sup>, and the tapped density was 0.621 ± 0.003 g/cm<sup>3</sup>, this values provide a Carr's index of 9 implying that the powder has good flowability properties<sup>22,23</sup>. As shown in Table 3, the amount of BDP emitted after each one of the eight actuations is never constant nor a decreasing trend can be described. Usually the first actuations release the highest amount of drug (and percentage of dose), and already seven of the eight actuations required are sufficient to deliver almost the totality of the dose. The same fluctuating trend is observed for the amount of powder emitted, this highlights how improvements on this type nasal powder device are needed, when compared to the liquid pumps that deliver always the same amount of drug solution/suspension after each spray. The same trend was observed for the other two parameters.

The interaction between the formulation and ambient environment (i.e. moisture) during use and storage is an important aspect to evaluate long-term stability and spray performances due to the

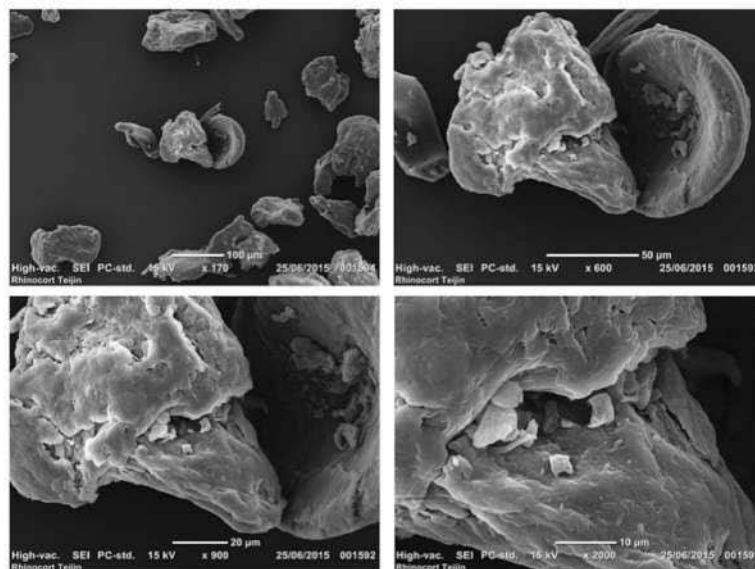


Figure 3. SEM micrographs of the Teijin Rhinocort powder blend.

Table 3. Amount of powder (mg) and BDP ( $\mu\text{g}$ ) emitted after each actuation ( $n=3 \pm \text{StDev}$ ).

	Actuation 1	Actuation 2	Actuation 3	Actuation 4	Actuation 5	Actuation 6	Actuation 7	Actuation 8
Emitted powder (mg)	$8.27 \pm 0.83$	$4.23 \pm 2.51$	$3.73 \pm 1.17$	$3.77 \pm 1.39$	$6.17 \pm 4.02$	$2.03 \pm 0.67$	$1.20 \pm 0.35$	$0.07 \pm 0.11$
Emitted BDP ( $\mu\text{g}$ )	$9.82 \pm 1.89$	$7.76 \pm 3.62$	$6.16 \pm 1.49$	$6.74 \pm 1.28$	$8.52 \pm 4.09$	$3.90 \pm 0.98$	$2.97 \pm 1.36$	$0.83 \pm 1.45$
Emitted BDP (%)	0.12	0.18	0.17	0.18	0.14	0.19	0.25	1.25
Emitted dose fraction (%)	20.7	16.3	13.0	14.2	17.9	8.2	6.3	1.7

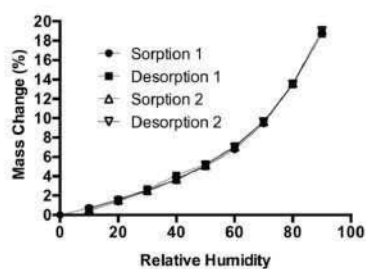


Figure 4. Dynamic vapor sorption isotherm (two cycles) of Rhinocort Teijin powder.

possibility of powder cohesion and increased retention of powder in the device with consequent reduced emitted dose<sup>32</sup>.

DVS was used in order to gain a better understanding of the behavior of the powder at different RH values. Figure 4 shows the moisture sorption isotherm (two cycles, sorption and desorption) for Rhinocort<sup>®</sup> formulation. The powder adsorbed roughly 20% w/w of moisture from 0 to 90% RH. The vapor sorption profile is comparable to reported values in literature for HPC over the same humidity range, which is the main component of the formulation

and is similar to an isotherm type III, characteristic of not porous, or possibly macro-porous materials with low energy of adsorption<sup>33–36</sup>.

There were no significant differences between two subsequent adsorption cycles, both cycles being completely reversible, suggesting moderate hygroscopicity<sup>37</sup>. The large amount of water that the powder can adsorb and the process of gelification observed during the hydration of the powder suggest the suitability of the formulation for nasal delivery allowing a longer residence time of the powder in the nasal cavity when hydrated<sup>33,38,39</sup>.

The specific surface area is a derived property of powders that can be used to determine the type and properties of a material and it is not linked to particle size, in fact powders with similar particle size can have different area, suggesting different particle porosity. A large surface area can ensure a better dissolution or hydration allowing the powder to hydrate and possibly dissolve the associated drug faster<sup>40</sup>.

The BET method was used to evaluate the surface area of the Teijin formulation and results showed a value of  $0.426 \pm 0.025 \text{ m}^2 \text{ g}^{-1}$ , comparable to low-substituted HPC available on the market, suggesting that the main component of the formulation is determining this property of the powder<sup>41</sup>.

In order to gain information regarding the powder particle size distribution, the capsule content was analyzed with Mastersizer 3000 (Malvern Instruments, Malvern, UK) equipped with Aero S system for dry dispersion. Figure 5 shows that the powder had a

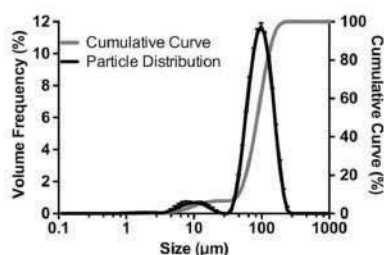


Figure 5. Particle size analysis by laser diffraction of Rhinocort Teijin powder blend measured with Malvern Mastersizer MS3000 ( $n=3 \pm \text{StDev}$ ).

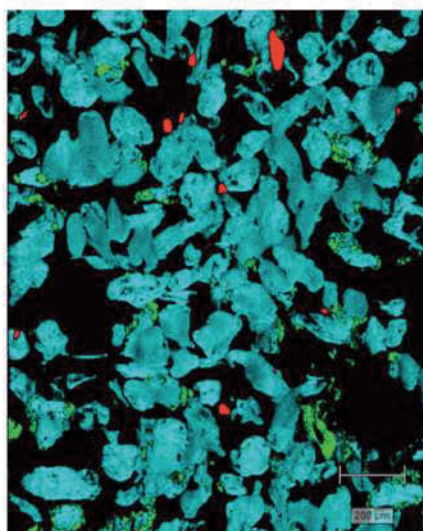


Figure 6. Overlay of Raman images on white light montage (BDP = green; HPC = blue and magnesium stearate = red).

Table 4. Percentage of Active Ingredient in each stage of the Apparatus E Impactor equipped with the 2L expansion glass chamber for nasal delivery ( $n=3 \pm \text{StDev}$ ).

Part or stage	Cut off diameter ( $\mu\text{m}$ )	% BDP ( $\pm \text{StDev}$ )
Expansion chamber	–	90.2 $\pm$ 4.78
Connection tube	–	0.57 $\pm$ 0.12
Stage 1	>14.1	4.64 $\pm$ 1.39
Stage 2	14.1–8.61	0.61 $\pm$ 0.25
Stage 3	8.61–5.39	0.36 $\pm$ 0.17
Stage 4	5.39–3.3	0.08 $\pm$ 0.14
Stage 5	3.3–2.08	NA
Stage 6	2.08–1.36	NA
Stage 7	1.36–0.98	NA
Final stage	<0.98	NA
Capsules (3)	–	2.01 $\pm$ 0.46
Device	–	0.74 $\pm$ 0.11

broad range of particle size (from 1 to 240  $\mu\text{m}$ ) divided into two distinct populations: 6.6% of the volume was in the small size population (peak at 9.9  $\mu\text{m}$ ), while the rest (93%) presented a peak at 98  $\mu\text{m}$ . The volume diameters characterizing the powder

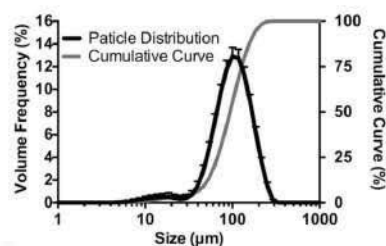


Figure 7. Particle size distribution of the powder emitted from Teijin Rhinocort using the Spraytech laser diffraction apparatus ( $n=3, \pm \text{StDev}$ ).

obtained from three capsules were:  $D_{v10}$  51.7  $\pm$  0.7  $\mu\text{m}$ ,  $D_{v50}$  98  $\pm$  1.3  $\mu\text{m}$  and  $D_{v90}$  162.3  $\pm$  4.0  $\mu\text{m}$ , respectively.

Figure 6 shows the scanning Raman map of the Teijin formulation powder, providing information about the localization of each component in the formulation blend. The larger and more abundant particles were hydroxyl propyl cellulose, supporting the DVS, BET and laser diffraction results. Sporadic particles of magnesium stearate were also observed. The BDP micronized particles were typically found on the surface of the large excipient particles but did not appear to be uniformly distributed, suggesting that probably the powder was not an ordered blend of the different components (Figure 6).

#### Aerosol performance of Teijin Rhinocort

The aerosol performance of the formulation was measured using Apparatus E equipped with a glass expansion chamber and by laser diffraction. According to the FDA draft guidance for industry, impactor and laser diffraction experiments should be performed to ascertain the absence of finer particles (aerodynamic diameter <10  $\mu\text{m}$ ) likely to penetrate the conductive airways and reach the lungs<sup>23</sup>.

As shown in Table 4 almost the total amount of the BDP was found in the expansion chamber and roughly 95% of the API was deposited in stages with a cutoff diameter larger than 10  $\mu\text{m}$ . Around 3% remained in the capsule and the device, indicating that the dose was not completely emitted. In only one experiment some BDP was detected (0.24% of the total) on stage 4; no drug was found in any lower cutoff stages.

In order to determine if any formulation excipient (i.e. HPC) could reach the lower airways, additional studies using Spraytech (Malvern Instruments, Malvern, UK) laser diffraction particle sizing were performed. The frequency and cumulative undersize particle size distribution profiles for the aerosolized powder are shown in Figure 7. It can be noticed that there are two populations, the first with a peak around 16  $\mu\text{m}$ , and the other one at 108  $\mu\text{m}$ . More than the 99% of the powder has a volume size larger than 10  $\mu\text{m}$  and the  $D_{v50}$  was 93.7  $\pm$  2.9  $\mu\text{m}$ . The  $D_{v50}$  value of the emitted dose is slightly smaller and significantly different from the one obtained for the capsule content, suggesting that a phenomenon of de-agglomeration is occurring during the *in vivo* simulated administration process using the Spraytech (Malvern Instruments, Malvern, UK).

The  $D_{v10}$ ,  $D_{v50}$  and  $D_{v90}$  for each actuation necessary to empty one capsule were determined with the Spraytech. Figure 8 shows  $D_{v10}$ ,  $D_{v50}$  and  $D_{v90}$  for each actuation obtained averaging three capsules. No statistical difference was observed. However, it was not possible to obtain data for the last two actuations of the eight

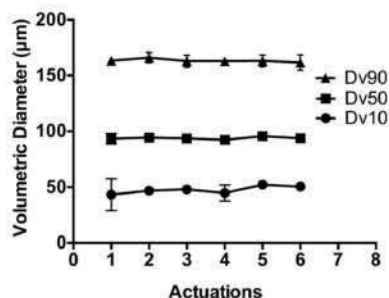


Figure 8. Equivalent volume diameter values ( $D_v$ , 90, 50 and 10) measured by laser diffraction for Teijin Rhinocort, eight insufflations for one dose ( $n = 3$ ,  $\pm$  StDev).

required for drug administration, since six actuations were enough to empty the capsule to the point where any further emitted powder was not enough to trigger the analysis, in disagreement to what is suggested on the patient information leaflet, where 4 actuation for each nostril are indicated to complete the process.

Clinical studies on the efficacy of Teijin formulation, on nasal allergies, were performed in Japan on over 220 people. Results from 1986 shows that the dry powder formulation was able to decrease the daily dosage by one quarter when compared to a pressurized nasal formulation (from 400  $\mu$ g to 100  $\mu$ g daily), with the same overall therapeutic improvement and less incidence of side effects<sup>42</sup>. The better efficacy of the powder formulation was explained as a result of the presence of HPC and its ability to prolong the residence of BDP in the nasal cavity. Furthermore, the fewer side effects were related to the lower daily frequency of administration needed and the reduced irritation due to the presence of the main excipient, HPC, compared to equivalent Freon based pMDI nasal formulations<sup>42</sup>. Similar results have been found in literature also for Rhinocort Turbohaler<sup>®</sup> (Budesonide, AstraZeneca, London, UK), where patients were found to prefer the use of a dry powder device (formulation) compared to a water nasal spray. Specifically, the patients found the DPI product to have a less unpleasant taste and to cause less nasal irritation, compared to the reference liquid product<sup>43</sup>.

In another study, the Optinose<sup>®</sup> device (Optinose, Yardley, PA) has been used for the systemic delivery of sumatriptan powder through the nose, reporting fast absorption ( $t_{max} = 20$  min) of the drug and no bitter aftertaste<sup>9</sup>. Furthermore, in another study, it was shown that when compared to water spray, the Optinose powder formulation had less clearance in the first two minutes after the administration due to lack of anterior drip-out and less sniffing that prevented further dripping<sup>15</sup>.

### Conclusion

Teijin Puvlizer Rhinocort<sup>®</sup> is one of the few nasal powder inhalers in the market worldwide and the oldest. The device comprises of a squeeze bulb-based insufflator able to administer the powder loaded in a capsule via repeated actuations. Despite the simple device, the particle size distribution was highly reproducible, suggesting a consistent deposition of the drug in the nasal cavity, complying with the FDA guidance requirements for nasal formulations. Practically, the fact that six consecutive and repeated steps are required to administer the required dose can be considered as a limiting step for patient compliance, in comparison with multi-dose pre-metered water nasal products now on the market.

### Disclosure statement

No conflicts of interest exist.

### Funding information

A/Professor Traini is the recipient of an Australian Research Council Future Fellowship (project number FT12010063). A/Professor Young is the recipient of an Australian Research Council Future Fellowship (project number FT110100996).

### References

1. Tafaghodi M, Rastegar S. Preparation and in vivo study of dry powder microspheres for nasal immunization. *J Drug Target* 2010;18:235–42.
2. Ishikawa F, Katsura M, Tamai I, Tsuji A. Improved nasal bio-availability of elcatonin by insoluble powder formulation. *Int J Pharm* 2001;224:105–14.
3. Kaye RS, Purewal TS, Alpar OH. Development and testing of particulate formulations for the nasal delivery of antibodies. *J Control Release* 2009;135:127–35.
4. Kamide N, Ogino M, Yamashina N, Fukuda M. Sniff nasal inspiratory pressure in healthy Japanese subjects: mean values and lower limits of normal. *Respiration* 2008;77:58–62.
5. Mistry A, Stolnik S, Illum L. Nanoparticles for direct nose-to-brain delivery of drugs. *Int J Pharm* 2009;379:146–57.
6. Djupesland PG, Skretting A. Nasal deposition and clearance in man: comparison of a bidirectional powder device and a traditional liquid spray pump. *J Aerosol Med Pulm Drug Deliv* 2012;25:280–9.
7. Djupesland PG, Skretting A, Winderen M, Holand T. Breath actuated device improves delivery to target sites beyond the nasal valve. *Laryngoscope* 2006;116:466–72.
8. Birkhoff M, Leitz M, Marx D. Advantages of intranasal vaccination and considerations on device selection. *Indian J Pharm Sci* 2009;71:729–31.
9. Luthringer R, Djupesland PG, Sheldrake CD, et al. Rapid absorption of sumatriptan powder and effects on glyceryl trinitrate model of headache following intranasal delivery using a novel bi-directional device. *J Pharm Pharmacol* 2009;61:1219–28.
10. Schroeter JD, Garcia GJM, Kimbell JS. A computational fluid dynamics approach to assess interhuman variability in hydrogen sulfide nasal dosimetry. *Inhal Toxicol* 2010;22:277–86.
11. Balducci AG, Ferraro L, Bortolotti F, et al. Antidiuretic effect of desmopressin chimera agglomerates by nasal administration in rats. *AAPS PharmSciTech* 2014;440:956–62.
12. Ishikawa F, Murano M, Hiraishi M, et al. Insoluble powder formulation as an effective nasal drug delivery system. *Pharm Res* 2002;19:1097–104.
13. Colombo G, Lorenzini L, Zironi E, et al. Brain distribution of ribavirin after intranasal administration. *Antiviral Res* 2011;92:408–14.
14. Tepper SJ, Cady RK, Silberstein S, et al. AVP-825 breath-powered intranasal delivery system containing 22 mg sumatriptan powder vs 100 mg oral sumatriptan in the acute treatment of migraines (The COMPASS study): a comparative randomized clinical trial across multiple attacks. *Headache* 2015;55:621–35.

15. Djupesland PG, Docekal P, Czech Migraine Investigators Group. Intranasal sumatriptan powder delivered by a novel breath-actuated bi-directional device for the acute treatment of migraine: a randomised, placebo-controlled study. *Cephalalgia* 2010;30:933–42.
16. Djupesland PG. Nasal drug delivery devices: characteristics and performance in a clinical perspective—a review. *Drug Deliv Transl Res* 2013;3:42–62.
17. Health USDO, Human Services F. Bioavailability and bioequivalence studies for nasal aerosols and nasal sprays for local action. Rockville (MD): Drug Administration, Center for Drug Evaluation, Research; 2003. Available from: <http://www.fda.gov/downloads/drugs/guidancecomplianceregulatoryinformation/guidances/ucm070111.pdf>.
18. Coowanitwong I, de S, Somaraju S, et al. Regional deposition of beclomethasone dipropionate powder exiting Puvlizer® in a nasal cast connected to a next generation impactor. *RDD Europe* 2011;2011:373–8.
19. Ottaviano G, Scadding GK, Coles S, Lund VJ. Peak nasal inspiratory flow; normal range in adult population. *Rhinology* 2006;44:32–5.
20. Papachristou A, Bourli E, Aivazi D, et al. Normal peak nasal inspiratory flow rate values in Greek children and adolescents. *Hippokratia* 2008;12:94–7.
21. Jallo LJ, Ghoroi C, Gurumurthy L, et al. Improvement of flow and bulk density of pharmaceutical powders using surface modification. *Int J Pharm* 2012;423:213–25.
22. Carr RL. Evaluating flow properties of solids. *Chem Eng* 1965;72:163–8.
23. Schüssele A, Bauer-Brandl A. Note on the measurement of flowability according to the European Pharmacopoeia. *Int J Pharm* 2003;257:301–4.
24. Dayal P, Shaik MS, Singh M. Evaluation of different parameters that affect droplet-size distribution from nasal sprays using the Malvern Spraytec®. *J Pharm Sci* 2004;93:1725–42.
25. U.S. Department of Health and Human Services, Food and Drug Administration, Center for Drug Evaluation and Research. Bioavailability and Bioequivalence Studies for Nasal Aerosols and Nasal Sprays for Local Action. 2003;1–37.
26. Doub WH, Adams WP, Wokovich AM, et al. Measurement of drug in small particles from aqueous nasal sprays by Andersen cascade impactor. *Pharm Res* 2012;29:3122–30.
27. Great Britain SO. British pharmacopoeia. Appendix XII C. Consistency of formulated preparations. London: Stationery Office; 2015.
28. Suzuki Y, Sekine K, Nagai T, et al. Powdery pharmaceutical composition for nasal administration. 1986:US4613500.
29. Dohi M, Nishibe Y, Makino Y, Fujii T. Powdery composition for nasal administration. 2010:US7731990B2.
30. Kobayashi H, Makino Y, Suzuki Y. Pharmaceutical preparation for intra-airway administration. 2001:EP0606486.
31. Makino Y, Kobayashi H, Suzuki Y. Pharmaceutical preparation for intra-airway administration. 1996:EP0606486A4.
32. Young PM, Price R, Tobyn MJ, et al. Effect of humidity on aerosolization of micronized drugs. *Drug Dev Ind Pharm* 2003;29:959–66.
33. Baumgartner S, Kristl J, Peppas NA. Network structure of cellulose ethers used in pharmaceutical applications during swelling and at equilibrium. *Pharm Res* 2002;19:1084–90.
34. Yakimets I, Paes SS, Wellner N, et al. Effect of water content on the structural reorganization and elastic properties of biopolymer films: a comparative study. *Biomacromolecules* 2007;8:1710–22.
35. Condon JB. Surface area and porosity determinations by physisorption: measurements and theory. Amsterdam: Elsevier Science; 2006:1–297.
36. Storey RA, Ymén I. Solid state characterization of pharmaceuticals. 3rd edn. New York, NY: John Wiley & Sons; 2011.
37. Callahan JC, Cleary GW, Elefant M, et al. Equilibrium moisture content of pharmaceutical excipients. *Drug Dev Ind Pharm* 1982;8:355–69.
38. Dohi M, Nishibe Y, Makino Y, Fujii T. Powdery composition for nasal administration. 2005:US6881423B2.
39. Hansen K, Kim G, Desai K-GH, et al. Feasibility investigation of cellulose polymers for mucoadhesive nasal drug delivery applications. *Mol Pharm* 2015;12:2732–41.
40. Khadka P, Ro J, Kim H, et al. Pharmaceutical particle technologies: an approach to improve drug solubility, dissolution and bioavailability. *Asian J Pharm Sci* 2014;9:304–16.
41. Rowe RC, Sheskey PJ, Cook WG, et al. Handbook of pharmaceutical excipients. London, UK: Royal Pharmaceutical Society; 2012.
42. Okuda M, Okamoto M, Nomura Y, Saito Y. Clinical study on beclomethasone dipropionate powder preparation (TL-102) in perennial nasal allergy. *Rhinology* 1986;24:113–23.
43. Yang WH, Dolovich J, Drouin MA, et al. Comparison of budesonide Turbuhaler with budesonide aqua in the treatment of seasonal allergic rhinitis. Rhinocort Study Group. *Can Respir J* 1998;5:455–60.

# Transport of Beclometasone Dipropionate Across RPMI 2650 Model of Nasal Epithelium: Evaluation of Two Different Approaches to Drug Delivery

Michele Pozzoli,<sup>1,2</sup> Hui Xin Ong,<sup>2</sup> Fabio Sonvico,<sup>1,3</sup>  
Paul M. Young,<sup>2</sup> and Daniela Traini<sup>2</sup>

<sup>1</sup>Graduate School of Health – Pharmacy,  
University of Technology Sydney, Sydney, Australia

<sup>2</sup>The Woolcock Institute for Medical Research and Discipline of Pharmacology,  
Sydney Medical School, University of Sydney, Sydney, Australia

<sup>3</sup>Department of Pharmacy, University of Parma, Italy

**KEYWORDS:** nasal epithelium model, nasal drug delivery,  
next generation cascade impactor, deposition,  
beclometasone dipropionate (BDP)

## INTRODUCTION

Allergic rhinitis is a hypersensitivity reaction to inhaled allergens. It produces inflammation of the nasal mucosa characterized by nasal congestion, sneezing, itching and rhinorrhoea [1]. Intranasal corticosteroids are highly effective in preventing and relieving early- and late-phase symptoms. Beclometasone dipropionate (BDP) is a commonly used glucocorticoid pro-drug which is hydrolyzed to its active form, beclometasone-17-monopropionate (BMP) [2]. In Australia, BDP is commercially available over the counter as an aqueous suspension, e.g., Beconase® (GSK), delivered via a nasal spray pump. In Japan, BDP is also available as a powder formulation commercialized as Rhinocort (Teijin Pharma) [3].

The conventional way to test *in vitro* permeation of drugs through cells is by the use of drug solution or suspension added at different concentrations to the apical side of cells growing on multi-well plates. However, this method is not representative of the *in vivo* processes occurring following nasal steroid administration, where aerosolized drugs in either suspension, or powder form is deposited on to nasal mucosa. Therefore, the aim of this study was to compare the conventional *in vitro* BDP drug permeation of a suspension with a novel deposition method that allows the delivery of drug aerosols generated from both liquid-based and powder-based nasal devices directly onto the surface of cultured nasal cells.



## METHODS

A nasal epithelia cell line (RPMI 2650; ATCC, USA), was grown and passaged according to ATCC protocol, with complete Minimum Essential Medium (Life Technologies, Australia) containing 10% fetal bovine serum (Life Technologies, Australia) 1X non-essential amino acid solution (Sigma Aldrich, Australia) and 2 mM L-glutamine, which was incubated at 37°C in a humidified atmosphere containing 5% CO<sub>2</sub>. To establish an air-liquid interface (ALI) model, 200 µl of nasal cells suspensions (2.5x10<sup>6</sup> cell/ml) were seeded on Snapwell™ polyester membrane inserts (1.13 cm<sup>2</sup>, 0.4 µm pore size, Corning Costar, USA). After 24 hours, the media from the apical compartment was removed. Transport studies were performed after 14 days of cell differentiation at the ALI configuration [4].

Beconase® (GSK, Australia) was chosen as the BDP water-based suspension nasal liquid product (50 µg/spray nominal dose). It contains cellulose, dextrose, polysorbate 80, phenylethyl alcohol (2.5 µL/g) and benzalkonium chloride (0.2 mg/g). Teijin Rhinocort® (Teijin, Japan) was used as the BDP nasal dry powder formulation. Teijin Rhinocort is a capsule-based device with each capsule containing a nominal dose of 50 µg of BDP, hydroxypropylcellulose (HPC) as carrier and magnesium stearate. To investigate and compare the effects of BDP aerosol deposition, a “conventional” transport study was performed by adding 250 µl of 15 µg/ml BDP of Hank's Balanced Salt Solution ((HBSS) Life Technologies, Australia) suspension directly to the apical surface of RPMI 2650 nasal cells (control formulation).

To study the transport of BDP after aerosol deposition, Apparatus E (Westech Ltd., UK) equipped with a previously described modified expansion chamber that holds Snapwell cell inserts, was used to mimic the deposition of BDP from both the dry powder and suspension nasal formulations [5]. Briefly, cell inserts were removed from the cultured plates and washed with pre-warmed HBSS. Subsequently, the Snapwell inserts were transferred into the modified nasal deposition chamber. For each formulation (dry powder and liquid suspension) a total of 150 µg of BDP was delivered into the chamber where the wells were located. Apparatus E was connected to a pump (Westech Scientific, UK) and flow rate was set to 15 L.min<sup>-1</sup>, using a calibrated flow-meter (Model 4040F; TSI Incorporated, MN, USA). Cell inserts after deposition were repositioned on culture plates and transport studies were performed for four hours. Samples (200 µl) were withdrawn every hour and media restored with fresh HBSS buffer to maintain sink condition. At the end of the experiment, the cell layer surface was washed to collect the drug on the surface of the cells before cell lysis to analyze the intracellular amount of drugs. BDP and BMP were quantified using validated high performance liquid chromatography (HPLC) method using a system equipped with UV-detector (Shimadzu Corporation, Japan) and a C18 column (Luna 3 µm, 4.6 x 150 mm, Phenomenex, Australia) operating at a flow rate of 0.8 mL.min<sup>-1</sup> and detector set to 243 nm. Mobile phase was a mixture of methanol: water (80:20 %v/v) and retention times of BDP and BMP were approximately six and nine minutes, respectively.

## RESULTS AND DISCUSSION

The sum of BDP and BMP (expressed as a percentage of total drug deposition) transported across the RPMI 2650 nasal cell model is shown in Figure 1. Overall, the 15µg/ml suspension delivered by direct addition on the surface of the cells, showed the highest drug permeation across the cell layer, with 35% of the drug transported after four hours. The Beconase aerosol suspension showed the highest drug permeation of 10.5% after one hour, while only 3.2% of drug was transported from the BDP dry powder formulation. This may be because dry powder aerosols require additional time

for wetting and dissolution once in contact with the nasal mucus layer. No statistical difference ( $p < 0.05$ ) was found between the two commercial formulations after four hours, suggesting that dissolution was the rate-limiting step for the transport of BDP across cells. It is envisaged that, upon deposition, the particles in both formulations start to dissolve in the nasal mucus creating an *in situ* saturated BDP area leading to a higher concentration gradient driving the diffusion process [6].

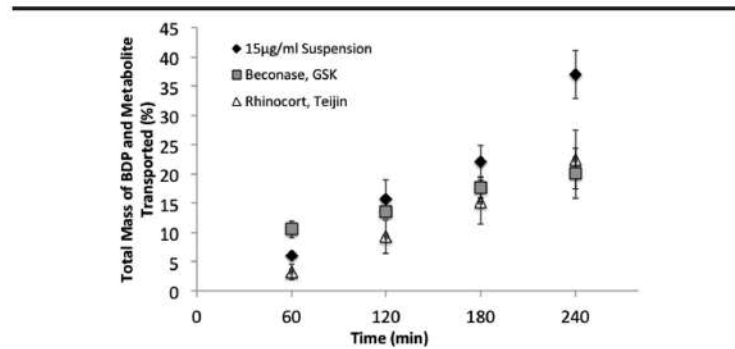


Figure 1. Total amount (%) of BDP and BMP transported over four hours ( $n = 3$ ,  $\pm$  StDev).

The amount (%) of BDP and BMP found on the surface and inside the nasal cells is shown in Table 2. It was found that around 25% of the BDP remained on the surface of the cell when BDP was delivered as suspensions, either by conventional transport method or as aerosols using the nasal spray. Meanwhile, for the dry powder formulation, only 9.4% was found to remain on the cells surface, confirming that the dry powder particles provide a higher permeation into the cell membrane after the deposition, which could be possibly due to a higher local concentration gradient during the powder dissolution. As for the values of BMP, the dry powder formulation showed the highest percentage of BMP inside the cells, with 64% of total drug deposited, suggesting that once penetrated into the cells, the BDP is rapidly converted into the active compound, BMP. No statistical differences were found between the Beconase and the Rhinocort formulations.

However, the 15 µg/ml suspension showed the lowest percentage of BMP inside the cell, but the highest drug transport across the cell layers. This could be due to the liquid-liquid interface conditions of the transport study. This approach may dilute the mucus layer barrier present on cell surface and ultimately maximize the paracellular permeation rate of the drug. Therefore, the new approach is believed to be more representative of the physiological conditions during nasal drug deposition.

	BDP		BMP	
	ON	IN	ON	IN
15µg/ml Suspension	25.4 $\pm$ 0.7	1.4 $\pm$ 0.2	0.7 $\pm$ 0.1	34.7 $\pm$ 2.1
Beconase, GSK	26.4 $\pm$ 8.4	1.0 $\pm$ 0.1	1.7 $\pm$ 1.2	52.9 $\pm$ 3.3
Rhinocort, Teijin	9.4 $\pm$ 3.6	3.0 $\pm$ 0.9	0.9 $\pm$ 0.6	64.0 $\pm$ 15.2

## CONCLUSIONS

This study has shown that there were no statistical differences between two commercially available nasal BDP formulations, for both the total drug permeated and the amount of active compound (BMP) recovered inside the cells after deposition studies. However, differences were found between classical aliquot addition based transport studies and the *in vitro* deposition method described herein, highlighting the importance of choosing a more physiological method to assess nasal formulations *in vitro*.

## REFERENCES

1. Trongsrud AJ, Whitaker AL, Small RE: Intranasal corticosteroids for allergic rhinitis, *Pharmacotherapy* 2002, 22: 1458-67.
2. Roberts JK, Moore CD, Ward RM, Yost GS, Reilly CA: Metabolism of beclomethasone dipropionate by cytochrome P450 3A enzymes. *J Pharmacol Exp Ther* 2013, 345: 308-16.
3. Okuda M, Okamoto M, Nomura Y, Saito Y: Clinical study on beclomethasone dipropionate powder preparation (TL-102) in perennial nasal allergy. *Rhinology* 1986, 24: 113-23.
4. Pozzoli M, Fabio S, Ong HX, Traini D, Young PM: Optimization of RPMI 2650 cells as a model for nasal mucosa. In *Respiratory Drug Delivery 2014. Volume 3*. Edited by Dalby RN, Byron PR, Peart J, Farr SJ, Suman JD, Young PM, Traini D. DHI Publishing; River Grove, IL: 2014: 739-42.
5. Pozzoli M, Zhu B, Traini D, Young PM, Fabio S: Validation of a novel apparatus for deposition studies of nasal products. In *Respiratory Drug Delivery Europe 2015. Volume 2*. Edited by Dalby RN, Byron PR, Peart J, Suman JD, Young PM, Traini D. DHI Publishing; River Grove, IL: 2015: 537-42.
6. Ong HX, Traini D, Loo C-Y, Sarkissian L, Lauretani G, Scalia S, Young PM: Is the cellular uptake of respiratory aerosols delivered from different devices equivalent? *Eur J Pharm Biopharm* 2015, 93: 320-27.



## Validation of a Novel Apparatus for Deposition Studies of Nasal Products

Michele Pozzoli,<sup>1,2</sup> Simone Cattaneo,<sup>4</sup> Bing Zhu,<sup>2</sup> Daniela Traini,<sup>2</sup>  
Paul M. Young,<sup>2</sup> and Fabio Sonvico<sup>1,3</sup>

<sup>1</sup>Graduate School of Health - Pharmacy,  
University of Technology Sydney, Sydney, Australia

<sup>2</sup>The Woolcock Institute for Medical Research and Discipline of Pharmacology,  
Sydney Medical School, University of Sydney, Sydney, Australia

<sup>3</sup>Department of Pharmacy, University of Parma, Italy

<sup>4</sup>Department of Aerospace Science and Technologies,  
Polytechnic University of Milan, Italy

**KEYWORDS:** Next Generation Impactor (NGI), cascade impactor (CI),  
beclomethasone dipropionate (BDP), deposition, particle size,  
nasal drug delivery, 3D printing

### INTRODUCTION

Particle size distribution is an important property of nasal sprays. Specifically, droplets with an aerodynamic diameter larger than 9  $\mu\text{m}$  are required to provide optimal nasal deposition and prevent inhalation into the lower airways [1]. According to the Food and Drug Administration (FDA) Guidance, the characterization of the nasal droplet size distribution can be evaluated by either laser diffraction or cascade impaction (CI), with an additional 2 L expansion chamber [2]. However, either method is not representative for investigating real time drug deposition in the nasal cavity.

Several cell culture models have been used to simulate the nasal mucosa, however to date no *in vitro* apparatus has been proposed to include simultaneous direct drug deposition and permeation experiments for nasal products [3-5].

The aim of this study was to modify the standard glass expansion chamber, proposed in the FDA guidance for nasal products, and validate a modified expansion chamber using both dry powder and liquid spray nasal products. This new expansion chamber allows *in vitro* cell-based deposition and permeation studies to be performed in conditions resembling drug administration process *in vivo*.

### METHODS

A Next Generation Impactor (NGI, Westech Ltd., UK) equipped with a standard glass expansion chamber for nasal testing was used for determining the aerodynamic particle size distribution of nasal product.

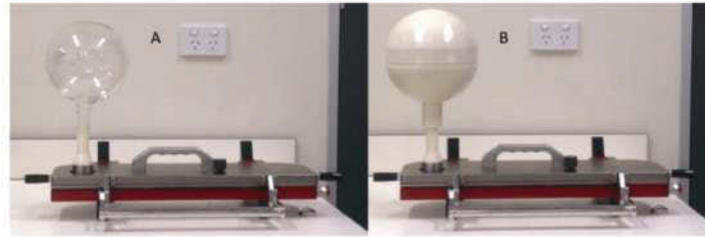


Figure 1. NGI configuration with glass expansion chamber (A) and modified 3D printed chamber (B).

A 2 L single-neck round bottomed glass flask with a 1 cm inlet hole at 30° from the neck axis was used as expansion chamber (EC) for the aerosol deposition experiments (Figure 1A). The modified expansion chamber (MC, Figure 1B and 2) was designed using Catia 3D design software (3DS, Boston, MA). Computer designed drawings were printed in acrylonitrile butadiene styrene (ABS) using a 3D printer (Dimension Elite). The internal and external surfaces were chemically treated with small quantities of acetone in order to eliminate the porosity associated with the printed material. Permeability was assessed using solutions of both water and methanol.

The modified expansion chamber was composed of two spherical interlocking hollow hemispheres. The lower hemisphere contained the opening for the NGI connection and the inlet hole for the nasal device at 30° from the neck axis. The upper hemisphere was designed in order to accommodate three cell culture inserts (Corning® Costar® Snapwell™, Sigma-Aldrich Corp., St. Louis, MO) located directly opposite to the inlet hole, Figure 2. The system design allowed easy access to the expansion chamber inner surface and handling of cell inserts.

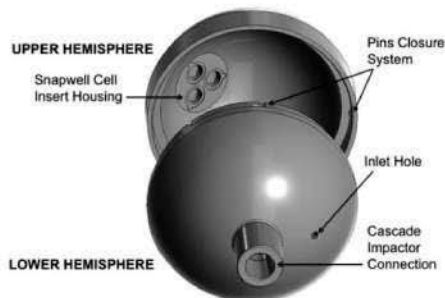


Figure 2. CAD 3D drawing of the modified expansion chamber.

Two different nasal products used for the treatment of rhinitis, both containing beclomethasone dipropionate (BDP) as active ingredient, were chosen to compare and validate the two expansion chambers. The two products were: Teijin Rhinocort® (Teijin, Japan), the only capsule-based nasal dry powder spray on the market (Japan) and Beconase® (GlaxoSmithKline, Australia) an aqueous suspension available over the counter, both products present a nominal dose of 50 µg of BDP.

For each product (dry powder and liquid suspension), aerosol deposition experiments were performed, using both the EC and MC. The NGI was connected to a pump (Westech Scientific, Bedfordshire, UK) and flow rate set at 15 L.min<sup>-1</sup>, using a calibrated flow meter (Model 4040F; TSI Incorporated, Shoreview, MN). BDP was quantified using reverse phase HPLC system equipped with UV-detector (Shimadzu Corporation, Japan) and Luna C18 column (3 µm, 4.6 x 150 mm, Phenomenex, NSW, Australia). Mobile phase was a mixture of methanol: water (80:20 %v/v), flow rate 1 mL.min<sup>-1</sup>, with detector operating at 243 nm and retention time of ~ six minutes. For each experiment, three dry powder capsules were used (eight actuations for each capsule) for the Teijin Rhinocort and three actuations for Beconase, respectively.

Particle sizing of the emitted dose was measured using laser diffraction (Spraytec™, Malvern Instruments, UK). Briefly, the device was placed at 2.5 cm from the Inhaler Nebulizer Accessory (i.e., 5.5 cm from the laser beam), tilted at a fixed angle of 30° and actuated at a flow rate of 15 L.min<sup>-1</sup>, resembling the *in vivo* process of drug administration. Particle size was calculated based on the stable phase of the spray. The results were presented in terms of D<sub>10</sub>, D<sub>50</sub>, and D<sub>90</sub> and percentage of particles ≤ 10 µm.

## RESULTS AND DISCUSSION

The difference in aerosol deposition between the modified expansion chamber and reference glass chamber for the two nasal products were evaluated using NGI and results are listed in Table 1.

	Mass BDP Expansion Chamber (µg)		Mass BDP Throat (Connection) (µg)		Mass BDP Stage 1 (µg)	
	Standard	Modified	Standard	Modified	Standard	Modified
Rhinocort	130.2 ± 6.9	126.8 ± 6.9	0.83 ± 0.17	0.85 ± 0.13	6.7 ± 2.0	6.4 ± 0.3
Beconase	158.1 ± 2.5	155.1 ± 2.5	0.44 ± 0.15	0.34 ± 0.13	NA	NA

No BDP was deposited on stages below Stage 1 of the NGI, confirming the efficiency of the products for nasal purposes. For both Rhinocort and Beconase, no statistical difference (p ≥ 0.05) was found between the amount of BDP deposited in the glass and the modified chamber, suggesting that the novel expansion chamber could be used routinely for aerodynamic size fractioning and deposition studies. For the powder formulation tested, Rhinocort, BDP deposited on the first stage of the NGI. On the contrary, no BDP reached Stage 1 of the NGI when the Beconase

suspension formulation was used. Regarding BDP deposited on the Snapwells using the modified chamber, for the liquid suspension formulation, 40.0% of the BDP was recovered on the three Snapwell inserts, while only 3.4% was recovered on the Snapwell inserts when the dry powder formulation was used. While the Snapwells were dry in this case, the low concentration on the filter membrane is likely due to the plume dynamics rather than adhesion to the membrane. Particle bounce of internal surfaces, including the Snapwells would have resulted in large increases in Stage 1 deposition, which was not observed. However, future studies conducted using Snapwell inserts with cells will be able to elucidate this.

Cascade impaction does not provide information about the final particle size of the whole formulation, but only the fraction containing the active ingredients. In order to fully characterize the particle size distribution of the emitted droplets/particles from the two nasal devices, laser diffraction was used.

As shown in Table 2, the particle size distribution of the BDP powder is larger than the particle size of the droplets obtained with the spray device.

	Rhinocort (µm)	Beconase (µm)
Dv10	46.7 ± 7.8	26.7 ± 3.0
Dv50	93.3 ± 2.8	58.5 ± 11.1
Dv90	163.0 ± 3.7	146.7 ± 48.6
% < 10	1.0 ± 0.8	1.1 ± 0.3

The absence of BDP on NGI Stage 1 for Beconase (despite a lower Dv50 and the higher percentage of deposition on the Snapwell) could be explained by the higher kinetic energy provided to the particles expelled from the liquid pump, resulting in the spray hitting the wall of the expansion chamber without complete aerosolization [1]. The lower energy provided by the dry powder formulation and device allows the plume complete development of the plume in the expansion chamber and the deposition of a small particle fraction in NGI Stage 1.

## CONCLUSIONS

This work has shown that the 3D printed modified expansion chamber for assessing nasal formulation can be reliably used as an alternative to the standard glass chamber when using the NGL. The ability to insert three Snapwell cell culture inserts within the impaction chamber open the possibility for nasal formulation deposition studies on nasal cells, permeation experiments and dissolution tests. Future studies will evaluate the use of a human nasal cell line in this modified nasal chamber for further characterization of nasal formulations.



## REFERENCES

1. Doub, WH *et al.*: Measurement of drug in small particles from aqueous nasal sprays by Andersen Cascade Impactor, *Pharm Res* 2012, 29: 3122-30.
2. FDA Draft Guidance (2003): Guidance for Industry (Draft). Bioavailability and bioequivalence studies for nasal aerosols and nasal sprays for local action.
3. Wengst, A, Reichl, S: RPMI 2650 epithelial model and three-dimensional reconstructed human nasal mucosa as *in vitro* models for nasal permeation studies, *Eur J Pharm Biopharm* 2010, 74: 290-97.
4. Bai, S *et al.*: Evaluation of human nasal RPMI 2650 cells grown at an air-liquid interface as a model for nasal drug transport studies, *J Pharm Sci* 2008, 97: 1165-78.
5. Kreft, ME *et al.*: The Characterization of the human nasal epithelial cell line RPMI 2650 under different culture conditions and their optimization for an appropriate *in vitro* nasal model, *Pharm Res* 2014, 32(2):665-79.

## Optimization of RPMI 2650 Cells as a Model for Nasal Mucosa

Michele Pozzoli,<sup>1</sup> Fabio Sonvico,<sup>1</sup> Hui Xin Ong,<sup>2</sup>  
Daniela Traini,<sup>2</sup> Mary Bebawy,<sup>1</sup> and Paul M. Young<sup>2</sup>

<sup>1</sup>*Graduate School of Health – Pharmacy,  
University of Technology Sydney, Sydney, Australia*

<sup>2</sup>*The Woolcock Institute for Medical Research and  
Discipline of Pharmacology, Sydney Medical School,  
University of Sydney, Sydney, Australia*

KEYWORDS: nasal mucosa, RPMI 2650, air liquid interface (ALI),  
nasal drug, trans-epithelial electrical resistance (TEER),  
mucus, delivery

[Production note:

This conference paper is not included in this digital copy due to copyright restrictions.]

Pozzoli, M., Sonvico, F., Ong, H., Traini, D., Bebawy, M. & Young, P. M. 2014, 'Optimization of RPMI 2650 Cells as a Model for Nasal Mucosa', *Respiratory Drug Delivery 2014*, Virginia Commonwealth University, Fajardo, Puerto Rico, pp. 739-742.

View/Download from: [UTS OPUS](#) or [Publisher's site](#)

## A.2 OTHER PUBLICATIONS DURING CANDIDACY UNRELATED TO THESIS

- Clementino, A., Batger, M., Garrastazu, G., Pozzoli, M., Del Favero, E., Rondelli, V., Gutfilen, B., Barboza, T., Sukkar, M.B., Souza, S.A.L., Cantù, L., Sonvico, F., 2016. The nasal delivery of nanoencapsulated statins - an approach for brain delivery. *Int J Nanomedicine* 11, 6575–6590. doi:10.2147/IJN.S119033
- Comfort, C., Garrastazu, G., Pozzoli, M., 2015. Opportunities and Challenges for the Nasal Administration of Nanoemulsions. *Current Topics in Medicinal Chemistry* 15, 356–368. doi:10.2174/1568026615666150108144655
- Martignoni, I., Trotta, V., Lee, W.-H., Loo, C.-Y., Pozzoli, M., Young, P.M., Scalia, S., Traini, D., 2016. Resveratrol solid lipid microparticles as dry powder formulation for nasal delivery, characterization and *in vitro* deposition study. *J Microencapsul* 1–8. doi:10.1080/02652048.2016.1260659



# The nasal delivery of nanoencapsulated statins – an approach for brain delivery

This article was published in the following Dove Press journal:  
International Journal of Nanomedicine  
7 December 2016  
Number of times this article has been viewed

Adryana Clementino<sup>1,2</sup>  
Mellissa Batger<sup>3</sup>  
Gabriela Garrastazu<sup>2,3</sup>  
Michele Pozzoli<sup>3</sup>  
Elena Del Favero<sup>4</sup>  
Valeria Rondelli<sup>4</sup>  
Bianca Gutfilen<sup>5</sup>  
Thiago Barboza<sup>5</sup>  
Maria B Sukkar<sup>3</sup>  
Sergio A L Souza<sup>5</sup>  
Laura Cantù<sup>4</sup>  
Fabio Sonvico<sup>1,3</sup>

<sup>1</sup>Department of Pharmacy, University of Parma, Parma, Italy; <sup>2</sup>National Council for Scientific and Technological Development – CNPq, Brasília, Brazil; <sup>3</sup>Graduate School of Health – Pharmacy, University of Technology Sydney, Ultimo, NSW, Australia; <sup>4</sup>Department of Medical Biotechnologies and Translational Medicine, LITA, University of Milan, Segrate, Italy; <sup>5</sup>Laboratório de Marcação de Células e Moléculas, Department of Radiology, Faculty of Medicine, Federal University of Rio de Janeiro, Rio de Janeiro, Brazil

Correspondence: Fabio Sonvico  
Graduate School of Health – Pharmacy,  
University of Technology Sydney,  
Building 7, Level 4, 67 Thomas Street,  
PO Box 123, Ultimo, NSW 2007,  
Australia  
Tel +61 2 9514 8303  
Email [fabio.sonvico@uts.edu.au](mailto:fabio.sonvico@uts.edu.au)

submit your manuscript | [www.dovepress.com](http://www.dovepress.com)  
Dovepress  
<https://doi.org/10.2147/IJN.S119017>

**Purpose:** Along with their cholesterol-lowering effect, statins have shown a wide range of pleiotropic effects potentially beneficial to neurodegenerative diseases. However, such effects are extremely elusive via the conventional oral administration. The purpose of the present study was to prepare and characterize the physicochemical properties and the in vivo biodistribution of simvastatin-loaded lecithin/chitosan nanoparticles (SVT-LCNs) suitable for nasal administration in view of an improved delivery of the statins to the brain.

**Materials and methods:** Chitosan, lecithin, and different oil excipients were used to prepare nanocapsules loaded with simvastatin. Particle size distribution, surface charge, structure, simvastatin loading and release, and interaction with mucus of nanoparticles were determined. The nanoparticle nasal toxicity was evaluated in vitro using RPMI 2651 nasal cell lines. Finally, in vivo biodistribution was assessed by gamma scintigraphy via Tc99m labeling of the particles.

**Results:** Among the different types of nanoparticles produced, the SVT-LCN\_MaiLab showed the most ideal physicochemical characteristics, with small diameter (200 nm), positive surface charge (+48 mV) and high encapsulation efficiency (EE; 98%). Size distribution was further confirmed by nanoparticle tracking analysis and electron microscopy. The particles showed a relatively fast release of simvastatin in vitro (35.6%±4.2% in 6 hours) in simulated nasal fluid. Blank nanoparticles did not show cytotoxicity, evidencing that the formulation is safe for nasal administration, while cytotoxicity of simvastatin-loaded nanoparticles (IC<sub>50</sub>) was found to be three times lower than the drug solution (9.92 vs 3.50 μM). In rats, a significantly higher radioactivity was evidenced in the brain after nasal delivery of simvastatin-loaded nanoparticles in comparison to the administration of a similar dose of simvastatin suspension.

**Conclusion:** The SVT-LCNs developed presented some of the most desirable characteristics for mucosal delivery, that is, small particle size, positive surface charge, long-term stability, high EE, and mucoadhesion. In addition, they displayed two exciting features: First was their biodegradability by enzymes present in the mucus layer, such as lysozyme. This indicates a new Trojan-horse strategy which may enhance drug release in the proximity of the nasal mucosa. Second was their ability to enhance the nose-to-brain transport as evidenced by preliminary gamma scintigraphy studies.

**Keywords:** nose-to-brain, simvastatin, nanoparticles, neurodegenerative diseases, gamma scintigraphy, small-angle X-ray scattering (SAXS), lysozyme, biodegradable nanoparticles

## Introduction

The 3-hydroxy-3-methylglutaryl coenzyme A (HMG-CoA) reductase inhibitors, or statins, are arguably among the biggest advances in cardiovascular care in the 20th century. Statins reduce cholesterol serum levels by reversibly inhibiting HMG-CoA reductase, an essential enzyme in cholesterol biosynthesis, reducing the risk of serious cardiovascular events.<sup>1,2</sup> Along with their lipid-lowering effects, statins have

International Journal of Nanomedicine 2016:11 6575–6590

6575

© 2014 Clementino et al. This work is published and licensed by Dove Medical Press Limited. The full terms of this license are available at <http://www.dovepress.com/terms.php> and incorporate the Creative Commons Attribution – Non Commercial (unported, v3.0) License (<http://creativecommons.org/licenses/by-nc/3.0/>). By accessing the work you hereby accept the Terms. Non-commercial uses of the work are permitted without any further permission from Dove Medical Press Limited, provided the work is properly attributed. For permission for commercial use of this work, please see paragraphs 4.2 and 5 of our Terms (<http://www.dovepress.com/terms.php>).

been credited for a range of outcomes or "pleiotropic effects".<sup>3</sup> The mechanisms by which pleiotropic outcomes occur are diverse and still not fully elucidated. Many of those effects are attributed to the inhibition of isoprenoid intermediates, that is, farnesyl pyrophosphate and geranylgeranyl pyrophosphate, and their downstream effects on intracellular signaling proteins Ras, Rho, and Rac.<sup>4</sup> Pleiotropic effects of statins include anti-inflammatory, antioxidant, immunomodulatory, and antithrombotic actions as well as the ability to stabilize atherosclerotic plaques and inhibit the proliferation of vascular smooth muscle.<sup>5-7</sup> Because of these pleiotropic effects, it is now believed that statins could be more widely employed in other diseases, such as rheumatoid arthritis, COPD, cancer, and neurodegenerative disorders.<sup>8-11</sup>

In the case of Alzheimer's disease, clinical research evidenced that an increase in brain cholesterol levels directly upregulates the production of  $\beta$ -amyloid protein, the major protein involved in the formation of senile plaques in the brain of Alzheimer's patients.<sup>12,13</sup> Moreover, the most widely recognized risk factor of late-onset Alzheimer's is the genetic variation in a transporter of cholesterol called apolipoprotein E  $\epsilon 4$  which supposedly alters the brain cholesterol homeostasis, leading to Alzheimer's disease development.<sup>14,15</sup> The inhibition of brain cholesterol synthesis has been shown to reduce  $\beta$ -amyloid accumulation, interfering with the production of  $\beta$ -amyloid and its accumulation as extracellular plaques.<sup>16,17</sup> These works suggest that the effects of statins in lowering the cholesterol levels may have a beneficial role on the pathogenesis of Alzheimer's disease. It has also been postulated that statin pleiotropic effects could provide further benefit to Alzheimer's patients via modulation of the chronic inflammatory response, another key factor in neurodegenerative process.<sup>11</sup> However, these effects of statins are only seen at high therapeutic concentrations at the target organ, and they are difficult to be observed when the conventional oral administration route is selected. In fact, statins undergo extensive first-pass metabolism, and their hydrophilic metabolites are prevented from crossing the blood-brain barrier (BBB), the principal biological barrier protecting the central nervous system (CNS).<sup>3</sup> Despite the fact that statins are generally well tolerated, this drug class has been associated with some adverse events, in particular myopathy. This side effect can be severe and progress to rhabdomyolysis, to the point that cerivastatin was withdrawn from the market in 2001 as a consequence of 52 drug-related fatalities worldwide.<sup>18</sup>

In the last few decades, the nasal mucosa has been demonstrated to be a site for drug administration that could

allow for fast and efficient absorption of drug molecules normally not suitable for oral administration.<sup>19</sup> More recently, the intranasal route has been increasingly investigated to deliver drugs to the brain aimed at the treatment of specific brain diseases, including neurological diseases, such as Parkinson's, schizophrenia, epilepsy, and Alzheimer's.<sup>20</sup> Several research suggest that the "nose-to-brain" route is one of the most important developments of pharmaceutical research in brain treatment, including the following: i) the potential to avoid gastrointestinal (GI) and hepatic first-pass metabolism; ii) the possibility of delivering drugs not suitable for oral administration, such as peptides and proteins; and iii) most importantly, the transport of exogenous material directly from the nasal cavity to the brain, thus bypassing the BBB.<sup>21,22</sup> It is known that the unique physiology of the olfactory region within the nasal cavity can provide a direct route of administration to the CNS, through the main innervation of the nasal cavity, that is, the olfactory and trigeminal nerves.<sup>23,24</sup> However, drug delivery via the nose is also limited by a number of factors such as the administration volume, the barrier of the nasal epithelium, the nasal metabolic activity and the presence of a protective mucus layer. Additionally, the amount of drug administered nasally which has been shown to be transported directly from nose-to-brain is very low, normally <0.1%. Hence, the system is not currently used in clinical practice.<sup>25</sup>

The extent of the nose-to-brain drug absorption has been shown to be highly dependent on the drug formulation.<sup>26,27</sup> The strategy of administering drugs encapsulated in nanoparticles via the olfactory epithelium could potentially improve the direct CNS delivery. Nanoparticles can improve nose-to-brain drug delivery, since they are able to interact with the nasal epithelium enhancing the drug absorption, protect the encapsulated drug from biological/chemical degradation and avoid the drug transport to the extracellular space by efflux proteins, such as P-glycoprotein. This could potentially increase CNS availability of the drug. In addition, their small diameter potentially allows for transcellular transport of nanoparticles through olfactory neurons to the brain, via the various endocytic pathways of neuronal cells in the olfactory region.<sup>21</sup>

From a drug delivery perspective, polymeric nanoparticles have proven to perform statistically better in delivering model drugs into CNS, in enhancing their pharmacological activity and/or reducing side effects, when compared to traditional formulations of drugs, when administered intranasally.<sup>28,29</sup> Colloid nanoparticles, composed of polysaccharides, such as chitosan, and phospholipids, have been proposed recently

as a biocompatible, biodegradable, and safe delivery system for poorly soluble drugs in order to overcome biological barriers.<sup>30,31</sup> Their chitosan surface layer in particular has the potential to facilitate nasal delivery, due to the polysaccharide mucoadhesive properties and its potential to increase epithelial permeability by interaction with the junctional complexes between cells.<sup>32,33</sup> In addition, this approach could potentially reduce classical statin side effects as nasal delivery allows dosage reduction and systemic exposure to the drug.

In the present study, a mucoadhesive formulation based on self-assembled lecithin/chitosan nanoparticles (LCNs) designed for intranasal administration was developed and optimized as a promising strategy for delivering simvastatin into the CNS. Desired features of this approach were high positive charge, small particle size and high drug content. In order to obtain these features, different oils were incorporated into LCNs in order to optimize the formulation. Physical and chemical stabilities were assessed along with drug release in simulated nasal fluid. Nanoparticle structure and interaction with mucus with and without lysozyme were investigated as well. The *in vitro* nasal toxicity of the nanoparticles alone or loaded with simvastatin was evaluated in a human nasal cell line (RPMI 2651). Finally, a preliminary gamma scintigraphy study of the biodistribution of simvastatin-loaded nanoparticles *in vivo* after intranasal instillation was carried out in rats.

## Materials and methods

### Materials

Chitosan (Chitoclear FG, deacetylation degree 95%, viscosity 45 cP) was provided by Primex (Siglufjörður, Iceland) and used without further purification. Lecithin (Lipoid S45) was obtained from Lipoid AG (Ludwigshafen, Germany). Pharmaceutical-grade oils Maisine™ 35-1 (glycerol monolinoleate), Labrafac™ Lipophile WL 1349 (medium-chain triglycerides, European Pharmacopoeia), Capryol™ PGMC (propylene glycol monocaprylate type I, National Formulary [NF]), and Capryol™ 90 (propylene glycol monocaprylate type II, NF), were a kind gift of Gattefossé (Saint-Priest, France). Simvastatin USP 99%, mucin from porcine stomach (type III), human lysozyme and bovine serum albumin (BSA) were supplied by Sigma-Aldrich (St Louis, MO, USA).

Centrifugal filter devices (Vivaspin® 2; 30,000 molecular weight cut-off [MWCO] HY) were obtained from Sartorius (Göttingen, Germany). Dialysis tubing cellulose (14,000 MWCO) was supplied by Sigma-Aldrich. Cell line RPMI 2650 (CCL-30) was purchased from American Type Culture Collection (ATCC) (Manassas, VA, USA). Minimum essential

medium (MEM) and fetal bovine serum (FBS) were acquired from Thermo Fisher Scientific (Waltham, MA, USA). Cell culture inserts and other culture plastics were from Corning Incorporated (Corning, NY, USA). All other chemicals were of analytical grade. Ultrapure and degassed ultrapure water (Purelab Flex; ELGA-Veolia LabWater, Windsor Court, UK) was used in all experiments.

## Methods

### Preparation of simvastatin-loaded LCNs

Simvastatin-loaded (SVT) LCNs were prepared as reported previously with slight modifications. In summary, 4 mL of an ethanol solution containing soybean lecithin (100 mg), simvastatin (50 mg) and different types of oils (Maisine [Mai], Labrafac [Lab], Capryol PGMC [Cap], and Capryol 90 [Cap<sub>90</sub>]) in 1:1 binary combination (100+100 mg) was injected, at controlled flow rate (15 mL/min), into 50 mL of 0.01% (w/v) chitosan aqueous solution, under constant mechanical stirring at 15,000 rpm for 10 minutes (Ultraturrax TP 18/10 – 10N; IKA-Werke GmbH, Staufen, Germany). The 0.01% chitosan aqueous solution was prepared from a 1% chitosan solution in 0.03 N HCl. Volume of organic phase and rate flow injection (15 mL/min) were controlled using a mechanical syringe pump coupled with a glass pipette (Model 200; KD Scientific, Holliston, MA, USA). Finally, ethanol phase was evaporated from the prepared colloidal suspension using a rotary evaporator (Heidolph WB/VV 2000; Schwabach, Germany) at the temperature of 40°C. Batches of LCNs loaded with simvastatin, without oil (SVT-LCNs) and with different oils (SVT-LCN\_MaiLab, SVT-LCN\_MaiCap<sub>90</sub>, SVT-LCN\_LabCap<sub>90</sub>, and SVT-LCN\_Cap<sub>90</sub>Cap<sub>90</sub>), were produced in order to optimize the formulation for stability and simvastatin encapsulation. All batches were prepared in at least triplicate and stored at room temperature for up to 3 months.

### Physicochemical characterization of SVT-LCNs

#### Determination of nanoparticle size and surface charge

The particle size and polydispersity index (PDI) of all nanoparticles were determined by dynamic light scattering (DLS) using Malvern Zetasizer Nano ZSP (Malvern Instruments Ltd., Malvern, UK).

For DLS measurements, the colloidal nanoparticle suspensions were diluted with distilled water filtered at 0.45 µm to avoid multiple scattering. The analysis was performed at 25°C and at a 90° scattering angle. Three measurements were performed for each sample, in triplicate (n=9± standard deviation [SD]).

The surface charge of the nanoparticles was measured using phase analysis light scattering. The same samples were used for both size and zeta potential determination, with the same instrument. For each measurement, nanoparticles were diluted (1:3) with distilled water filtered at 0.45  $\mu\text{m}$  to achieve a desired conductance (300  $\mu\text{S}$ ) without altering the surface charge properties of nanoparticles. Zeta potential values were presented as means of triplicate runs (six sub-runs) per sample ( $n=9\pm\text{SD}$ ).

#### Nanoparticle tracking analysis

In order to further confirm the particle size distribution and have an evaluation of particle concentration in suspension, a nanoparticles tracking analysis (NTA) experiment was conducted using NanoSight NS300 (Malvern Instruments Ltd.) equipped with a 480 nm laser light source, and a 20 $\times$  magnification microscope was used to carry out the particle tracking analysis with a field of view of approximately 100 $\times$ 80 $\times$ 10  $\mu\text{m}$ . The built-in sCMOS camera was used to record videos, and the particle tracking was analyzed by NTA 3.1 software. NTA tracks single particles in Brownian motion through the light they scatter. Videos of the particle's tracks, projected on the  $x$ - $y$  plane, observed through a 20 $\times$  microscope, were analyzed by the built-in NTA 3.1 software that locates and follows the center of each individual particle moving in the observation volume, determining the average distance moved by each particle in the  $x$  and  $y$  directions. This value is then converted into particle size on the basis of a variation of Stokes-Einstein equation taking into account that the motion is tracked in two dimensions:

$$\overline{(x, y)^2} = \frac{4T k_B}{3\pi\eta d_h}$$

where  $k_B$  is the Boltzmann constant and  $\overline{(x, y)^2}$  is the mean-squared displacement of a particle during time  $t$  at temperature  $T$ , in a medium of viscosity  $\eta$ , with a hydrodynamic diameter of  $d_h$ .<sup>34</sup>

Furthermore, knowing the volume of the suspension and the dilution, the associated NTA software is capable of calculating an approximate concentration of the nanoparticles inside the colloidal suspension.<sup>35</sup>

Only SVT-LCN\_MaiLab were analyzed by NTA. The nanoemulsion was highly diluted (1:630,000) with ultrapure water to allow single particle tracking. After that, sample was drawn into a 1 mL plastic syringe, which was used for full-sample injection into the instrument sample chamber. The nanoparticle images were acquired using a video capture

mode of the sample for three 60-second analyses, which were used for subsequent analysis. Measurement was carried out at a defined temperature (28 $^{\circ}\text{C}$ –28.2 $^{\circ}\text{C}$ ) and viscosity (0.828–0.832 cP). The results were obtained as mean and SD of three runs.

#### Nanoparticle imaging by scanning transmission electron microscopy

The morphology of simvastatin raw material, simvastatin-loaded lecithin/chitosan nanospheres (without oily core), blank LCN\_MaiLab nanocapsules and SVT-LCN\_MaiLab nanocapsules, was observed by scanning transmission electron microscopy (STEM) using an EVO<sup>®</sup> electron microscope (ZEISS International, Oberkochen, Germany) operating at an accelerating voltage of 30 kV. A drop of sample solution was placed onto a 200 mesh copper grid coated with carbon (Agar Scientific, Stansted, UK) and air dried for 1 minute, after which excess solution was removed gently with filter paper. Subsequently, a drop of 2% (w/v) phosphotungstic acid was used as a staining agent and removed after 30 seconds. The images were obtained via inverse contrast imaging with magnification between 75,000 $\times$  and 150,000 $\times$ .

#### Determination of nanoparticle structure and interaction with a nasal mucus model by SAXS

The internal structure of nanoparticles and the structural changes occurring upon their interaction with a model of nasal mucus were investigated by Synchrotron small-angle X-ray scattering (SAXS) technique. Experiments were performed at the ID02 high-brilliance beamline (ESRF, Grenoble, France). The X-ray beam cross section was 200 $\times$ 400  $\mu\text{m}$  with  $\lambda=0.1$  nm. All measurements were performed at  $T=25^{\circ}\text{C}$ . Samples were put in plastic capillaries (KI-BEAM; ENKI srl, Concesio, Italy) with 2 mm internal diameter, mounted horizontally onto a thermostated sample holder. The region of investigated momentum transfer,  $q = (4\pi/\lambda) \sin(\theta)$ , was  $0.0116 < q < 6.43$  nm $^{-1}$ , where  $2\theta$  is the scattering angle. In order to prevent any radiation damage, several frames with very short exposure time (0.1 second) were acquired, and then checked and averaged. After solvent subtraction, the measured SAXS profiles reported the nanoparticles' scattered radiation intensity as a function of the momentum transfer,  $q$ . SVT-LCN\_MaiLab were prepared according to the above-described protocol at a final concentration of 7.1 mg/mL. In order to assess the stability of SVT-LCN\_MaiLab in the presence of artificial mucus and their interaction with lysozyme, SAXS analyses were also

performed on nanoparticle dispersions in simulated nasal fluid (8.77 mg/mL sodium chloride, 2.98 mg/mL potassium chloride, and 0.59 mg/mL calcium chloride dihydrate) at three different mucus concentrations 2%, 1%, and 0.5% (w/v), and the kinetics of interaction in the presence of both mucus (0.5%) and lysozyme (0.5 mg/mL) was followed within 8 hours.

#### Quantification of simvastatin in LCNs

The simvastatin content in nanoparticles was measured using a high-performance liquid chromatography (HPLC) system. The instrumentation consisted of ESA model 542 autosampler (Chelmsford, MA, USA), ESA model 584 pump and Shimadzu SPD10A UV detector (Kyoto, Japan). A reverse phase  $C_{18}$  column (Luna, 250×3.0 mm, 5  $\mu$ m; Phenomenex, Torrance, CA, USA) was employed for chromatographic separation of both simvastatin's isoforms, that is, lactone and hydroxy-acid form,<sup>36</sup> with a mobile phase consisting of a 65:35 (v/v) mixture of acetonitrile and 0.025 M sodium dihydrogen phosphate buffer (pH 4.5) at a flow rate of 0.8 mL/min. The UV detector was set at 238 nm with a sample injection volume of 50  $\mu$ L. In order to quantitatively convert simvastatin into its hydroxy-acid form, simvastatin was dissolved in ethanol and added to 1.5 volumes of 1 N NaOH and heated at 50°C for 2 hours. Next, the pH of the solution was adjusted to 7.2 with HCl, and the volume was made up with water to 10 mL. Linearity of calibration curves for both simvastatin and its hydroxy-acid form was verified in the range of 0.5–50  $\mu$ g/mL ( $r=0.998$  and  $r=0.999$ , respectively). Limit of detection and limit of quantification were 0.02 and 0.08  $\mu$ g/mL for simvastatin and 0.06 and 0.18  $\mu$ g/mL for simvastatin hydroxy-acid form, respectively.

The encapsulation efficiency (EE) of nanoparticles was determined by an indirect method; that is, the amount of precipitated and free simvastatin were quantified and subtracted from the total amount of the drug quantified in the total preparation, and all amounts were determined by HPLC, and then expressed as a percentage of the total drug in the preparation. The total amount of simvastatin in the formulations was quantified. Firstly, 100  $\mu$ L of the preparation was dispersed in 10 mL of ethanol by sonication for 15 minutes (ultrasonic cleaner; VWR, Radnor, PA, USA) to extract the entire amount of drug. Then, the ethanol dispersion was heated at 60°C in a tightly closed container for 5 minutes to solubilize the drug content extracted from the nanoparticles and directly assayed for HPLC. For the quantification of precipitated and free simvastatin in the aqueous medium, colloidal suspensions were first centrifuged at 1,500× g for

10 minutes (Medifuge; Heraeus Sepatech GmbH, Hanau, Germany) to separate the nanoparticles from any large precipitate. The pellet obtained for each sample was resuspended with ethanol, submitted to a brief sonication process to solubilize the drug and then analyzed by HPLC. An aliquot of 2 mL of supernatant obtained in the previous step was further centrifuged using Vivaspin® Centrifugal Concentrator (MWCO 30,000 Da; Sartorius) at 4,000× g for 10 minutes (Medifuge, Heraeus Sepatech GmbH) to separate the dissolved and hence non-encapsulated simvastatin. The ultrafiltered solution was diluted with ethanol by the same method used for pellet quantification and analyzed by HPLC as well. All analyses were performed in triplicate ( $n=9 \pm$  SD). EE of simvastatin was determined by using the following formula:

$$EE\% = \frac{\text{Total amount of SVT} - (\text{Precipitated SVT} + \text{Dissolved SVT})}{\text{Total amount of SVT}} * 100$$

#### In vitro drug release from LCNs

In vitro release from SVT-LCN\_MaiLab nanocapsules was studied using simulated nasal electrolytic solution (SNES) containing potassium, calcium, and sodium at biologic human concentrations of the nasal fluid, as described by Castile et al.<sup>37</sup> In order to obtain sink conditions during the release experiments, simvastatin solubility in SNES was increased by adding 0.5% (w/v) BSA to the dissolution medium.

The test for in vitro release from SVT-LCN\_MaiLab in the SNES-0.5% BSA release medium at pH 6.5 was conducted using the dialysis bag technique (dialysis tube membrane, MWCO 14,000 kDa; Sigma-Aldrich). A volume of 1 mL of the nanoemulsion was diluted with 1 mL of SNES at pH 6.5 and placed in the dialysis bags. The sealed bags were immersed into 100 mL of the release medium containing 0.5% BSA kept at 37°C and magnetically stirred at 100 rpm. At predetermined time points (0, 1, 2, 3, 4, 5, 6, 7, 8, and 24 hours), 1.5 mL aliquots of the dissolution medium were taken and replaced with an equivalent amount of fresh release medium. Samples were analyzed by HPLC to determine the released simvastatin. The same experiment was conducted using a 1 mg/mL simvastatin suspension in ultrapure water used as control. In vitro release studies were replicated three times for both simvastatin nanoparticles and simvastatin suspension.

#### Cytotoxicity assay of SVT-LCNs

Cytotoxicity assays of simvastatin suspension, SVT-LCN\_MaiLab and Blank-LCN\_MaiLab were conducted using the human nasal septum carcinoma cell line RPMI 2650 (ATCC)



and performing an MTT [3-(4,5-dimethylthiazol-2-yl)-2,5-diphenyltetrazolium bromide] cytotoxicity assay. The RPMI 2650 cell line was cultured in a MEM containing 10% (v/v) FBS and 1% nonessential amino acid solution and incubated at 37°C with 95% air humidity and 5% CO<sub>2</sub> atmosphere. Cells were seeded at an initial density of 50,000 cells per well and incubated for 24 hours to allow cell adhesion in 96-well cell culture cluster (Costar; Coming Incorporated). Different concentrations from 0 to 240 µM of simvastatin nanoparticles, SVT-LCN\_MaiLab and Blank-LCN\_MaiLab were prepared by direct dilution in cell culture medium. To prepare the raw simvastatin solution, dimethyl sulfoxide (DMSO) was used as simvastatin solvent and diluted to low final concentration (<0.1%) to avoid toxicity effects of the solvent on the cell viability. The cells were treated with the formulations for 72 hours, followed by incubation in MTT reagent for 2 hours at 37°C. Next, the cell medium was removed, and 120 µL of DMSO was added to each well to dissolve the violet-colored metabolite. The plates were shaken for 15 minutes, the contents were pipetted and transferred to new plates and the absorbance was measured at 570 nm using a microplate reader (Spark 10 M; Tecan, Männedorf, Switzerland). Absorbance values were considered directly proportional to cell viability, and percentage cell viability was calculated by comparison to control values obtained for untreated cells.

#### Gamma scintigraphy studies

##### Particles labeling with <sup>99m</sup>Tc

A preliminary experiment to evaluate the administration of simvastatin-loaded nanoparticles was carried out in rats by gamma scintigraphy. SVT-LCN\_MaiLab and a simvastatin suspension were both labeled with <sup>99m</sup>Tc based on previous experiences, in which anti-CD3 monoclonal antibody was successfully labeled.<sup>38-40</sup>

Briefly, 60 µL of simvastatin nanoparticles or simvastatin suspension (1 mg/mL) was incubated with 100 µL of SnCl<sub>2</sub> (0.6, 6, or 60 µg) (Sigma-Aldrich) in 0.9% NaCl for 20 minutes at room temperature. Afterward, 100 µL (100 µCi) of pertechnetate (<sup>99m</sup>TcO<sup>4-</sup>; CNEN/IPEN, São Paulo, Brazil) was added, and the reaction mixture was incubated for further 10 minutes at room temperature. The radiolabeling efficiency of the nanoparticle and the simvastatin was evaluated using thin-layer chromatography (TLC), which was carried out using Whatman filter paper No 1 and acetone as mobile phase. The radioactivity of the strips was quantified in a gamma counter (Wizard2; PerkinElmer, Waltham, MA, USA). The nanoparticle and the simvastatin were both successfully labeled using 6 µg of SnCl<sub>2</sub> reaching an average 94% labeling efficiency. To quantify the TLC results, the

distance traveled by the substance being considered is divided by the total distance traveled by the mobile phase. This is called the retention factor (Rf); in this experiment, free <sup>99m</sup>Tc pertechnetate had a high Rf being transported with the mobile phase. When the particle labeling was carried out, the new radiopharmaceutical conjugate was not efficiently eluted by the mobile phase; that is, Rf=0. Efficient radiolabeling was considered for a signal at Rf=0%>80%.

##### *In vivo* biodistribution study

All animal experiments were approved by the Ethics in Research Committee of University Hospital Clementino Fraga Filho (affiliated university Federal University of Rio de Janeiro, Rio de Janeiro, Brazil; [CECA/CCS/UFRJ 129/14]). All animals were handled in accordance with Brazilian guidelines for the care and use of animals for scientific and educational purposes (Conselho Nacional de Controle de Experimentação Animal – CONCEA, 2016). Nine Wistar rats weighing 300–350 g obtained from the central vivarium were used. The animals had free access to a standard rat diet and tap water at all times during the studies. Three Wistar rats per group were placed individually in an induction chamber, and anesthesia was induced with 1% isoflurane. Then, 10 µL of the radiolabeled formulation, that is, SVT-LCN\_MaiLab, simvastatin suspension or a simple pertechnetate solution (TcO<sup>4-</sup>), was instilled with a micropipette in each nostril of the animal. Ninety minutes post-administration, the animals were sacrificed with a high dose of isoflurane (5%), and the organs were collected for biodistribution analysis.

For quantitative biodistribution analysis, the brain, heart, lungs, liver, kidneys, spleen, and stomach of rats were removed and weighed. The total radioactivity administered to each animal and the radioactivity present in each organ were measured in a gamma counter (Packard Cobra II Auto-Gamma Counter; PerkinElmer). The percentage of the dose per gram of the organ (% gram/tissue: % dose/organ/mass in grams) was determined for each sample.

##### Statistics

All results were reported as mean and SD of at least three replicates, unless stated otherwise. Cytotoxicity IC<sub>50</sub> values were calculated by using a nonlinear (sigmoidal, 4PL) fitting of each data set (Prism, Version 7.0a; GraphPad Software Inc., La Jolla, CA, USA). The differences between data were tested using Student's *t*-test (paired, two-tailed) considering significant differences with *P*<0.05. The results of the biodistribution assays were analyzed using two-way analysis of variance, and a Tukey's multiple comparisons test was used to compare the groups. Differences were considered to

be statistically significant at  $P < 0.001$  (Prism, Version 7.0a; GraphPad Software Inc.).

## Results

### Preparation and physicochemical characterization of SVT-LCNs

Simvastatin nanoparticles were formed via the electrostatic self-assembly of lecithin and chitosan. In previous papers, this system was shown to be adapted for the encapsulation of lipophilic drugs, but the loading efficiency was limited by the affinity of the drug for the phospholipid component of the nanosystem.<sup>31,41</sup>

In this study, in order to improve their loading capacity, nanoparticles were produced by adding to the formulation different oils on the basis of literature solubility studies of simvastatin. Maisine, Labrafac, Capryol PGMC, and Capryol 90 were chosen, and formulated with lecithin/chitosan in binary combinations, at the maximum amount compatible with the production of stable nanoparticles. Preliminary experiments were carried out to determine the maximum amount of oils that could be used to produce stable nanoparticles (data not shown).

To select the optimal formulation, all nanoparticles prepared were characterized for size, PDI, zeta potential, drug-loading efficiency, and stability during 3-month storage at room temperature. Table 1 reports the average size, PDI, zeta potential, and drug-loading efficiency of SVT-LCNs produced without oil and with different oil combinations.

SVT-LCNs produced without oily excipients showed higher average size (around 270 nm) and smaller positive surface charge compared to blank nanoparticles (LCNs). Furthermore, substantial precipitation of simvastatin affected the EE of SVT-LCN. The EE was approximately 22%. In all the examined cases, the addition of oil significantly reduced the amount of drug precipitated during preparation of nanoparticles. This was consistent with an improved loading

capacity provided by adding an oily core to nanoparticles, leading to a fourfold increase in EE. In preliminary studies carried out with only Maisine, it was observed that the EE of simvastatin was increasing with increasing oil concentration (Table 1 presents the data for LCN\_Mai and LCN\_Mai<sub>2</sub>). It was hypothesized that the combination of different types of oils could promote a further improvement in EE. In most cases, no significant improvement was obtained. It can be seen in Table 1 that the addition of the oil combinations Cap<sub>1</sub>Cap<sub>1</sub> and LabCap<sub>1</sub> in formulations (SVT-LCN\_Cap<sub>1</sub>Cap<sub>1</sub> and SVT-LCN\_LabCap<sub>1</sub>) did not result in a significant variation in the average size compared to SVT-LCNs or EE when compared to lecithin/chitosan Maisine-containing nanoparticles (SVT-LCN\_Mai<sub>2</sub>). On the other hand, SVT-LCN\_MaiCap<sub>1</sub> showed larger particle size (352 nm) but not a dramatic increase in loading capacity. All the oil-containing formulations evidenced a positive surface charge with values ranging from +11 to +48 mV. The preparations with higher particle sizes also showed reduced surface charge and higher PDI, with a potential negative effect on their long-term stability. In fact, SVT-LCN\_Cap<sub>1</sub>Cap<sub>1</sub> and SVT-LCN\_MaiCap<sub>1</sub> preparations evidenced precipitation or flocculation just few days after preparation. SVT-LCN\_LabCap<sub>1</sub> was apparently stable over 1-month storage but displayed a slight phase separation over longer times.

On the other hand, the addition of the oil combination Maisine and Labrafac had a huge positive effect. In fact, simvastatin-loaded nanoparticles produced using Maisine and Labrafac (SVT-LCN\_MaiLab) showed a significantly smaller particle size (204 nm), elevated positive surface charge (nearly 50 mV) and high drug-loading efficiency, encapsulating 98% of the total amount of simvastatin. Moreover, SVT-LCN\_MaiLab were found to be monodispersed (PDI < 0.1). In addition, the system remained chemically and physically stable at room temperature up to 3 months, as shown in Table 2. Therefore, the SVT-LCN\_MaiLab

**Table 1** Physicochemical properties and EE of simvastatin-loaded nanoparticles (n=9±SD)

Formulation	Oil ratio	Particle size (nm)	Zeta potential (mV)	PDI	EE (%)
LCN	–	146.7±26.2	+57.26±2.57	0.380±0.025	–
SVT-LCN	–	272.0±12.6	+34.43±2.13	0.263±0.040	22.60±20.80
SVT-LCN_Mai	1:0	192.4±22.5	+36.63±2.25	0.120±0.035	74.13±6.04
SVT-LCN_Mai <sub>2</sub>	2:0	184.9±9.5	+45.30±1.08	0.089±0.004	86.90±6.28
LCN_MaiLab	1:1	205.6±10.2	+50.20±2.17	0.129±0.017	–
SVT-LCN_MaiLab	1:1	204.5±15.4	+48.45±4.09	0.098±0.040	98.52±1.33
SVT-LCN_Cap <sub>1</sub> Cap <sub>1</sub>	1:1	280.4±9.2	+20.17±2.03	0.185±0.045	88.78±0.99
SVT-LCN_MaiCap <sub>1</sub>	1:1	352.0±33.9	+11.34±3.21	0.223±0.020	90.74±0.87
SVT-LCN_LabCap <sub>1</sub>	1:1	271.1±8.1	+17.01±2.98	0.154±0.040	94.68±0.65

Note: – indicates no data.

Abbreviations: EE, encapsulation efficiency; SD, standard deviation; PDI, polydispersity index; LCN, lecithin/chitosan nanoparticle; SVT-LCN, simvastatin-loaded lecithin/chitosan nanoparticle; Mai, Maisine; Mai<sub>2</sub>, double Maisine; Lab, Labrafac; Cap<sub>1</sub>, propylene glycol monocaprylate type I; Cap<sub>2</sub>, propylene glycol monocaprylate type II.

**Table 2** Physical and chemical stability study at room temperature of simvastatin-loaded nanoparticles (SVT-LCN\_MaiLab)

Storage time (months)	Particle size (nm)	Zeta potential (mV)	PDI	EE (%)
0	204.5±15.4	48.4±4.1	0.098±0.040	98.52±1.33
1	205.5±15.2	48.1±3.2	0.166±0.024	97.11±1.25
3	201.9±18.6	40.0±2.5	0.131±0.033	96.54±1.13

**Abbreviations:** PDI, polydispersity index; EE, encapsulation efficiency; SVT-LCN, simvastatin-loaded lecithin/chitosan nanoparticle; Mai, Maisine; Lab, Labrafac.

formulation was selected for further experiments, as it presented small and narrow particle size distribution, positive and sufficiently high superficial charge and optimal drug entrapment efficiency.

### Nanoparticle tracking analysis

In order to confirm the particle-sizing data obtained by DLS, SVT-LCN\_MaiLab particle size distribution and concentration were measured using NTA. NTA is a relatively new investigation technique that offers direct and real-time visualization, sizing, and counting of nanoparticles, allowing high-resolution particle size distributions to be obtained.<sup>42</sup> Results are shown in Figure 1. The particle size distribution showed a peak at 101.0±4.6 nm with 90% of the particles being <132.1±13.0 nm, confirming the narrow size distribution of the nanoparticles. A smaller NTA average particle size in comparison with DLS results was expected due to the different weighting functions and the intensity scattered by particles for DLS which is much larger for large particles. NTA provides complementary information to both DLS and microscopy. In fact, as it follows individual particles, it enhances the resolution of polydispersed particle population

which is usually obtained by DLS. The technique still operates on a statistically significant number of particles, larger than for microscopy, although not determining their morphology.<sup>43</sup>

NTA measurements also confirmed the stability of the lecithin/chitosan oil core nanoparticles prepared using Maisine and Labrafac combination, as similar results were obtained for the same formulation stored for 3 months at room temperature (data not shown).

### Nanoparticles imaging by STEM

LCNs were further characterized by STEM (Figure 2). Simvastatin raw material, SVT-LCNs and SVT-LCNs prepared using Maisine and Labrafac (SVT-LCN\_MaiLab) are shown in Figure 2A–C, respectively. Simvastatin suspension was organized as agglomerates of individual elongated crystals of few micrometers in size (Figure 2A). LCNs prepared without oil loaded with simvastatin produced spherical spongy particles in the range of 100–500 nm, as shown in Figure 2B. Large simvastatin crystals were also observed within this formulation, as a consequence of low encapsulation efficacy, and consistently showed extensive precipitation during nanoparticle preparation. The incorporation of oils, that is, Maisine

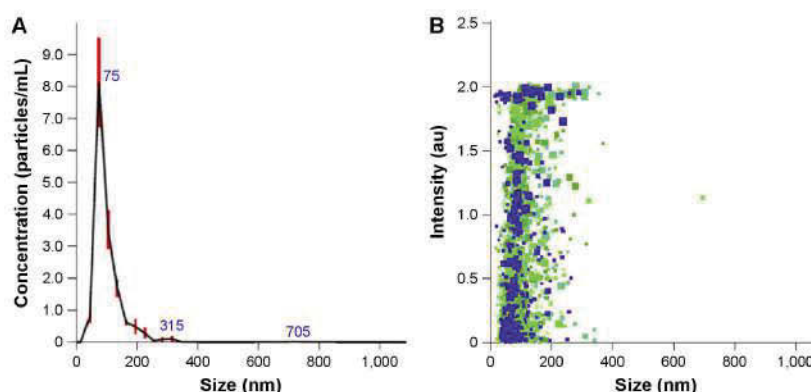


**Figure 1** Particle size distribution vs nanoparticles concentration and intensity of scattered light obtained by NTA. **Notes:** Particle size distribution is expressed as average and standard error of the mean of nanoparticle concentration ( $n=5$ ) (A). Different colors and sizes of markers represent measures of particle size and scattered light intensity of single particles from the five independent experiments (B). **Abbreviation:** NTA, nanoparticles tracking analysis.

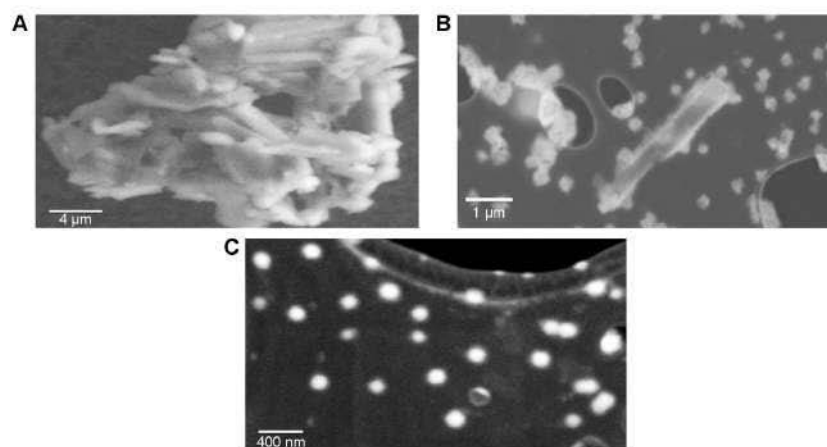


**Figure 2** STEM images of simvastatin crystals (A), SVT-LCNs (B), and SVT-LCN\_MaiLab (C)

**Abbreviations:** STEM, scanning transmission electron microscopy; SVT-LCNs, simvastatin-loaded lecithin/chitosan nanoparticles; Mai, Maisine; Lab, Labrafac

and Labrafac, into the formulation of the LCNs significantly improved the nanoparticle morphology and size distribution. SVT-LCN\_MaiLab (Figure 2C) appeared as small almost perfectly spherical nanoparticles with narrow size distribution (150–250 nm). Additionally, the increased EE of simvastatin following incorporation of oils into the formulation was confirmed by the absence of large simvastatin crystals.

### Nanoparticles structure and interaction with the nasal mucus model

To investigate the internal structure of nanoparticles, SAXS measurements were performed on blank and simvastatin-loaded nanoparticles. In Figure 3, we report the scattered X-ray intensity profiles for LCN, LCN\_MaiLab, and SVT-LCN\_MaiLab.

Spectra were very different all over the investigated  $q$  region. Blank LCNs (bottom black line in Figure 3) showed the characteristic features of closed lamellar structures, such as vesicles, with low multilamellar layering as evidenced previously.<sup>30</sup> The structure peak at  $q = 1.13 \text{ nm}^{-1}$  corresponded to a characteristic interlamellar distance of 5.6 nm. In fact, the momentum transfer  $q$  was related to the characteristic scattering distance of supramolecular structures  $d$  by the equation:

$$d = \frac{2\pi}{q}$$

The obtained bilayer contrast profile is reported in the insert of Figure 3 (bottom black profile). The structural

parameters were in agreement with typical values for lipid/polysaccharide nanoparticles:<sup>30</sup> the overall size was  $140 \pm 20 \text{ nm}$ , and the hollow water core was surrounded by one or more lipid bilayers, each 5 nm thick, with the interlayer regions containing water and chitosan.

Intensity spectra of LCN systems containing Maisine and Labrafac oils (LCN\_MaiLab, blue line in Figure 3) clearly revealed the presence of an oil core that definitely changed the

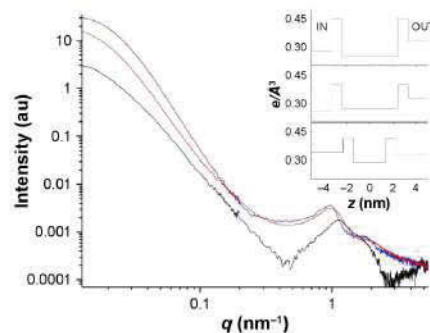


**Figure 3** SAXS intensity spectra of LCN (black line), LCN\_MaiLab (blue line), and SVT-LCN\_MaiLab (red line)

**Notes:** The corresponding electron density profiles ( $e/\text{\AA}^3$ ) across the bilayer are shown in the insert. IN is the core region, and OUT is the bulk solvent region and  $z$  is the distance from the center of the bilayer. ( $e/\text{\AA}^3$ ) is the electron density for number of electrons/ volume.

**Abbreviations:** SAXS, small-angle X-ray scattering; LCNs, lecithin/chitosan nanoparticles; Mai, Maisine; Lab, Labrafac;  $q$ , momentum transfer.

contrast of the inner region, the "IN" electron density being lower than the "OUT" (insert of Figure 3, central blue profile). The intensity decay in the low- $q$  region was proportional to  $q^{-4}$ , as expected for globular particles with well-defined interfaces. The overall size of oil-containing particles was roughly 200 nm. The nanoparticle structure was core-shell type: the oil core was surrounded by a multilayer shell, as visible in the high- $q$  region of the spectra. The obtained profile of bilayers belonging to the shell showed that their structure was affected by the presence of the oil component, as reported in Figure 3. The internal hydrophobic region of the lamellae was thicker than for blank nanoparticles. Accordingly, the interlamellar peak appeared at lower  $q$  values ( $1 \text{ nm}^{-1}$ ) corresponding to a characteristic distance of 6.3 nm, larger than for oil-free nanoparticles. Simvastatin-loaded nanoparticles (SVT-LCN\_MaiLab) showed a structure quite similar to the unloaded ones. Interestingly, simvastatin seemed not only to be embedded in the oil core, but also in the shell structure, lowering its electron density as compared to the unloaded nanoparticles.

To investigate the structural changes induced by the interaction of the nanoparticles with mucus, SAXS analyses were also performed on SVT-LCN\_MaiLab dispersions in the presence of artificial mucus in simulated nasal fluid (2%, 1%, 0.5% [w/v]). Figure 4, left panel, reports the intensity spectrum of the nanoparticles in 0.5% artificial mucus together with that of the mucus itself. In the right panel, the spectrum obtained originally for the nanoparticles in simulated nasal fluid is compared to the one of the nanoparticles inside the mucus, after subtraction of the mucus contribution to the scattered intensity.

First, it was observed that in the presence of mucus, nanoparticles were still detected and kept the same core-shell

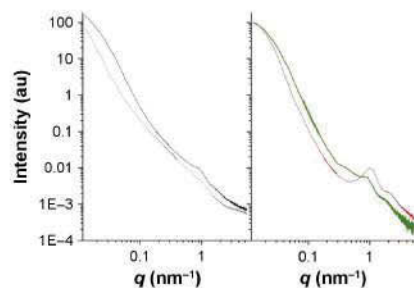


**Figure 4** SAXS intensity spectra of SVT-LCN\_MaiLab dispersed in artificial mucus. **Notes:** Left panel: SVT-LCN\_MaiLab in 0.5% artificial mucus (black line) and 0.5% mucus (gray line). Right panel: SVT-LCN\_MaiLab before interaction with artificial mucus (red line) and in mucus, after mucus spectrum subtraction (green line). **Abbreviations:** SAXS, small-angle X-ray scattering;  $q$ , momentum transfer; SVT-LCNs, simvastatin-loaded lecithin/chitosan nanoparticles; Mai, Malsine; Lab, Labrafac.

structure. Differences were visible in the high- $q$  region of the spectra, corresponding to the local scale. The characteristic structure peak shifted to  $q = 0.89 \text{ nm}^{-1}$ , corresponding to an interlamellar distance of 7 nm. The adjacent bilayers swelled, as indicated by the increased thickness of the interlamellar solvent layer, showing that the particle was stretched by the presence of the mucus matrix. Meanwhile, the intensity of the structure peak was decreased, suggesting a peeling off of layers from the multilayer shell. Moreover, an additional small peak at  $q = 0.38 \text{ nm}^{-1}$  stemmed for polymer (chitosan and/or mucin) coordination, with a correlation length of  $\sim 16.5 \text{ nm}$ .

Finally, the effect and kinetics of the interaction upon addition of lysozyme to the mucus/nanoparticles system were tested, following its structural evolution over several hours. Lysozyme is a protein widely present in natural mucosal secretions, being one of the most abundant antimicrobial factors that constitute the innate immunity.<sup>44</sup> Lysozyme at a physiological concentration ( $0.5 \text{ mg/mL}$ )<sup>45</sup> was added in mucus plus SVT-LCN\_MaiLab dispersion, and subsequent SAXS spectra were acquired at different incubation times. The corresponding intensity spectra are reported in Figure 5. Experimental results revealed that lysozyme interacts with nanoparticles helping the peeling process of the multilayer shell. In fact, both the characteristic structure peaks were moving to lower  $q$  values, and the associated intensity decreased. After 6 hours, the effect was almost complete. In the first hours, the external

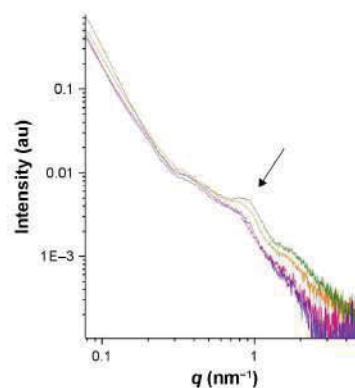


**Figure 5** SVT-LCN\_MaiLab interaction with mucus plus lysozyme. **Notes:** SAXS intensity spectra of SVT-LCN\_MaiLab in artificial mucus (0.5%) after mucus subtraction: without lysozyme (green line) and in interaction with lysozyme at different times:  $t=0$  hours (orange line),  $t=6$  hours (pink line), and  $t=8$  hours (violet line). The arrow indicates the position of the characteristic structure peak of nanoparticles.

**Abbreviations:** SAXS, small-angle X-ray scattering; SVT-LCNs, simvastatin-loaded lecithin/chitosan nanoparticles; Mai, Malsine; Lab, Labrafac;  $q$ , momentum transfer.

layers of the shell progressively swelled and peeled off suggesting a specific biodegradation of the nanoparticles as a consequence of the interaction with the enzyme.

### Simvastatin release studies

In vitro release testing is an important analytical tool, used to investigate and establish product behavior and stability during each step of the drug development.<sup>46</sup> The in vitro drug release was measured via the dialysis bag diffusion method which is one of the most commonly used dissolution methods for the testing of nanoformulations designed for nasal drug delivery.<sup>47-49</sup> SVT-LCN\_MaiLab were chosen for testing due to their optimal EE of drug and suitable physicochemical features, and a suspension of simvastatin was used as control. The simvastatin release profile from SVT-LCN\_MaiLab can be seen in Figure 6. A simulated nasal fluid at pH 6.5, containing sodium, potassium, and calcium salts, was used to simulate the nasal conditions. Due to the low solubility of simvastatin in aqueous solution, BSA was used to increase simvastatin solubility in the dissolution medium outside the dialysis bag to achieve sink conditions throughout the experiment. BSA was selected for being closer to physiological conditions in comparison to surfactants or co-solvents generally used to increase the solubility of poorly soluble drugs. The in vitro release tests were performed over 24 hours for SVT-LCN\_MaiLab and simvastatin suspension. For the suspension, after an initial rapid release in the first hour, a plateau characterized by a very low dissolution rate was reached. This was not observed for the nanoparticle formulation. In fact, the nanoparticles kept releasing simvastatin at a constant release rate from the second hour to the end of the experiment. As shown in Figure 6, 40% of simvastatin was released from

SVT-LCN\_MaiLab within 8 hours and >50% in 24 hours, displaying a significantly faster release than the simvastatin suspension (21.17% simvastatin released after 8 hours by the suspension).

### Cytotoxicity studies

In the last few years, the human RPMI 2650 epidermoid carcinoma cells have been proposed as a suitable model of nasal mucosa for in vitro studies simulating nasal drug transport.<sup>50</sup> Recently, this nasal epithelial cell line has been grown in air-liquid interface conditions to develop an in vitro model of the nasal mucosa suitable for studies of deposition and permeation of nasally administered formulations. These cells also appear a good choice for in vitro cytotoxicity assay of a new formulation such as SVT-LCNs. For this purpose, RPMI 2650 cells were incubated for 72 hours with increasing concentrations of simvastatin solution, blank nanoparticles, and simvastatin-loaded nanoparticles. The cells viability was recorded as percentage in comparison to untreated cells and plotted in Figure 7 against the simvastatin concentration. In the case of blank nanoparticles, this value corresponded to the equivalent amount of carrier nanoparticles.

Blank particles did not show any cytotoxicity indicating that the carrier is suitable for nasal administration. Results showed that cells viability also remained around 100% in the highest concentration, suggesting that our LCNs containing oil are highly biocompatible.

Cytotoxicity of simvastatin and SVT-LCN\_MaiLab appeared to be dose-dependent, as seen through the cells viability. For SVT-LCN\_MaiLab,  $IC_{50}$  was found to be 9.92  $\mu$ M, which was nearly three times that of pure simvastatin (3.50  $\mu$ M), and displayed a reduced toxicity compared to the pure drug.

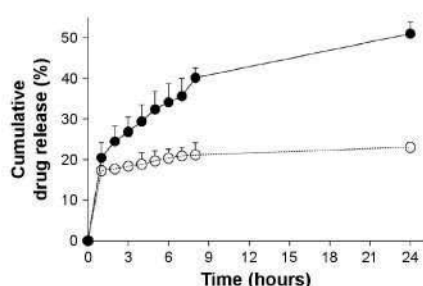


**Figure 6** Simvastatin release profile from SVT-LCN\_MaiLab (filled circle) and a control simvastatin suspension (open circle) in simulated nasal fluid with 0.5% BSA at pH 6.5 and 37°C.

**Abbreviations:** BSA, bovine serum albumin; SVT-LCNs, simvastatin-loaded lecithin/chitosan nanoparticles; Mai, Maisine; Lab, Labrafac.

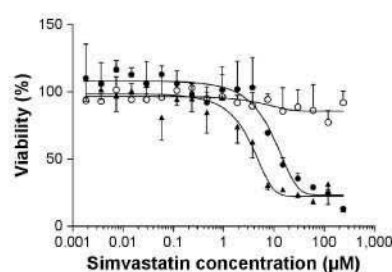


**Figure 7** In vitro cytotoxicity studies on human nasal cell line RPMI 2650 of simvastatin (filled triangle), simvastatin-loaded nanoparticles (SVT-LCN\_MaiLab, filled circle), and blank nanoparticles (LCN\_MaiLab, open circle).

**Notes:** Cell viability is plotted against the logarithm of simvastatin concentration. **Abbreviations:** SVT-LCNs, simvastatin-loaded lecithin/chitosan nanoparticles; Mai, Maisine; Lab, Labrafac.

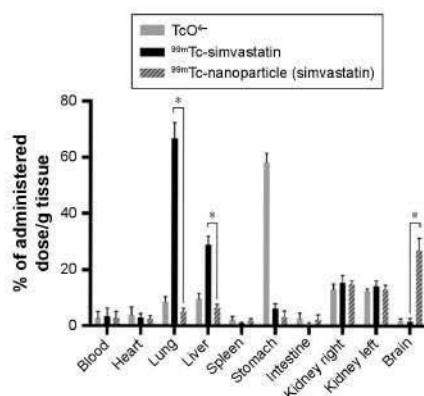


**Figure 8** Radioactivity biodistribution in Wistar rats 90 minutes after the nasal instillation of 20  $\mu\text{L}$  (10  $\mu\text{L}$  in each nostril) of  $^{99\text{m}}\text{Tc}$ -labeled simvastatin-loaded nanoparticles, simvastatin suspension, and pertechnetate ( $\text{TcO}_4^-$ ) expressed as percentage of administered dose (%D) per gram of tissue ( $n=3$ ,  $^*P<0.001$ ).

### Gamma scintigraphy studies

A preliminary study of biodistribution in rats after nasal administration of  $^{99\text{m}}\text{Tc}$ -labeled nanoparticles was carried out by gamma scintigraphy which was compared to the administration of a radiolabeled suspension of simvastatin and pertechnetate solution alone, used as controls. Figure 8 shows organ distribution of the radioactivity detected 90 minutes after the nasal instillation in each nostril of 10  $\mu\text{L}$  nanoparticles or drug suspension. The radioactivity distributions were very different. In the case of the drug suspension, most of the radioactivity was found in the lung, followed by far by the stomach and the liver. Only a very limited amount of radioactivity was found in other organs or in the brain. In the case of the pertechnetate solution, radioactivity was mainly found in the stomach. On the contrary, after the nasal administration of nanoparticle formulation, a significant fraction of the radioactivity (more than 20%) was localized in the brain, followed by an accumulation in the kidneys comparable to the levels observed for controls. Other organs such as the liver, lung, heart, and stomach contained progressively decreasing amounts of radioactivity.

### Discussion

Administration of poorly soluble drugs intranasally for systemic and CNS therapeutic action can be extremely challenging due to the low volume of nasal secretions, the barrier provided by the mucus layer and the short time available for dissolution/absorption because of mucociliary clearance.<sup>51,52</sup>

It is considered that nanoparticles could improve the bio-availability of nasally administered substances.<sup>53,54</sup> Chitosan and lecithin have been used to produce nanoparticles and liposomes for many years.<sup>55–57</sup> The main advantages attributed to these components are their biocompatibility and biodegradability, and in fact, liposomes are still by far the most successful nanomedicines on the market.<sup>58</sup> Recently, our research group proposed hybrid nanoparticles formed by the electrostatic interaction of these two components, that is, the positively charged polysaccharide chitosan and the negatively charged phospholipids of soybean lecithin.<sup>59,60</sup> These nanoparticles were demonstrated to be extremely effective in the improvement of accumulation of corticosteroid drugs in skin layers and of the permeation of tamoxifen through the intestinal epithelium.<sup>31,61,62</sup>

As a consequence, it has been hypothesized that this delivery system could be an interesting candidate for the nasal administration of lipophilic drugs, in particular for the nose-to-brain pathway. Simvastatin was selected as an ideal model drug as it has a sound rationale for its use in neurodegenerative diseases and could benefit from an alternative administration route, providing a direct access to the CNS.<sup>63</sup>

In order to efficiently load simvastatin into LCNs, it was necessary to add into the formulation an oily component. Various pharmaceutical lipophilic solvents were selected based on simvastatin solubility data reported in the literature. In a systematic study of simvastatin solubility in oils and surfactants, Capryol PGMC and Capryol 90 were found to be the best solvents for simvastatin (~105 mg/mL), followed by other oily excipients, such as Maisine (~60 mg/mL) and Labrafac (~25 mg/mL).<sup>64</sup> Therefore, combinations of these oils were used in order to optimize EE of simvastatin in LCNs. Nanoparticles with a positive surface charge and a size of around 200–300 nm in size were obtained, showing a good EE of simvastatin and providing a 30-fold increase in simvastatin apparent solubility in water. Interestingly, the best formulation, containing the combination of glyceryl monolinoleate (Maisine) and medium-chain triglycerides (Labrafac), reached an apparent simvastatin solubility which is fivefold of that expected by extrapolating from the solubility of the drug in the two solvents and from their respective amounts in the formulation, showing a synergistic effect. This suggests an optimized accommodation of the simvastatin into the oily core of the particles surrounded by a lecithin/chitosan shell, as evidenced by the SAXS experiments. It could be hypothesized that Maisine, a lipid with a slightly higher melting point than the others selected (Maisine is liquid at 40°C),

can intimately mix with the molecules of Labrafac when heated, forming a semisolid oil core when cooled down at room temperature, favoring simvastatin entrapment. In fact, LCN\_MaiLab showed the highest EE of formulated drug, encapsulating it almost entirely.

Concerning the stability of the preparations, it has been previously reported that surface charge is an important indicator of the stability of nanoparticles. In particular, when the zeta potential exceeds 30 mV, nanoparticles are regarded as stable, their stability increasing along with net surface charge.<sup>65</sup> Blank nanoparticles displayed similar values of zeta potential, generally higher than their equivalent loaded nanoparticles (Table 1). The surface charge of all LCNs was highly positive, as expected due to the presence of chitosan, a positive polysaccharide covering the surface of the nanoparticles, as reported previously. The introduction of simvastatin and of some oils into LCNs resulted in a decrease in their surface charge (SVT-LCN\_Cap, Cap<sub>1</sub>, SVT-LCN\_MaiCap<sub>1</sub>, and SVT-LCN\_LabCap). As the simvastatin hydroxy-acid form is capable of deprotonating to a negatively charged ion, this could lead to charge neutralization and loading close to the external shell.

On the contrary, the addition of the oil combination Maisine plus Labrafac into LCNs (SVT-LCN\_MaiLab) did not result in an important reduction of the positive surface charge, in line with the already suggested efficient trapping of simvastatin in a solid lipid core. A similar behavior was also observed for SVT-LCN\_Mai<sub>2</sub>, supporting the effectiveness of this oil in embedding simvastatin inside the core, thus conferring great stability to the nanoparticles system.

This core-shell organization evidenced from the nanoparticle structure investigation by SAXS is maintained upon interaction with mucus. The interaction of the superficial shell with the mucus is in agreement with a number of previous studies that indicate mucoadhesion as an important feature of nasal preparations. In particular, this may provide a much higher residence time in the nasal cavity, pivotal to allow an enhancement of drug availability.<sup>66</sup>

For the *in vitro* release studies, a simulated nasal electrolyte solution containing BSA was preferred to surfactant solutions<sup>48</sup> or mixtures with organic solvents miscible with water<sup>47</sup>, as a physiological dissolution medium. Generally, drug inclusion in nanoparticles is a strategy to prolong the release. In this study, on the contrary, after a similar initial "burst" release, a faster release rate was evidenced for nanoparticles in comparison to a simple simvastatin suspension, likely resulting from the high surface area of nanoparticles and the efficient dispersion of the drug in the nanoparticle core.

This result is even more relevant as usually, apparent drug release in dialysis methods is hindered by the dialysis membrane itself, which poses an additional barrier to the diffusion of the drug to the receiver compartment.<sup>68</sup>

As already pointed out, the major drawback affecting the nasal administration is the removal of the formulation through the mucociliary clearance, a mechanism that can reduce the bioavailability of poorly water-soluble drugs.<sup>52</sup> Hence, fast absorption is required in order to achieve the needed therapeutic concentrations. The role of chitosan in promoting mucoadhesion and penetration is well known. Several studies suggest that chitosan nanoparticles are transported by transmucosal route with increased uptake when compared to other nanoparticles as a result of the chitosan mucoadhesivity.<sup>69,70</sup> However, it is doubtful that slow-release nanoparticles would provide a significant improvement of intranasal drug delivery.<sup>71</sup> For this reason, the present system, which is both mucoadhesive and fast releasing as compared to a typical formulation for nasal administration of drug suspensions, could overcome limitation on delivery due to clearance. Moreover, previous studies have shown that LCNs are highly susceptible to degradation by GI enzymes, thus promoting drug release and drug permeation through intestinal epithelium via an enhanced paracellular transport.<sup>31</sup> This degradation is also likely to occur on the nasal mucosal surface. Degradation has been evidenced in the presence of mucus and lysozyme, where a breakdown of the original particle structure occurs over time (Figure 5). In fact, nasal secretions are rich in antibacterial peptides and proteins that are part of the innate immune defenses of the body.<sup>44</sup> Among these proteins, one of the most abundant is lysozyme, an enzyme able to degrade proteoglycans of bacterial cell wall, but also able to degrade chitosan.<sup>72</sup> The degradation of the nanoparticles by endogenous enzymatic process constitutes a new approach for nasal delivery and could represent an interesting Trojan-horse strategy for improving the nasal bioavailability of statins and other poorly soluble drugs.

Interestingly, despite reports of concerns in the literature regarding the biocompatibility of positively charged chitosan nanoparticles, the cytotoxicity studies carried out evidenced no apparent toxicity of the proposed drug nanocarriers. This is of course an important result, as safety is a prerequisite to the use of the formulation. In fact, the nasal epithelial layer represents one of the first body's defense lines, and materials harming the mucosal barrier constitute a potential health risk.<sup>73</sup>

The cytotoxicity evidenced by simvastatin-loaded nanoparticles is actually related to the statin itself. In fact, several



recent studies have demonstrated the anticancer activity of statins in various cancer cells.<sup>10,74,75</sup> Since RPMI 2650 cells are derived from an epidermoid carcinoma of the nasal septum, the cytotoxic activity detected is to be attributed to the drug released by nanoparticles or by the direct uptake of nanoparticles by the cells. As nanoparticles degradation and/or drug release is time dependent, SVT-LCN\_MaiLab showed lower IC<sub>50</sub> values than simvastatin.

In vivo preliminary studies were carried out to assess the potential of the formulation for the proposed nose-to-brain delivery of statins. Gamma scintigraphy was selected as a powerful and rapid method to evaluate the biodistribution of the formulation after nasal administration in rodents.<sup>76</sup> A suspension of simvastatin was used as a control. It is worth pointing out that the radioactivity that is detected cannot be considered permanently bound to the particles or to the drug molecule. However, it appears clear that after the nasal instillation of the nanoparticle formulation, the radioactivity was localized mainly in the kidneys and in the brain. This biodistribution implies a significant absorption of the radiolabel through the nasal mucosa, which accounts for the localization in the kidney where the radioisotope will be eliminated by filtration and an efficient transfer via the nose-to-brain pathway of around 20% of the administered radioactivity dose. This was not observed for the controls, that is, simvastatin suspension and the solution of the radioisotope itself, where the radioactivity mainly localized in the lungs and GI tract of the animals, as often happens for rodents that are obligate nose breather. It can be hypothesized that the nanoparticle formulation is more effective through both chitosan-mediated mucoadhesion<sup>77</sup> and penetration enhancement via tight-junction opening,<sup>78</sup> but also most likely as a consequence of mucosal biodegradation of the nanoparticle structure. Overall, these processes are able to favor the transmucosal absorption of the radioactivity, independently from the form it may assume: isotopes linked to entire nanoparticles, particle fragments, polysaccharide chains or free from linkage to any of nanoparticle structures.

## Conclusion

Although some brain-targeted nanoparticles loaded with statins have been proposed by some other authors, this is to our knowledge the first research proposing nanoparticles to be administered nasally to deliver statins to the brain. The particles were designed to optimize the loading of a lipophilic drug such as simvastatin and to provide multiple features helpful for nasal delivery, such as physical and chemical stability, biocompatibility, mucoadhesion, and a

rapid drug release. Furthermore, the nanoparticles appear to be prone to a mucus-specific biodegradation process that represents an innovative Trojan-horse strategy able to boost the permeation of the encapsulated drug. Preliminary in vivo gamma scintigraphy studies showed an enhanced nose-to-brain transport of the radioactivity administered nasally for the SVT-LCNs but not for a more traditional formulation such as a suspension. Although further studies are necessary to elucidate if the nanoparticles are taken up by the nasal epithelium or simply favor the drug absorption without crossing the mucosa and to investigate the pharmacokinetics and efficacy of the nanoformulated statin after administration via the nasal route, the proposed nanoformulation appears to be an optimal drug delivery platform for poorly soluble drugs that need to get administered to the nasal mucosa for systemic or CNS delivery.

## Acknowledgments

Adryana Clementino and Gabriela Garrastazu would like to acknowledge the Brazilian government as recipients of CNPq grants in the program "Ciências sem Fronteiras". Fabio Sonvico would like to thank the University of Technology Sydney for the support received for his research through Early Career Researcher Grant program.

## Disclosure

The authors report no conflicts of interest in this work.

## References

- Bonetti PO, Lerman LO, Napoli C, Lerman A. Statin effects beyond lipid lowering – are they clinically relevant? *Eur Heart J*. 2003;24(3):225–248.
- Heart Protection Study Collaborative Group. MRC/BHF Heart Protection Study of cholesterol lowering with simvastatin in 20,536 high-risk individuals: a randomised placebo-controlled trial. *Lancet*. 2002;360(9326):7–22.
- Romana B, Batger M, Prestidge CA, Colombo G, Sonvico F. Expanding the therapeutic potential of statins by means of nanotechnology enabled drug delivery systems. *Curr Top Med Chem*. 2014;14(9):1182–1193.
- Liao JK, Laufs U. Pleiotropic effects of statins. *Annu Rev Pharmacol Toxicol*. 2005;45:89–118.
- Palinski W, Napoli C. Unraveling pleiotropic effects of statins on plaque rupture. *Arterioscler Thromb Vasc Biol*. 2002;22(11):1745–1750.
- Blanco-Colio LM, Tuñón J, Martín-Ventura JL, Egido J. Anti-inflammatory and immunomodulatory effects of statins. *Kidney Int*. 2003;63(1):12–23.
- Jain MK, Ridker PM. Anti-inflammatory effects of statins: clinical evidence and basic mechanisms. *Nat Rev Drug Discov*. 2005;4(12):977–987.
- McCarty DW, McClines IB, Madhok R, et al. Trial of Atorvastatin in Rheumatoid Arthritis (TARA): double-blind, randomised placebo-controlled trial. *Lancet*. 2004;363(9426):2015–2021.
- Marin L, Colombo P, Bebawy M, Young PM, Traini D. Chronic obstructive pulmonary disease: patho-physiology, current methods of treatment and the potential for simvastatin in disease management. *Expert Opin Drug Deliv*. 2011;8(9):1205–1220.

10. Gopalan A, Yu W, Sanders BG, Kline K, Simvastatin inhibition of mevalonate pathway induces apoptosis in human breast cancer cells via activation of JNK/CHOP/DRS signaling pathway. *Cancer Lett.* 2013; 329(1):9–16.
11. Wang Q, Yan J, Chen X, et al. Statins: multiple neuroprotective mechanisms in neurodegenerative diseases. *Exp Neurol.* 2011;230(1): 27–34.
12. Ghribi O, Larsen B, Schrag M, Herman MM. High cholesterol content in neurons increases BACE,  $\beta$ -amyloid, and phosphorylated tau levels in rabbit hippocampus. *Exp Neurol.* 2006;200(2):460–467.
13. Pugliese L, Tanzi RE, Kovacs DM. Alzheimer's disease: the cholesterol connection. *Nat Neurosci.* 2003;6(4):345–351.
14. Bu G. Apolipoprotein E and its receptors in Alzheimer's disease: pathways, pathogenesis and therapy. *Nat Rev Neurosci.* 2009;10(5): 333–344.
15. Kivipelto M, Helkala EL, Laakso MP, et al. Apolipoprotein E epsilon4 allele, elevated midlife total cholesterol level, and high midlife systolic blood pressure are independent risk factors for late-life Alzheimer disease. *Ann Intern Med.* 2002;137(3):149–155.
16. Fassbender K, Simons M, Bergmann C, et al. Simvastatin strongly reduces levels of Alzheimer's disease  $\beta$ -amyloid peptides A $\beta$ 42 and A $\beta$ 40 *in vitro* and *in vivo*. *Proc Natl Acad Sci U S A.* 2001;98(10):5856–5861.
17. Ehehalt R, Keller P, Haass C, Thiele C, Simons K. Amyloidogenic processing of the Alzheimer  $\beta$ -amyloid precursor protein depends on lipid rafts. *J Cell Biol.* 2003;160(1):113–123.
18. Schachter M. Chemical, pharmacokinetic and pharmacodynamic properties of statins: an update. *Fundam Clin Pharmacol.* 2005;19(1): 117–125.
19. Pires A, Fortuna A, Alves G, Falcão A. Intranasal drug delivery: how, why and what for? *J Pharm Pharm Sci.* 2009;12(3):288–311.
20. Suman JD. Current understanding of nasal morphology and physiology as a drug delivery target. *Drug Deliv Transl Res.* 2013;3(1):4–15.
21. Mistry A, Glud SZ, Kjemis J, et al. Effect of physicochemical properties on intranasal nanoparticle transit into murine olfactory epithelium. *J Drug Target.* 2009;17(7):543–552.
22. Kozlovskaya L, Abou-Kaoud M, Stepensky D. Quantitative analysis of drug delivery to the brain via nasal route. *J Control Release.* 2014; 189:133–140.
23. Tayebati SK, Nwankwo IE, Amenta F. Intranasal drug delivery to the central nervous system: present status and future outlook. *Curr Pharm Dev.* 2013;19(3):510–526.
24. Illum L. Transport of drugs from the nasal cavity to the central nervous system. *Eur J Pharm Sci.* 2000;11(1):1–18.
25. Illum L. Is nose-to-brain transport of drugs in man a reality? *J Pharm Pharmacol.* 2004;56(1):3–17.
26. Horvát S, Fehér A, Wolburg H, et al. Sodium hyaluronate as a mucoadhesive component in nasal formulation enhances delivery of molecules to brain tissue. *Eur J Pharm Biopharm.* 2009;72(1):252–259.
27. Wu H, Hu K, Jiang X. From nose to brain: understanding transport capacity and transport rate of drugs. *Expert Opin Drug Deliv.* 2008;5(10):1159–1168.
28. Zhang QZ, Zha LS, Zhang Y, et al. The brain targeting efficiency following nasally applied MPEG-PLA nanoparticles in rats. *J Drug Target.* 2008;14(5):281–290.
29. Betbeder D, Spérando S, Latapie JP, et al. Biovector nanoparticles improve antinociceptive efficacy of nasal morphine. *Pharm Res.* 2000; 17(6):743–748.
30. Gerelli Y, Di Bari MT, Deriu A, et al. Structure and organization of phospholipid/polysaccharide nanoparticles. *J Phys Condens Matter.* 2008; 20(10):104211.
31. Barbieri S, Buttini F, Rossi A, et al. Ex vivo permeation of tamoxifen and its 4-OH metabolite through rat intestine from lecithin/chitosan nanoparticles. *Int J Pharm.* 2015;491(1–2):99–104.
32. Takeuchi H, Matsui Y, Yamamoto H, Kawashima Y. Mucoadhesive properties of carboxyl or chitosan-coated liposomes and their effectiveness in the oral administration of calcitonin to rats. *J Control Release.* 2003;86(2–3):235–242.
33. Smith JM, Dornish M, Wood EJ. Involvement of protein kinase C in chitosan glutamate-mediated tight junction disruption. *Biomaterials.* 2005;26(16):3269–3276.
34. Hole P, Silence K, Hannell C, et al. Interlaboratory comparison of size measurements on nanoparticles using nanoparticle tracking analysis (NTA). *J Nanopart Res.* 2013;15(12):2101.
35. Filipe V, Hawe A, Jiskoot W. Critical evaluation of Nanoparticle Tracking Analysis (NTA) by NanoSight for the measurement of nanoparticles and protein aggregates. *Pharm Res.* 2010;27(5):796–810.
36. Yang DJ, Hwang LS. Study on the conversion of three natural statins from lactone forms to their corresponding hydroxy acid forms and their determination in Pu-Erh tea. *J Chromatogr A.* 2006;1119(1–2):277–284.
37. Castile J, Cheng YH, Simmons B, Perelman M, Smith A, Watts P. Development of *in vitro* models to demonstrate the ability of PecSys<sup>®</sup>, an *in situ* nasal gelling technology, to reduce nasal run-off and drip. *Drug Dev Ind Pharm.* 2013;39(5):816–824.
38. Martins FP, Gutfilen B, de Souza SA, et al. Monitoring rheumatoid arthritis synovitis with <sup>99m</sup>Tc-anti-CD3. *Br J Radiol.* 2008; 81(961):25–29.
39. Martins FP, Souza SA, Gonçalves RT, Fonseca LM, Gutfilen B. Preliminary results of [<sup>99m</sup>Tc]OKT3 scintigraphy to evaluate acute rejection in renal transplants. *Transplant Proc.* 2004;36(9):2664–2667.
40. Lopes FP, de Azevedo MN, Marchiori E, da Fonseca LM, de Souza SA, Gutfilen B. Use of <sup>99m</sup>Tc-anti-CD3 scintigraphy in the differential diagnosis of rheumatic diseases. *Rheumatology (Oxford).* 2010;49(5): 933–939.
41. Gerelli Y, Di Bari MT, Barbieri S, et al. Flexibility and drug release features of lipid/saccharide nanoparticles. *Soft Matter.* 2010;6(3): 685–691.
42. Wright M. Nanoparticle tracking analysis for the multiparameter characterization and counting of nanoparticle suspensions. *Methods Mol Biol.* 2012;906:511–524.
43. Sokolova V, Ludwig AK, Hornung S, et al. Characterisation of exosomes derived from human cells by nanoparticle tracking analysis and scanning electron microscopy. *Colloids Surf B Biointerfaces.* 2011;87(1):146–150.
44. Travis SM, Singh PK, Welsh MJ. Antimicrobial peptides and proteins in the innate defense of the airway surface. *Curr Opin Immunol.* 2001; 13(1):89–95.
45. Cole AM, Dewan P, Ganz T. Innate antimicrobial activity of nasal secretions. *Infect Immun.* 1999;67(7):3267–3275.
46. D'Souza SS, DeLuca PP. Methods to assess *in vitro* drug release from injectable polymeric particulate systems. *Pharm Res.* 2006; 23(3):460–474.
47. Chen KH, Di Sabatino M, Albertini B, Passerini N, Kett VL. The effect of polymer coatings on physicochemical properties of spray-dried liposomes for nasal delivery of BSA. *Eur J Pharm Sci.* 2013;50(3–4):312–322.
48. Sood S, Jain K, Gowthamarajan K. Optimization of curcumin nanoemulsion for intranasal delivery using design of experiment and its toxicity assessment. *Colloids Surf B Biointerfaces.* 2014;113:330–337.
49. Seju U, Kumar A, Sawant KK. Development and evaluation of olanzapine-loaded PLGA nanoparticles for nose-to-brain delivery: *in vitro* and *in vivo* studies. *Acta Biomater.* 2011;7(12):4169–4176.
50. Bai S, Yang T, Abbruscato TJ, Ahsan F. Evaluation of human nasal RPMI 2650 cells grown at an air-liquid interface as a model for nasal drug transport studies. *J Pharm Sci.* 2008;97(3):1165–1178.
51. Lochhead JJ, Thorne RG. Intranasal delivery of biologics to the central nervous system. *Adv Drug Deliv Rev.* 2012;64(7):614–628.
52. Sigurdsson HH, Kirch J, Lehr CM. Mucus as a barrier to lipophilic drugs. *Int J Pharm.* 2013;453(1):56–64.
53. Mistry A, Stolnik S, Illum L. Nanoparticles for direct nose-to-brain delivery of drugs. *Int J Pharm.* 2009;379(1):146–157.
54. Kumar A, Pandey AN, Jain SK. Nasal-nanotechnology: revolution for efficient therapeutics delivery. *Drug Deliv.* 2016;23(3):681–693.
55. Bernkop-Schnürch A, Dünnhaupt S. Chitosan-based drug delivery systems. *Eur J Pharm Biopharm.* 2012;81(3):463–469.

56. Akbarzadeh A, Rezaei-Sadabady R, Davaran S, et al. Liposome: classification, preparation, and applications. *Nanoscale Res Lett*. 2013;8(1):102.
57. Gabizon AA, Shmeeda H, Zalipsky S. Pros and cons of the liposome platform in cancer drug targeting. *J Liposome Res*. 2006;16(3):175–183.
58. Barenholz Y. Doxil® – the first FDA-approved nano-drug: lessons learned. *J Control Release*. 2012;160(2):117–134.
59. Di Bari MT, Gerelli Y, Sonvico F, et al. Dynamics of lipid-saccharide nanoparticles by quasielastic neutron scattering. *Chem Phys*. 2008;345(2–3):239–244.
60. Sonvico F, Di Bari MT, Bove L, Deriu A, Cavatorta F, Albanese G. Mean square hydrogen fluctuations in chitosan/lecithin nanoparticles from elastic neutron scattering experiments. *Physica B*. 2006;385–386:725–727.
61. Senyigit T, Sonvico F, Barbieri S, Ozer O, Santi P, Colombo P. Lecithin/chitosan nanoparticles of clobetasol-17-propionate capable of accumulation in pig skin. *J Control Release*. 2010;142(3):368–373.
62. Barbieri S, Sonvico F, Como C, et al. Lecithin/chitosan controlled release nanopreparations of tamoxifen citrate: loading, enzyme-triggered release and cell uptake. *J Control Release*. 2013;167(3):276–283.
63. Jiang Y, Li Y, Liu X. Intranasal delivery: circumventing the iron curtain to treat neurological disorders. *Expert Opin Drug Deliv*. 2015;12(11):1717–1725.
64. Karim FT, Kalam A, Anwar R, Miah MM, Rahman MS, Islam SM. Preparation and evaluation of SEDDS of simvastatin by in vivo, in vitro and ex vivo technique. *Drug Dev Ind Pharm*. 2014;41(8):1338–1342.
65. Müller RH, Jacobs C, Kayser O. Nanosuspensions as particulate drug formulations in therapy. Rationale for development and what we can expect for the future. *Adv Drug Deliv Rev*. 2001;47(1):3–19.
66. Casettari L, Illum L. Chitosan in nasal delivery systems for therapeutic drugs. *J Control Release*. 2014;190:189–200.
67. Dalpiaz A, Ferraro L, Perrone D, et al. Brain uptake of a Zidovudine prodrug after nasal administration of solid lipid microparticles. *Mol Pharm*. 2014;11(5):1550–1561.
68. Modi S, Anderson BD. Determination of drug release kinetics from nanoparticles: overcoming pitfalls of the dynamic dialysis method. *Mol Pharm*. 2013;10(8):3076–3089.
69. Artursson P, Lindmark T, Davis SS, Illum L. Effect of chitosan on the permeability of monolayers of intestinal epithelial cells (Caco-2). *Pharm Res*. 1994;11(9):1358–1361.
70. Prego C, Garcia M, Torres D, Alonso MJ. Transmucosal macromolecular drug delivery. *J Control Release*. 2005;101(1–3):151–162.
71. Illum L. Nanoparticulate systems for nasal delivery of drugs: a real improvement over simple systems? *J Pharm Sci*. 2007;96(3):473–483.
72. Nordtveit RJ, Vårum KM, Smidsrød O. Degradation of partially N-acetylated chitosans with hen egg white and human lysozyme. *Carbohydr Polym*. 1996;29(2):163–167.
73. Ekelund K, Östh K, Pålstorp C, Björk E, Ulvenlund S, Johansson F. Correlation between epithelial toxicity and surfactant structure as derived from the effects of polyethyleneoxide surfactants on eaco-2 cell monolayers and pig nasal mucosa. *J Pharm Sci*. 2005;94(4):730–744.
74. Wu H, Jiang H, Lu D, et al. Effect of simvastatin on glioma cell proliferation, migration, and apoptosis. *Neurosurgery*. 2009;65(6):1087–1096; discussion 1096–1097.
75. Ali H, Shirode AB, Sylvester PW, Nazzari S. Preparation, characterization, and anticancer effects of simvastatin-tocotrienol lipid nanoparticles. *Int J Pharm*. 2010;389(1–2):223–231.
76. Alam S, Khan ZI, Mustafa G, et al. Development and evaluation of thymoquinone-encapsulated chitosan nanoparticles for nose-to-brain targeting: a pharmacoscintigraphic study. *Int J Nanomedicine*. 2012;7:5705–5718.
77. Jogani VV, Shah PJ, Mishra P, Mishra AK, Misra AR. Intranasal mucoadhesive microemulsion of tacrine to improve brain targeting. *Alzheimer Dis Assoc Disord*. 2008;22(2):116–124.
78. Vilasalu D, Exposito-Harris R, Heras A, et al. Tight junction modulation by chitosan nanoparticles: comparison with chitosan solution. *Int J Pharm*. 2010;400(1–2):183–193.

## International Journal of Nanomedicine

## Publish your work in this journal

The International Journal of Nanomedicine is an international, peer-reviewed journal focusing on the application of nanotechnology in diagnostics, therapeutics, and drug delivery systems throughout the biomedical field. This journal is indexed on PubMed Central, MedLine, CAS, SciSearch®, Current Contents®/Clinical Medicine,


Submit your manuscript here: <http://www.dovepress.com/international-journal-of-nanomedicine-journal>

Dovepress

Journal Citation Reports/Science Edition, EMBASE, Scopus and the Elsevier Bibliographic databases. The manuscript management system is completely online and includes a very quick and fair peer-review system, which is all easy to use. Visit <http://www.dovepress.com/testimonials.php> to read real quotes from published authors.

RESEARCH ARTICLE

**Resveratrol solid lipid microparticles as dry powder formulation for nasal delivery, characterization and *in vitro* deposition study**

Isabella Martignoni<sup>a</sup>, Valentina Trotta<sup>a</sup>, Wing-Hin Lee<sup>b</sup>, Ching-Yee Loo<sup>b</sup>, Michele Pozzoli<sup>b,c</sup>, Paul M. Young<sup>b</sup>, Santo Scalia<sup>a</sup> and Daniela Traini<sup>b</sup> 

<sup>a</sup>Department of Chemical and Pharmaceutical Sciences, University of Ferrara, Ferrara, Italy; <sup>b</sup>Respiratory Technology, Woolcock Institute of Medical Research and Discipline of Pharmacology, Sydney Medical School, The University of Sydney, NSW, Australia; <sup>c</sup>Graduate School of Health-Pharmacy, University of Technology Sydney, NSW, Australia

**ABSTRACT**

This study focuses on development and *in vitro* characterisation of a nasal delivery system based on uncoated or chitosan-coated solid lipid microparticles (SLMs) containing resveratrol, a natural anti-inflammatory molecule, as an effective alternative to the conventional steroidal drugs. The physico-chemical characteristics of the SLMs loaded with resveratrol were evaluated in terms of morphology, size, thermal behaviour and moisture sorption. The SLMs appeared as aggregates larger than 20 µm. *In vitro* nasal deposition was evaluated using a USP specification Apparatus E 7-stage cascade impactor equipped with a standard or a modified nasal deposition apparatus. More than 95% of resveratrol was recovered onto the nasal deposition chamber and stage 1 of impactor, suggesting that the SLMs mostly deposited in the nasal cavity. Additionally, the SLMs were not toxic on RPMI 2650 nasal cell line up to a concentration of approximately 40 µM of resveratrol.

**ARTICLE HISTORY**

Received 10 May 2016  
Revised 19 October 2016  
Accepted 7 November 2016

**KEYWORDS**

Nasal drug delivery;  
solid lipid microparticles;  
chitosan; *in vitro* models

[Production note:

This paper is not included in this digital copy due to copyright restrictions.]

Martignoni, I., Trotta, V., Lee, W.-H., Loo, C.-Y., Pozzoli, M., Young, P.M., Scalia, S. & Traini, D. 2016, 'Resveratrol solid lipid microparticles as dry powder formulation for nasal delivery, characterization and *in vitro* deposition study', *Journal of Microencapsulation*, 33(8):735-742.

DOI: 10.1080/02652048.2016.1260659

View/Download from: [Publisher's site](#)

## Opportunities and Challenges for the Nasal Administration of Nanoemulsions

Claurice Comfort<sup>1</sup>, Gabriela Garrastazu<sup>1,2</sup>, Michele Pozzoli<sup>1</sup> and Fabio Sonvico<sup>1,\*</sup>

<sup>1</sup>Graduate School of Health - Pharmacy, University of Technology, Sydney, 15 Broadway, Ultimo, NSW, 2007, Australia; <sup>2</sup>Coordenação de Aperfeiçoamento de Pessoal de Nível Superior, Brazil



**Abstract:** Nasal delivery has become a growing area of interest for drug administration as a consequence of several practical advantages, such as ease of administration and non-invasiveness. Moreover, the avoidance of hepatic first-pass metabolism and rapid and efficient absorption across the permeable nasal mucosa offer a promising alternative to other traditional administration routes, such as oral or parenteral delivery. In fact, nasal delivery has been proposed for a number of applications, including local, systemic, direct nose-to-brain and mucosal vaccine delivery. Nanoemulsions, due to their stability, small droplet size and optimal solubilization properties, represent a versatile formulation approach suitable for several administration routes. Nanoemulsions demonstrated great potential in nasal drug delivery, increasing the absorption and the bioavailability of many drugs for systemic and nose-to-brain delivery. Furthermore, they act as an active component, i.e. an adjuvant, in nasal mucosal vaccinations, displaying the ability to induce robust mucosal immunity, high serum antibodies titres and a cellular immune response avoiding inflammatory response. Interestingly, nanoemulsions have not been proposed for the treatment of local ailments of the nose. Despite the promising results *in vitro* and *in vivo*, the application of nanoemulsions for nasal delivery in humans appears mainly hindered by the lack of detailed toxicology studies to determine the effect of these formulations on the nasal mucosa and cilia and the lack of extensive clinical trials.

**Keywords:** Drug delivery, mucosal vaccine, nanoemulsions, nasal delivery, nose to brain, pharmaceutical nanotechnology.

[Production note:

This paper is not included in this digital copy due to copyright restrictions.]

Comfort, C., Garrastazu, G., Pozzoli, M. & Sonvico, F. 2015, 'Opportunities and Challenges for the Nasal Administration of Nanoemulsions', *Current Topics in Medicinal Chemistry*, 15(4):356-368.

DOI: 10.2174/1568026615666150108144655

View/Download from: [UTS OPUS](#) or [Publisher's site](#)

## A.3 COPYRIGHTS PERMISSIONS

### ELSEVIER LICENSE TERMS AND CONDITIONS

Dec 19, 2016

---

This Agreement between Michele Pozzoli ("You") and Elsevier ("Elsevier") consists of your license details and the terms and conditions provided by Elsevier and Copyright Clearance Center.

License Number	4012720727216
License date	Dec 19, 2016
Licensed Content Publisher	Elsevier
Licensed Content Publication	European Journal of Pharmaceutics and Biopharmaceutics
Licensed Content Title	Application of RPMI 2650 nasal cell model to a 3D printed apparatus for the testing of drug deposition and permeation of nasal products
Licensed Content Author	Michele Pozzoli,Hui Xin Ong, Lucy Morgan, Maria Sukkar, Daniela Traini, Paul M. Young, Fabio Sonvico
Licensed Content Date	October 2016
Licensed Content Volume Number	107
Licensed Content Issue Number	n/a
Licensed Content Pages	11
Start Page	223
End Page	233
Type of Use	reuse in a thesis/dissertation
Intended publisher of new work	other
Portion	full article
Format	both print and electronic
Are you the author of this Elsevier article?	Yes
Will you be translating?	No
Order reference number	
Title of your thesis/dissertation	Drug delivery to the nose: formulation, deposition and permeation of poorly soluble drugs
Expected completion date	Jan 2017
Estimated size (number of pages)	200
Elsevier VAT number	GB 494 6272 12
Requestor Location	Michele Pozzoli 15 Broadway, Building 7 level 4 Graduate School of Health Pharmacy



**Taylor & Francis**  
Taylor & Francis Group

**Title:**

Dry powder nasal drug delivery: challenges, opportunities and a study of the commercial Teijin Puvlizer Rhinocort device and formulation

**Author:**

Michele Pozzoli, Philippe Rogueda, Bing Zhu, et al

**Publication:**

Drug Development and Industrial Pharmacy

**Publisher:**

Taylor & Francis

**Date:**

Oct 2, 2016

Copyright © 2016 Taylor & Francis

Logged in as:

Michele Pozzoli

Account #:

3001094314

LOGOUT

**Thesis/Dissertation Reuse Request**

Taylor & Francis is pleased to offer reuses of its content for a thesis or dissertation free of charge contingent on resubmission of permission request if work is published.

BACK

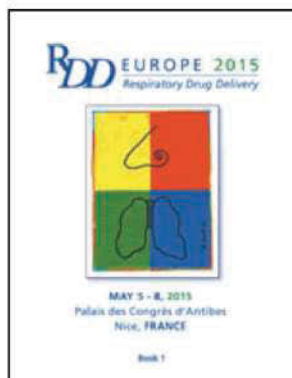
CLOSE WINDOW

Copyright © 2016 [Copyright Clearance Center, Inc.](#) All Rights Reserved. [Privacy statement.](#) [Terms and Conditions.](#) Comments? We would like to hear from you. E-mail us at [customercare@copyright.com](mailto:customercare@copyright.com)



**Dear Michele,**

We are pleased to grant you permission to use the following:



[Validation of a Novel Apparatus for Deposition Studies of Nasal Products](#)

Pozzoli M, Cattaneo S, Zhu B, Traini D, Young PM, Sonvico F

RDD Europe 2015. Volume 2, 2015: 537-542.

**What you will reproduce:**

The main test and figures with some adaptations

**How you will use it:**

Material is needed to be included in full in my PhD thesis

Please acknowledge the source of the material used and the publisher, e.g. "Reproduced with permission from RDD Europe 2015, Virginia Commonwealth University and RDD Online".

**RDD Online**

Virginia Biotechnology Research Park,  
[800 East Leigh Street, Suite 206-10](#)  
[Richmond, VA 23219-1534, USA](#)

Phone: +1 (804) 827-1490

Fax: +1 (804) 828-8277

Email: [info@rddonline.com](mailto:info@rddonline.com)

Web: [www.rddonline.com](http://www.rddonline.com)

---

RDD Online

Virginia Biotechnology Research Park, [Suite 206-10, 800 East Leigh Street, Richmond, VA 23219, USA](#).

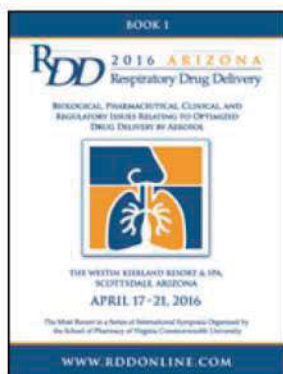
[Unsubscribe from receiving further emails from RDD Online.](#)





Dear Michele,

We are pleased to grant you permission to use the following:



[Transport of Beclometasone Dipropionate Across RPMI 2650 Model of Nasal Epithelium: Evaluation of Two Different Approaches to Drug Delivery](#)

Pozzoli M, Ong H, Sonvico F, Young PM, Traini D

Respiratory Drug Delivery 2016. Volume 3, 2016: 607-610.

**What you will reproduce:**

Main text

**How you will use it:**

Material is need for my PhD thesis or dissertation

Please acknowledge the source of the material used and the publisher, e.g. "Reproduced with permission from Respiratory Drug Delivery 2016, Virginia Commonwealth University and RDD Online".

**RDD Online**

Virginia Biotechnology Research Park,  
[800 East Leigh Street, Suite 206-10](#)  
[Richmond, VA 23219-1534, USA](#)

Phone: +1 (804) 827-1490  
Fax: +1 (804) 828-8277  
Email: [info@rddonline.com](mailto:info@rddonline.com)  
Web: [www.rddonline.com](http://www.rddonline.com)

---

RDD Online

Virginia Biotechnology Research Park, [Suite 206-10, 800 East Leigh Street, Richmond, VA 23219, USA](#).

[Unsubscribe from receiving further emails from RDD Online.](#)



**Title:** Creation of a standardized geometry of the human nasal cavity

**Author:** Y. Liu, M. R. Johnson, E. A. Matida, S. Kherani, J. Marsan

**Publication:** Journal of Applied Physiology

**Publisher:** The American Physiological Society

**Date:** Mar 1, 2009

Copyright © 2009, Copyright © 2009 the American Physiological Society

Logged in as:  
Michele Pozzoli  
Account #:  
3001094314

LOGOUT

### Permission Not Required

Permission is not required for this type of use.

This Agreement between Michele Pozzoli ("You") and Elsevier ("Elsevier") consists of your license details and the terms and conditions provided by Elsevier and Copyright Clearance Center.

Your confirmation email will contain your order number for future reference.

#### Printable details.

License Number	4012730539670
License date	Dec 19, 2016
Licensed Content Publisher	Elsevier
Licensed Content Publication	Advanced Drug Delivery Reviews
Licensed Content Title	Nasal delivery systems and their effect on deposition and absorption
Licensed Content Author	H Kublik, M.T Vidgren
Licensed Content Date	5 January 1998
Licensed Content Volume	29
Licensed Content Issue	1-2
Licensed Content Pages	21
Type of Use	reuse in a thesis/dissertation
Portion	figures/tables/illustrations
Number of figures/tables/illustrations	2
Format	both print and electronic
Are you the author of this Elsevier article?	No
Will you be translating?	No
Order reference number	
Original figure numbers	figure 4 and 6
Title of your thesis/dissertation	Drug delivery to the nose: formulation, deposition and permeation of poorly soluble drugs
Expected completion date	Jan 2017
Estimated size (number of pages)	200
Elsevier VAT number	GB 494 6272 12
Requestor Location	Michele Pozzoli 15 Broadway, Building 7 level 4 Graduate School of Health Pharmacy  Ultimo, NSW 2007 Australia Attn: Michele Pozzoli



**Title:** Nasal drug delivery devices: characteristics and performance in a clinical perspective—a review

**Author:** Per Gisle Djupesland

**Publication:** Drug Delivery and Translational Research

**Publisher:** Springer

**Date:** Jan 1, 2012

Copyright © 2012, The Author(s)

Logged in as:  
Michele Pozzoli  
Account #:  
3001094314

[LOGOUT](#)

**Permissions Request**

This is an open access article distributed under the terms of the Creative Commons Attribution License, which permits unrestricted use, distribution, and reproduction in any medium, provided the original work is properly cited.

Springer and BioMed Central offer a reprint service for those who require professionally produced copies of articles published under Creative Commons Attribution (CC BY) licenses. To obtain a quotation, please email [reprints@springeropen.com](mailto:reprints@springeropen.com) with the article details, quantity(ies) and delivery destination. Minimum order 25 copies.



**Title:** Creation of a standardized geometry of the human nasal cavity

**Author:** Y. Liu, M. R. Johnson, E. A. Matida, S. Kherani, J. Marsan

**Publication:** Journal of Applied Physiology

**Publisher:** The American Physiological Society

**Date:** Mar 1, 2009

Copyright © 2009, Copyright © 2009 the American Physiological Society

Logged in as:  
Michele Pozzoli  
Account #:  
3001094314

[LOGOUT](#)

**Permission Not Required**

Permission is not required for this type of use.

**ELSEVIER LICENSE  
TERMS AND CONDITIONS**

Dec 19, 2016

---

This Agreement between Michele Pozzoli ("You") and Elsevier ("Elsevier") consists of your license details and the terms and conditions provided by Elsevier and Copyright Clearance Center.

License Number	4012720557908
License date	Dec 19, 2016
Licensed Content Publisher	Elsevier
Licensed Content Publication	Procedia Vaccinology
Licensed Content Title	Novel Formulation Concept for Particulate Uptake of Vaccines via the Nasal Associated Lymphoid Tissue
Licensed Content Author	Regina Scherließ,Sabrina Trows
Licensed Content Date	2011
Licensed Content Volume Number	4
Licensed Content Issue Number	n/a
Licensed Content Pages	7
Start Page	113
End Page	119
Type of Use	reuse in a thesis/dissertation
Portion	figures/tables/illustrations
Number of figures/tables/illustrations	1
Format	both print and electronic
Are you the author of this Elsevier article?	No
Will you be translating?	No
Order reference number	
Original figure numbers	figure 1
Title of your thesis/dissertation	Drug delivery to the nose: formulation, deposition and permeation of poorly soluble drugs
Expected completion date	Jan 2017
Estimated size (number of pages)	200
Elsevier VAT number	GB 494 6272 12
Requestor Location	Michele Pozzoli 15 Broadway, Building 7 level 4 Graduate School of Health Pharmacy

**ELSEVIER LICENSE  
TERMS AND CONDITIONS**

Dec 19, 2016

This Agreement between Michele Pozzoli ("You") and Elsevier ("Elsevier") consists of your license details and the terms and conditions provided by Elsevier and Copyright Clearance Center.

License Number	4012730817645
License date	Dec 19, 2016
Licensed Content Publisher	Elsevier
Licensed Content Publication	Journal of Controlled Release
Licensed Content Title	Development and testing of particulate formulations for the nasal delivery of antibodies
Licensed Content Author	Richard S. Kaye, Tarlochan S. Purewal, Oya H. Alpar
Licensed Content Date	17 April 2009
Licensed Content Volume Number	135
Licensed Content Issue Number	2
Licensed Content Pages	9
Start Page	127
End Page	135
Type of Use	reuse in a thesis/dissertation
Intended publisher of new work	other
Portion	figures/tables/illustrations
Number of figures/tables/illustrations	1
Format	both print and electronic
Are you the author of this Elsevier article?	No
Will you be translating?	No
Order reference number	
Original figure numbers	Figure 2
Title of your thesis/dissertation	Drug delivery to the nose: formulation, deposition and permeation of poorly soluble drugs
Expected completion date	Jan 2017
Estimated size (number of pages)	200
Elsevier VAT number	GB 494 6272 12
Requestor Location	Michele Pozzoli 15 Broadway, Building 7 level 4 Graduate School of Health Pharmacy  Ultimo, NSW 2007 Australia Attn: Michele Pozzoli
Total	0.00 USD
Terms and Conditions	

*“Okay, geez! Taylor's right, haters gonna hate, hate, hate, hate, hate”*

*Sheldon Cooper*

The Big Bang Theory – Season 8 Episode 13:

- The Anxiety Optimization –